



**University of  
Zurich**<sup>UZH</sup>

**Zurich Open Repository and  
Archive**

University of Zurich  
Main Library  
Strickhofstrasse 39  
CH-8057 Zurich  
[www.zora.uzh.ch](http://www.zora.uzh.ch)

---

Year: 2011

---

## **Raffinose Oligosaccharide Catabolism in *Arabidopsis thaliana***

Egert, A

Posted at the Zurich Open Repository and Archive, University of Zurich

ZORA URL: <https://doi.org/10.5167/uzh-59358>

Dissertation

Published Version

Originally published at:

Egert, A. Raffinose Oligosaccharide Catabolism in *Arabidopsis thaliana*. 2011, University of Zurich, Faculty of Science.

# **Raffinose Oligosaccharide Catabolism in *Arabidopsis thaliana***

---

**Dissertation**

**zur**

**Erlangung der naturwissenschaftlichen Doktorwürde  
(Dr. sc. nat.)**

**vorgelegt der**

**Mathematisch-naturwissenschaftlichen Fakultät**

**der**

**Universität Zürich**

**von**

**Aurélie Egert**

**aus**

**Frankreich**

**Promotionskomitee**

**Prof. Dr. Enrico Martinoia (Vorsitz)**

**Prof. Dr. Felix Keller (Leitung der Dissertation)**

**Dr. Norbert Sprenger**

**Zürich, 2011**

Die vorliegende Arbeit wurde von der Mathematisch-naturwissenschaftlichen Fakultät der Universität Zürich auf Antrag von Prof. Dr. Enrico Martinoia, Prof. Dr. Felix Keller und Dr. Norbert Sprenger als Dissertation angenommen.

*« La nature est remplie d'une infinité de raisons  
dont l'expérience n'a jamais vu la trace. »*

*Leonard de Vinci*



## INDEX

SUMMARY .....	v
ZUSAMMENFASSUNG.....	vii

## CHAPTER I: General Introduction ..... 1

### 1.1 RFO biosynthesis ..... 5

1.1.1 Galactinol synthase (GolS) catalyzes the formation of the RFO precursor Gol.....	6
1.1.2 Raffinose synthase (RafS) catalyzes the synthesis of the first RFO member .....	7
1.1.3 Stachyose synthase (StaS) catalyzes the synthesis of the second RFO member .....	8
1.1.4 Higher DP RFO are mainly synthesized <i>via</i> a Gol-independent pathway.....	9

### 1.2 RFO catabolism .....11

1.2.1 RFO degradation starts with the hydrolytic action of $\alpha$ -D-galactosidases ( $\alpha$ Gals) .....	12
1.2.2 Galactokinase (GALK) phosphorylates free Gal produced by the degradation of Gal-containing compounds .....	16
1.2.3 Free Gal is toxic.....	17
1.2.4 The Gal salvage pathway continues .....	18

### 1.3 RFOs play a role in abiotic stress tolerance.....21

1.3.1 Plants are frequently exposed to abiotic stress .....	21
1.3.2 RFOs accumulate during stress and may act as osmoprotectants.....	23
1.3.3 Cold stress involves molecular regulation and incudes RFO accumulation .....	25
1.3.4 Water deficit and salt stress may induce RFO accumulation.....	28
1.3.5 Other abiotic stress and RFO accumulation.....	29

### 1.4 RFOs play a role in carbon partitioning and storage.....31

1.4.1 Transport RFOs move in the phloem from source to sink .....	31
1.4.2 Storage RFOs accumulate in the vacuole and can be easily mobilized.....	33

### 1.5 Aims of my thesis .....35

## CHAPTER II: Functional identification of Arabidopsis alkaline $\alpha$ -galactosidases ATSIP1 (At1g55740) and ATSIP2 (At3g57520) .....37

### 2.1 Introduction.....39

### 2.2 Materials and methods.....41

2.2.1 Plants material and growth conditions .....	41
2.2.2 Screening for T-DNA insertion lines.....	41
2.2.3 Heterologous expression of ATSIP1 and -2 in <i>Sf9</i> insect cells.....	42
2.2.3.1 Bacmid construction and transfection .....	42
2.2.3.2 Expression of ATSIP1 and -2 in <i>Sf9</i> cells .....	43
2.2.3.3 RNA isolation from <i>Sf9</i> cells and cDNA synthesis.....	44
2.2.4 $\alpha$ -Galactosidase activity assays of recombinant ATSIP1 and -2.....	45
2.2.5 Desalting of extracts.....	45
2.2.6 HPLC-PAD analysis.....	46
2.2.7 Biochemical characterization of recombinant ATSIP1 and -2 .....	46

2.2.8	Cold acclimation and deacclimation treatments .....	47
2.2.9	Water-deficit and rehydration treatments .....	47
2.2.10	Plant enzyme extraction and activity assays.....	47
2.2.11	EDTA-mediated phloem exudation and <sup>14</sup> C pulse-chase experiment.....	48
2.2.12	RNA isolation from plant tissue and semi-quantitative PCR (sqPCR).....	48
2.2.13	Promoter-β-glucuronidase (GUS) plants .....	49
2.2.14	Histochemical staining for β-glucuronidase (GUS) activity .....	49
2.2.15	Preparation of root cross sections for light microscopy .....	50
2.2.16	Seed germination assays .....	50
2.2.17	Water soluble carbohydrate (WSC) extractions.....	50
<b>2.3</b>	<b>Results.....</b>	<b>51</b>
2.3.1	ATSIP1 and -2 are <i>bona-fide</i> αGals with different substrate specificities .....	51
2.3.2	Biochemical characterization of recombinant ATSIP1 and -2 .....	53
2.3.3	ATSIP2 does not seem to play an important role during deacclimation of cold-acclimated plants .....	54
2.3.4	ATSIP2 does not seem to play an important role during rehydration of dehydrated plants...	56
2.3.5	Investigating the role of ATSIP1 and -2 role in phloem unloading in leaves.....	58
2.3.5.1	ATSIP2 has a sink-specific expression and αGal activity pattern .....	60
2.3.5.2	ATSIP1 has a sink-specific expression pattern but the Sta and Gol-specific αGal activity remains low .....	61
2.3.6	Physiological functions of ATSIP1 and -2 during seed germination .....	62
<b>2.4</b>	<b>Discussion .....</b>	<b>65</b>
<b>CHAPTER III: AtDIN10 (At5g20250) is an alkaline αGal located in the chloroplast.....</b>		<b>67</b>
<b>3.1</b>	<b>Introduction .....</b>	<b>69</b>
<b>3.2</b>	<b>Materials and methods.....</b>	<b>71</b>
3.2.1	Plant material and growth conditions .....	71
3.2.2	Recombinant AtDIN10 expression and characterization in <i>Sf9</i> insect cells .....	71
3.2.3	GFP fusion protein analysis .....	71
3.2.4	Biochemical characterization of recombinant AtDIN10.....	72
<b>3.3</b>	<b>Results.....</b>	<b>73</b>
3.3.1	<i>AtDIN10</i> contains a putative chloroplast transit peptide (cTP).....	73
3.3.2	AtDIN10 is localized in the chloroplast.....	73
3.3.3	AtDIN10 is an alkaline αGal .....	74
<b>3.4</b>	<b>Discussion .....</b>	<b>76</b>
<b>CHAPTER IV: An Arabidopsis T-DNA insertion mutant for galactokinase (AtGALK, At3g06580) hyperaccumulates free galactose and exhibits insensitivity to exogenous galactose.....</b>		<b>79</b>
<b>4.1</b>	<b>Introduction.....</b>	<b>81</b>
<b>4.2</b>	<b>Materials and methods.....</b>	<b>83</b>
4.2.1	Plant materials and growth conditions .....	83

4.2.2	Screening for T-DNA insertion lines.....	83
4.2.3	Recombinant AtGALK expression in <i>Sf9</i> insect cells.....	83
4.2.4	GALK activity assay and biochemical characterization of recombinant AtGALK.....	84
4.2.5	GALK analysis of plant crude extract .....	84
4.2.6	Construction of <i>atgalk/35S: AtGALK</i> rescued lines .....	84
4.2.7	RNA isolation and semi-quantitative PCR (sqPCR) .....	84
4.2.8	Water soluble carbohydrate (WSCs) extraction.....	85
4.2.9	Isolation of mesophyll protoplasts and vacuoles from Arabidopsis .....	85
4.2.10	Enzymatic quantification of Gal.....	85
4.2.11	Gal toxicity assays.....	86
<b>4.3</b>	<b>Results.....</b>	<b>87</b>
4.3.1	AtGALK was functionally expressed and biochemically characterized .....	87
4.3.2	Characterization of an <i>atgalk</i> T-DNA insertion line .....	88
4.3.3	Functional rescue of <i>atgalk</i> .....	90
4.3.4	<i>In vitro</i> -grown <i>atgalk</i> seedlings exhibit insensitivity to exogenous Gal .....	91
4.3.5	Free Gal accumulates in leaf mesophyll vacuoles of <i>atgalk</i> plants.....	92
4.3.6	Uptake mechanisms for free Gal are unaffected in <i>atgalk</i> plants .....	93
<b>4.4</b>	<b>Discussion .....</b>	<b>96</b>
<b>CHAPTER V:</b>	<b>General summary, conclusions and outlook .....</b>	<b>101</b>
<b>5.1</b>	<b>General discussions and conclusions .....</b>	<b>103</b>
5.1.1	AtSIP2 is a <i>bona fide</i> Raf-specific alkaline $\alpha$ Gal proposed to be involved in phloem unloading .....	105
5.1.2	ATsIP1 is a <i>bona fide</i> Sta- and Gol-specific alkaline $\alpha$ Gal with a yet unknown physiological function.....	106
5.1.3	AtDIN10 is an alkaline $\alpha$ Gal located in the chloroplast, proposed to degrade DGDG during dark-induced senescence .....	107
5.1.4	Are the other annotated RafSs genuine RafSs?.....	108
5.1.5	AtGALK is a <i>bona fide</i> GALK and the study of <i>atgalk</i> reveals a putative new Gal detoxification pathway involving a tonoplast transporter.....	109
5.1.6	Does the conversion of $\beta$ -form of Gal to $\alpha$ -form via a mutarotase exist in Arabidopsis?.....	111
<b>5.2</b>	<b>Outlook.....</b>	<b>114</b>
<b>REFERENCE LIST.....</b>		<b>115</b>
<b>APPENDICES</b>		
I	List of abbreviations.....	129
II	PETERS S., EGERT A., STIEGER B., KELLER F. (2010) Plant and Cell Physiology .....	131
III	<i>Curriculum Vitae</i> .....	137
IV	Acknowledgments .....	139





## SUMMARY

Raffinose family oligosaccharides (RFOs) are  $\alpha$ 1,6-galactosyl extensions of sucrose, occurring exclusively in plants and some photoautotrophic algae. In plants, they fulfill important functions such as carbon translocation and storage and abiotic stress protection. Contrary to RFO biosynthesis, its catabolism has received little attention in research, despite its putative importance in phloem unloading, abiotic stress relief and remobilization of seed carbohydrate reserves. The following experiments were conducted to define the first two steps of RFO catabolism in *Arabidopsis* catalyzed by  $\alpha$ -galactosidases ( $\alpha$ Gals) and galactokinase (GALK), respectively.

(i) *Arabidopsis* *ATSIP2* has recently been suggested to be a raffinose synthase (RafS) gene. However, using the *Sf9* insect cell expression system, I demonstrated that recombinant *ATSIP2* is a genuine alkaline  $\alpha$ Gal with high substrate specificity for Raffinose (Raf) (and not a RafS). Recombinant *ATSIP2* hydrolyzed only the  $\alpha$ - and not the  $\beta$ -variant of the artificial substrate, *p*-nitrophenol-*D*-galactopyranoside (pNPGal), displayed a pH optimum of 7.5-8.0 and was inhibited by a potent  $\alpha$ Gal inhibitor, deoxygalactonojirimycin (DGJ), as well as by high galactose (Gal) concentrations. Using a reverse genetic approach, I found that *ATSIP2* does not play a role in the low temperature and dehydration stress relief of abiotic stress-induced Raf accumulation. However, a  $\beta$ -glucuronidase (GUS) reporter construct using the *ATSIP2* promoter showed that *ATSIP2* is strongly expressed in sink tissues of *Arabidopsis*, *i.e.* sink leaves and non-xylem parts of the root stele, suggesting a physiological function of *ATSIP2* in Raf phloem unloading.

(ii) *Arabidopsis* *ATSIP1* was also proposed to be a RafS. However, I showed that *ATSIP1* is rather a genuine alkaline  $\alpha$ Gal (like *ATSIP2*), with equally high specificities for stachyose (Sta) and galactinol (Gol) and a pH optimum of 8.5. The recombinant protein only hydrolyzed the  $\alpha$ - and not the  $\beta$ -variant of pNPGal and was strongly inhibited by DGJ and partially inhibited by Gal. A GUS reporter construct using the *ATSIP1* promoter showed that *ATSIP1* is strongly expressed in sink tissues of *Arabidopsis*. However, enzyme activities with Sta and Gol as substrates and *ATSIP1* transcript levels in these tissues remained low. The Sta specificity suggests a physiological role of *ATSIP1* in seed germination, because seeds are the only known *Arabidopsis* organs where Sta is present.

(iii) The third alkaline  $\alpha$ Gal candidate from *Arabidopsis*, *AtDIN10*, was reported to be up-regulated during dark-induced senescence. Using *Sf9* insect cell system, I established that *AtDIN10* is also an alkaline  $\alpha$ Gal with a pH optimum of 8.0 and broad substrate specificity for different galacto-

oligosaccharides. Transient expression with an N-terminal *AtDIN10::GFP* fusion in Arabidopsis mesophyll protoplasts showed that AtDIN10 is located in the chloroplast, most likely in the stroma.

(iv) GALK is a cytosolic enzyme which catalyzes the ATP-dependent conversion of  $\alpha$ -D-Gal to  $\alpha$ -D-Gal-1-P. AtGALK had recently been identified, cloned and functionally characterized in *E. coli*. I conducted the expression and biochemical characterization in *Sf9* cells confirming its identity. I then constructed and identified an *AtGALK* T-DNA *loss-of-function* mutant (*atgalk*) that displays no GALK activity and accumulates free Gal up to 7 mg g<sup>-1</sup> FW in leaves and roots, compared to trace amounts in wild-type plants. Because free Gal is generally cytotoxic, it was surprising to find that *atgalk* plants exhibited no growth or morphological defects and were insensitive to exogenous Gal up to 100mM. Conversely, wild-type plants exhibited sensitivity to even low concentrations of exogenous Gal (10mM). The leaves of *atgalk* plants constitutively over-expressing the *AtGALK* cDNA reverted to Gal concentrations of leaves from wild-type plants, but still retained the *atgalk* Gal insensitivity. Finally, I demonstrated that (i) the Gal in the leaves of *atgalk* plants accumulated totally in the mesophyll vacuoles, and (ii) that the *atgalk* mutant was not impaired in Gal uptake through the roots. A previously unknown detoxification pathway targeting free Gal to the vacuole seems to be constitutively active in the *atgalk* mutant background.

## ZUSAMMENFASSUNG

Raffinose Familie Oligosaccharide (RFOs) sind  $\alpha$ 1,6 Galactosyl-Verlängerungen der Saccharose, die ausschliesslich in Pflanzen und einigen photautotrophen Algen vorkommen. Sie spielen eine wichtige Rolle als Phloemzucker, Kohlenhydratspeicher und Schutzstoffe gegen abiotischen Stress. Im Gegensatz zur Biosynthese der RFOs ist deren Katabolismus nur wenig untersucht, obwohl er bei der Phloementladung, Stressentlastung und Samenkeimung sehr wichtig ist. Folgende Experimente wurden durchgeführt, um die ersten beiden Schritte des RFO Katabolismus, katalysiert durch  $\alpha$ -Galactosidasen ( $\alpha$ Gal) und Galactokinasen (GALK), zu entschlüsseln:

(i) Arabidopsis *ATSIP2* wird in der Literatur als ein Raffinose Synthase (RafS) Gen beschrieben. Mittels heterologer Expression von *ATSIP2* in *Sf9* Insektenzellen konnte ich zeigen, dass *ATSIP2* eine echte alkalische  $\alpha$ Gal mit einer hohen Spezifität für Raffinose (Raf) (und keine RafS) ist. Rekombinantes *ATSIP2* Protein hydrolysierte nur die  $\alpha$ - und nicht die  $\beta$ -Form des künstlichen Substrates *p*-Nitrophenyl-D-Galactopyranosid (pNPGal), zeigte ein pH Optimum von 7,5-8,0, wurde von Deoxygalactonojirimycin (DGJ), einem potenten Hemmstoff der  $\alpha$ Gal, und hohen Galactosekonzentrationen gehemmt. Mittels eines "reverse genetic" Ansatzes konnte ich zeigen, dass *ATSIP2* bei der Hydrolyse von unter Kälte- und Trockenstress gebildeter Raf, während der Stressentlastung keine Rolle spielt. Untersuchungen mit *ATSIP2*-Promotor- $\beta$ -Glucuronidase (GUS) Konstrukten zeigten, dass *ATSIP2* vor allem in Sink Blättern und in Wurzel Stelen exprimiert war. Dieses Expressionsmuster deutet klar darauf hin, dass *ATSIP2* eine physiologische Funktion bei der Phloementladung von Raf hat.

(ii) Arabidopsis *ATSIP1* wird ebenfalls als eine RafS beschrieben. Mittels heterologer Expression von *ATSIP1* in *Sf9* Insektenzellen konnte ich zeigen, dass *ATSIP1* eine echte alkalische  $\alpha$ Gal mit einer hohen Spezifität für Stachyose (Sta) und Galactinol (Gol) (und keine RafS) ist. Rekombinantes *ATSIP1* Protein hydrolysierte nur die  $\alpha$ - und nicht die  $\beta$ -Form von pNPGal, zeigte ein pH Optimum von 8,5, wurde von DGJ und hohen Galactosekonzentrationen gehemmt. Mit einem *ATSIP1*-GUS-Promotor Konstrukt konnte ich zeigen, dass die Expression besonders hoch in Sink Gewebe ist. Jedoch waren die Enzymaktivitäten mit Sta und Gol als Substrat und die *ATSIP1* Transkripte in diesen Geweben schwach. Die beobachtete hohe Spezifität von *ATSIP1* für Sta deutet also eher auf eine physiologische Rolle bei der Samenkeimung hin, da die Samen das einzige Organ von Arabidopsis sind, das Sta enthält.

(iii) Vom dritten alkalischen  $\alpha$ Gal Kandidaten aus Arabidopsis, AtDIN10, war bekannt, dass er während der dunkelinduzierten Seneszenz hochreguliert wird. Mittels *Sf9* Insektenzellen konnte ich zeigen, dass AtDIN10 ebenfalls eine alkalische  $\alpha$ Gal ist, mit einer breiten Substratspezifität für verschiedene Galacto-Oligosaccharide und einem pH Optimum von 8,0. Transiente Expression mit einer N-terminalen *AtDIN10::GFP* Fusion in Arabidopsis Mesophyllprotoplasten zeigte eindeutig, dass AtDIN10 in Chloroplasten lokalisiert ist, höchstwahrscheinlich im Stroma.

(iv) GALK ist ein cytosolisches Enzym, welches die ATP-abhängige Umformung von  $\alpha$ -D-Gal zu  $\alpha$ -D-Gal-1-P katalysiert. AtGALK wurde kürzlich identifiziert, kloniert und funktionell in *E. coli* charakterisiert. Ich exprimierte und charakterisierte AtGALK in *Sf9* Zellen und bestätigte ihre Identität. Ich produzierte und identifizierte eine *AtGALK* T-DNA *loss-of-function* Mutante (*atgalk*), die keine GALK Aktivität zeigte und bis zu 7 mg g<sup>-1</sup> Trockengewicht Gal in ihren Blättern und Wurzeln akkumulierte. Im Vergleich dazu wies der Wildtyp nur geringe Spuren von Gal auf. Da Gal generell cytotoxisch ist, kam der Befund überraschend, dass *atgalk* Pflanzen keine Entwicklungsstörungen aufwiesen und gegenüber exogener Gal bis zu 100mM insensitiv waren. Im Gegenzug waren Wildtyp Pflanzen klar sensitiv gegenüber geringen Konzentrationen exogener Gal (10mM). Blätter von *atgalk* Pflanzen, die *AtGALK* überexprimierten, zeigten wildtypähnliche Gal Konzentrationen, blieben aber gleich Gal-insensitiv wie die *atgalk* Pflanzen. Schliesslich konnte ich noch zeigen, dass (i) in den Blättern der *atgalk* Pflanzen die Gal vollständig in den Vakuolen der Mesophyllzellen akkumuliert und (ii) *atgalk* Pflanzen exogene Gal durch die Wurzeln aufnehmen können. Diese Resultate deuten auf einen neuen Gal-Detoxifikationsmechanismus hin, der freie Gal in die Vakuole transportiert und in Pflanzen mit *atgalk* Hintergrund operativ ist.

# **Chapter I:**

## **General introduction**



Plants are sessile organisms and are frequently subjected to various and adverse environmental conditions. Abiotic stresses such as drought, cold, heat, salt or nutrient availability result in developmental, growth or shape constraints. Each organism has a unique range of genetically determined and phylogenetically adapted physiological resistance within which a factor affecting it is tolerable. Plants have complex and dynamic systems to respond to stress stimuli that involve a myriad of biochemical and physiological processes. Upon exposure to abiotic stresses, many plants accumulate compatible solutes (also known as osmoprotectants or compatible osmolytes), consisting of non-toxic organic molecules that protect the cells against deleterious osmotic and metabolic imbalances caused by stress (see section 1.3.2; Hare et al., 1998; Majumder et al., 2010). Compatible solutes include the raffinose family oligosaccharides (RFOs; **Fig.1**) that rank as the second most abundant soluble carbohydrates in the plant kingdom and are the focus of this thesis. RFOs are ubiquitous in plants and are known to accumulate during abiotic stress and to be catabolized after stress relief (Kandler and Hopf, 1982; Keller and Pharr, 1996; Avigad and Dey, 1997; Peterbauer and Richter, 2001; Taji et al., 2002; Nishizawa-Yokoi et al., 2008).

As primary photosynthetic products, RFOs also have prominent additional roles in plants, such as storage and transport of carbon (Dey, 1985; Keller and Matile, 1985; Bachmann et al., 1994; Sprenger and Keller, 2000). It is crucial for a plant to store and/or transport the carbon fixed in photosynthesis during the day, which can be mobilized at night to sustain growth and development. Starch is, for example, temporarily synthesized as a carbon reserve in the chloroplasts during the day and utilized as carbon source during the night (for review see Mullen and Koller, 1988; Smith et al., 2005; Grennan, 2006; Graf et al., 2010), thereby sustaining continuous metabolism. Generally speaking, starch is the common storage form and sucrose (Suc) the common translocation form of carbon. However, many plants show diverse alternative strategies for carbon storage and transport. Well-known examples include RFOs (*e.g.* raffinose (Raf) and stachyose (Sta) in the *Cucurbitaceae* and *Lamiaceae*) and sugar alcohols (*e.g.* sorbitol in the *Plantaginaceae* and *Rosaceae*, mannitol in the *Apiaceae* and *Oleaceae*, volemistol in the *Primulaceae*) which may serve for carbon storage and transport, in addition to starch and Suc, respectively (Häfliger et al., 1999; Loescher and Everard, 2000; Turgeon and Wolf, 2009).

RFO biosynthesis and degradation pathways have been described in different plant species and tissues (see sections 1.1 and 1.2). Chemically, RFOs [Suc-(Gal)<sub>n</sub>, 1≤n<13] are non-reducing oligosaccharides that consist of galactose (Gal) units linked to Suc via α-(1→6) glycosidic linkages (**Fig.1**). The trisaccharide Raf (O-α-D-galactopyranosyl-(1→6)-α-D-glucopyranosyl-(1←→2)-β-D-fructofuranoside) was first detected in sugar beet molasses (Loiseau, 1876) and constitutes the



smallest member of the RFO series and is the most widely spread RFO in the plant kingdom. The second member, the tetrasaccharide Sta, was first isolated from *Stachys sieboldii* tubers (Japanese artichoke; Planta and Schultze, 1890), and the third member, the pentasaccharide verbascode (Ver), was first isolated from *Verbascum thapsus* roots (Bourquelot and Bridel, 1910). The fourth, less common member, ajugose (Aju), first isolated from *Ajuga nipponensis* roots (Murakami, 1941), mostly occurs in storage organs like seeds of dicots, particularly of legumes (Kotiguda et al., 2006), but also in roots, rhizomes, tubers, and leaves (Dey, 1990; Bachmann et al., 1994). Much less is known about the occurrence of the longer-chain RFOs. They have, for instance, been described in vegetative tissues of cold-tolerant *Laminaceae* such as *Ajuga reptans* (common bugle) and *Glechoma hederaceae* (ground ivy; Bachmann et al., 1994; Bachmann et al., 1995). In cold-acclimated common bugle leaves they occur exclusively in the vacuole up to the degree of polymerization (DP) of fifteen (Bachmann et al., 1994).

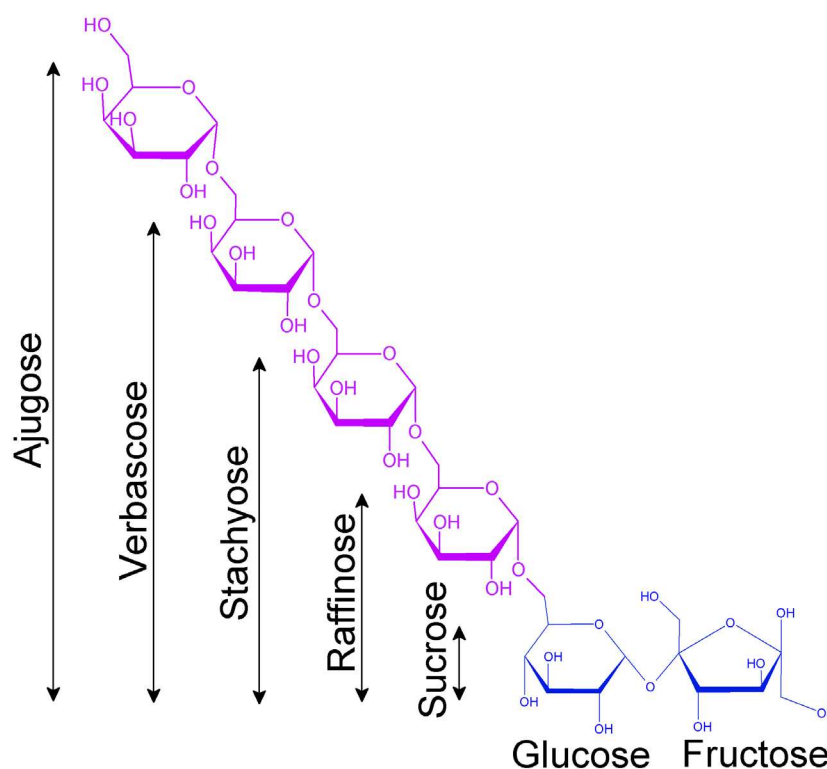


**Fig.1.** Structure of the first four RFO members (DP<sub>3-6</sub>).

In this chapter, I will give a general overview of plant RFO metabolism with an emphasis on its catabolism which constitutes the main focus of my thesis. The enzymes involved in the biosynthetic and catabolic steps will be presented with their characteristics and functions both from the biochemical, the physiological and molecular points of view.

## 1.1 RFO biosynthesis

The RFO biosynthetic pathway is well established (**Fig.2**). It proceeds by the stepwise addition of Gal units from the donor galactinol (Gol; O- $\alpha$ -D-galactopyranosyl-(1 $\rightarrow$ 1)-L-*myo*-inositol) to Suc in the cytosol (at least up to DP<sub>4</sub>).

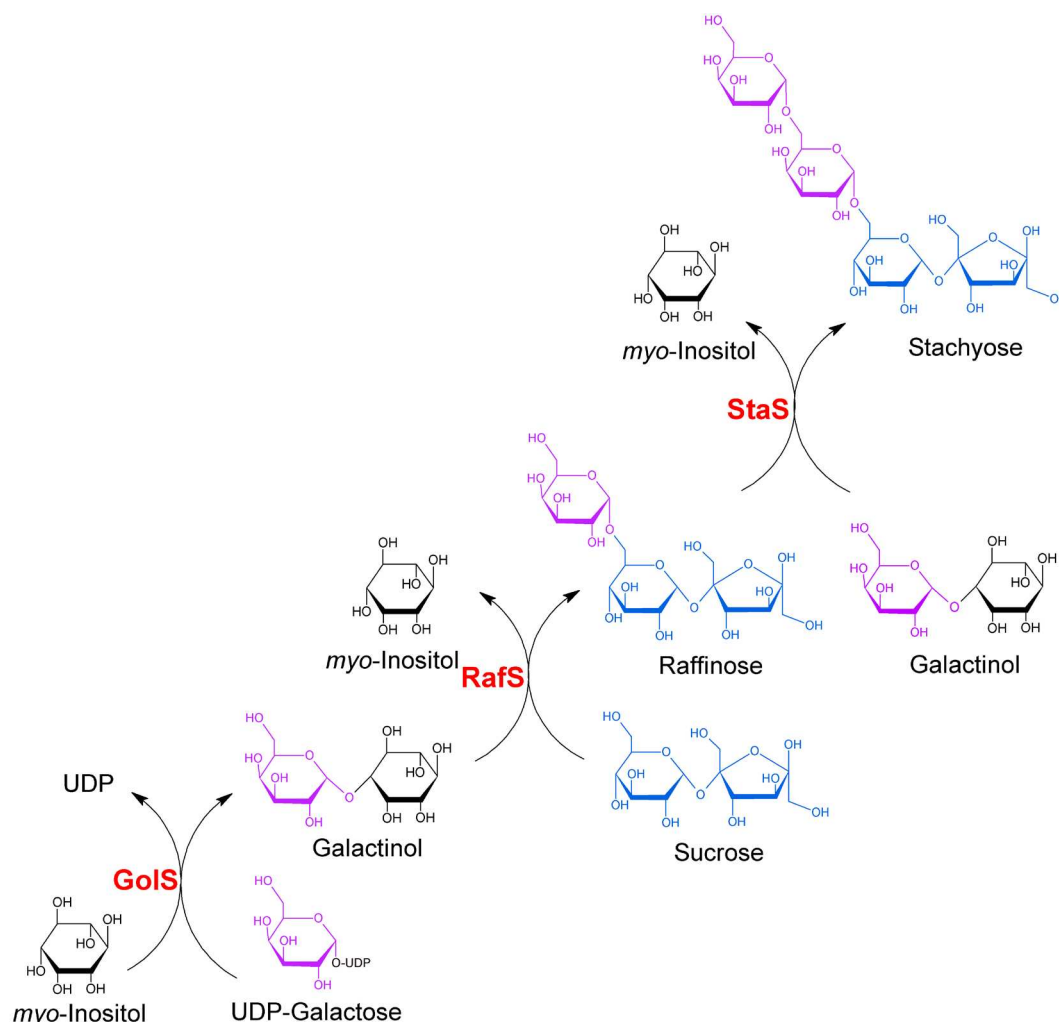


**Fig.2.** The three first steps of RFO anabolism catalyzed by galactinol synthase (GoIS), raffinose synthase (Rafs), and a stachyose synthase (StaS). Gal molecules are represented in purple and Suc molecules in blue.

For a long time, it was speculated that Gol's main function in plants was exclusively to act as a galactosyl donor for RFO formation. More recently, an additional function as a signal molecule was proposed (Kim et al., 2008). Gol synthesis is catalyzed by galactinol synthase (GoIS; UDP-D- $\alpha$ -galactose:*myo*-inositol-1- $\alpha$ -D-galactosyltransferase; EC 2.4.1.123; Frydman and Neufeld, 1963; Keller and Pharr, 1996; Taji et al., 2002) which uses the substrates, UDP-galactose (UDP-Gal) and *myo*-inositol (Ino) (**Fig.2**). The second step is the synthesis of Raf by Raffinose synthase (RafS; Gol:Suc-6-galactosyltransferase; EC 2.4.1.82; Lehle and Tanner, 1973) that involves the transfer of the

galactosyl moiety from a Gol molecule to the glucose (Glc) moiety of Suc (**Fig.2**). The third step is the synthesis of Sta catalyzed by Sta synthase (StaS; Gol:Raf-6-galactosyltransferase; EC 2.4.1.67; Tanner and Kandler, 1968; Peterbauer et al., 2002a) that involves the transfer of the galactosyl moiety from a Gol molecule to the Gal moiety of Raf (**Fig.2**). The higher DP (DP>4) RFO biosynthesis proceeds by galactinol-independent galactosyltransferase reactions in the vacuole employing galactan:galactan galactosyltransferase (GGT) which catalyzes the transfer of the terminal Gal residue from one RFO to another, resulting in the formation of RFOs of the next higher and lower degree of polymerization (Bachmann et al., 1994; Inan Haab and Keller, 2002; Tapernoux-Lüthi et al., 2004).

### 1.1.1 Galactinol synthase (GoS) catalyzes the formation of the RFO precursor Gol

The first committed step of RFO biosynthesis is the production of Gol from Ino and UDP-Gal, a reaction catalyzed by a GoS (for review see Keller and Pharr, 1996). Gol itself was first isolated and identified from *Beta vulgaris* juice (sugar beet; Brown and Serro, 1953) and chemically characterized by methylation and hydrolysis (Kabat et al., 1953). Two pieces of evidence support that Gol is the galactosyl donor for RFO biosynthesis. Firstly, Gol is only found in plants containing RFOs (Senser and Kandler, 1967b) and secondly, it shows all the characteristics of a precursor (Senser and Kandler, 1967; Tanner, 1969). Photosynthetic studies with leaves and  $^{14}\text{CO}_2$  showed that the labeling of Gol was much faster and the  $^{14}\text{C}$ -Gol pool size became rapidly enlarged compared with that of the RFOs; however, upon chasing with unlabeled  $^{12}\text{CO}_2$ , the radioactivity in Gol decreased while it increased in the RFOs.

The GoS reaction was first detected in crude extracts from maturing *Pisum sativum* seeds (pea; Frydman and Neufeld, 1963). The enzyme was partially purified from *Cucumis sativus* leaves (cucumber; Pharr et al., 1981) and highly purified from *Cucurbita pepo* leaves (squash; Smith et al., 1991). In leaves, GoS shows a pH optimum between 7 and 8 and is dependent on sulfhydryl groups and  $\text{Mn}^{2+}$  ions (Handley and Pharr, 1982). GoS activity is highly specific for both UDP-Gal and Ino substrates, with apparent  $K_m$  values of 0.2 to 2mM and 4 to 6.5mM, respectively. In pea seeds, however, GoS exhibits a pH optimum of 5.6 (Frydman and Neufeld, 1963). Subcellular localization studies showed that both Gol and GoS occur outside the vacuole, most probably in the cytosol (Keller, 1992; Bachmann and Keller, 1995).

As the first enzymatic step of a metabolic sequence GoS might be tightly regulated (Keller and Pharr, 1996). The regulation of RFO biosynthesis has been documented in a comparative study involving 20 plant species and GoS activity positively correlated with the RFO proportion of soluble

carbohydrates, negatively correlated the Suc level, and did not correlate with the hexose levels (Handley et al., 1983). These relations were also observed during plant development *e.g.* in the cucumber leaves (Pharr and Sox, 1984) and seeds, *e.g.* of *Glycine max* (soybean; Saravitz et al., 1987), in *Medicago sativa* (alfalfa; Blöchl et al., 2005) and in *Brassica napus* (rapeseeds; Li et al., 2011).

GolS involvement in abiotic stress is well established (see sections 1.3.3 and 1.3.4; Liu et al., 1998; Sprenger and Keller, 2000; Taji et al., 2002). Liu et al. (1998) found that GolS activity in *Phaseolus vulgaris* seeds (kidney bean) increased upon the exposure of plants to cold. *GolS* genes from *Arabidopsis thaliana*, common bugle, *Lycopersicon esculentum* (tomato), *Xerophyta viscosa* and *Coffea Arabica* (coffee) have been cloned and functionally expressed (Sprenger and Keller, 2000; Taji et al., 2002; Downie et al., 2003; Peters et al., 2007; dos Santos et al., 2011). In *Oryza sativa* (rice), a protein comparison identified a *GolS* homolog that belongs to a group of ABA-independent desiccation stress-inducible genes. In tomato seeds, the presence of *GolS* transcripts showed a correlation with desiccation tolerance; the transcripts declined during imbibition, and in tomato seedling leaves, *GolS* transcripts were induced by cold and desiccation (Downie et al., 2003). In *Arabidopsis*, ten members constitute the *GolS* gene family, of which *AtGolS1* and 2 are induced by water-deficit and high-salinity stresses, but not by cold stress, whereas *AtGolS3* is induced by cold stress and regulated by DREB/CBF transcription factors (see section 1.3.3), but not by water-deficit or salt stress (Taji et al., 2002). *AtGolS1* was also shown to be a heat shock target gene responsible for heat-induced RFO accumulation since Raf levels did not increase under heat exposure in the *AtGolS1* knock-out plants (Panikulangara et al., 2004). *AtGolS2* overexpression of caused an increase in endogenous Gol and Raf and reduced transpiration. These results show that the stress-inducible GolS plays a key role in the accumulation of Gol and Raf under abiotic stress conditions (Taji et al., 2002). However, Gol does not only serve as galactosyl donor and regulator of RFO synthesis, it also acts as a signal molecule during induced systemic resistance in cucumber after *Pseudomonas chlororaphis* O6 root colonization (Kim et al., 2008). The increase of Gol in plant leaves, both endogenously through the transgene expression of *CsGolS1* and exogenously through sugar treatment of the roots, correlated with resistance against bacterial and fungal infections. This suggests that Gol can act as an endogenous molecular signal induction of defense responses in plants in biotic stress cases (Kim et al., 2008).

### 1.1.2 Raffinose synthase (RafS) catalyzes the synthesis of the first RFO member

The second step of RFO biosynthesis is the formation of Raf from Suc and Gol by RafS (Fig.2, for review see Keller and Pharr, 1996). RafS has only been characterized from *Vicia faba* seeds (broad

bean; Lehle and Tanner, 1973) and exhibits a neutral pH optimum apparent  $K_m$  values for Gol of 4.8 and 7mM and for Suc of 1 and 16.4mM, for broad bean and common bugle crude extracts, respectively (Lehle and Tanner, 1973; Bachmann et al., 1994). RafS from pea has been cloned and heterologously expressed in *Spodoptera frugiperda* Sf21 insect cells, and the biochemical properties of the recombinant enzyme correlated with previous data from broad bean purified extracts (Peterbauer et al., 2002a). More recently, RafS from rice was expressed in *E. coli* (Li et al., 2007). At the amino acid level, RafS sequences show homologies to StaSs (Peterbauer et al., 1999; Peterbauer et al., 2002a) and a class of unidentified seed imbibition proteins (SIPs; Anderson and Kohorn, 2001; Romo et al., 2001). At the structural level, RafSs have similarities with  $\alpha$ -D-galactosidases ( $\alpha$ Gals). Their inhibition by the  $\alpha$ Gal-specific inhibitor, 1-deoxygalactonojirimycin (DGJ), suggests a possible minor hydrolase activity (Peterbauer et al., 2002a). The information on the subcellular localization of RafS is minimal in the literature, but suggests that RafS is present in the cytosol (Keller and Pharr, 1996; Schneider and Keller, 2009). In Arabidopsis, six genes have been annotated as RafS by sequence homologies but their functional identities remain uncharacterized (Nishizawa et al., 2008). In Chapters II and III of this thesis, I will demonstrate that three of these putative RafS genes actually encode functional  $\alpha$ Gals (and not RafSs).

### 1.1.3 Stachyose synthase (StaS) catalyzes the synthesis of the second RFO member

The third step of RFO anabolism is the production of Sta from Raf and Gol by a StaS (for review see Keller and Pharr, 1996). StaS was first isolated and characterized from kidney bean seeds (Tanner and Kandler, 1966, 1968) and purified and/or characterized in broad bean seeds (Tanner et al., 1967) and in some cucurbit leaves (Gaudreault and Webb, 1981; Huber et al., 1990; Holthaus and Schmitz, 1991), common bugle leaves (Bachmann et al., 1994), *Vigna angularis* seeds (adzuki bean; Peterbauer and Richter, 1998), and *Lens culinaris* seeds (lentil; Hoch et al., 1999). In common bugle leaves, StaS is localized in the cytosol and its product, Sta, may be transported to the vacuole for storage or RFO chain elongation in mesophyll cells or be used for phloem transport if it is synthesized in the intermediary cells (Bachmann and Keller, 1995). StaS exhibits a neutral pH optimum and apparent  $K_m$  values for Gol between 2.4 and 11mM and for Raf between 0.85 and 15mM (Keller and Pharr, 1996). In addition to the formation of Sta, it is also able to synthesize galactocyclitols, such as galactopinitol A from D-pinitol, ciceritol from galactopinitol A, and the Gol-dependent synthesis of galactosylononitol from D-ononitol (Hoch et al., 1999). Galactosylononitol could also substitute for Gol in the synthesis of Sta from Raf, indicating that StaS is a multi-substrate enzyme that can mediate a redistribution of galactosyl residues from different carbohydrate species (Peterbauer and Richter, 1998). A cDNA encoding StaS from adzuki bean has been cloned and functionally expressed in Sf21

insect cells. The native and heterologous StaS showed similar catalytic properties for both cyclitols and RFOs (Peterbauer et al., 1999).

#### 1.1.4 Higher DP RFOs are mainly synthesized *via* a Gol-independent pathway

Relatively little information is available on the synthesis of Ver, Aju and higher DP RFOs. The transfer of a further Gal residue from Gol to Sta to produce Ver is possibly catalyzed by a bifunctional StaS or by a very similar verbascose synthase (VerS; Tanner et al., 1967; Kandler and Hopf, 1982; Peterbauer et al., 2002a).

In addition, a Gol-independent pathway was identified in common bugle leaves, which catalyzes the transfer of the terminal Gal unit from one RFO molecule to another by an enzyme named galactan:galactan galactosyltransferase (GGT) by analogy with the fructosyltransferases of the fructan biosynthetic pathway (Fig.3; Bachmann et al., 1994). This was confirmed in crude extracts of pea seeds where both pathways are active (Peterbauer et al., 2001). GGT activity was first detected in leaves of cold-grown common bugle plant (Bachmann et al., 1994) and has later been detected in leaves of salt-stressed *Coleus blumei* plants (Gilbert et al., 1997); it has not yet been found in seeds. Compartmentation studies indicated that both GGT activity and higher DP RFOs, starting from Sta, are located within the vacuoles of mesophyll cells of the common bugle (Bachmann and Keller, 1995; Braun and Keller, 2000). Consistent with its subcellular localization, GGT activity exhibited an acidic pH optimum (Bachmann et al., 1994; Inan Haab and Keller, 2002), while the Gol-dependent transferase were extravacuolar in location and display pH optima at neutral pH values (Bachmann et al., 1994; Bachmann and Keller, 1995). *ArGGT* was purified 200-fold and its transferase reaction displayed saturable concentration dependence for both Raf and Sta with apparent *K<sub>m</sub>* values of 42 and 58mM, respectively (Inan Haab and Keller, 2002). *ArGGT* was later cloned, functionally expressed and characterized in tobacco protoplasts. *ArGGT* is structurally and functionally related to acid plant  $\alpha$ Gals of the glycosylhydrolase (GH) family 27 and the C-terminal extension share a vacuolar sorting determinant targeting it to the vacuole (Tapernoux-Lüthi et al., 2007). Transcript levels, enzyme activities and long-chain RFOs increased during cold treatment suggesting an important role of GGT in long-chain RFO accumulation (Inan Haab and Keller, 2002; Tapernoux-Lüthi et al., 2004). Using excised common bugle leaves grown in the warm, it was further shown that the RFO concentration correlates positively with frost tolerance clearly suggesting a protective role for RFOs in this type of abiotic stress (Peters and Keller, 2009).

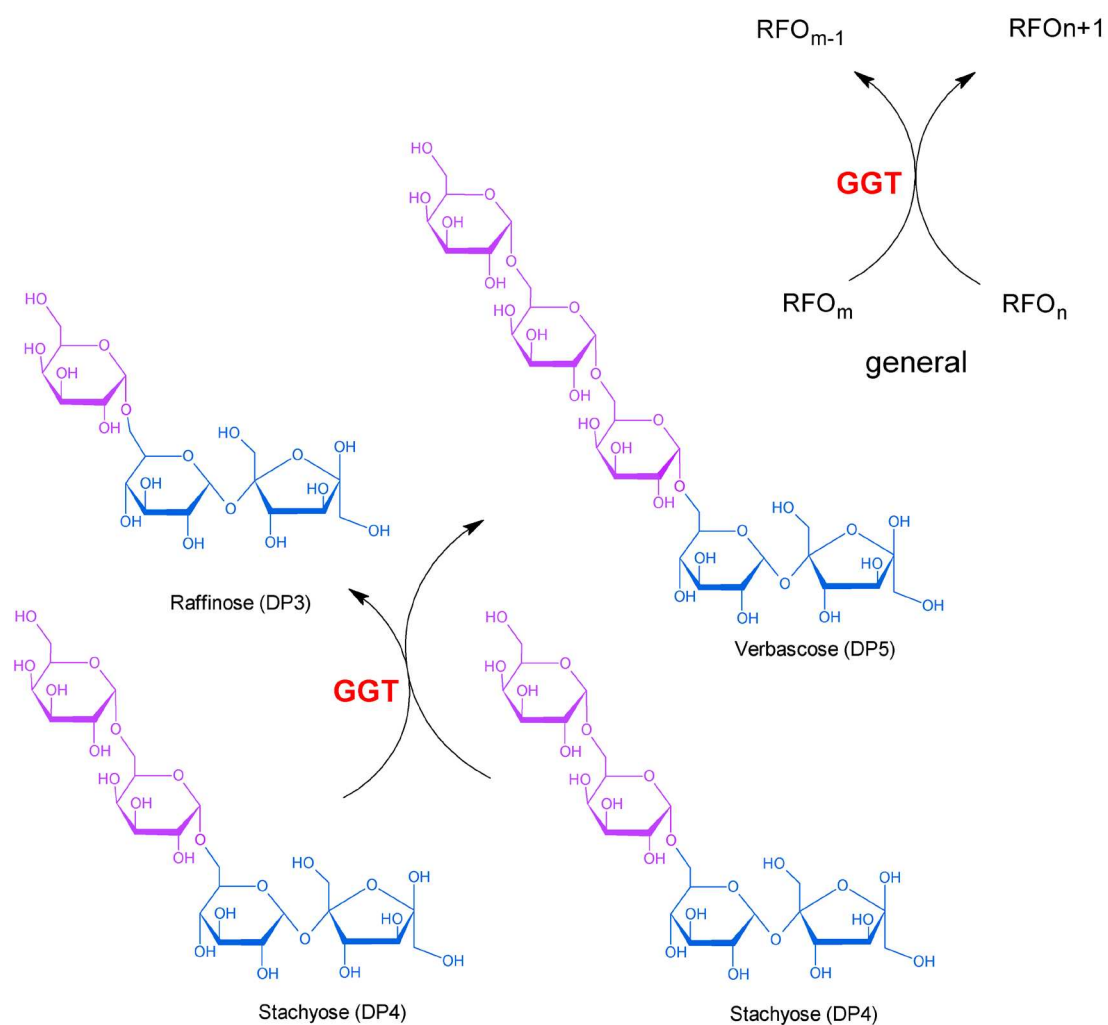


**Fig.3.** High DP RFO biosynthesis catalyzed by galactan:galactan galactosyltransferase (GGT) that transfers a Gal moiety from an RFO to another. Gal molecules are represented in purple and Suc molecules in blue.

## 1.2 RFO catabolism

RFO catabolism occurs at different times and in different location in plants. For instance, RFOs are (i) catabolized early during seed imbibition to allow proper germination. (ii) After the relief of a stress, RFO that had accumulated during abiotic stress events are rapidly catabolized to provide metabolizable energy and carbon skeletons. (iii) RFOs may also be catabolized during phloem unloading. A good example of RFO catabolism in phloem unloading is melon where Raf and Sta (together with Suc) are the primary translocated sugars in the phloem. The very low concentrations of Raf and Sta and high concentration of Suc in fruits suggest that RFOs unloaded from phloem are rapidly catabolized (Mitchell et al., 1992; Chrost and Schmitz, 1997; Carmi et al., 2003; Dai et al., 2006).

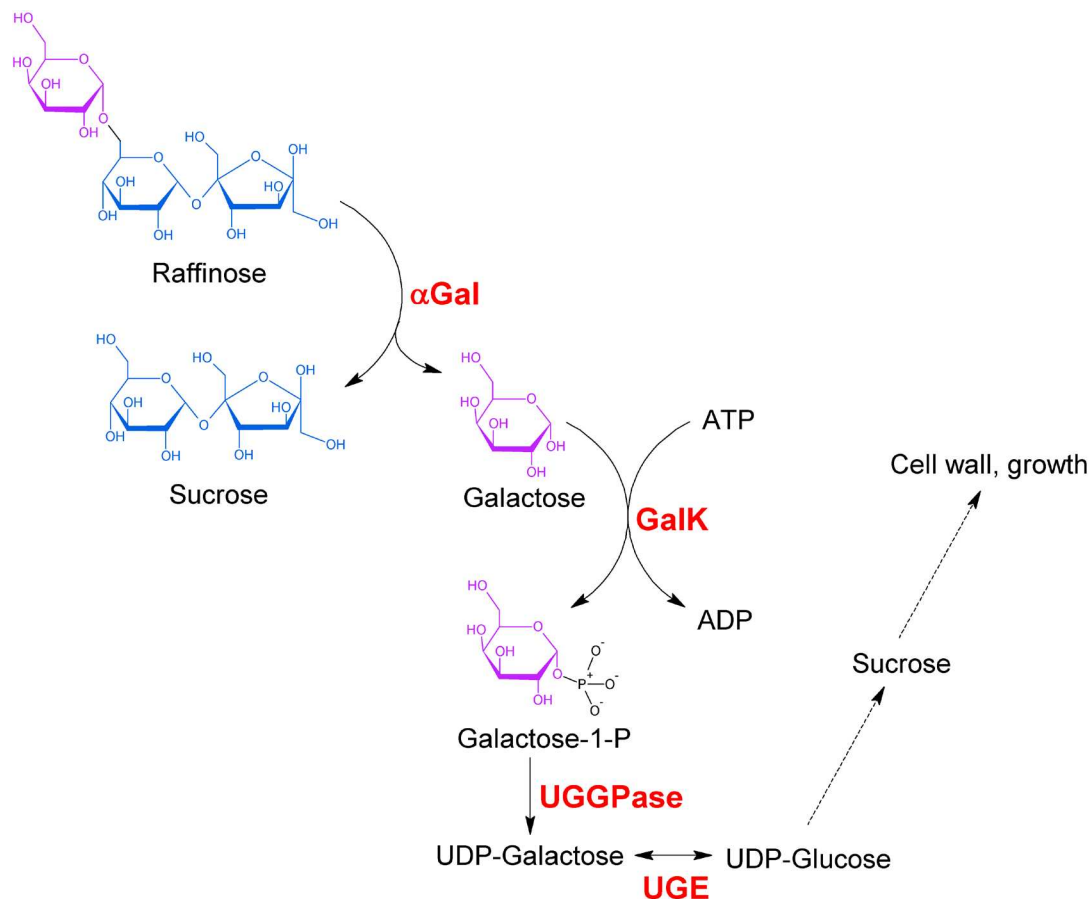


**Fig.4.** Schematic representation of RFO catabolism. The first step is catalyzed by an  $\alpha$ Gal that converts Raf or higher DP RFOs into Suc (or lower DP RFOs) and free Gal. Gal salvage pathway starts with GALK that converts Gal to Galactose-1-P (Gal1P). The continuation of the Gal salvage pathway involves the conversion of Gal1P to UDP-Gal by an UDP Glc/Gal Pyrophosphorylase followed by the epimerization of UDP-Gal to UDP-Glc by an UDP-Glc/UDP-Gal 4-epimerase. Gal, galactose;  $\alpha$ Gal,  $\alpha$ -galactosidase; GALK, galactokinase; UGGPase, UDP Glc/Gal Pyrophosphorylase; UGE, UDP-Glc/UDP-Gal 4-epimerase.



RFO catabolism starts with the hydrolytic action of  $\alpha$ Gal ( $\alpha$ -D-galactoside galactosylhydrolase; EC 3.2.1.22; Dey and Pridham, 1972; Porter et al., 1990) that removes the terminal galactosyl moieties from the RFOs to generate lower DP RFOs (or finally Suc) and free Gal (**Fig.4**). Because free Gal is toxic in living cells (Ordin and Bonner, 1957; Roberts et al., 1971) Gal is usually quickly converted to useful metabolites in the so-called “Gal salvage pathway” (**Fig.4**). Depending on the metabolic activities in a given tissue, carbon may flow to respiratory pathways or to the synthesis of starch, Suc, oligosaccharides, polysaccharides or other cellular components such as glycolipids and glycoproteins.

### 1.2.1 RFO degradation starts with the hydrolytic action of $\alpha$ -D-galactosidases ( $\alpha$ Gals)

$\alpha$ Gals mainly catalyze the hydrolysis of terminal  $\alpha$ -D-galactosyl units from galacto-oligosaccharides, polysaccharides and galactolipids. They are often described as hydrolases, but some of them also show transgalactosylation activity (Hashimoto et al., 1995; Zhao et al., 2008; Nakai et al., 2010). They are widely distributed in bacteria, fungi, plants and animals (Keller and Pharr, 1996; Fernandez-Leiro et al., 2010; Guce et al., 2010; Kulik et al., 2010). In humans, mutations of the  *$\alpha$ GalA* gene cause incomplete degradation of neutral glycosphingolipids, resulting in Fabry disease, an inherited, life-threatening, disorder (Calhoun et al., 1985). Different strategies involving recombinant  $\alpha$ Gals, are being developed for the treatment of this disease (Blom et al., 2003). A further applied use of recombinant  $\alpha$ Gals in humans is their use in the conversion between ABO blood groups that are determined by variations in polysaccharide structures present on the surface of red blood cells. Some  $\alpha$ Gals are able to remove the  $\alpha$ -linked terminal Gal that differs between O antigen (universal blood) and B antigen, and processes involving plant  $\alpha$ Gals are being developed to obtain O-type blood from B-type donors (Zhang et al., 2007). Further,  $\alpha$ Gals are extensively used for industrial applications, such as improving the quality and yield of Suc in the sugar beet industry by achieving efficient Raf and other galacto-oligosaccharide hydrolysis (Suzuki et al., 1969), reducing the content of nondigestible oligosaccharides in legume-derived food (Thanankul et al., 1976) and modifying the gelling properties of guar gum (*Cyamopsis tetragonoloba*) by hydrolysis of polymeric galactomannans to improve textures (food, textile, paper, cosmetics, pharmaceutical products) (Bulpin et al., 1990).

Plant  $\alpha$ Gals from numerous sources have been studied and multiple forms of the enzyme have been described (Barham et al., 1971; Dey and del Campillo, 1984; Keller and Pharr, 1996). They may be classified according to their pH optimum and substrate specificity (Dey and del Campillo, 1984; Keller and Pharr, 1996) as well as their amino acid sequence similarity (Cantarel et al., 2009). Acid  $\alpha$ Gals belong to the glycoside hydrolase (GH) family 27 (**Fig.6**). In seeds they are used to mobilize  $\alpha$ -D-Gal

residues stored within RFOs and other storage oligo- and polysaccharides mainly during germination of seeds, such as those of fenugreek (Dey and Pridham, 1972), *Trifolium repens* (white clover; Williams et al., 1978), tomato (Feurtado et al., 2001), soybean (Guimaraes et al., 2001), coffee (Marraccini et al., 2005). In leaves, acid  $\alpha$ Gals have been shown to play an important role for leaf development in cell wall loosening during cell growth (Chrost et al., 2007). During fruit ripening acid  $\alpha$ Gals hydrolyze cell wall components which leads to the softening of fruit tissues of, for instance, olive, grape berries and papaya (Heredia et al., 1993; Nunan et al., 2001; Soh et al., 2006). Finally, acid  $\alpha$ Gals have also been described to occur in leaves (common bugle; Bachmann et al., 1994) and tubers (Japanese artichoke; Ueno et al., 1980; Keller and Matile, 1985) which store large amounts of RFOs and use acid  $\alpha$ Gals to mobilize RFOs.

Alkaline  $\alpha$ Gals belong to the GH36 family. The first alkaline  $\alpha$ Gal was discovered in *Cucurbita melo* leaves (squash; Gaudreault and Webb, 1982, 1983; Gaudreault and Webb, 1986; Carmi et al., 2003). Later, a similar alkaline  $\alpha$ Gal was described in sink leaves of RFO-translocating common bugle plants (Bachmann et al., 1994) and more recently, two alkaline  $\alpha$ Gals were characterized in *Cucumis melo* (melon) fruit, CmAGA1 and CmAGA2, which differed in their substrate specificity towards the natural substrates, Raf and Sta, respectively (Gao and Schaffer, 1999; Carmi et al., 2003). Alkaline activity, and not acid activity, correlates temporally with the developmental leaf sink-to-source transition (Pharr and Sox, 1984; Gaudreault and Webb, 1986; Bachmann et al., 1994; Irving et al., 1997; Carmi et al., 2003). Spatially, only the alkaline activity correlates with Sta levels along the cucumber pedicel (Pharr and Hubbard, 1994). Therefore, the alkaline  $\alpha$ Gals play an important role in phloem unloading and catabolism of imported RFOs in sink tissues.

On theoretical grounds, the importance of  $\alpha$ Gals in abiotic stress is indicated, but has only received very little attention in research. In *Tetragonia tetragonides* (New Zealand spinach), an alkaline  $\alpha$ Gal was identified as a drought stress-responsive gene. It was suggested to be involved in galactosyl-saccharide degradation for enhancing carbohydrate utilization under abiotic stress (Hara et al., 2008). In petunia, the downregulation of an acid  $\alpha$ Gal enhanced freezing tolerance at the whole-plant level in non-acclimated and cold-acclimated plants, whereas overexpression of the  $\alpha$ Gal gene caused a decrease in endogenous Raf and impaired freezing tolerance (Pennycooke et al., 2003). This suggests that  $\alpha$ Gals play an important regulatory role during abiotic stress and, in particular, after the relief of the stress to permit rapid RFO utilization.

$\alpha$ Gals are known to cleave various galactosyl substrates. Indeed, an alkaline  $\alpha$ Gal isolated from rice was shown to degrade galactolipids, in addition to galacto-oligosaccharides, during natural leaf

senescence, dark-induced senescence, hormone treatments (methyl jasmonic acid and salicylic acid) and abiotic stresses ( $\text{H}_2\text{O}_2$  and wounding). This particular alkaline  $\alpha$ Gal (Osh69; GenBank Accession no. AF251068) is exclusively localized in senescing chloroplasts, strongly suggesting a further physiological role of alkaline  $\alpha$ Gals in chloroplast degradation during leaf senescence (Lee et al., 2004; Lee et al., 2009). Chloroplasts are the first organelles subjected to degradation during leaf senescence, and breakdown of chlorophyll takes place when thylakoid membranes are disrupted. Thylakoid membranes are the most abundant membrane system in biology and may account for up to 90% of all membranes in a green leaf (Gray, 1996). Galactolipid monogalactosyl and digalactosyl diacylglycerol (MGDG and DGDG, **Fig.5**) represent almost 70% of thylakoid and envelope membrane lipids of chloroplasts (Joyard et al., 1996). They play important roles in the assembly of photosynthetic membrane proteins. For example, in the DGDG-deficient mutant, *dgdg1*, light harvesting chlorophyll a/b-binding protein (LHCII) loses the ability to form trimers (Dörmann et al., 1995). Osh69 was shown to preferentially degrade chloroplast galactolipids during leaf senescence (Lee et al., 2004; Lee et al., 2009). Arabidopsis RFO metabolism might also play a role in dark-adapted and senescent leaves. Raf is known to be transported to the chloroplast (Schneider and Keller, 2009) and dark-induced genes (*DIN*) have been identified (Fujiki et al., 2000; Fujiki et al., 2001). One of them (*AtDIN10*) could be a good candidate for an alkaline  $\alpha$ Gal function during leaf senescence. In the chapter III of this thesis I will be presenting a preliminary biochemical characterization of AtDIN10 with the aim to test whether it could be a potential galactolipid degrading enzyme.

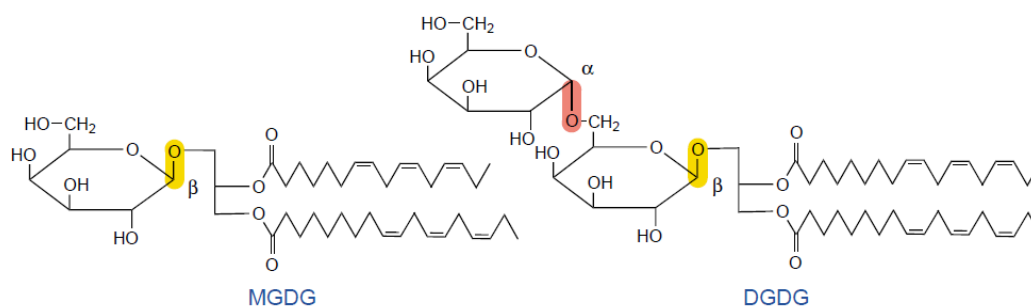


**Fig.5.** Structure of the two major galactolipid types present in chloroplast thylakoids. DGDG: digalactosyl diacylglycerol. MGDG: monogalactosyl diacylglycerol. The conformation of the anomeric carbon atom is indicated in red ( $\alpha$ ) or yellow ( $\beta$ ) (Dörmann and Benning, 2002).

Alkaline  $\alpha$ Gals also play important roles during seed germination of *Zea mays* (maize), barley and pea (Carmi et al., 2003; Zhao et al., 2006; Blöchl et al., 2008). In maize, one of three putative alkaline  $\alpha$ Gals (*ZmAGA1*) was expressed in seeds and callus tissues; transcripts increased when seed germination was interrupted by heat, cold or dehydration stresses. The acidic  $\alpha$ Gal activity and sub-cellular localization did not correlate with Raf depletion, suggesting that alkaline  $\alpha$ Gals may be responsible for RFO hydrolysis in germinating maize seeds (Zhao et al., 2006). Contrary to maize, both acid and alkaline  $\alpha$ Gals have been shown to be important (sequentially) in the mobilization of

seed RFO reserves in pea. Based on these data, a proposed model suggested that acid  $\alpha$ Gals localized in the vacuoles are not active in dry seeds due to the high pH and low water content (about 7%) in this compartment. However, during imbibition, protein storage vacuoles are acidified by proton pumps and merge to re-build the central vacuole, restoring acidic  $\alpha$ Gals activity to rapidly mobilize RFOs. Suc and Gal, in addition to starch, being the main energy sources for seed metabolism, may still be reutilized to form RFOs under unfavorable conditions. At later stages of germination, alkaline  $\alpha$ Gals degrade RFOs in the cytosol in addition to the acidic enzyme in the vacuoles (Blöchl et al., 2008).

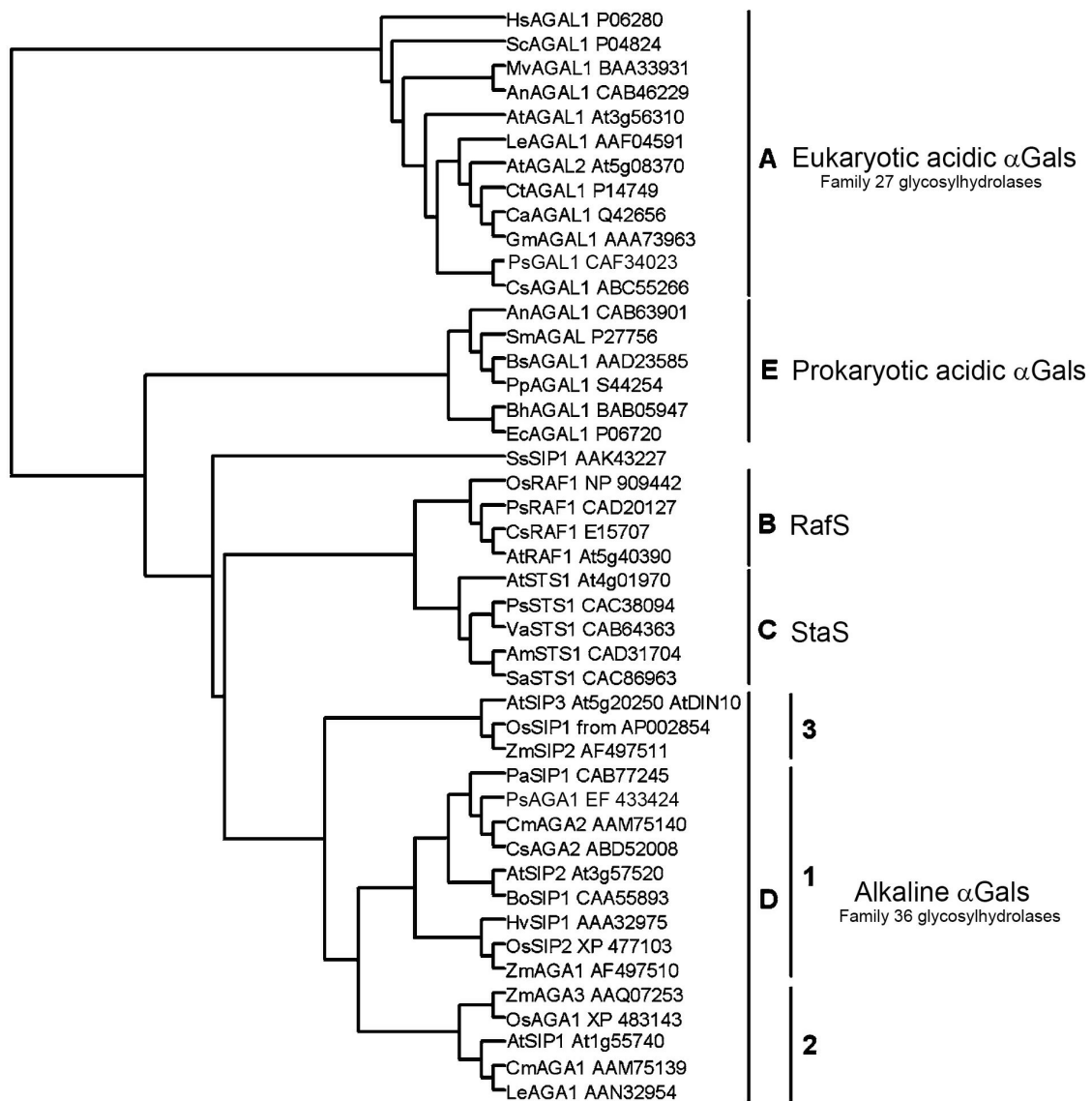


**Fig.6.** Phylogenetic tree based on sequence alignment between acid  $\alpha$ Gals (AGAL), RafS (RAF), StaS (STS), and alkaline  $\alpha$ Gals/seed imbibition proteins (AGA/SIP). Clade A includes eukaryotic  $\alpha$ Gals (Family 27; Henrissat and Davis, 2000; Carmi et al., 2003; Zhao et al., 2006), clade B represents RafS, clade C represents StaS, clade D represents alkaline  $\alpha$ Gals/seed imbibition proteins, and clade E represents prokaryotic  $\alpha$ Gals (Family 36; Henrissat and Davis, 2000). The AGA/SIP clade D was sub-divided into three sub-clades (Zhao et al., 2006). Consensus branch lengths in the phylogram are proportional to the number of inferred amino acid changes (Adapted from Blöchl et al., 2008).

In Arabidopsis, little is known about  $\alpha$ Gals. An acid  $\alpha$ Gal (ATAGAL2; At5g08370) was shown to play an important role in leaf development by functioning in cell wall loosening and cell wall expansion (Chrost et al., 2007). Interestingly, no alkaline  $\alpha$ Gal has been characterized so far. Sequence alignments identified a group of seed imbibition proteins (SIPs) as alkaline  $\alpha$ Gals (Fig.6; Carmi et al., 2003). SIPs were initially reported in germinating barley seed embryos (Heck et al., 1991) and homologs were discovered in tomato (SIP1, AF512549, Carmi et al., 2003), in maize seeds (ZmAGA1 and ZmAGA3; Zhao et al., 2006) and in pea seeds (PsAGA1; Blöchl et al., 2008). In Arabidopsis, SIPs (ATSIP1, At1g55740, ATSIP2, At3g57520 and ATSIP3 or AtDIN10, At5g20250) were identified as putative RafSs with O-glycosyl hydrolase activities and were suggested to function accordingly in both biosynthesis and degradation of Raf (Anderson and Kohorn, 2001; Nishizawa et al., 2008; Maruyama et al., 2009). In the Chapters II and III of this thesis, the functional identification and characterization of these three ambiguously annotated ATSIPs enzymes will be presented.

### **1.2.2 Galactokinase (GALK) phosphorylates free Gal produced by the degradation of Gal-containing compounds**

Galactokinase (GALK; EC 2.7.1.6) is a cytosolic enzyme with a wide occurrence across the taxonomic kingdoms ranging from bacteria to mammals and plants. It catalyzes the MgATP-dependent phosphorylation of  $\alpha$ -D-Gal at the C1 position to  $\alpha$ -D-Gal1P and is, therefore, distinctly different from hexokinases, which phosphorylate hexoses at the C6 position (Granot, 2008). Gal1P may then be further metabolized to Glc1P and UDP-Glc either by (i) the Leloir pathway (mainly found in non-plant organisms), involving a Gal1P uridylyltransferase (UT; EC 2.7.7.12) and a UDP-Glc/UDPGal 4-epimerase (UGE; EC 5.1.3.2; Leloir, 1951; Frey, 1996; Holden et al., 2003) or by (ii) the pyrophosphorylase pathway (mainly found in plants), involving the novel UDP-Gal/UDP-Glc pyrophosphorylase and UGE (Dai et al., 2006; Dai et al., 2011; Kleczkowski et al., 2011).

Gal1P was first isolated by Kosterlitz (1943) from rabbit liver that had been fed with Gal. GALK activity has been widely studied from yeast (Caputto et al., 1948; Wilkinson, 1949; Timson and Reece, 2002; Stagoj and Komel, 2008), *E. coli* (Schümperli et al., 1982), *Mus musculus* (mouse; Ai et al., 1995), plants (Neufeld et al., 1960; Foglietti and Percheron, 1974; Dey et al., 1980; Yang et al., 2009), and humans (Timson and Reece, 2003).

In plant seeds, Gal-rich oligosaccharides and cell wall polymers form an important reserve and are mobilized during early germination by the action of  $\alpha$ Gals (Pridham et al., 1969; Foglietti and

Percheron, 1976), however free Gal is generally not detectable at any stage of seed germination (Dey et al., 1980), except during the germination of isolated endosperms of *Trigonella foenum-graecum* seeds (fenugreek; Reid, 1971). It was thus suggested that the cotyledons were the site of Gal metabolism and the presence of an efficient GALK that converts free Gal into Gal1P in seeds could explain this phenomenon. Later, Gaudreault and Webb (1986) detected twice as much GALK activity in immature squash leaves than in mature ones and suggested that immature leaf tissues have a high potential for hydrolyzing RFOs and for incorporating free Gal into the hexose phosphate pool.

Although the presence of GALK can be predicted in all plant storage organs which contain  $\alpha$ -D-galactosyl-substituted carbohydrate reserves, the enzyme has only been purified from seeds, namely, of *Phaseolus aureus* (mung bean; 158-fold; Chan and Hassid, 1975), of fenugreek (400-fold; Foglietti and Percheron, 1976) and of broad bean (1300-fold; Dey, 1983). The biochemical characterization of GALK in broad beans showed that the enzyme is composed of two identical 30 kDa subunits, exhibits a pH optimum of 7.3 and an apparent  $K_m$  of 0.5mM for Gal and 1.5mM for ATP, respectively. This activity was inhibited by Gal at a concentration between 2-10mM (Dey, 1983).

Arabidopsis GALK (*AtGALK*, At3g06580) was fortuitously identified *via* the ability of the cDNA to functionally rescue the growth deficiency of a yeast GALK mutant ( $\Delta gal1$ , Kaplan et al., 1997). It was shown that *AtGALK* is a single copy gene and is expressed in all major organs of the plant. *AtGALK* transcripts were also detected in whole young seedlings 2.5 days after imbibition, a stage which coincides with cotyledon expansion, radicle elongation and the development of root hairs, confirming the previous hypothesis that cotyledons are a major location for GALK activity (Kaplan et al., 1997). Further evidence for the identity of *AtGALK* was reported by expression of the cDNA in an *E. coli* GALK mutant deficient in GALK activity (Sherson et al., 1999). In that study, GALK activity was measured in mutants heterologously expressing *AtGALK*. More recently, *AtGALK* was comprehensively biochemically characterized after expression of the cDNA in *E. coli* (Yang et al., 2009). *AtGALK* has a total molecular weight of 50kDa, a pH optimum similar to broad bean GALK, an apparent  $K_m$  of 0.7mM for Gal and 0.7mM for ATP, respectively, and requires  $Mg^{2+}$  for optimum activity. To date this remains the only GALK reported from Arabidopsis.

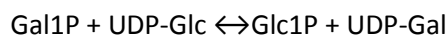
### 1.2.3. Free Gal is toxic

Gal toxicity in living cells is well established and wide spread ranging from bacteria (Zeng et al., 2010) to humans, where it causes the inherited metabolic disorder, galactosemia (Fridovich-Keil, 2006). In

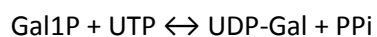
plants, a number of early reports have documented deleterious physiological effects in the presence of excess Gal, for instance, (i) the inhibition of root or shoot growth (Ordin and Bonner, 1957; Ferguson et al., 1958; Roberts et al., 1971; Yamamoto et al., 1988; Seifert et al., 2004; Rösti et al., 2007), (ii) inhibition of auxin biosynthesis and translocation (Anker, 1974; Krul and Colclasure, 1977), and (iii) induction of leaf senescence (Morre, 1968). Free Gal is known to be toxic for the cell even at low concentration (1mM external concentration; Ordin and Bonner, 1957; Roberts et al., 1971). Moreover, it also interferes with normal carbohydrate metabolism (Göring and Reckin, 1968). The exact mechanism of Gal toxicity in plants is largely unknown. It is thought to occur as a consequence of the buildup of Gal1P which in turn inhibits phosphoglucomutase (catalyzing  $\text{Glc1P} \leftrightarrow \text{Glc6P}$ ). Although this hypothesis argues for a direct role of GALK in Gal toxicity, other mechanisms of toxicity are also proposed to exist (Dey, 1985). Regardless of the actual mechanism of toxicity it is clear that plants must be able to exercise tight control over the levels of Gal and its phosphorylated derivatives, especially during growth when the plant needs to build up cellulose and other Glc-based compounds. If plant GALKs play a similar role than yeast GALKs in signaling (Johnston, 1987), the presence of Gal to the transcriptional machinery may be the key component of this mechanism. In chapter IV of this thesis I will be describing the characterization of an *atgalk* mutant line that accumulates Gal and exhibits an unexpected Gal insensitivity.

#### 1.2.4 The Gal salvage pathway continues

To keep the intracellular Gal pool low,  $\alpha$ Gals are strongly inhibited by free Gal, and Gal is efficiently phosphorylated by GALK to form Gal1P, indicating an efficient continuation of free Gal metabolism. Following phosphorylation, two alternative pathways exist for the fate of the Gal1P in plants leading to the production of glucose-1-phosphate (Glc1P) or UDP-Glc, the Leloir pathway involving a uridylyltransferase (UT) and the pyrophosphorylase (PPase) pathway, respectively (Keller and Pharr, 1996). The Leloir pathway is catalyzed by an uridylyltransferase (UT; Wong et al., 1977) utilizing UDP-Glc in the transferase reaction:

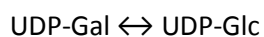


The UT pathway is considered to be of central importance to the metabolism of Gal in mammals, yeast and bacteria but has also been demonstrated to occur to a much lesser extent in plants (Feingold and Avigad, 1980). The only reports of its occurrence are in soybean seeds where UT showed significant activity in embryonic axis of germinating seeds (Main et al., 1983). An additional way of integrating Gal1P into metabolism is via a UDP-Gal/Glc PPase (UGGPase, EC. 2.7.7.10) utilizing UTP:



This pathway is apparently more widespread in plants (Wong et al., 1977). UGGPase can utilise both Gal1P and Glc1P as substrates. There is no reported UGGPase specific for Gal. In addition to this dual PPase, there exists other PPases specific for Glc (Smart and Pharr, 1981; Gao et al., 1999; Kleczkowski et al., 2011). UGGPase activity has been reported to be present in extracts from *Saccharum officinarum* (sugar cane; Maretzki and Thom, 1978), cucumber (Smart and Pharr, 1981), soybean (Main et al., 1983), squash (Gaudreault and Webb, 1986) and tomato (Kim et al., 1991). UGGPase activity increased in immature tissues of squash and coincided with increased GALK activity (Gaudreault and Webb, 1986). The co-localization of the two enzymes suggests that UGGPase could be the main pathway of Gal metabolism following the GALK phosphorylation in squash.  $\alpha$ Gals, GALK and PPase activities was also detected in cucumber peduncles consistent with the predicted Sta degradation location (Smart and Pharr, 1981; Gross and Pharr, 1982). The UGGPase from melon fruit was cloned and characterized and the results indicated that the flux of Gal in the fruit of the RFO-translocating cucurbits from Gal1P to Glc1P is carried out by this enzyme and not by UT (Dai et al., 2006).

The UDP-Gal product is further metabolized to UDP-Glc via an epimerase reaction carried out by a UDP-Glc/UDP-Gal 4-epimerase (UGE, EC 5.1.3.2, Dey, 1984; Holden et al., 2003):



This enzyme was discovered by Leloir (1951) from Gal-adapted *Saccharomyces fragilis*, and has been isolated from a number of microbial, plant and animal sources (Feingold and Avigad, 1980; Dey, 1984). UGE freely interconverts UDP-Glc and UDP-Gal (Barber et al., 2006). *UGE* genes have been characterized in various plants; the Arabidopsis genome contains five genes predicted to encode *UGE* (Barber et al., 2006), rice contains four putative *UGE* genes, and three cDNA clones putatively encoding *UGE* isoforms were isolated from *Hordeum vulgare* (barley; Zhang et al., 2006a). In Arabidopsis, expression levels and experiments with *UGE1* antisense lines both suggest that *UGE1* might be the dominant isoform in green plants (Dormann and Benning, 1998). *UGE1* to *UGE5* show *in vitro* variations in substrate affinity, cofactor requirement, metabolite inhibition profile and appear to have adapted to different metabolic roles *in vivo* (Barber et al., 2006). *UGE2* and *UGE4* together play a major role in vegetative growth and cell wall carbohydrate biosynthesis (Rösti et al., 2007). *UGE2* and *UGE3* cooperate in pollen development, and *UGE1* and *UGE5* contribute nonspecifically to *UGE* activity and growth under unstressed conditions but might be more specifically involved in



stress situations (Rösti et al., 2007). One possible explanation of the apparent biochemical redundancy of UGE and other nucleotide sugar interconversion enzymes in plants is the abundance and complexity of plant carbohydrates, in particular their developmental heterogeneity. The differential expression of kinetically diverse isoforms of nucleotide sugar metabolic enzymes might reflect the ability of each cell to adjust the activity of glycosyltransferases in response to external stresses. Kinetically diverse isoforms might be better adapted to different physiological intracellular environments in different cell types and organs (Barber et al., 2006).

The UDP-Glc generated from these reactions can be directly utilized for numerous sugar metabolism reactions, particularly cell wall synthesis (Kleczkowski, 1994). Alternatively, and in the case of the Suc-accumulating melon fruit, UDP-Glc is converted to Glc1P for the continuation of hexose metabolism leading to the synthesis of Suc, the major stored sugar of *Cucurbita melo* (melon; Dai et al., 2006).

## 1.3 RFOs play a role in abiotic stress tolerance

### 1.3.1 Plants are frequently exposed to abiotic stress

Abiotic stress arises from an excess or a deficit in the physical or chemical environment of a plant. Environmental stresses are very diverse; they may be caused by high and low temperature, water deficit, high salinity, strong wind, oxygen excess or deprivation, heavy metals, wounding, nutrient deprivation or excessive light (Jones et al., 1989; Lichtenthaler, 1998; Mahajan and Tuteja, 2005). Various abiotic stresses result in both general and specific effects on plant growth and development. For example, water-deficit limits plant growth due to photosynthetic decline, osmotic stress-imposed constraints on plant processes and interference with nutrient availability as the soil dries (Schulze, 1986; Chaves, 1991). Salinity interferes with plant growth as it leads to physiological drought and ion toxicity (Zhu, 2001). Chilling (temperatures below optimal but above freezing) and freezing temperatures can also cause osmotic stress in addition to their direct effect on metabolism (Thomashow, 1999). Therefore, osmotic stress and the associated oxidative stress appear to be common consequences of exposure to drought, salinity and low temperature. Tolerance or susceptibility to these abiotic stresses is a very complex phenomenon, in part, because (i) stress may occur at multiple stages of plant development and (ii) often more than one stress type affects the plant simultaneously. Perception of stress cues and relay of the signals to switch on adaptive responses are the key steps leading to plant stress tolerance (**Fig.7**). At the transcriptional level, regulation of specific gene expression by *cis*-acting elements (*e.g.* CRT/DRE, ABRE elements) and transcription factors (*e.g.* CBF/DREB1 in cold stress, AREB/ABF in osmotic stress) are important to determine cross talk in stress signaling pathways (Yamaguchi-Shinozaki and Shinozaki, 2006).

Plants employ three major strategies to cope with abiotic stress, *i.e.* stress escape, stress avoidance, and stress tolerance. The plants that escape stress conditions never experience environmental stress by completing their life cycle during a period of adequate conditions, for example annual plants or ephemeral plants in deserts that form dormant seeds before the onset of the dry season. Another way to survive stress conditions is the stress avoidance that involves preventing the plant being exposed to stress and reducing the impact of stress when it is present. Avoidance is also achieved by specialized morphological adaptations, for example, the development of specialized leaf surfaces to decrease the rate of transpiration, the reduction of leaf area, sunken stomata or the increase in root length and density to use water more efficiently. In fact, desert plants, like mesquite trees, may avoid water stress by expanding roots into the water table; cacti have succulent photosynthetic stems and leaves reduced to thorns to avoid water stress. More impressive are the true desiccation tolerant

plants, for example resurrection plants, that display the rare phenomenon of being completely tolerant to vegetative desiccation, effectively remaining in metabolic stasis in the air-dried state (0% relative humidity) and resuming normal cellular metabolism within a short period after water has become available again (for reviews see Gaff, 1989; Farrant, 2000; Scott, 2000; Vitré et al., 2004).

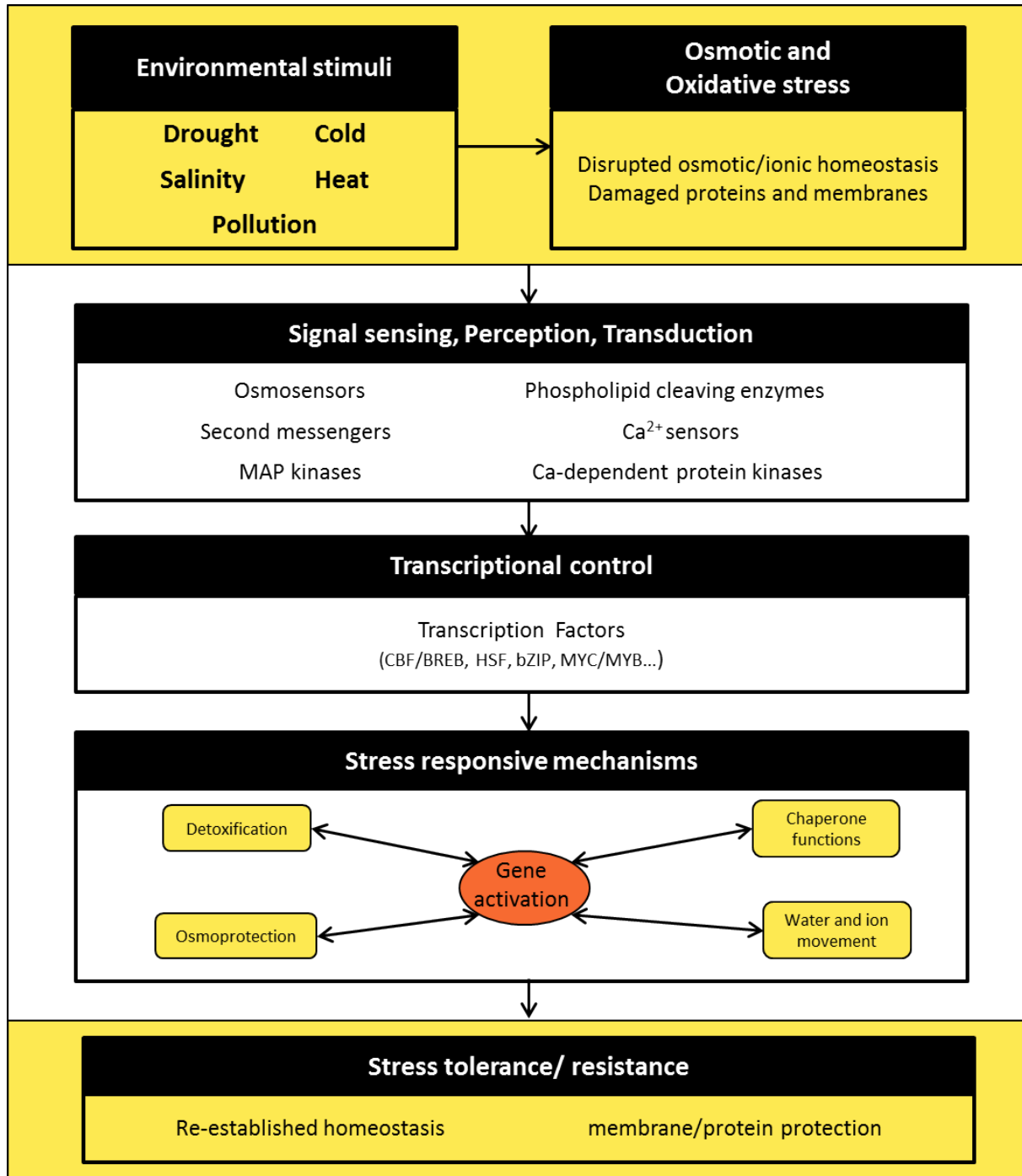


**Fig.7.** Plant responses to abiotic stress. Primary stresses are often interconnected and cause cellular damage and secondary stresses such as osmotic and oxidative stresses. The initial stress signals trigger the downstream signaling process and transcription controls which activate stress-responsive mechanisms. Inadequate response at one or several steps in the signaling and gene activation may ultimately result in irreversible changes leading to cell death. Adapted from Wang et al. (2003b) and Jewell et al. (2010).

### 1.3.2 RFOs accumulate during abiotic stress and may act as osmoprotectants

Many plants accumulate compatible solutes, or osmolytes, in response to cellular dehydration caused by cold temperature, drought, salt, heat or oxidative stress. These compounds are termed compatible solutes because even at high concentrations in the cytoplasm they do not interfere with normal metabolism (Rhodes et al., 2004). These non-toxic molecules tend to be neutrally charged at physiological pH, present low molecular masses and protect and stabilize cellular structures by interacting with membranes, protein complexes or enzymes (Yancey et al., 1982; Bohnert et al., 1995). Two theoretical models have been proposed to explain the physicochemical basis of this protective effect (**Fig.8**; Hoekstra et al., 2001).

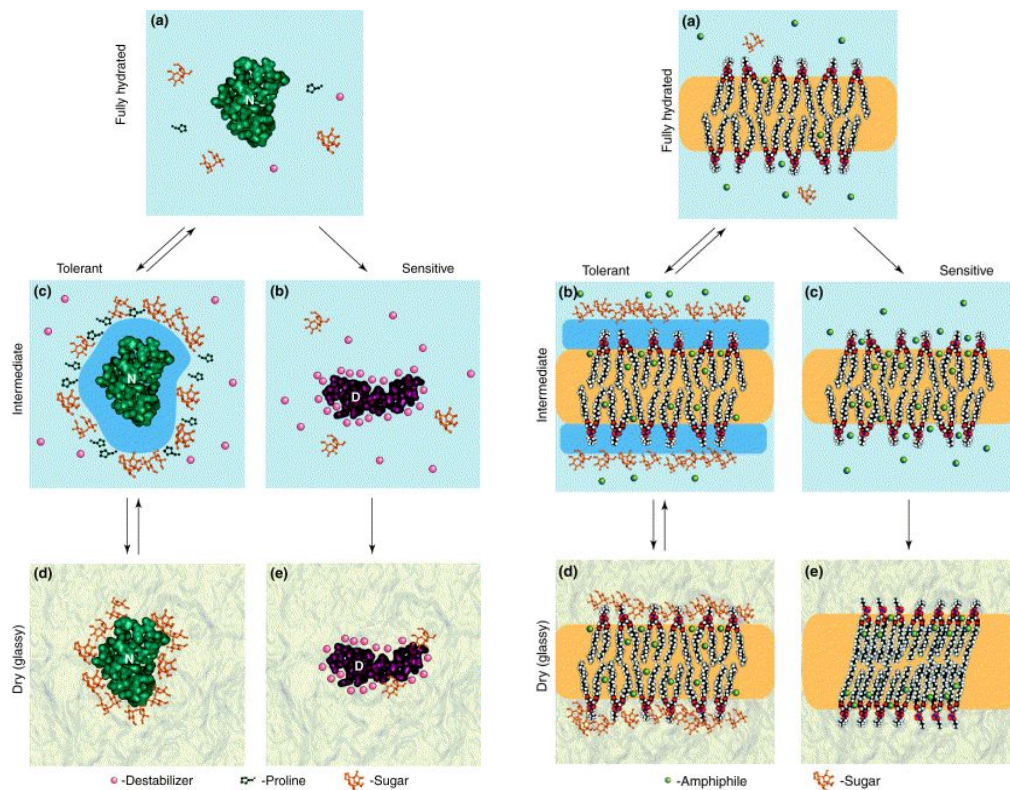


**Fig.8.** Mechanisms of protein structure stabilization and membrane behavior at different stages of water loss. 1. (a) Native form of a thermodynamically stable protein. During water loss the amount of cytoplasmic solutes increase and might interact with the protein. (b) The lack of compatible solute in sensitive plants causes preferential interactions leading to protein unfolding. (c) In tolerant plants, preferential exclusion from the protein surface (blue band) maintains native conformation and hydration of the proteins. (d) Compatible solutes, especially sugars stabilize proteins in the dried state. (e) In dried sensitive cells, the previously unfolded proteins are fixed and can't be reversed. 2. (a) Membrane lipids in hydrated state. (b) The presence of compatible solutes in tolerant cells keeps the membrane surface hydrated (blue band) and prevents membrane fusion. (c-e) In sensitive cells, the absence of compatible solutes leads to packing of the phospholipid molecules and membrane fusion. (d) In tolerant cells, compatible solutes replace water and maintain the spacing between phospholipids molecules (Hoekstra et al., 2001).

In the case of the “preferential exclusion model”, molecules that tend to decrease the solubility of proteins by being excluded from the hydration sphere of protein are stabilizing them (Timasheff, 1992; Hoekstra et al., 2001). This creates a situation where native protein structures are thermodynamically favored because their surface is still surrounded by a water shell and destabilizing solutes would only interact with the water phase in the cytosol. In contrast, according to the “preferential interaction model”, the solutes that can enter the hydration sphere and interact directly with protein surfaces are causing protein unfolding (Yancey, 1994). Both models may, in fact, play functional roles under osmotic stress (Fig.8). The structure of different solutes could accommodate hydrophobic, Van-der-Waals and electrostatic interactions (Shinozaki and Yamaguchi-Shinozaki, 1999).

Chemically, osmoprotectants are generally grouped into three classes (Fig.9): (i) betaines (fully *N*-methylated amino acid derivatives) and related compounds such as 3-dimethylsulfoniopropionate (DMSP) and choline-*O*-sulfate, (ii) certain amino acids like proline, and (iii) polyols (mannitol, sorbitol, Gol, *D*-ononitol, *D*-pinitol etc.) and non-reducing sugars such as the disaccharides (Suc and trehalose) and the oligosaccharides (fructans and RFOs).

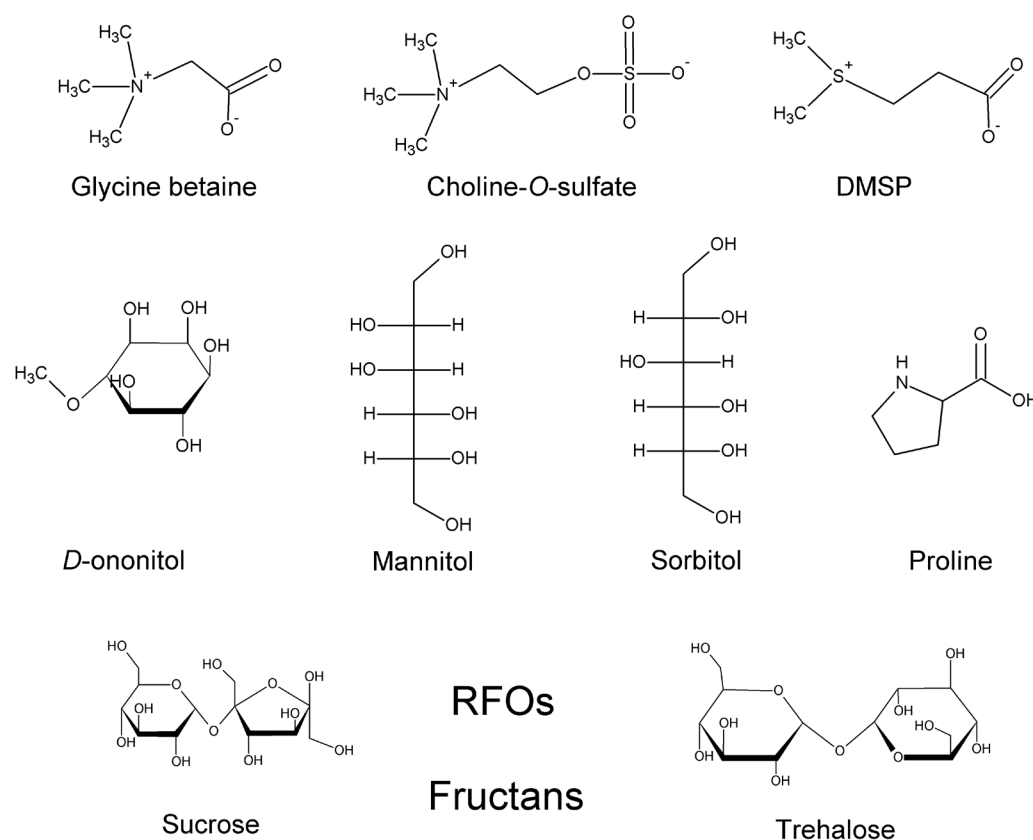


**Fig.9.** Structure of representative osmoprotectants found in plants. DMSP, 3-dimethylsulfoniopropionate.

Proline (Hare et al., 1998; Verbruggen and Hermans, 2008), glycine-betaine (Chen and Murata, 2008) and mannitol (Tarczynski et al., 1993) occur commonly in plants, while DMSP, choline-*O*-sulfate (Rhodes, 1993), *D*-ononitol (Sheveleva et al., 1997), and trehalose (Penna, 2003) occur rarely (Rontein et al., 2002). In the case of mannitol accumulation, it appears that the mode of action of this osmoprotectant may not be only in cytoplasmic osmotic adjustment. It may play a more significant role as a hydroxyl radical scavenger in the chloroplast (Shen et al., 1997). During water loss, RFOs and other carbohydrates are able to keep the surface of proteins and lipid bilayers hydrated by water replacement (Crowe et al., 1992; Hoekstra et al., 2001; Valluru and Van den Ende, 2008). In seedlings of *Vicia villosa* (winter vetch), for example, osmotic stress induced by polyethylene glycol (PEG) solution induced the activity of crucial enzymes of the RFO biosynthetic pathway, *i.e.* GolS and RafS, in both the root and epicotyl. The root and epicotyl transiently accumulated elevated amounts of Gol and Raf and when the PEG solution was replaced by water, Gol and Raf were degraded, thus suggesting their involvement in the response of tissues to osmotic stress (Lahuta, 2010).

External addition or molecular genetic engineering of osmoprotectants has shown a positive correlation between elevated concentrations and improved stress tolerance in yeast (Takagi, 2006) and plants (Tarczynski et al., 1993; Sheveleva et al., 1997; McNeil et al., 1999; Huang et al., 2000; Rathinasabapathi, 2000; Penna, 2003; Chen and Murata, 2008). In some cases, however, the absolute osmolyte concentration reached by genetic modulation of one compatible solute accumulation is unlikely to mediate osmotic adjustment in response to stress (Hare et al., 1998; Serraj and Sinclair, 2002). Genetic modulations of osmoprotectants also have their limitations: (i) The introduction of a foreign gene conferring synthesis of a solute may substantially disturb normal metabolism and growth. (ii) The engineered gene may often be embedded in a rigid metabolic network that resists change and resists solute accumulation. (iii) The accumulation of one single compatible solute is not enough to perform an osmotic adjustment in response to stress (for review see Serraj and Sinclair, 2002; Rhodes et al., 2004). (iv) A combination of many different gene activations or molecule accumulation is needed to acquire stress tolerance (Zuther et al., 2004; Bhatnagar-Mathur et al., 2008).

### **1.3.3 Cold stress involves molecular regulation and induces RFOs accumulation**

Each plant has its unique set of temperature requirements, which are optimal for its proper growth and development. Importantly, what is optimal for one plant may be stressful for another. Cold stress includes low chilling and freezing. Chilling results primarily in the *loss-of-function* of

biomembranes connected with a decrease of their fluidity and an inactivation or at least deceleration of the membrane-bound ion pumps (Sakai and Larcher, 1987). Light energy which is absorbed independently of the temperature produces oxidative stress, if metabolism cannot keep pace with the energizing of the photosynthetic membranes (Beck et al., 2004). The main cause of freeze-induced injury to plants is ice formation rather than low temperature. Ice formation in plants begins in the apoplastic space as it has relatively low solute concentration. As the vapor pressure of ice is much lower than that of water at any given temperature, ice formation in the apoplast establishes a vapor pressure gradient between the apoplast and surrounding cells. The unfrozen cytoplasmic water migrates down the gradient from the cell cytosol to the apoplast, which contributes to the enlargement of existing ice crystals and causes a mechanical strain on the cell wall and plasma membrane leading to cell rupture (Olien and Smith, 1977). Whether and to what extent a plant becomes damaged by exposure to low temperature depends on many factors, such as its developmental stage, the duration and severity of frost, the rates of cooling (and rewarming) and whether ice formation takes place intracellularly or extracellularly.

Frost hardiness or sensitivity is a quality of each individual plant and tissue and is governed by its genetic potential as well as by environmental factors and, therefore, usually changes with time. Cold resistance involves many genes and traits such as fluidity of the biomembranes, synthesis and accumulation of high and low molecular weight osmoprotectants, increase the potential to cope with oxidative and dehydration stresses (Nanjo et al., 1999). It becomes even more complex because the various tissues of a plant are differentially frost resistant, whereby juvenile/meristematic tissues are generally more frost sensitive than mature tissues (Sakai and Larcher, 1987). A recent study on metabolic profiling proposed that combinations of metabolites can be predictive of leaf freezing tolerance and of heterosis in freezing tolerance (Korn et al., 2010).

In nature, plants may exhibit cold tolerance due to gradual exposure to low non-freezing temperatures, a process known as cold acclimation (Thomashow, 1999). The accumulation of water-soluble carbohydrates (including RFOs) typically occurring during cold acclimation also seems likely to contribute to the stabilization of membranes as these molecules can protect membranes against freeze-induced damage *in vitro*. Increases in concentrations of soluble sugars are very rapid responses of *Arabidopsis* to low temperature occurring as rapidly as 2h after exposure to 1°C (Wanner and Junttila, 1999). At low concentrations, Suc serves as a substrate for low temperature-induced metabolic alterations, while at higher concentrations, it has a direct cryoprotective effect on cellular membranes (Uemura and Steponkus, 2003). The presence of high Raf concentrations during abiotic stress is also well-established (Taji et al., 2002; Pennycooke et al., 2003). However, Raf was

recently demonstrated to be neither necessary nor sufficient for improved freezing tolerance in *Arabidopsis* (Zuther et al., 2004). In a follow up study, Raf was shown to occur in the chloroplasts of cold-acclimated *Arabidopsis* and demonstrated to be effective in stabilizing, protecting the photosynthetic apparatus of cold acclimated leaves against damage during freezing (Knaupp et al., 2011).

Cold acclimation is accomplished by the expression of many cold-regulated genes (Thomashow, 2001; Zhu, 2001). In *Arabidopsis*, these genes are called *RD* (responsive to dehydration), *ERD* (early responsive to dehydration), *LTI* (low-temperature induced), *KIN* (cold induced) and *COR* (cold regulated). These genes are also induced by dehydration (directly by water deficit or indirectly by high salt) and ABA, and can be collectively called cold-responsive genes. Cold-responsive genes are regulated via transcription factors binding sites in their promoter region (e.g. C repeat/dehydration-responsive elements (*CRT/DRE*) and abscisic acid (ABA)-responsive elements). Corresponding transcription factors that function in osmotic- and cold-stress-responsive gene expression [e.g. C-repeated binding factors/dehydration-responsive element binding proteins (CBFs/DREBs) and basic leucine zippers (bZIPs), respectively]] are binding specifically to the above mentioned *cis*-elements (Yamaguchi-Shinozaki and Shinozaki, 2006). It has been reported that the expression of key regulators of abiotic stress responses such as CBF3, COR15A and RD29A were induced by both Glc and ABA. Constitutive expression of CBF3 in transgenic *Arabidopsis* plants induces expression of target *COR* genes to enhance freezing tolerance in non-acclimated plants. Expression of *COR15A* and *RD29A* is regulated by CBF3, suggesting that glucose may contribute to the regulation of cold stress tolerance (Uddin et al., 2008; Wang et al., 2008). *GoS* transcripts are also induced during cold stress in parallel to RFO increase in leaves of *Arabidopsis* and *A. reptans* (Liu et al., 1998; Sprenger and Keller, 2000). In *Arabidopsis*, the *AtGoS3* promoter contains two *DRE* and two *DRE-like* core motifs and is a target gene of DREB1A and increased Raf concentrations in transgenic *35S:DREB1A* is correlated with increase expression of *AtGoS3* (Taji et al., 2002). Recently, metabolomics studies showed that *AtGoS3* transcripts also increased in the transgenic *35S:DREB2A-CA* plants, but Gol and Raf levels did not increase compared with *35S:DREB1A* lines, suggesting that (i) dynamic changes in gene expression may be necessary for plants to accumulate these metabolites and (ii) strong freezing stress tolerance of the *35S:DREB1A* lines may depend on the accumulation of these metabolites (Maruyama et al., 2009).



#### 1.3.4 Water deficit and salt stress may induce RFO accumulation

Plants are often subjected to periods of soil and atmospheric water deficits during their life cycle as well as, in many areas of the globe, to high soil salinity. Both water deficit and high salinity manifest at the cellular level as physiological dehydration. Salinity reduces the ability of plants to take up water, and this quickly causes reductions in growth rate, along with a series of metabolic changes, e.g. osmotic adjustment, identical to those caused by water stress. However, under prolonged salt stress, plants respond additionally to dehydration to hyper-ionic and hyper-osmotic stress. Salt will eventually rise to toxic levels in the older transpiring leaves, causing premature senescence, and reduce the photosynthetic leaf area of the plant to a level that cannot sustain growth (Munns, 2002). The effects of drought and salinity on photosynthesis range from the restriction on CO<sub>2</sub> diffusion into the chloroplast, *via* limitations on stomatal opening mediated by shoot- and root-generated hormones, and on the mesophyll transport of CO<sub>2</sub>, to alterations in leaf photochemistry and carbon metabolism (Chaves et al., 2009). Salt-tolerant plants differ from salt-sensitive ones in having a low rate of Na<sup>+</sup> and Cl<sup>-</sup> transport to leaves and the ability to sequester these ions into vacuoles to prevent their build-up in cytoplasm or cell walls and thus avoid salt toxicity (Munns, 2002). Mechanisms for salt tolerance are, therefore, of two main types, firstly those minimizing the entry of salt into the plant, and secondly, those minimizing the entry of salt into the cytoplasm. The mechanisms of water-deficit response have been investigated most extensively in *Arabidopsis* and other plants including crops and resurrection plants (Ingram and Bartels, 1996; Bray, 1997; Shinozaki and Yamaguchi-Shinozaki, 1997; Chaves et al., 2003; Yamaguchi-Shinozaki and Shinozaki, 2006). The drought stress signal is mediated via both ABA-dependent and ABA-independent pathways to regulate expression of various genes involved in drought stress tolerance and response. These gene products are thought to function in the accumulation of osmoprotectants, detoxification protection of cells, protein turnover, stress-signaling pathways, transcriptional regulation etc. (Bohnert et al., 1995; Ingram and Bartels, 1996; Bray, 1997; Shinozaki and Yamaguchi-Shinozaki, 1997, 1999; Zhu, 2002).

RFOs, such as Raf and Sta, accumulate in seeds during seed development and are thought to play some role in desiccation tolerance of seeds. In soybean seeds, RFOs accumulate at the late stage of maturation and desiccation (Castillo et al., 1990). In maize, Raf accumulates in seed embryos during drying and is thought to function in stress tolerance, whereas Suc accumulates independently of desiccation tolerance. Desiccation tolerance of seeds is not achieved in the absence of Raf accumulation (Brenac et al., 1997). These results suggest that the Suc-to-RFO ratio is critical for seed desiccation tolerance, rather than the total amount of sugars. Although young, excised soybean seeds are not tolerant to desiccation, slow-induced dehydration confers them desiccation tolerance,

which is strongly correlated with a significant increase in Sta content (Blackman et al., 1992). In general, under salt and drought stress, soluble carbohydrate concentrations tend to increase, while starch concentrations decrease (Chaves, 1991). Under very severe dehydration stress, soluble carbohydrates may decrease (Pinheiro et al., 2001). Soluble carbohydrates will modify gene expression and proteomic patterns, namely those governing photosynthetic metabolism. It is accepted that transcripts for genes involved in photosynthesis and other source activities (e.g. photoassimilate export and nutrient mobilization) are repressed under high sugar content, whereas those involved in sink activities, like degradation of carbohydrates and the synthesis of storage polysaccharides, lipids and proteins are induced (Stitt et al., 2007).

### 1.3.5 Other abiotic stress and RFO accumulation

Heat stress is often defined as the rise in temperature beyond a threshold level for a period of time sufficient to cause irreversible damage to plant growth and development. Although limited details are available, anatomical changes under high ambient temperatures are generally similar to those under drought stress. In wild-type *Arabidopsis* plants, it was shown that *AtGolS1* is transcriptionally regulated by HSF2 (heat shock transcription factor) and its expression levels showed a strong correlation with the Gol and Raf concentrations in the leaves (Panikulangara et al., 2004). Another putative heat shock factor, *HsfA2*, is a key regulator in the induction of the defense mechanism under several types of environmental stress (Nishizawa et al., 2006). In *HsfA2*-overexpressing transgenic *Arabidopsis* plants, the transcription of *AtGolS1*, *AtGolS2* and *AtGolS4* was highly induced in leaves compared to the wild-type plants. This higher expression correlated positively with higher Gol and Raf concentrations (Nishizawa et al., 2008). However, down-regulation of *AtGolS1* or *AtGolS2* had no effect on the Raf levels or the total GolS activities under heat stress. This suggests that the suppression of the different *GolS* genes may be compensated by the other *GolS* genes (Panikulangara et al., 2004; Nishizawa et al., 2008).

Oxidative stress is often induced by other stresses that give rise to excess concentrations of reactive oxygen species (ROS) at the cellular level. Therefore, antioxidants and antioxidant enzymes such as ascorbate (AsA), glutathione (GSH), superoxide dismutase, AsA peroxidase, GSH peroxidase, thioredoxin peroxidase and catalase function to interrupt the cascades of uncontrolled oxidation in some organelles (Nishizawa-Yokoi et al., 2008). Recently, Nishizawa *et al.* (2008) demonstrated that RFOs might also play a role to protect plants from oxidative damages. In fact, the expression of most of the *Arabidopsis GolS* and *RafS* genes was induced under oxidative stress caused by environmental changes, resulting in increased leaf Raf and Gol concentrations. Plants overexpressing *GolS1* or *GolS2*

resulted in an oxidative stress-tolerant phenotype with enhanced Gol and Raf levels both under control and oxidative stress conditions. The increase in Gol and Raf concentration had no effect on the levels of Glc, fructose (Fru) and Suc, suggesting that the oxidative stress-tolerant phenotype of these transgenic plants is due to the increases in Gol and Raf (Nishizawa et al., 2006; Nishizawa et al., 2008). These findings indicate that Gol and Raf act not only as osmoprotectants, but also as antioxidants in the leaves of *Arabidopsis* plants.

## 1.4 RFOs play a role in carbon partitioning and storage

### 1.4.1 Transport RFOs move in the phloem from source to sink

Assimilation of carbon and nutrient resources and subsequent distribution throughout the plant are closely linked events. The phloem is a central component of the plant's complex vascular system that plays a vital role in moving photoassimilates from sites of primary production, *e.g.* photosynthesizing leaves (sources; net exporters) to the region of resource utilization (sinks; net importers) of a plant. Recently, studies have shown that the phloem also plays a key role in moving informational signals that coordinates many facets of plant growth and development (for review see Turgeon and Wolf, 2009; Ainsworth and Bush, 2011). The export of carbohydrates from source leaves provides the substrates for growth and maintenance of sink tissues, and the phloem is its delivery system. High concentrations of carbohydrates, mainly Suc, but also Raf, Sta and/or sugar alcohols (for review see Turgeon and Ayre, 2005; Turgeon and Wolf, 2009; Ainsworth and Bush, 2011), raise the turgor pressure in the phloem of source tissues. This finally results in hydrostatic pressure-driven mass flow of carbohydrates to the sieve elements of sink tissues, where the turgor pressure is lower and the translocated carbohydrates are unloaded and further metabolized. Three different strategies for loading carbohydrates into the phloem have been described (Fig.10; Rennie and Turgeon, 2009; Slewinski and Braun, 2010). The most common one is through the apoplast, where photoassimilates are loaded into the phloem by specific transporters (for review see Lalonde et al., 2003; Sauer, 2007). The two other loading mechanisms are symplastic, driven by a downhill concentration gradient from the mesophyll to the minor veins. The first symplastic loading mechanism, especially found in woody plants, occurs via a process driven by diffusion alone (passive) (Reidel et al., 2009; Rennie and Turgeon, 2009). The second symplastic mechanism can be found in plants with specialized companion cells (intermediary cells, ICs) which are linked to bundle sheath cells by extremely high numbers of asymmetrically branched plasmodesmata. This symplastic transport mechanism appears to be found in RFO-transporting plants (*e.g.* in Cucurbitaceae and Lamiaceae) suggesting that the synthesis of these sugars is an integral part of the phloem-loading mechanism (Turgeon et al., 1993; Turgeon and Medville, 2004). According to the polymer trap model, Suc diffuses from the mesophyll to the IC symplastically, where it is used for the *in situ* Raf and Sta synthesis. Within the IC, Raf and Sta are physically trapped and concentrated because they are larger than the exclusion limit of the plasmodesmata facing the mesophyll and, therefore, cannot diffuse back into the mesophyll (Turgeon, 1996). The polymer trap hypothesis is supported by recent evidence that loading is insensitive to down-regulation of the Suc transporter (Zhang and Turgeon, 2009), but highly sensitive

to down-regulation of Raf and Sta synthesis via the suppression of a *Go/S* gene (McCaskill and Turgeon, 2007). Conversely, overexpression of a *Go/S* gene in apoplastic loading species that do not naturally transport RFOs in the phloem leads to Gol and Raf transport (Hannah et al., 2006). The presence of IC (and accordingly symplastic loading) does not exclude the possibility of apoplastic phloem loading since some species have more than one type of sieve element/companion cell complex types, resulting in so called mixed loading (Voitsekhovskaja et al., 2009). The presence of Suc in the phloem of some RFO transporting species and the absence of Gol transport, despite its high concentration in ICs, were highlighted as aspects of the polymer trap hypothesis that are not fully understood (Turgeon, 1996). Recently, it was proposed that small molecules in the companion cells enter the sieve elements indiscriminately but that differential retention and retrieval mechanisms are responsible for differences in the efficiency of their transport (Ayre et al., 2003).

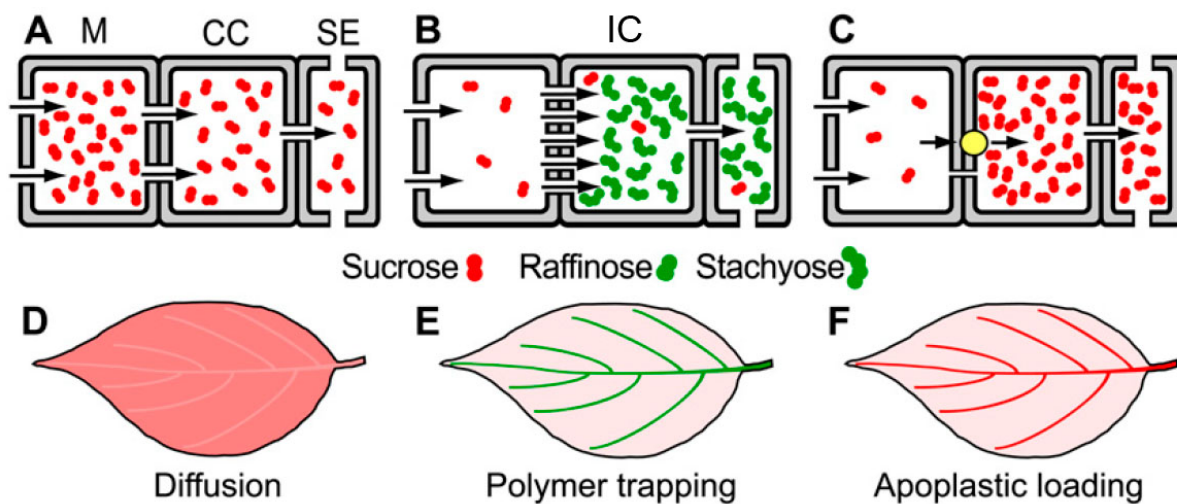


**Fig.10.** Schematic representation of different phloem loading strategies. A,D. Symplastic phloem loading utilizes abundant plasmodesmata, allowing thermodynamically favorable diffusion of sugars down a concentration gradient from the photosynthetic cells into the phloem. B,E. In the polymer trapping model of phloem loading, RFOs are synthesized in the intermediary cells. This decreases the Suc concentration and establishes a Suc gradient to drive phloem transport. C,F. Apoplastic phloem loading requires transporters (yellow circle) to actively retrieve and concentrate Suc from the apoplast into phloem cells. M, mesophyll cell; CC, companion cell; SE, sieve element cell; IC, intermediary cell. Arrows indicate the directional flow of sugar through cells. Adapted from Rennie and Turgeon, 2009; Slewinski and Braun, 2010; Turgeon, 2010.

The final phase of carbohydrate translocation from source to sink is the removal of the translocates from the phloem and their delivery to recipient sink cells, a process called phloem unloading. Within sink cells, cellular metabolism and compartmentation are the key-events. Irrespective of sink function, a portion of imported carbohydrates is respired to provide energy for maintenance of cell function and structure. In growing organs, imported photoassimilates become substrates for the synthesis of new cell material either directly or indirectly, after biochemical transformations. In storage organs, they may be (i) stored in the large central vacuole either directly or indirectly, (ii) in

plastids (as starch), or (iii) in the cell wall (as different polysaccharides). The mechanisms of phloem unloading have been much less studied and are only poorly understood compared to those of phloem loading. Like phloem loading, the unloading mechanisms may be symplastic or apoplastic. The unloading type is species- and organs-specific and even depends on the developmental stage. Symplastic unloading seems to be most common, predominating in developing leaves, roots, tubers and meristems. Apoplastic unloading, occurs in developed seeds and fruits (Patrick, 1997). In Japanese artichoke tubers, there is evidence that phloem-imported Sta is unloaded symplastically and subsequently accumulated in the vacuoles of the storage parenchyma by a concentration step involving an active proton-Sta antiporter situated on the tonoplast (Keller, 1992; Greutert and Keller, 1993). Conversely, RFOs (Raf and Sta) arriving at the growing melon fruit are rapidly catabolized to Suc. In melon young fruits, transcriptional analysis showed that imported Raf and Sta are hydrolyzed primarily by acidic  $\alpha$ Gals, whereas in older fruits, they are initially hydrolyzed by alkaline  $\alpha$ Gals (Dai et al., 2011). Interestingly, a developmental switch from symplastic to apoplastic unloading or *vice versa* has also been described, *e.g.* for grape berries and potato tubers, respectively (Viola et al., 2001; Zhang et al., 2006b).

In *Arabidopsis* seedling roots, phloem transport processes were studied by real-time imaging with the fluorescent probe, carboxyfluorescein. It was shown that symplastic transport following unloading was confined to the elongation zone of the root (Oparka et al., 1994). More recently, the phloem unloading and post-phloem transport was also studied in developing *Arabidopsis* flowers, as important sink tissues. Using phloem-mobile fluorescent tracers, it was shown that phloem unloading into cells of ovule primordial followed a symplastic pathway. Subsequently, the same tracers could not move out of phloem cells into mature ovules anymore suggesting a further change in the mode of phloem unloading. In open flowers as well as in outgrowing siliques, the phloem was again unloaded via the symplast. The results indicated that symplast connectivity is highly regulated and varies not only between different sink tissues but also between different developmental stages (Werner et al., 2011). In chapter II of this thesis I will report on experiments conducted to study the possible role of alkaline  $\alpha$ Gals (ATSIP1 and -2) in RFOs unloaded in *Arabidopsis* sink tissues.

#### **1.4.2 Storage RFOs accumulate in the vacuole and can be easily mobilized**

Storage carbohydrates are generally defined to occur at more than 1% of the dry weight (DW) of a given tissue (Drew, 1984). In plants, RFOs can accumulate up to 80 % of the DW of a tissue, for example in Japanese artichoke tubers (Keller and Matile, 1985), but occur more commonly in a range of 25 to 50% of the dry weight (Keller and Pharr, 1996). RFOs have been found to be stored in

numerous plant organs such as photosynthesizing leaves (*e.g.* common bugle; Bachmann et al., 1994), roots (*e.g.* common bugle; Bachmann et al., 1994), stems (*e.g.* *Cornus sericea* L.; Ashworth et al., 1993), tubers (*e.g.* Japanese artichoke; Keller and Matile, 1985) and seeds (pea; Peterbauer and Richter, 2001), where they fulfill their short - or long-term storage functions, *i.e.* temporary (reversible, *e.g.* in tubers) or permanent (irreversible, *e.g.*, in fruits). In mature cells, imported carbohydrates enter physical (*e.g.* vacuoles) and chemical (*e.g.* starch) storage pools.

Plant seeds are entirely dependent on their stored reserves for germination. They contain a wide range of storage compounds, among which carbohydrates occupy a special position. The most prominent soluble sugars are Suc and RFOs, the latter being almost ubiquitous in plant seeds (Peterbauer and Richter, 2001). It is known that RFOs rapidly disappear after imbibition and their degradation is often completed before polymeric carbohydrates are mobilized, indicating that they may play a special role during early germination (Blöchl et al., 2007). Seeds have a high demand for energy during early germination. Neither polymeric carbohydrates nor proteins or lipids are able to meet this demand, as their degradation is slow (several days) rather fast (hours; Bewley and Black, 1994). RFOs may, therefore, be an essential source of rapidly metabolizable carbon for early germination events (Downie and Bewley, 2000). Inhibition of the hydrolytic enzyme,  $\alpha$ Gal, during germination leads to delayed germination in pea and winter vetch *in vivo* (Blöchl et al., 2007; Lahuta and Goszczynska, 2009). In soybean, however, Sta or Raf are not necessary for efficient germination (Dierking and Bilyeu, 2009). Further RFO accumulation coincides in seeds of many species, with the development of desiccation tolerance during maturation (Obendorf, 1997) and RFO content correlates positively with seed longevity (Horbowicz and Obendorf, 1994). In chapter II of this thesis, I will report on experiments conducted to test if RFO storage pools contained in dry Arabidopsis seeds are mobilized by  $\alpha$ Gals during imbibition and early germination.

## 1.5 Aims of my thesis

The general aim of this thesis was to study RFO catabolism in *Arabidopsis thaliana*. To this end, I aimed at the cloning, functional identification and biochemical characterization of genes/enzymes involved in the two first steps of RFO catabolism and defining their putative *in vivo* functions.

In this thesis, I report on:

- (i) The cloning, functional identification and biochemical characterization of the two putative *Arabidopsis* alkaline  $\alpha$ Gals, ATSIP1 and ATSIP2, by heterologous expression in *Sf9* insect cells. They both revealed to be *bona fide* alkaline  $\alpha$ Gals with distinct substrate specificities. I tested their putative roles during cold-stress and water-deficit relief, phloem unloading and seed germination.
- (ii) The cloning, functional identification and partial biochemical characterization of *AtDIN10* by heterologous expression in *Sf9* insect cells which confirmed that *AtDIN10* is also an alkaline  $\alpha$ Gal. A transient expression of an *AtDIN10-GFP* fusion located the protein in the stroma part of the chloroplast.
- (iii) The cloning, functional identification and biochemical characterization of *AtGALK* by heterologous expression in *Sf9* insect cells and the characterization of an *atgalk* T-DNA *loss-of-function* mutant line that hyper-accumulates Gal in its vacuoles and displays insensitivity to exogenous Gal. I created a constitutive *AtGALK* overexpression line in the *atgalk* background that restored leaf Gal concentrations to those of leaves from wild-type plants. The unexpected chemotype indicated a possible new Gal detoxification pathway that targets Gal to vacuoles.





## **Chapter II:**

**Functional identification of the Arabidopsis alkaline  $\alpha$ -galactosidases, ATSIP1 (At1g55740) and ATSIP2 (At3g57520)**



## 2.1 Introduction

The *Arabidopsis* genes, *ATSIP1* (At1g55740) and *ATSIP2* (At3g57520), exhibit controversial annotations and functions. They have been annotated as putative RafSs or seed imbibition proteins (SIPs) with *O*-glycosyl hydrolase (mainly  $\alpha$ Gal) activity and suggested to function accordingly in both the biosynthetic and hydrolytic directions of Raf metabolism, especially under certain abiotic stress conditions (drought, high salinity, high temperature; Nishizawa et al., 2008; Maruyama et al., 2009; Wu et al., 2009).

Interestingly, *ATSIP1* shares amino acid similarities of 72% to *CmAGA1* while *ATSIP2* shares 78% to *CmAGA2*, both functionally identified as alkaline  $\alpha$ Gals from melon fruit with distinct substrate specificities for Raf and Sta, respectively (Gao and Schaffer, 1999; Carmi et al., 2003). *ATSIP1* and *ATSIP2* share 59% amino acid similarity to each other. Numerous higher plant  $\alpha$ Gals have been identified and described from a variety of species (for reviews see Dey and del Campillo, 1984; Keller and Pharr, 1996; Peterbauer and Richter, 2001). Most studies have dealt with acidic isoforms, which appear to play important roles in seed development and germination as well as in sprouting of Sta-containing tubers (see reviews cited above). Alkaline  $\alpha$ Gals, however, have been mostly associated with sink activities, hydrolyzing phloem-translocated Raf and Sta in sink leaves and developing fruits (Gaudreault and Webb, 1986; Bachmann et al., 1994; Carmi et al., 2003) as well as with thylakoid galactolipid breakdown during leaf senescence (Lee et al., 2009). It was also shown that they play a role during seed germination in maize, barley and pea (Carmi et al., 2003; Zhao et al., 2006; Blöchl et al., 2008). In pea seeds, it was proposed that alkaline  $\alpha$ Gals mobilizes RFO reserves in the cytosol sequentially with acid  $\alpha$ Gals located in the vacuole (Blöchl et al., 2008). Another possible role of acid and alkaline  $\alpha$ Gals that has not received much attention is the degradation of stressed-induced RFOs during and after abiotic stress relief. Indeed, recent studies proposed a role of alkaline  $\alpha$ Gals during drought stress in New Zealand spinach (Hara et al., 2008) and of acid  $\alpha$ Gals during low temperature deacclimation in petunia (Pennycooke et al., 2004).

The cloning and functional expression of two cDNAs from melon fruit (*CmAGA1* and -2) showed that they displayed distinct  $\alpha$ Gal activity at alkaline pH. Most importantly, these genes showed highest homology to *SIP* genes, suggesting that SIPs are likely to represent alkaline  $\alpha$ Gals in plants and revealing a hitherto unknown sub-family of glycosyl hydrolases (Carmi et al., 2003). On the basis of sequence homology, *SIP* genes have been identified in at least five other plant families including Poacea (barley, *SIP*: M77475), Fabaceae (*Cicer arietum*, *SIP*: X95875), Solanaceae (tomato, *SIP*:

TC94379), Vitaceae (grape, SIP1: EU543561), and Brassicaceae (Arabidopsis, SIPs: AAC83062, CAB66109).

In this chapter, I describe the functional identification and the biochemical characterization of ATSIP1 and ATSIP2 (i) to determine if they encode RafSs and/or alkaline  $\alpha$ Gals and (ii) to identify possible physiological functions *in vivo*. I will be presenting clear evidence that both *ATSIP1* and *ATSIP2* encode alkaline  $\alpha$ Gals and not RafSs or VerSs as proposed in recent papers (Anderson and Kohorn, 2001; Nishizawa et al., 2008). ATSIP2 has a distinct substrate specificity for Raf and shows promoter activity restricted to sink tissues, suggesting that it is involved sink metabolism, most probably in the unloading of phloem-mobile Raf. ATSIP1, however, has distinct substrate specificities for Sta and Gol and a function in seed germination is postulated, because (i) Sta is present in seeds but not in vegetative tissues of Arabidopsis and (ii) alkaline  $\alpha$ Gal activity was absent or very low in crude extracts of Arabidopsis leaves when Sta and Gol were used as substrates.

This work was initiated by Dr. Shaun Peters who performed the cloning and the optimization of ATSIP2 expression of in *Sf9* insect cells. Parts of the results presented here on ATSIP2 were published last year (Peters et al., 2010).

## 2.2 Materials and Methods

### 2.2.1 Plant material and growth conditions

*Arabidopsis* Col-0 ecotype seeds were surface sterilized by soaking them in 1ml seed sterilization solution [70% EtOH, 0.1% (v/v) Tween] for 15min and then in 1ml 100% EtOH for another 15min. Following stratification (48h, 4°C), the seeds were propagated on soil (Einheitserde, type ED73, Gebr. Patzer GmbH & Co. KG, Schopfheim, Germany) pretreated with a *Steinernema feltiae* (0.6g l<sup>-1</sup>) solution (Traunem Andermatt Biocontrole AG, Grossdietwil, Switzerland) to prevent inoculation of the soil with black fly larvae. Plants were grown in a controlled environment chamber [8h light, 120μmol photons m<sup>-2</sup> s<sup>-1</sup>, 22°C, 16h dark, 60% relative humidity (RH)].

### 2.2.2 Screening for T-DNA insertion lines

Two independent T-DNA insertion lines for ATSIP1 (SALK\_090247 and SAIL\_87\_E04) and ATSIP2 (SALK\_038166, SALK\_113663) were identified by genomic DNA extractions (Edwards et al., 1991) followed by PCRs using two different primer pairs: a fragment of the wild-type (WT) allele of At1g55740 was amplified with the primers *SALK\_090247<sub>LP</sub>* and *SALK\_090247<sub>RP</sub>* or with the primers *SAIL\_87\_E04<sub>LP</sub>* and *SAIL\_87\_E04<sub>RP</sub>*. The mutant alleles were traced with the *SALK\_090247<sub>RP</sub>* and the T-DNA-3' primer *Lbb1.3* for the mutant line SALK\_090247 and with the *SAIL\_87\_E04<sub>RP</sub>* and the T-DNA-3' *PSCA110<sub>LB1</sub>* for the mutant line SAIL\_87\_E04 (**Table1**). For ATSIP2, a fragment of the WT allele of At3g57520 was amplified with the primers *SALK\_038166<sub>LP</sub>* and *SALK\_038166<sub>RP</sub>* or with the primers *SALK\_113663<sub>LP</sub>* and *SALK\_113663<sub>RP</sub>*. The mutant alleles were traced with the *SALK\_038166<sub>RP</sub>* and the T-DNA-3' *Lbb1.3* or with the *SALK\_113663<sub>RP</sub>* and *Lbb1.3*.

**Table1.** Primer list used for screening of ATSIPs T-DNA insertion mutant lines.

Primer name	Sequence
<i>SALK_090247<sub>LP</sub></i>	5'-TCATTGATTCGATCCCTTTTCG-3'
<i>SALK_090247<sub>RP</sub></i>	5'-TGATGCCACGTGAATACGAAG-3'
<i>Lbb1.3</i>	5'-ATTTTGCCGATTTCGGAAC-3'
<i>SAIL_87_E04<sub>LP</sub></i>	5'-TCGAGACGTTCCATACTCAG-3'
<i>SAIL_87_E04<sub>RP</sub></i>	5'-CGTCTGGTTGTTCTCTTGTTGG-3'
<i>PSCA110<sub>LB1</sub></i>	5'-GCCTTTTCAGAAATGGATAAATAGCCTTGCTTCC-3'
<i>SALK_038166<sub>LP</sub></i>	5'-TCGAATTGTTTGGCTAAGACG-3'
<i>SALK_038166<sub>RP</sub></i>	5'-GCTTCAATTCCTCTCACCTC-3'
<i>SALK_113663<sub>LP</sub></i>	5'-TTTGTAAGCGCCAACAATTC-3'
<i>SALK_113663<sub>RP</sub></i>	5'-TTCAATAGTCTATGCATACAGATCAGG-3'

### 2.2.3 Heterologous expression of ATSIP1 and -2 in *Sf9* insect cells

#### 2.2.3.1 Bacmid construction and transfection

*ATSIP1* (At1g55740) and *ATSIP2* (At3g57520) were obtained as full length cDNAs from the Riken Arabidopsis full length clone database (pda02775 and pda18685, respectively; <http://www.brc.riken.jp>; Seki et al., 1998; Seki et al., 2002) and amplified using a high fidelity PCR (Expand High Fidelity PCR System, Roche, Basel, Switzerland) according to the manufacturer's instructions, using coding sequence (CDS)-specific primers (*ATSIP1*<sub>fwd</sub>, *ATSIP1*<sub>rev</sub> or *ATSIP2*<sub>fwd</sub>, *ATSIP2*<sub>rev</sub>, **Table2**) at a primer annealing temperature of 58°C.

**Table2.** Primer list used for the expression of recombinant ATSIP1 and -2.

Primer name	Sequence
<i>ATSIP1</i> <sub>fwd</sub>	5'-ATGACCGTTGGTGCCGG-3'
<i>ATSIP1</i> <sub>rev</sub>	5'-TTATTGGATGACCACGTCCC-3'
<i>ATSIP2</i> <sub>fwd</sub>	5'-ATGACGATTACATCAAATATCTCTG-3'
<i>ATSIP2</i> <sub>rev</sub>	5'-CTAGACCAGAATCTCAACATG-3'
<i>pFastBac</i> <sub>fwd</sub>	5'- ATTAAATGATAACCATCTCG-3'
<i>M13</i> <sub>fwd</sub>	5'- TGTAACGACGCGCCAGT-3'

The resulting products were purified using the Wizard SV Gel and PCR Clean-Up System (Promega, Dübendorf, Switzerland) were cloned in pGEM-TEasy vector (Promega) according to the manufacturer's instructions and the construct was transformed by heat shock into Dh10b *E. coli* cells (Invitrogen, Basel, Switzerland) and spread onto LB plates [1.0% (w/v) Bacto-tryptone, 0.5% (w/v) Bacto-yeast extract, 1.0% (w/v), 1.5% (w/v) Bacto-agar] with appropriate antibiotic selection (100µg ml<sup>-1</sup> ampicillin). After 18h incubation at 37°C, antibiotic-resistant colonies were used for colony PCRs to confirm the presence of the respective cDNAs. Plasmid-DNAs from positives colonies were isolated from *E. coli* overnight cultures using the Wizard Plus Minipreps DNA purification system (Promega) and the CDS were excised using the *NotI* restriction endonuclease. *ATSIP1* was subcloned into the pFastBac1 vector and *ATSIP2* into the pFastbac HTc (Invitrogen) after the dephosphorylation of the 5' phosphates end of the vector with a shrimp alkaline phosphatase (SAP, Promega). Ligation reactions and transformations into Dh10b *E. coli* cells followed the same protocol than the ligations and transformations into pGEM-TEasy vector.

Positive colonies were selected for gene orientation (5'-3') by PCR using an orientation-specific primer pair (*pFastBac*<sub>fwd</sub>, *ATSIP1*<sub>rev</sub> or *pFastBac*<sub>fwd</sub>, *ATSIP2*<sub>rev</sub>; **Table2**). The pFastBac constructs (1ng) were used to transform DH10Bac-competent cells (**Fig.1**). Briefly, 100µl of DH10Bac cells were thawed 30min on ice with the pFastBac construct, heat-shocked (45s, 42°C; 2min, 4°C) and incubated

for 4h (37°C, 225rpm) with 900µl SOC medium [2.0% (w/v) Bacto-tryptone, 0.5% (w/v) Bacto-yeast extract, 8.6mM NaCl, 2.5mM KCl, pH7.0] prior to spreading the cells onto LB plates with appropriate antibiotic selection (50µg ml<sup>-1</sup> Kanamycin, 7µg ml<sup>-1</sup> Gentamicin, 10µg ml<sup>-1</sup> Tetracycline) and with Blue-White select screening reagent (Sigma-Aldrich, Buchs, Switzerland). Gene transposition was confirmed for positive colonies using colony PCR (*M13<sub>fwd</sub>*, *ATSIP1<sub>rev</sub>* or *M13<sub>fwd</sub>*, *ATSIP2<sub>rev</sub>*, **Table.2**).

Bacmid preparation, insect cell transfection and recombinant protein expression were conducted as outlined in the Bac-to-Bac manual (Invitrogen) using *Sf9* cells grown in monolayer cultures (**Fig.1**) with minor modifications. For the Bacmid isolation, DH10Bac cells from an overnight culture were harvested by centrifugation, resuspended, lysed, and neutralized following the Miniprep DNA purification system procedure (Promega). However, instead of using a column, Bacmid-DNA was precipitated overnight by adding one volume of isopropanol, pelleted by centrifugation, rinsed with 70% cold EtOH and resolubilized in 50µl of TE buffer (10mM Tris-HCl, 1mM EDTA, pH8.0) prior to transfection.

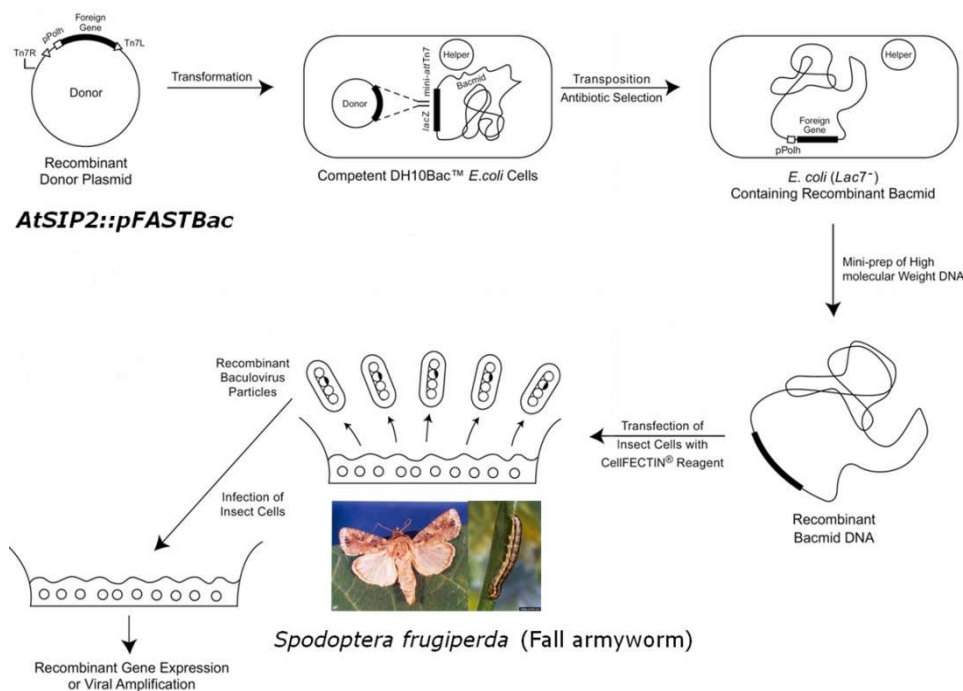


**Fig.1.** Diagram of the Bac-to-Bac System (adapted from the Bac-to-Bac manual, Invitrogen)

### 2.2.3.2 Expression of ATSIP1 and -2 in *Sf9* cells

After 72h transfection at 27°C, the entire medium was collected and clarified by centrifugation (500g, 10min). Supernatant constituted the P<sub>0</sub> viral stock and was stored protected from light at 4°C for 6 months or -80°C for months. P<sub>0</sub> was amplified by successive 48h infections in a 10cm culture dish seeded with 5x10<sup>6</sup> cells in a total volume of 10ml. After each infection the medium was clarified by centrifugation and the new virus stock was assumed to be amplified 10-fold. Usually P<sub>2</sub> or P<sub>3</sub> (visual



multiplicity of infection (MOI) of 5-10 correlating approximately to a virus titer of  $2 \times 10^8$  pfu  $\text{ml}^{-1}$ ) were utilized for assaying recombinant protein. For a standard infection expressing ATSIP1 or-2, *Sf9* cells were seeded at  $5 \times 10^6$  cells, into a 10cm-culture dish containing 10ml BaculoGold TNM-FH medium (BD Biosciences, Allschwil, Switzerland) supplemented with  $1 \text{U ml}^{-1}$  Penicillin and  $1 \mu\text{g ml}^{-1}$  Streptomycin (Pen strep, GIBCO, Invitrogen) and incubated at room temperature (RT) for 15min. Baculovirus stock was added to the medium at MOI 7.5 and the plates were incubated for 72h at  $27^\circ\text{C}$ . Using a compound light microscope, infected cells were observed due to their detachment from the surface of the plate and their enlarged size 72h after inoculation (**Fig.2**).

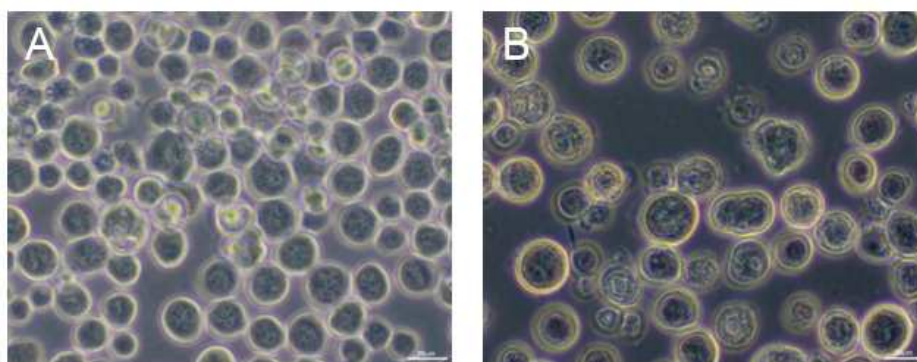


**Fig.2.** Light microscopy of *Sf9* cells after 72h of incubation without infection (A) or with infection (B).

### 2.2.3.3 RNA isolation from *Sf9* cells and cDNA synthesis

RNA was isolated from *Sf9* cells using the TRIzol LS reagent (Invitrogen) following the manufacturer's instructions. Briefly, cells were pelleted (500g, 10min,  $4^\circ\text{C}$ ) 72h after infection and resuspended directly into 3ml TRIzol LS reagent and lysed by pipetting. RNA was separated by adding chloroform and precipitated by mixing it with isopropyl alcohol. The amount of RNA isolated corresponded to  $3\text{--}4 \mu\text{g} \mu\text{l}^{-1}$  RNA. The cDNA template for PCR was obtained by reverse transcribing  $1 \mu\text{g}$  total RNA with  $1 \mu\text{g}$  oligo (dT<sub>15</sub>) primer and 200U M-MLV (H<sup>-</sup>) reverse transcriptase (Promega) according to the manufacturer's protocol. One  $\mu\text{l}$  of RNasin Plus RNase Inhibitor (Promega) was added to the reaction to avoid any RNA degradation. The PCR was carried out with CDS specific primers (*ATSIP1*<sub>fwd</sub>, *ATSIP1*<sub>rev</sub> or *ATSIP2*<sub>fwd</sub>, *ATSIP2*<sub>rev</sub>) in  $50 \mu\text{l}$  containing  $5 \mu\text{l}$  cDNA, 1.25U GoTaq DNA polymerase (Promega), 1×PCR buffer, 0.5mM of each dNTP, and  $0.5 \mu\text{mol}$  of each primer, at a primer annealing temperature of  $58^\circ\text{C}$  for 30 cycles. The number of cycles was chosen to give a strong signal in case the *Sf9* cells effectively contained *ATSIPs* mRNAs. The PCR products were loaded into a 1% agarose gel, analyzed by electrophoresis using 1×TAE buffer (40mM Tris, 20mM acetic acid, 1mM EDTA), stained with ethidium bromide and the picture was captured with a digital camera.

### 2.2.4 $\alpha$ -Galactosidase activity assays of recombinant ATSIP1 and -2

*Sf9* cells were collected by centrifugation (500g, RT, 5min) 72h after baculovirus infection. Cell pellets were resuspended in 2ml of extraction buffer [100mM Hepes-KOH, pH 7.5, 5mM MgCl<sub>2</sub>, 1mM EDTA (ethylenediaminetetraacetic acid), 10mM DTT (1,4 dithiothreitol), 1mM benzamidine, 1mM PMSF (phenylmethanesulfonylfluoride), 0.05% (v/v) Triton X-100] and homogenized on ice using a Potter homogenizer connected to an electric drill. After centrifugation (12000g, 4°C, 10min), total protein concentration of the clarified extract was determined photometrically with a Bradford assay (Bio-Rad Protein Assay, Reinach, Switzerland). Briefly, 1-2 $\mu$ l were pipetted in 1ml of the Protein Assay reagent diluted 5x, incubated for 30min and the absorbance at 595nm was recorded by a spectrophotometer (Bio-Rad Smart Spec Plus). The results were compared to a bovine serum albumin (BSA) standard curve. Aliquots (100 $\mu$ l) of clarified extracts were centrifuge-desalted by gel filtration (1700g, 4°C, 2min) through 5ml Sephadex G-25 columns (fine, final bed volume of 2ml). Columns were pre-equilibrated with assay buffer (100mM Hepes-KOH, pH7.5 or 8.5). Pre-equilibration was performed twice with 2ml of assay buffer.

For the enzyme activity assays, 20 $\mu$ l aliquots of clarified crude extracts were incubated with 20 $\mu$ l of assay buffer (100mM Hepes-KOH, pH 7.5, 200mM Sta or Gol for ATSIP1, 100mM Raf for ATSIP2) at 30°C for 30min (ATSIP1) or 1h (ATSIP2). The reactions were stopped by boiling the samples for 6min in a water bath. Clarified crude extracts were also assayed for RafS activity as described except that assay buffer contained 100mM Suc and 10mM Gol. After desalting of the extracts (2.2.5), the products formed, Gal when RFOs (when the substrates) or Ino (when Gol was the substrate), were measured by HPLC-PAD (2.2.6).

### 2.2.5 Desalting of extracts

Desalting of carbohydrate and enzyme assay samples was conducted prior to analysis using “French columns” as previously described (Bachmann, 1993, Bachmann *et al.* 1994, Peters *et al.* 2007, Peters and Keller 2009). Briefly, a 1ml MoBiCol column (MobiTec, Göttingen, Germany) fitted with a 10 $\mu$ m pore size filter was prepared by adding 150 $\mu$ l of alkaline anion-exchanger resin AG 1-X8 (HCO<sub>2</sub><sup>-</sup>-form, 200-400 mesh, Bio-Rad), 100 $\mu$ l of the phenolic trapper, polyvinylpolypyrrolidone (PVPP), and 50 $\mu$ l of acidic anion-exchanger Sordolite CS-2C (H<sup>+</sup>-form). The “French columns” were first washed by centrifugation (3000g, 4°C, 4min) with 600 $\mu$ l H<sub>2</sub>O, the samples were then applied and eluted with a second step of centrifugation (same conditions) and finally the columns were rinsed with an additional 100 $\mu$ l water step under identical centrifugation conditions.

### 2.2.6 HPLC-PAD analysis

The desalted samples were analyzed by HPLC-PAD, using a  $\text{Ca}^{2+}/\text{Na}^{+}$ -moderated ion partitioning carbohydrate column (Table3, Peters et al., 2007; Peters and Keller, 2009).

**Table3.** HPLC system specifications.

Degassing	Erma ERC-3510
Pump	Gynkotek model 480
Injector	Gynkotek Gina 50
Stationary phase	$\text{Ca}^{2+}$ -column Benson BC100 (7.8x300mm; Benson Polymeric; Reno, Nevada; USA)
Precolumn	Carbo- $\text{Ca}^{2+}$ Security guard cartridge (4.0x3.0mm; Phenomenex, Brechbühler, Schlieren, Switzerland)
Mobile phase	$\text{H}_2\text{O}$ with $\text{Ca}/\text{Na}$ -EDTA (50mg $\text{l}^{-1}$ )
Flow rate	0.6ml $\text{min}^{-1}$
Temperature	90°C
Elution	Isocratic
Post column addition	300mM NaOH (0.6ml $\text{min}^{-1}$ )
Detection	PAD ESA 5040 analytic cell ESA Coulochem II
Integration	Chromeleon V 6.4 Dionex

### 2.2.7 Biochemical characterization of recombinant ATSIP1 and -2

The pH optimum of recombinant ATSIP1 and ATSIP2 was determined using crude extracts prepared from *Sf9* cells as described above and 100mM Sta or Raf, respectively, in the following buffers: (i) for ATSIP1, 100mM MES-KOH buffer (pH 5.0, 5.5, 6.0, 6.5), 100mM Hepes-KOH buffer (pH 6.5, 7.0, 7.5, 8.0) and 100mM Tris-HCl buffer (pH 8.0, 8.5, 9), (ii) for ATSIP2 full strength Mcllvaine buffer (pH 5.0, 5.5, 6.0), 100mM MES-KOH buffer (pH 6.0, 6.5, 7.0) and 100mM Hepes-KOH buffer (pH 7.0, 7.5, 8.0, 9.0). Enzyme activity assays were conducted in a total volume of 50 $\mu\text{l}$  containing 25 $\mu\text{l}$  of clarified crude extract and 25  $\mu\text{l}$  of assay buffer. The final concentration of Sta and Raf was 50mM.

The specificity of recombinant ATSIP2 for the linkage type  $\alpha$ - or  $\beta$ -galactoside, respectively, was tested using the artificial substrate, *p*-nitrophenyl-*D*-galactopyranoside (pNPGal, Sigma), as previously described (Gao and Schaffer, 1999). Briefly, 10 $\mu\text{l}$  of clarified crude extract was incubated with 90 $\mu\text{l}$  of assay buffer (100mM Hepes-KOH pH7.5) containing 3mM pNP $\alpha$ Gal or pNP $\beta$ Gal. The assay mixture was incubated in a 96-well microtiter plate at 30°C and the reaction stopped by the addition of 160 $\mu\text{l}$  of 1M  $\text{Na}_2\text{CO}_3$ . Absorbance of the pNP formed was read with a plate reader spectrophotometer at 405nm (Fusion Universal Microplate Analyzer, Packard, Meriden, USA).

Inhibition assays with the specific  $\alpha$ Gal inhibitor, deoxygalactonojirimycin-HCl (DGJ; Industrial Research, Lower Hutt, New Zealand), were conducted by incubating clarified crude extracts at RT for 10min with 10 $\mu$ M DGJ. Samples were then assayed for  $\alpha$ Gal activity as described above.

The specificities for the natural substrates, Raf, Sta, Ver, Gol, and melibiose (Mel), were tested as described in 2.2.4 with 100mM final concentration of sugar for ATSIP1 and 50mM for ATSIP2.

### **2.2.8 Cold acclimation and deacclimation treatments**

For cold stress experiments 6-week-old plants were transferred to a cold chamber (8h light, 120 $\mu$ mol photons m<sup>-2</sup> s<sup>-1</sup>, 4°C, 16h dark, 60% RH) for 14d followed by 14d of deacclimation in the standard growing chamber at 22°C. Plant leaf material was sampled at various time points for enzymatic assays (acidic  $\alpha$ Gal, alkaline  $\alpha$ Gal and RafS, see section 2.2.4) and WSCs (see section 2.2.14).

### **2.2.9 Water-deficit and rehydration treatments**

Water deficit stress was imposed on whole potted plants by withholding irrigation over a period of 11d, at the end of which the RWC was determined to be around 50% and visual signs of turgor loss appeared in the leaves. Leaf samples were excised at various intervals for WSCs (see section 2.2.14). Rehydration was conducted by watering the plants and sampling after 3d. RWC (relative water content) was determined as previously described (Peters et al., 2007).

### **2.2.10 Plant enzyme extraction and activity assays**

For the determination of  $\alpha$ Gal activities in crude leaf extracts, 5-week-old soil-grown *Arabidopsis* plants were separated into source, intermediary and sink leaves as well as roots. Tissue (100mg) was homogenized in 200 $\mu$ l of an alkaline extraction buffer [50mM Hepes-KOH pH7.5, 2mM MnCl<sub>2</sub>, 2mM MgCl<sub>2</sub>, 40mM DTT, 1mM NaEDTA, 2% (w/v) PVP K30, 2% (w/v) PEG 20 000, 2% (w/v) PVPP, 0,1% (v/v) Triton X-100] or an acidic extraction buffer [McIlvaine buffer pH5.0, 2mM MnCl<sub>2</sub>, 2mM MgCl<sub>2</sub>, 20mM DTT, 2% (w/v) PVP K30, 2% (w/v) PEG 20 000, 2% (w/v) PVPP] as previously described (Peters et al. 2007, Peters and Keller 2009) and aliquots (200 $\mu$ l) were centrifuge-desalted over Sephadex columns as described above. Aliquots (10 $\mu$ l) of clarified crude extracts were incubated with 10 $\mu$ l of 100mM Raf assay buffer for the  $\alpha$ Gal activity or with 10mM Gol and 100mM Suc for the RafS activity, at 30°C for 1h and the activity was determined as described above.

### 2.2.11 EDTA-mediated phloem exudation and $^{14}\text{C}$ pulse-chase treatment

Mature leaves of 6-week-old WT plants were excised from the rosettes, the petioles were then cut under water and immediately placed into 1.5ml Eppendorf tubes filled with fresh water. To label the leaves with  $^{14}\text{CO}_2$ , the tubes were placed into a TLC chamber containing aliquots of  $\text{NaH}^{14}\text{CO}_3$  solution ( $25\mu\text{Ci g}^{-1}\text{ FW}$ ). Lactic acid (one drop) was added to release the  $^{14}\text{CO}_2$  and the chamber was immediately closed and exposed to a light source (about  $100\mu\text{mol m}^{-2}\text{ s}^{-1}$ ) for 10min (=pulse). After this treatment, the leaves were removed from the chamber, cut again under water, placed into new Eppendorf tubes containing 1ml exudation buffer (5mM EDTA, 5mM  $\text{KHPO}_4$ , pH7.5; King and Zeveaart, 1974) and kept in a moist chamber to prevent wilting and transpiration for 1h or 3h (=chase). Radio-labeled WSCs present in the leaves were detected by HPLC-PAD analysis (see 4.2.11) after a cryosap extraction. Briefly, leaf material was finely chopped and placed into a 1ml MoBiCol column fitted with a  $10\mu\text{m}$  pore size frit. The leaf material was frozen in liquid nitrogen and thawed at  $4^\circ\text{C}$ . The column was placed in a 2ml Eppendorf tube and centrifuged ( $12\,000g$ ,  $4^\circ\text{C}$ , 15min). To prevent enzymatic digestion of the WSCs in the cryosap, it was stored on ice and desalted immediately as previously described (2.2.5). The phloem exudate was concentrated, desalted and radio-labeled WSCs detected by HPLC-PAD as previously described.

### 2.2.12 RNA isolation from plant tissue and semi-quantitative PCR (sqPCR)

Total RNA was extracted from source, intermediary and sink leaves as well as roots using the Plant RNeasy<sup>®</sup>mini kit (Qiagen AG, Hombrechtikon, Switzerland). Total RNA was quantified using the NanoDrop ND-1000 spectrophotometer (NanoDrop, Wilmington, USA). The reverse transcription and cDNA synthesis was carried out as previously described (2.2.3.3). The sqPCR was carried out in  $50\mu\text{l}$  containing  $5\mu\text{l}$  cDNA, 1.25U GoTaq DNA polymerase (Promega),  $1\times\text{PCR}$  buffer, 0.5mM of each dNTP, and  $0.5\mu\text{mol}$  of each primer, at a primer annealing temperature of  $58^\circ\text{C}$  for 23 cycles. The number of cycles chosen for the sqPCR was determined to occur in the linear range of the constitutively expressed *ACTIN2* gene (*ACT2*, At3g18780). The *ACT2* primer amplified a 1.1kB fragment and the *ATSIP2* primer pair amplified a 1.0kB fragment of the cDNA.

<i>ATSIP2</i> <sub>fwd</sub>	5' - ATGACGATTACATCAAATATCTCTG-3'
<i>ATSIP2sq</i> <sub>rev</sub>	5' - TGAAGTGGGTATGCTAATGC-3'
<i>ACT2</i> <sub>fwd</sub>	5' - ATGGCTGAGGCTGATGATAT-3'
<i>ACT2</i> <sub>rev</sub>	5' - TTAGAAACATTTTCTGTGAACGAT-3'

The PCR products were analyzed as previously described (2.2.3).

### 2.2.13 Promoter- $\beta$ -glucuronidase (GUS) plants

0.5kB Fragments of Arabidopsis genomic DNA, upstream from the *ATSIP1* and *ATSIP2* start codons, were amplified using a high fidelity PCR (Expand High Fidelity PCR System, Roche), following the manufacturer's instructions (**Table4**). These fragments were cloned into the pCR8/GW/TOPO vector system (Invitrogen) and subcloned into the Gateway destination vector pMDC163 (Curtis and Grossniklaus, 2003) using a conventional LR clonase reaction (Invitrogen).

**Table4.** Primer list used for *ATSIPs* promoter analysis.

Primer name	Sequence
<i>PrATSIP1_1487<sub>fwd</sub></i>	5' ACAGGCTTTGAGGACTTAC-3'
<i>PrATSIP1_527<sub>fwd</sub></i>	5' TCATAGCATTTCGATTTTCATA-3'
<i>PrATSIP1<sub>rev</sub></i>	5' TGTTACTTCCTTGTAGGGAAAAC-3'
<i>PrATSIP2_1572<sub>fwd</sub></i>	5' TAATAGCGCATATAGAAGAAAAACG-3'
<i>PrATSIP2_450<sub>fwd</sub></i>	5' AGCCAAACACACCGTTCTGA-3'
<i>PrATSIP2<sub>rev</sub></i>	5' TTCTAGATTAACGTATCAGATAATCACAAGG-3'

This *ATSIPs*-promoter- $\beta$ -glucuronidase reporter constructs were transformed into *Agrobacterium tumefaciens* (GV3101) by electroporation, using a Genepulser (2.5kV; 100 $\Omega$ ; 25  $\mu$ F, Bio-Rad). A second reporter construct included the 0.5kB described above and an additional 1kB of upstream sequence (**Table4**). Col-0 Arabidopsis plants were transformed using a floral dip method (Clough and Bent, 1998). Hygromycin B-resistant plants grown onto half strength MS agar (Duchefa Biochemie BV, Haarlem, The Netherlands; Murashige and Skoog, 1962), supplemented with Suc (5%, w/v) and Hygromycin B (25 $\mu$ g ml<sup>-1</sup>) were selected as previously described (Harrison et al., 2006). Transgenic plants (T3) were used to assay for  $\beta$ -glucuronidase activity.

### 2.2.14 Histochemical staining for $\beta$ -glucuronidase (GUS) activity

One week after germination, T3 transgenic plants were transferred onto soil and used to stain for GUS activity (Parcy et al., 1998) four weeks later. Briefly, tissue was harvested and placed in 90% acetone for 20min. For the staining procedure, samples were infiltrated under vacuum in staining buffer containing X-Gluc (5-bromo-4-chloro-3-indolyl- $\beta$ -D-glucuronic acid) [0.2% (v/v) Triton X-100, 50mM NaHPO<sub>4</sub>, K<sub>4</sub>[Fe(CN)<sub>6</sub>], 2mM K<sub>3</sub>[Fe(CN)<sub>6</sub>], pH7.2, 2mM X-Gluc] for 20min. The tubes were sealed for 16h incubation at 37°C in dark, and were treated with an ethanol series to bleach the tissue of chlorophyll (successively in 20%, 35% and 50% EtOH at RT for 30min each). For fixation, samples were incubated 30min in formalin-acetic acid-alcohol (FAA; 50% EtOH, 5% formaldehyde, 10% acetic acid) and were finally stored in 70% EtOH at 4°C.

### 2.2.15 Preparation of root cross sections for light microscopy

For the preparation of root cross sections, roots of 10d-old plants grown on half-strength MS agar were used. They were stained for GUS activity, fixed for 3min under vacuum in 4% (v/v) glutaraldehyde and incubated for 4h at RT. The tissue was washed thrice with ddH<sub>2</sub>O and dehydrated using an ethanol series (70%, 30min; 90%, 30min; 100%, 1h). The final dehydration step using 100% ethanol was repeated once. Embedding of the tissue was conducted using Technovit 7100 (Heraeus Kulzer, Dübendorf, Switzerland), following the manufacturer's instructions and root cross sections (2-3µm) were cut using a hand operated microtome.

### 2.2.16 Seed germination assays

Arabidopsis seeds were surface-sterilized and imbibed at 4°C in either sterile water or water supplemented with 10µM DGJ for 16h. Imbibed seeds were then transferred to Petri dishes (wetted filter paper with water or DGJ) and kept at 22°C in the dark for germination. Germination was defined as the time between imbibition and protrusion of the radicle, *i.e.* a seed was considered to be germinated when the radicle pierced the seed coat.

### 2.2.17 Water soluble carbohydrate (WSC) extraction

WSCs were extracted using an ethanol series as previously described (Peters et al., 2007; Peters and Keller, 2009) with minor modifications. For seed WSCs extractions, ground, freeze-dried Arabidopsis seeds (20mg) were flash-frozen in liquid N<sub>2</sub> and homogenized for 30s in the presence of 5 steel balls (2.5mm diameter) in a Retsch mill (MM 300, Retsch, Haan, Germany). For cold acclimation-deacclimation experiment, 100mg of fresh tissue was flash-frozen in liquid N<sub>2</sub> and ground prior to the extraction. For water-deficit-rehydration experiment, 15mg of previously ground and freeze-dried leaf material was used as a basis for the extraction. WSCs were extracted twice (per step) in a three-step sequential process, using 1ml each of 80% EtOH, 50% EtOH and dH<sub>2</sub>O. Extractions were conducted at 80°C for 10min and the tubes centrifuged at 15 000g (5min, 4°C). WSCs were desalted (see section 2.2.5) and washed twice through the "French columns" prior to their analysis by HPLC-PAD, using Ca<sub>2</sub><sup>+</sup>/Na<sup>+</sup>-moderated ion partitioning column (see section 2.2.6).



## 2.3. Results

### 2.3.1 ATSIP1 and -2 are *bona-fide* $\alpha$ Gals with different substrate specificities

*ATSIP1* and *ATSIP2* were heterologously expressed in *Sf9* insect cells. The presence of *ATSIP1* and -2 RNA in the infected cells was confirmed by RT-PCR (**Fig.3**).

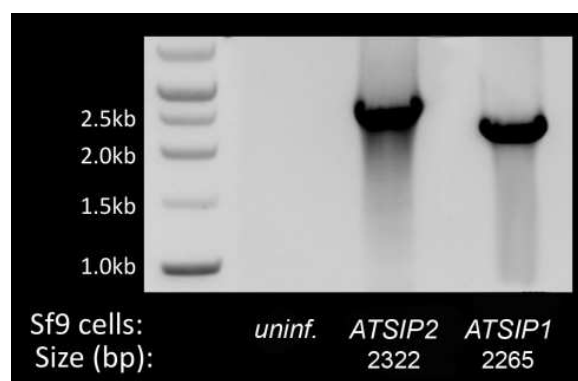


**Fig.3.** RT-PCR performed with *ATSIP1* and *ATSIP2* CDS-specific primers. RNAs were isolated from uninfected *Sf9* cells (*uninf.*) or *Sf9* cells infected with baculovirus containing *ATSIP1* or *ATSIP2* constructs.

Crude extracts of *Sf9* cells infected with a baculovirus carrying the *ATSIP1* cDNA were clearly able to hydrolyze Sta and Gol at pH 8.5, contrary to crude extracts from uninfected *Sf9* cells (**Fig.4A, 4B**). This hydrolase activity was completely abolished when the enzyme assay was performed in the presence of 10  $\mu$ M DGJ, a potent  $\alpha$ Gal inhibitor (Butters et al., 2005; Blöchl et al., 2007; **Fig.4A, 4B**). RafS activity was also tested using the substrates Suc and Gol; no Raf was produced confirming that the enzyme is only active hydrolytically (**Fig.4C**).

Crude extracts carrying *ATSIP2* protein were able to hydrolyze Raf at pH 7.5, contrary to crude extracts from uninfected *Sf9* cells (**Fig.4D**). As observed for *ATSIP1*, the hydrolase activity of the recombinant *ATSIP2* was completely abolished in the presence of 10  $\mu$ M DGJ (**Fig.4D**). *ATSIP1* and -2 displayed no RafS activity (**Fig.4E**), thus revealing that both enzymes are *bona fide*  $\alpha$ Gals and not RafSs or VerS as previously proposed for *ATSIP1* (Anderson and Kohorn, 2001). The substrate preference of the recombinant *ATSIP1* and -2 was tested using the natural substrates, Raf, Sta, Ver, Gol and Mel. *ATSIP1* showed hydrolytic activity towards Sta and Gol, with a preference for Gol (**Fig.4F**) while *ATSIP2* showed a high specificity only towards Raf (**Fig.4G**).



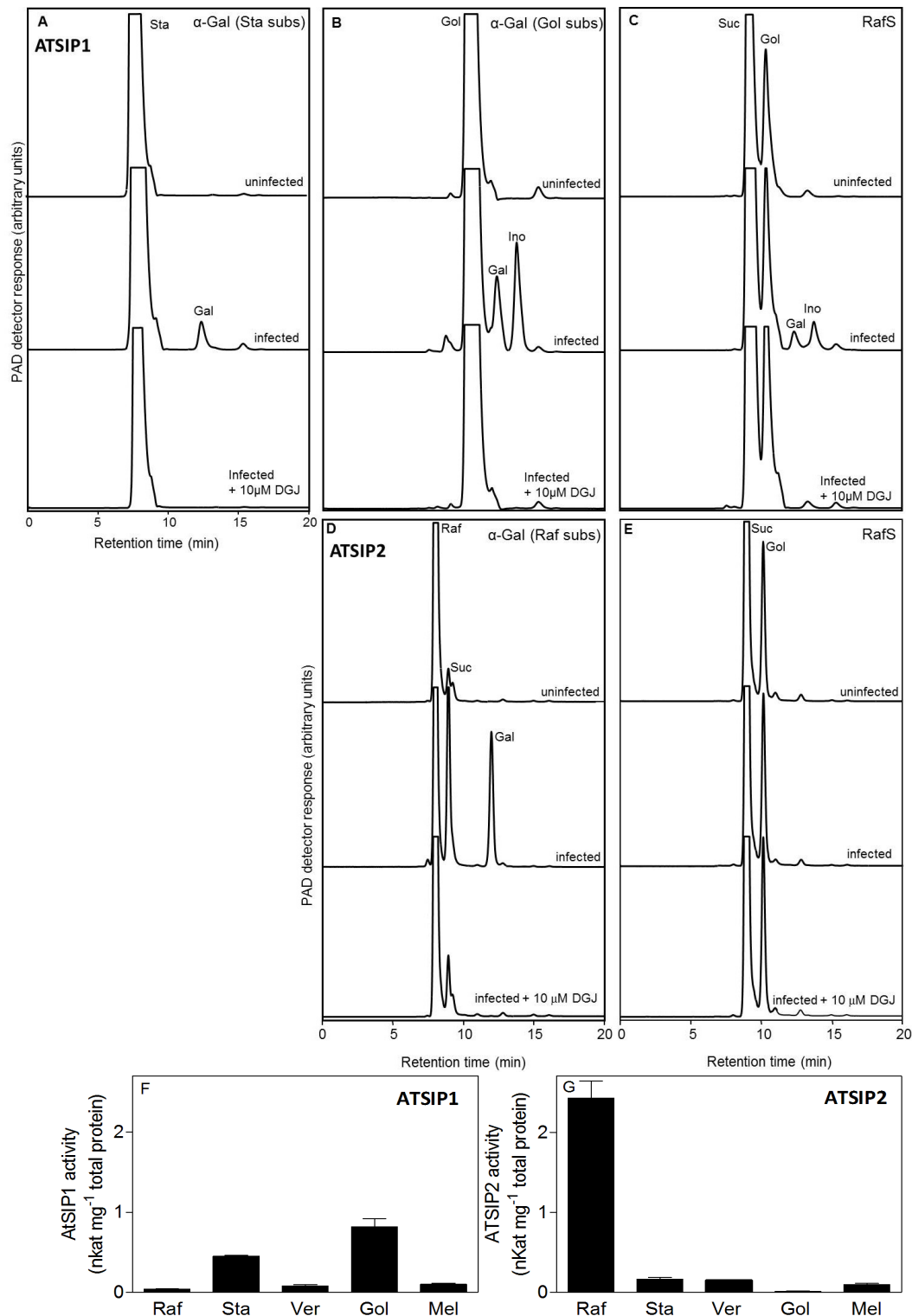


**Fig.4.** Enzyme activities with different substrates of *Sf9* cells infected or uninfected (controls) with an *ATSIP1*- or *ATSIP2*- carrying baculovirus. Crude cell lysates containing *ATSIP1* recombinant protein were incubated at pH 8.5 either with 100mM Sta (A) or Gol (B) to assay for alkaline αGal activity or with 10mM Gol and 100mM Suc to assay for RafS activity (C). Crude cell lysates containing *ATSIP2* recombinant protein were incubated at pH 7.5 either with 50mM Raf to assay for alkaline α-Gal activity (D) or with 10mM Gol and 100mM Suc to assay for RafS activity (E). DGJ is a potent inhibitor of α-Gals (Butters et al., 2005; Blöchl et al., 2007). The *ATSIP1* protein showed activity towards Sta and Gol with a preference for Gol when different natural substrates are compared (measured at pH 8.5 with 100mM each of Raf, Sta, Ver, Gol, and Mel) (F). The *ATSIP2* activity shows clear Raf specificity when different natural substrates are compared (measured at pH 7.5 with 50mM each of Raf, Sta, Ver, Gol, and Mel) (G). subs, substrate.

### 2.3.2 Biochemical characterization of recombinant ATSIP1 and -2

Recombinant ATSIP1 and -2 both showed alkaline hydrolase activities. To determine their pH dependencies, ATSIP1 and -2 activities were measured with 50mM of the RFO substrates, Sta and Raf, respectively. ATSIP1 was most active between pH 8.0 and 9.0 with a maximum activity at pH 8.5 in HEPES buffer (**Fig.5A**). ATSIP2 showed a lower and broader pH optimum between pH 6.5 and 8.5 with maximum activity at pH 8.0 in HEPES buffer (**Fig.5B**).

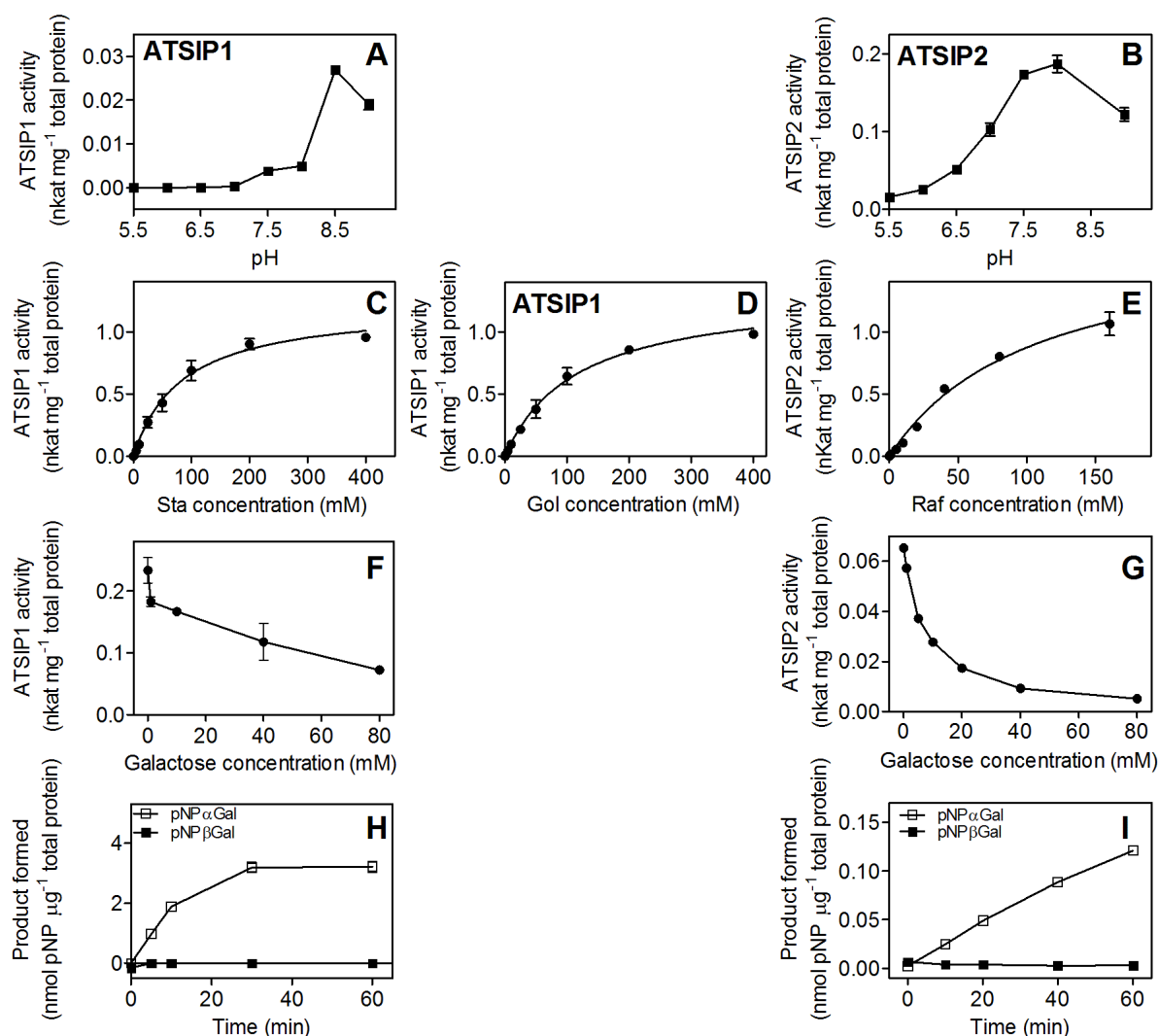


**Fig.5.** Biochemical characterization of recombinant ATSIP1 and ATSIP2 enzymes. The pH dependency of ATSIP1 shows a pH optimum around pH 8.5 with 50mM Sta and pH 8.0 with 50 mM Raf as substrate for ATSIP1 (A) and ATSIP2 (B), respectively. The Sta and Gol concentration dependency of ATSIP1 shows Michaelis-Menten type kinetics with apparent  $K_m$  values of  $83\text{mM} \pm 13\text{mM}$  (C) and of  $115\text{mM} \pm 17\text{mM}$  (D) for Sta and Gol, respectively. The Raf concentration dependency of ATSIP2 shows Michaelis-Menten type kinetics with apparent  $K_m$  value of  $105 \pm 18\text{mM}$  (E). The Gal inhibition curve of ATSIP1 at pH 8.5 with 100mM Gol shows 50% inhibition at 15mM Gal (F). The Gal inhibition curve of ATSIP2 at pH7.5 with 50mM Raf shows 50% inhibition at 7.4mM Gal (G). The activities of ATSIP1 (H) and ATSIP2 (I) with pNPαGal or pNPβGal show that ATSIPs only cleaves α-galactosidic linkages. Data are means  $\pm$  SE of three to six replicates.

Both recombinant ATSIPs showed Michaelis-Menten-type kinetics. ATSIP1 has an apparent  $K_m$  of  $83\text{mM} \pm 13\text{mM}$  and  $v_{\max}$  value of  $1.21 \pm 0.06 \text{ nkat mg}^{-1} \text{ protein}$  for Sta (**Fig.5C**) and an apparent  $K_m$  of  $115\text{mM} \pm 17\text{mM}$  and  $v_{\max}$  value of  $1.32 \pm 0.09 \text{ nkat mg}^{-1} \text{ protein}$  for Gol (**Fig.5D**). ATSIP2 has apparent  $K_m$  and  $v_{\max}$  values of  $105 \pm 18\text{mM}$  and  $1.80 \pm 0.16 \text{ nkat mg}^{-1} \text{ protein}$ , respectively (**Fig.5E**). To get some idea of the end product inhibition of ATSIP1 and -2, we assayed various Gal concentrations with one substrate concentration for each protein tested. The  $\alpha$ Gal activity was end product-inhibited by Gal displaying a 50% inhibition at  $15\text{mM}$  Gal (with  $100\text{mM}$  Gol as substrate) for ATSIP1 and at  $7.4\text{mM}$  Gal (with  $50\text{mM}$  Raf as substrate, **Fig.5F**) for ATSIP2 (**Fig.5G**). The ATSIP1 activity was not inhibited by Ino, the second end-product of Gol hydrolysis (data not shown). When tested with the natural  $\alpha$ -galactosyl substrates, Raf, Sta, Ver, Gol, and melibiose (Mel), both Sta and Gol were recognized as efficient substrates for ATSIP1, but only Raf for ATSIP2 (**Fig.4G**). When tested with the artificial substrate, *p*-nitrophenyl- $\alpha$ -D-galactopyranoside (pNP $\alpha$ Gal), both ATSIPs were able to hydrolyze the pNP $\alpha$ Gal (**Fig.5H, 5I**). Conversely, the  $\beta$ -linked variant of pNPGal, *p*-nitrophenyl- $\beta$ -D-galactopyranoside (pNP $\beta$ Gal) did not show any detectable activity, indicating that ATSIP1 and ATSIP2 are indeed  $\alpha$ Gals (and not  $\beta$ Gals).

### 2.3.3. ATSIP2 does not seem to play an important role during deacclimation of cold-acclimated plants

Considering that (i) Sta rarely occurs in vegetative tissues of Arabidopsis and (ii) Raf is ATSIP2's main natural substrate the most logical putative physiological function for ATSIP2 would be RFO degradation in leaves. Conversely, the most logical putative function of ATSIP1 would be the RFO degradation in the seeds where Sta is known to be present (Bentsink et al., 2000).

It is well documented that Raf is accumulating in Arabidopsis leaves during various abiotic stresses and degraded when the stress is relieved (*e.g.* Taji et al., 2002). In a first approach, we explored therefore the possibility that alkaline  $\alpha$ Gals could play a role in Raf degradation during the cold deacclimation phase. By cold acclimating 6-week-old WT plants at  $4^\circ\text{C}$ , we observed a gradual increase of Raf starting from  $0.25\text{mg g}^{-1} \text{ FW}$  ( $22^\circ\text{C}$ ) and increasing to  $7.0\text{mg g}^{-1} \text{ FW}$  after 14d cold acclimation ( $4^\circ\text{C}$ ; **Fig.6A**). During the deacclimation phase, when the plants were transferred again to  $22^\circ\text{C}$ , Raf quickly decreased, reaching  $1.0\text{mg g}^{-1} \text{ FW}$  after 1d deacclimation (**Fig.6A**). The Raf increase during the acclimation phase correlated positively with RafS activity increase (from  $0.054 \text{ nkat g}^{-1} \text{ FW}$  at the beginning to  $0.121 \text{ nkat g}^{-1} \text{ FW}$  after 14d acclimation) (**Fig.6B**). Acid and alkaline  $\alpha$ Gals activities, however, increased mostly during the deacclimation phase (from  $0.050 \text{ nkat g}^{-1} \text{ FW}$  at 14d

to  $0.107 \text{ nkat g}^{-1} \text{ FW}$  at 17d for the alkaline  $\alpha\text{Gal}$  activity and from  $0.102 \text{ nkat g}^{-1} \text{ FW}$  at 14d to  $0.327 \text{ nkat g}^{-1} \text{ FW}$  for the acidic  $\alpha\text{Gal}$  activity), in parallel with Raf depletion, suggesting that  $\alpha\text{Gals}$  play an important role in Raf degradation in the deacclimation phase (**Fig.6C, 6D**).

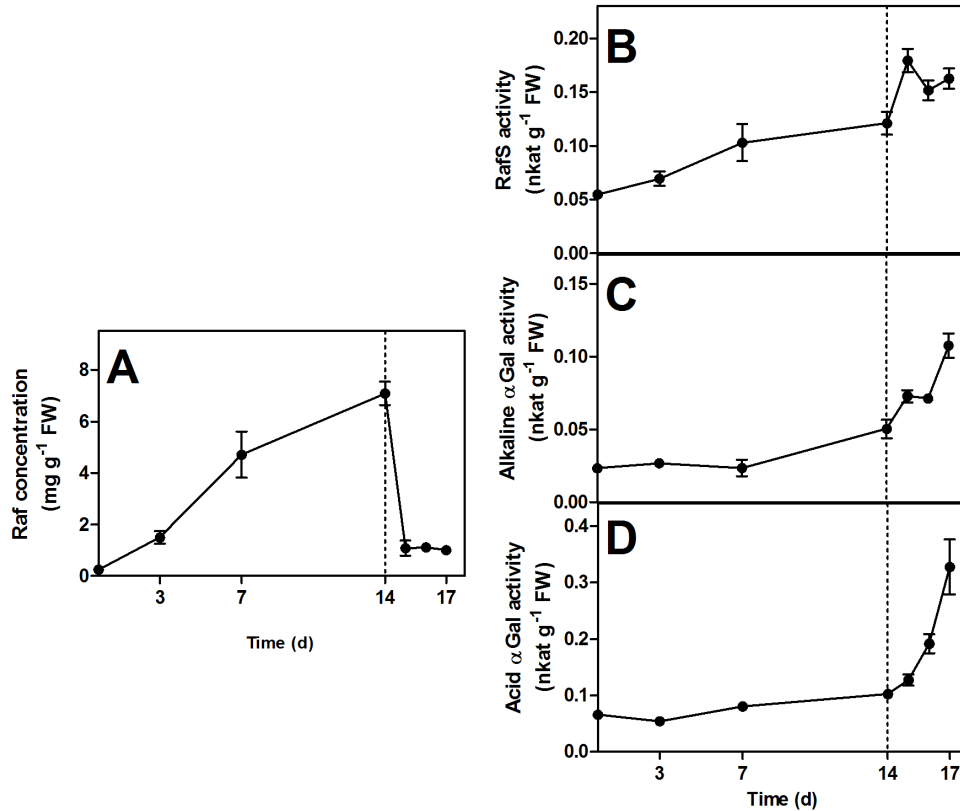


**Fig.6.** RFO Enzyme activities and Raf concentration changes in wild-type *Arabidopsis* plants during 14d of cold acclimation (4°C) and 3d of deacclimation (22°C). The dotted line indicates the transfer of the plants to the deacclimation phase. Raf concentration was determined by HPLC-PAD (A). RafS activity was measured with 5mM Gol and 50mM Suc as substrates at pH7.5 (B).  $\alpha\text{Gal}$  activities were measured with 50mM Raf as substrate at pH7.5 (alkaline  $\alpha\text{Gal}$ , C) or pH5.0 (acid  $\alpha\text{Gal}$ , D). Enzyme assay samples were analyzed by HPLC-PAD. Data points represent the means  $\pm$  SE of six replicates. Raf, Raffinose;  $\alpha\text{Gal}$ ,  $\alpha$ -galactosidase; RafS, raffinose synthase.

To determine whether ATSIP2 is responsible for Raf degradation observed during deacclimation, we performed a cold acclimation and deacclimation experiment with an *atsip2* T-DNA insertion line (SALK\_038166) compared with a WT plant (**Fig.7**). The *atsip2* line did not show any phenotype during the experiment. WSCs analyses confirmed that Raf increased similarly in both the WT and *atsip2* mutant line (from  $0.25 \text{ mg g}^{-1} \text{ FW}$  to  $6.16 \text{ mg g}^{-1} \text{ FW}$  for the WT and from  $0.42 \text{ mg g}^{-1} \text{ FW}$  to  $7.08 \text{ mg g}^{-1} \text{ FW}$  for the *atsip2* line). Other WSCs (Gol, Ino, Suc, Gal, Glc and Fru) were also similar in WT and *atsip2* plants during cold acclimation and deacclimation and followed a gradual increase during cold acclimation and a rapid decrease during deacclimation (**Fig.7**).

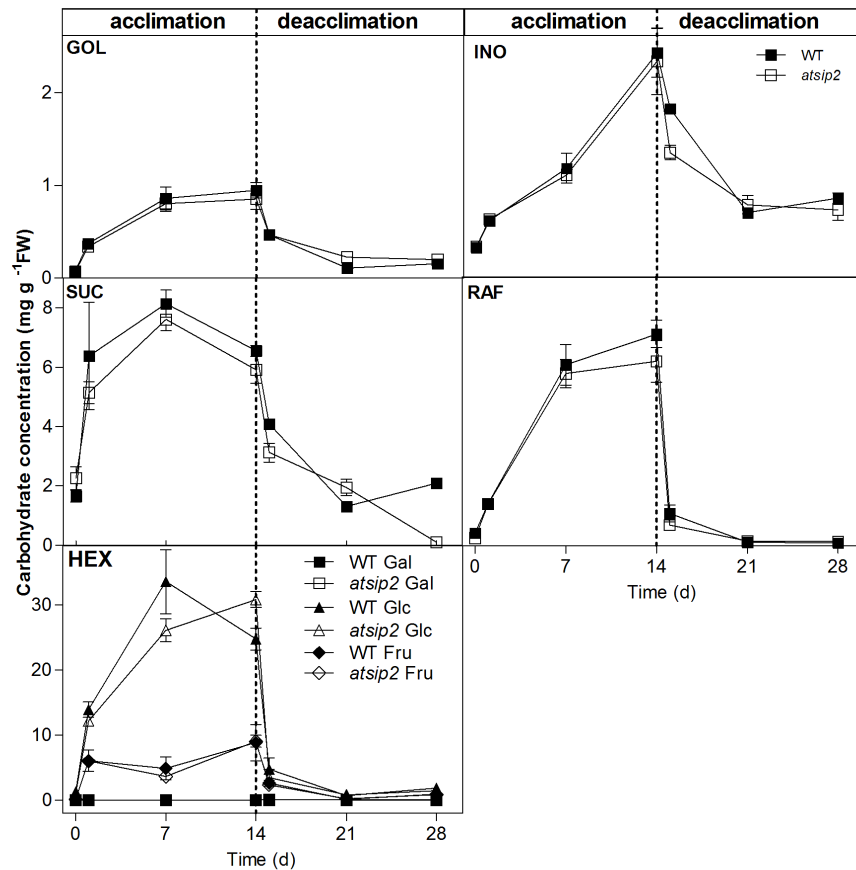


**Fig.7.** Changes in the carbohydrate concentrations in the leaves of WT and *atsip2* plants subjected to cold acclimation over a period of 14d, followed by 14d of deacclimation at 22°C. Samples were collected at regular intervals and WSCs were extracted and analyzed as described above. Data points represent the means  $\pm$  SE of six replicates. Gol, galactinol; Ino, *myo*-inositol; Suc, sucrose; Raf, Raffinose; Hex, hexoses.

These results suggest that the lack of ATSIP2 does not seem to be responsible for Raf degradation during the deacclimation phase. However, it has to be kept in mind that the acid  $\alpha$ Gals have a quite broad pH range of hydrolytic activity and may well contribute to the Raf degradation observed compensating the effect of ATSIP2 loss in the *atsip2* plants. The absence of a phenotype during deacclimation may also be attributed to other alkaline  $\alpha$ Gals that would take over the function of Raf degradation. Because the subcellular location of Raf degradation is still unknown (vacuole and/or cytoplasm) and because the enzyme assays were performed on crude extracts we cannot discriminate between  $\alpha$ Gal isoforms. Despite the reservations, the results presented suggest that ATSIP2 does not seem to play a major role in Raf degradation during the deacclimation.

#### 2.3.4. ATSIP2 does not seem to play an important role during rehydration of dehydrated plants

It is well known that *GoISs* are tightly regulated and function in a stress-specific manner (*e.g.* *AtGoIS1* and -2 are specific for water deficit stress and *AtGoIS3* is specific for cold stress). It was, therefore,

tempting to consider another putative role for ATSIP2, and examine whether ATSIP2 is involved in the relief of a water deficit stress (*i.e.* during rehydration). To this end, we performed a water deficit experiment by withholding irrigation until leaves started to lose turgor (approximately after 11d) and subsequently re-watering the plants (**Fig.8**). The drying curve shows that *Arabidopsis* leaves can maintain a RWC at 80% for 9d, and once the RWC starts to decline, the plants rapidly display a loss of turgor. Lethal dehydration occurs below a RWC of 50%. Thus, we performed the water-deficit stress experiment until the plants reached a RWC of 50% and we immediately re-hydrated them by re-watering. Like for the cold deacclimation experiment (see 2.3.3), we used the *atsip2* T-DNA insertion line (SALK\_038166) and compared it to WT plants. The dehydration and rehydration curves of *atsip2* plants were very similar to the WT plants.

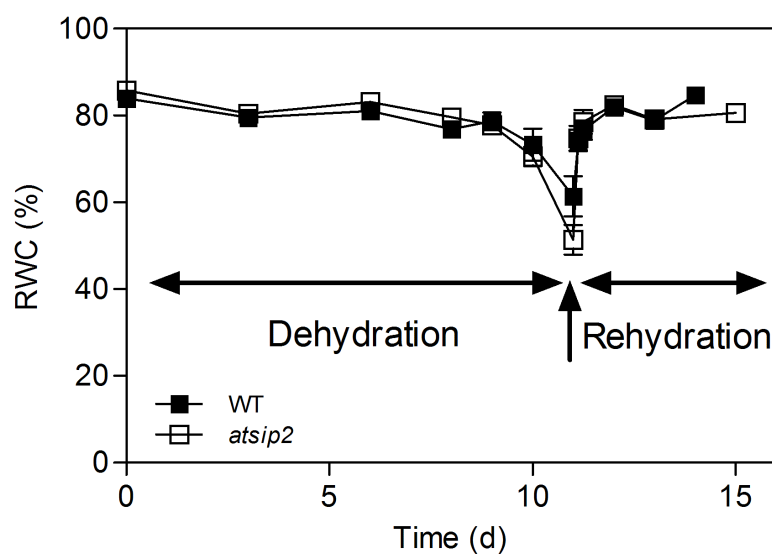


**Fig.8.** Dehydration/rehydration cycle of *Arabidopsis* plants. Water was withheld for 11d until the leaves reached about 50% RWC. They were then re-watered immediately. WT, wild-type Col-0 plants; *atsip2*, *atsip2* T-DNA insertion mutant line (SALK\_038166).

WSCs were extracted at four specific time points and analyzed by HPLC-PAD: at the beginning of withholding water (0), after 8d (RWC of 80%, FT) and 11d (RWC of 50%, S) without watering and 3d after the rehydration (RWC of 80%, R, **Fig.9**). We observed an increase in Ino, Gol Raf and Suc concentrations after 8d when the plants still displayed a RWC of 80%, suggesting that the plants had already perceived the stress and started to accumulate protective metabolites before the turgor decreased. Raf still increased after 11d in WT and even more in the *atsip2* plants [from 0.38mg g<sup>-1</sup>DW (0) to 11.99mg g<sup>-1</sup>DW (stressed, S) for the WT and from 0.9mg g<sup>-1</sup>DW (0) to 18.27mg g<sup>-1</sup>DW (S) in the *atsip2* plants]. After 3d of rehydration, the WSCs concentrations reached again the normal levels in both WT and *atsip2* plants. These results showed that *atsip2* plants accumulated more Raf during water deficit, possibly due to the lack of the alkaline  $\alpha$ Gal that might act as a Raf feedback regulating enzyme. However, during the rehydration phase Raf was degraded in the *atsip2* plants as well as in

the WT plants, suggesting that ATSIP2 does not seem to play an important role for Raf degradation during the rehydration phase of a water-deficit stress.

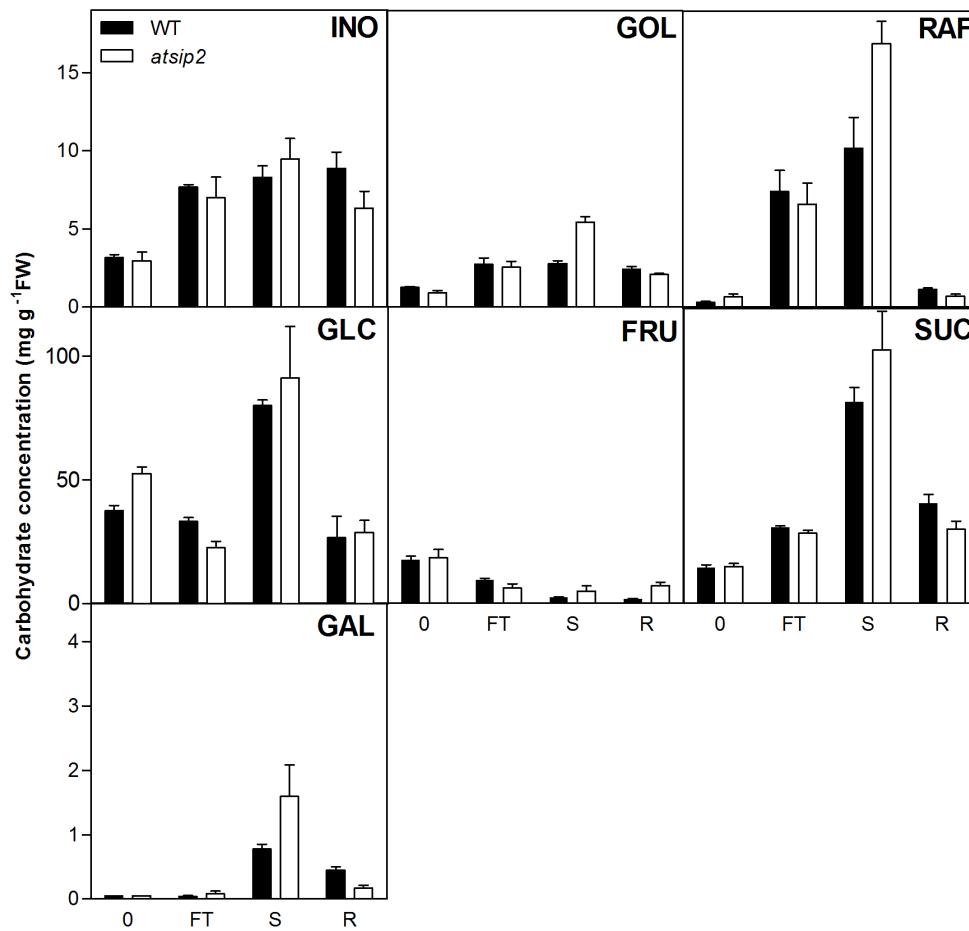


**Fig.9.** Changes in the carbohydrate concentrations in the leaves of plants subjected to a water deficit stress over a period of 11d, followed by a rehydration period of one week. Samples were collected the day after the last watering, at 8d where the plant still were at full turgor (FT), at 11d, when the plants were stressed (S) and reached 50% RWC and after 3d of rehydration (R). Error bars indicate the standard error between the mean of six replicates.

### 2.3.5. Investigating the role of ATSIP1 and -2 in phloem unloading in leaves

Since ATSIP2 does not seem to play an important role during cold and dehydration stress relief, we thought it worthwhile to investigate a putative function in phloem unloading. However we first needed to confirm that Raf is indeed present in the phloem sap and could, therefore, be a potential substrate for an alkaline  $\alpha$ Gal at the sink part of the plant. We chose a <sup>14</sup>C phloem exudation method that allowed the detection of radio-labeled WSCs in the leaves and in the phloem sap. After 10min pulse, followed by 1h chase, we detected a significant amount of *de novo*-synthesized <sup>14</sup>C-Raf in the leaves in addition to the known carbohydrates, <sup>14</sup>C-Suc, <sup>14</sup>C-Glc and <sup>14</sup>C-Fru (**Fig.10**). When we

analyzed the phloem sap (3h chase), we could also detect a  $^{14}\text{C}$ -Raf peak which represented 1.46% of the total WSCs present in the phloem exudate (**Fig.10**).

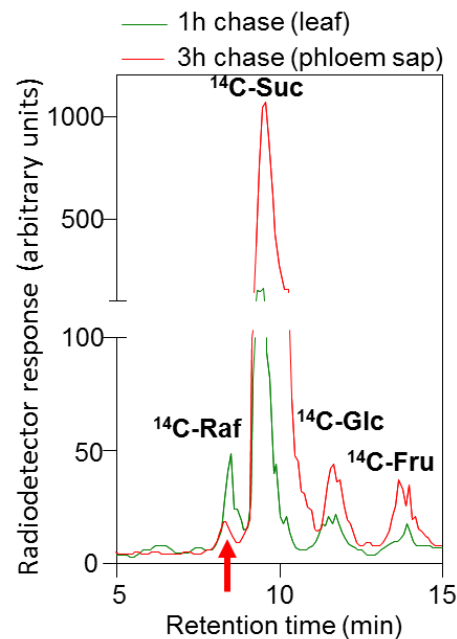


**Fig.10.** HPLC traces representing radio-labeled carbohydrate peaks of 6-week-old wild-type plants exposed to a  $^{14}\text{CO}_2$  pulse-chase treatment and analyzed with the BC-100 column coupled to a FLO-ONE radio chromatography detector. The green trace represents the WSCs extracted from the leaves after 10min pulse followed by 1h chase and the red trace correspond to the phloem exudate collected after 10min pulse followed by 3h chase.

Knowing that Raf could be translocated in the phloem we examined the pattern of expression driven by the *ATSIP2* native promoter fused with a reporter gene. *ATSIP2* promoter:β-glucuronidase (GUS) fusion was created using the Gateway-compatible vector pMDC163 (Curtis and Grossniklaus, 2003), and a 0.5kB fragment of genomic DNA, upstream of the start codon of *ATSIP2* (**Fig.11B**). A second fusion included this 0.5kB plus an additional 1kB of upstream DNA (**Fig.11B**). A similar construct with *ATSIP1* promoter was created for a comparison (**Fig.11A**).



**Fig.11.** Scheme of the promoter sequence used for the GUS constructs. The short promoter constructs incorporate fragments of 450-550bp upstream the start codon of *ATSIPs* genes and the large promoter construct incorporate fragments of 1480-1580bp upstream the start codon of *ATSIPs* genes.



### 2.3.5.1. *ATSIP2* has a sink-specific expression and $\alpha$ Gal activity pattern

*Arabidopsis* (Col-0) transformed with these *ATSIP2* promoter constructs showed strong GUS activity in sink leaves of 5-week-old soil-grown plants (**Fig.12A, B**), suggesting that *ATSIP2* is expressed in these tissues. *ATSIP2* promoter expression was also found in steles of lateral roots (**Fig.12C, D**). Cross sections of young roots further revealed that this expression is located in the non-xylem parts of the stele, including the phloem (**Fig.12E, F**).

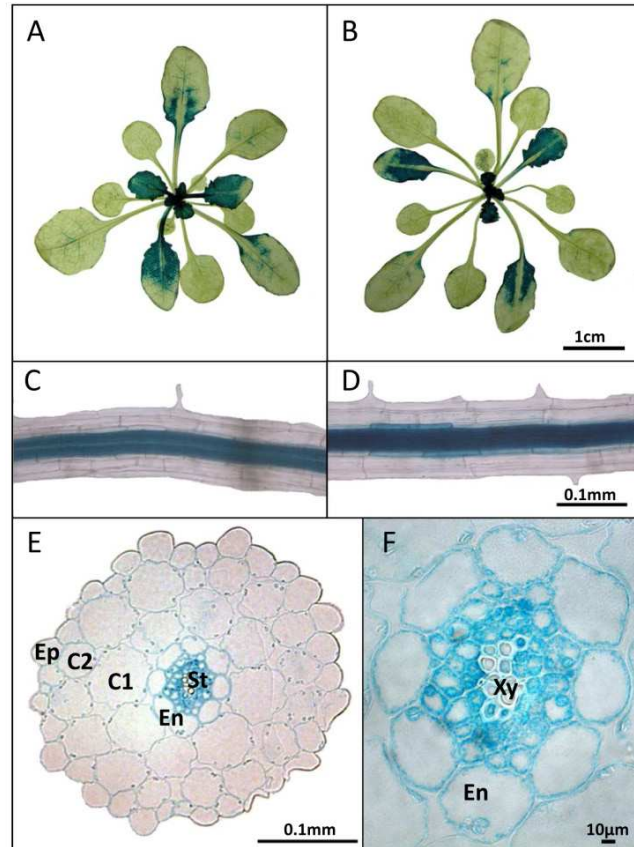


**Fig.12.** The *ATSIP2* promoter is active in sink leaves and the non-xylem parts of the root stele (blue GUS staining). A. Sink leaf-specific expression pattern in the 1.14 stage rosettes of *pATSIP2<sub>500</sub>::pMDC163* and B. of *pATSIP2<sub>1500</sub>::pMDC163*. C. Root stele-specific expression of *pATSIP2<sub>500</sub>::pMDC163* and D. of *pATSIP2<sub>1500</sub>::pMDC163*. E and F. Cross sections of roots of young *pATSIP2<sub>500</sub>::pMDC163* plants showing promoter activity in the non-xylem parts of the root stele. Ep, Epidermis; C1-C2, cortex; En, endodermis, St, stele; Xy, xylem vessels. All plants were of the same age (5 weeks; soil-grown), except for E and F (10d-old, half-strength MS agar-grown).

Finally, we were able to correlate this GUS-expression pattern to *in vivo* alkaline  $\alpha$ Gal activity. Using Raf as substrate at pH 7.5, the  $\alpha$ Gal activity was significantly higher in sink tissues (roots and young leaves) than in source tissues (old leaves) (**Fig.13A**). Using semi-quantitative reverse transcription PCR (sqPCR), these  $\alpha$ Gal activities were positively correlated to the presence of *ATSIP2* transcripts in all tissue types described (**Fig.13B**). These results gave us strong indication that *ATSIP2* is involved in Raf phloem unloading.

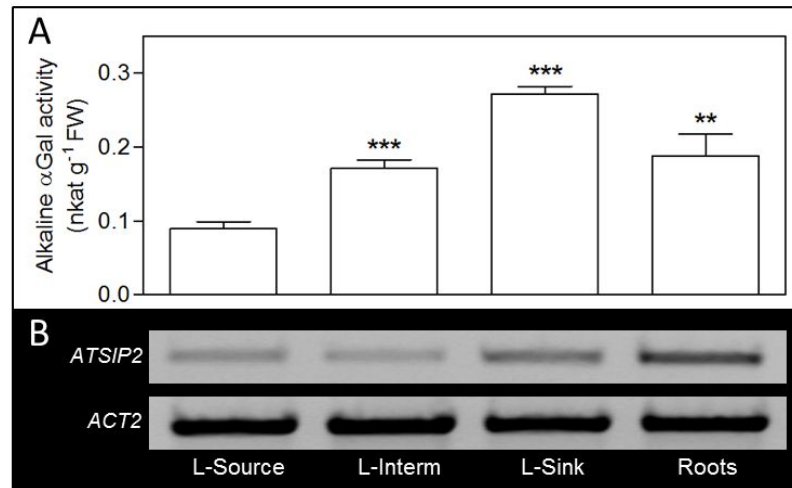


**Fig.13.** A. The extractable Raf-specific alkaline  $\alpha$ Gal activity of wild-type plants is highest in the sink tissues.  $\alpha$ Gal activity was measured at pH7.5 with 50mM Raf. All plants were 5 weeks old. B. sqPCR of cDNA from the four tissues described shows that the *ATSIP2* transcripts are most abundant in sink tissues. The *ACTIN2* gene was used as a constitutively expressed control. The statistical probabilities represented by stars reflect an unpaired t-test (\*\*\*,  $p < 0.0001$ ; \*\*,  $p < 0.006$ ). L-Source, source leaves; L-Interm, intermediate leaves; L-Sink, sink leaves.

#### 2.3.5.2. *ATSIP1* has a sink-specific expression pattern, but the *Sta*- and *Gol*-specific $\alpha$ Gal activity remains low

The *ATSIP1* promoter GUS-expression pattern is somewhat similar to *ATSIP2* with a strong promoter activity in sink leaves, but differed slightly in intermediate and source leaves (**Fig.14A,B**), where it is rather located in the periphery of the leaves. This is in contrast to the *ATSIP2* GUS staining which was restricted to the phloem unloading parts of the leaves (**Fig.12A,B, 14A,B**). Despite clear GUS staining pattern, the *in vivo* alkaline  $\alpha$ Gal activity at pH8.5 with the possible natural substrates, Raf, *Sta* and *Gol*, remained relatively low in all the GUS-staining tissues compared to the  $\alpha$ Gal activities (**Fig.14C**). Nevertheless, in sink leaves, we observe a 3-fold increase ( $35.4 \text{ nkat mg}^{-1} \text{ FW}$  in sink leaves and  $11.2 \text{ nkat mg}^{-1} \text{ FW}$  in source leaves) for Raf as substrate, a 2.2-fold increase ( $10.4 \text{ nkat mg}^{-1} \text{ FW}$  in sink leaves and  $4.6 \text{ nkat mg}^{-1} \text{ FW}$  in source leaves) for *Sta* as substrate and a 1.7-fold increase ( $8.9 \text{ nkat mg}^{-1} \text{ FW}$  in sink leaves and  $5.2 \text{ nkat mg}^{-1} \text{ FW}$  in source leaves) for *Gol* as substrate. The activity on Raf is possibly a residual *ATSIP2* activity, which was shown to be still active at pH8.5 (**Fig.5B**). The sqPCR correlated with the *ATSIP1* promoter GUS activity and the  $\alpha$ Gals assays confirming that *ATSIP1* is mostly expressed in sink vegetative tissues but at a lower level compared to *ATSIP2* (**Fig.14D; Fig.13B**).

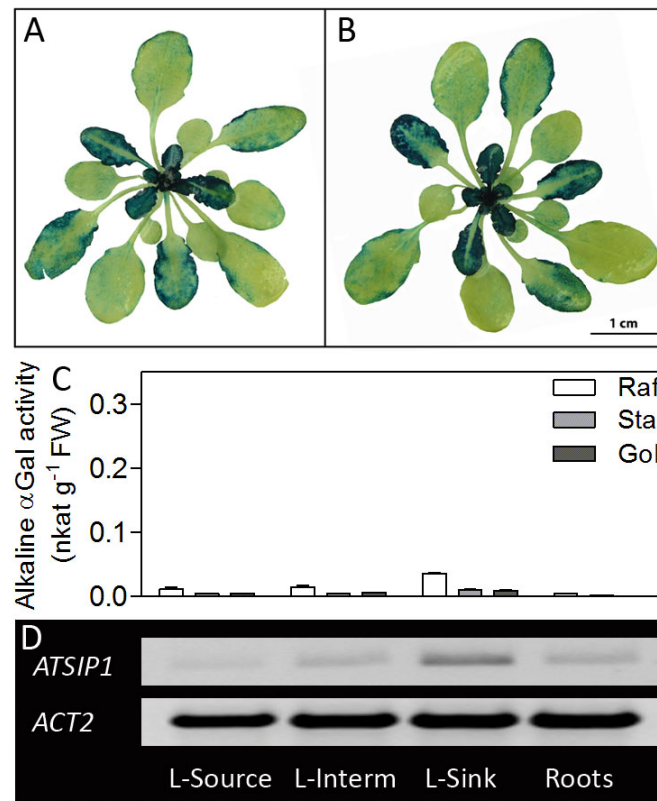


**Fig.14.** The *ATSIP1* promoter is active in sink leaves. Sink leaf-specific expression pattern in the 1.16 stage rosettes of *pATSIP1<sub>500</sub>::pMDC163* (A) and of *pATSIP1<sub>1500</sub>::pMDC163* (B). The extractable alkaline  $\alpha$ Gal activity of wild-type plants is highest with Raf as substrate in the sink tissues and very low with Sta and Gol as substrates in all tissues-types tested.  $\alpha$ Gal activity was measured at pH8.5 with 100mM Raf, Sta and Gol (C). For easy comparison, the  $\alpha$ Gal activity scale is the same as in Fig.13A. All plants were 5 weeks old (soil-grown). SqPCR of cDNA from the three tissues described shows that the *ATSIP1* transcripts are most abundant in sink tissues (D). The *ACTIN2* gene was used as a constitutively expressed control. L-Source, source leaves; L-Interm, intermediate leaves; L-Sink, sink leaves.

### 2.3.6. Physiological functions of *ATSIP1* and -2 during seed germination

To determine if *ATSIP1* and -2 play a role during seed germination, T-DNA insertion lines for *ATSIP1* and *ATSIP2* were used to compare their germination rates. We used two homozygous T-DNA insertion lines each for *ATSIP1* (SALK\_090247, SAIL\_87\_E04) and *ATSIP2* (SALK\_038166, SALK\_113663) (Fig.15A). All these lines had an insertion in the last exon of the gene. We created an *atsip1-atsip2* double mutant plant by crossing the single mutant lines, SALK\_090247 and SALK\_038166. In all these lines, 100% of the seeds started to germinate after 54h of imbibition at 20°C in the dark. We observed a small delay at 44h imbibition for the *atsip1-atsip2* double mutant line, but no delay for the single lines (Fig.15B). This suggests that the single mutant lines, *atsip1* or *atsip2*, did not affect the germination process but a lack of both enzymes could slightly impair the process. Germination was also tested in the presence of 10 $\mu$ M DGJ and WT. Mutant lines showed a reduction of germination rate between 30 and 70% (data not shown). By measuring  $\alpha$ Gal activities

after 1d of imbibition on crude extracts of seeds kept in the dark at 22°C with the corresponding substrates and pH optima of both ATSIP1 and -2 (Raf as a substrate at pH7.5, Sta as a substrate at pH8.5 and Gol as a substrate at pH8.5), we detected a good activity towards Raf (0.46nkat g<sup>-1</sup> DW, **Fig. 15C**), but the activities towards Gol (0.038nkat g<sup>-1</sup> DW, **Fig.15C**) and Sta (0.029nkat g<sup>-1</sup> DW, **Fig.15C**) were lower. This suggests a putative role of ATSIP2 in Raf degradation after 1d imbibition, but only a minor role for ATSIP1.

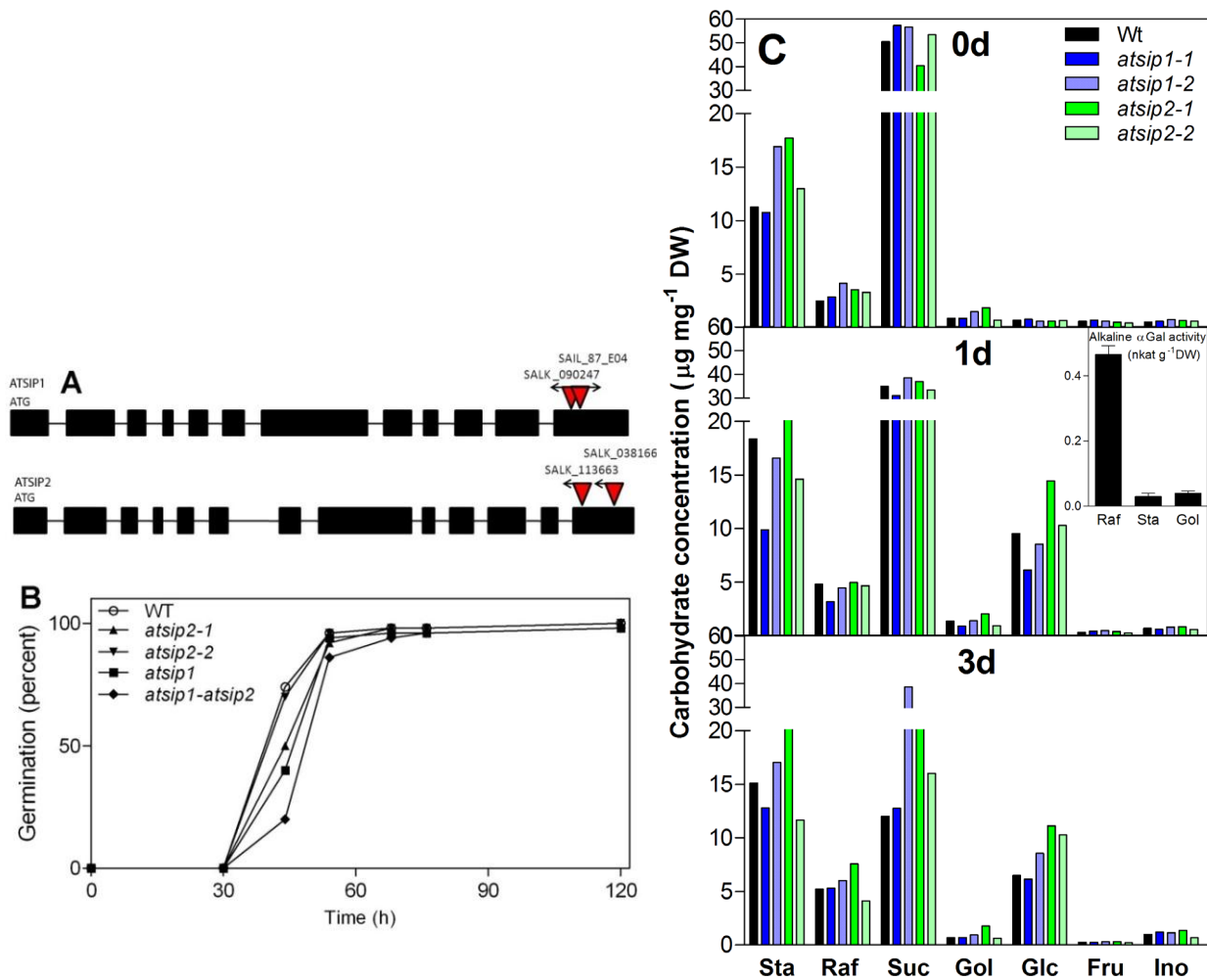


**Fig.15.** Seed imbibition and germination in WT, *atsip1*, *atsip2* and *atsip1-atsip2* lines. **A.** Schematic illustration of the structures of the *ATSIP1* and *ATSIP2* genes, respectively. Black boxes correspond to exons and lines to introns. Insertion T-DNA sites are indicated above the genes. **B.** Germination kinetics of different lines tested (*atsip2-1* for SALK\_038166, *atsip2-2* for SALK\_113663, *atsip1-1* for SALK\_090247, *atsip1-2* for SAIL\_87\_E04, *atsip1-atsip2* for SALK\_090247- SALK\_038166). Germination assay was performed at 20°C in the dark. **C.** Carbohydrate concentrations of the different seed lines before imbibition and after 1d and 3d imbibition in water at 22°C in the dark. The extractable alkaline  $\alpha$ Gal activity of wild-type seeds was measured after 1d imbibition. Activity was measured by HPLC-PAD after the incubation of crude extract for 1h with 50mM Raf at pH7.5 or with 100mM Sta and Gol, respectively, at pH8.5. The substrate concentrations and pH values were chosen according to the specificity and optimum pH of ATSIP1 and -2. WT; wild-type.

Conversely, RFO concentration did not decrease after 1d or 3d of imbibition in WT and mutant line seeds. We observed a 10-fold increase in Glc (*e.g.* from 0.67nkat g<sup>-1</sup> DW in dry seeds to 6.49nkat g<sup>-1</sup> DW after 3d imbibition for the WT) a 2-fold increase in Ino (*e.g.* from 0.51nkat g<sup>-1</sup> DW in dry seeds to 0.97nkat g<sup>-1</sup> DW after 3d imbibition for the WT) and a 5-fold decrease in Suc (*e.g.* from 50.49nkat g<sup>-1</sup> DW in dry seeds to 11.99nkat g<sup>-1</sup> DW after 3d imbibition for the WT). Surprisingly, Raf concentrations increased (*e.g.* from 2.49nkat g<sup>-1</sup> DW in the dried seeds to 5.19nkat g<sup>-1</sup> DW after 3d imbibition for the WT) as well as Sta (*e.g.* from 11.25nkat g<sup>-1</sup> DW in the dried seeds to 15.08nkat g<sup>-1</sup> DW after 3d imbibition for the WT).

## 2.4 Discussion

The presented data on the biochemical characterization of recombinant ATSIP1 and -2 unambiguously identify both enzymes as alkaline  $\alpha$ Gals with different substrate specificities and not as RafSs or VerS as reported (Anderson and Kohorn, 2001; Nishizawa et al., 2008; Maruyama et al., 2009; Wu et al., 2009). We showed that ATSIP1 and -2 were able to hydrolyze the  $\alpha$ -variant but not the  $\beta$ -variant of the artificial substrate pNPGal. Both enzymes were only active at alkaline pH (optimum pH of 7.5 for ATSIP2 and 8.5 for ATSIP1; **Fig5A, 5B**) and showed only hydrolytic and no synthetic RafS or VerS activities. However, the substrate specificity differed, ATSIP2 being Raf-specific (2.42nkat mg<sup>-1</sup> total protein) and ATSIP1 being Sta- (0.45nkat mg<sup>-1</sup> total protein) and Gol-specific (0.81nkat mg<sup>-1</sup> total protein). ATSIP1 and -2 were inhibited by the known  $\alpha$ Gal-specific inhibitor, DJG, and also partially by the end-product, Gal. Because recombinant ATSIP1 showed a substrate preference for Sta and Gol and because Sta is reported to be only present in Arabidopsis seeds, ATSIP1 was thought to hydrolyze Sta in seeds and probably during early germination. Raf-specific ATSIP2 however was rather thought to have a function in leaves.

In a first approach, we focused on ATSIP2 and tested the possibility that alkaline  $\alpha$ Gal could play a role in degradation during cold deacclimation of cold-acclimated plants. Despite a decrease in Raf during the relief of the stress, correlated with an increase of alkaline  $\alpha$ Gal activity in WT plants, the *atsip2* line did not show any difference in WSC concentration during the deacclimation, suggesting that ATSIP2 does not seem to play an important role in Raf degradation during deacclimation. Similarly, we tested whether ATSIP2 could play a role during rehydration after dehydration. The results showed that the *atsip2* line, as well as the WT plants, accumulated Raf during 11d of dehydration and degraded Raf up to non-stressed values within 3d, therefore suggesting that ATSIP2 does not seem to play an important role in Raf degradation during rehydration after a water-deficit stress.

According to the transcript abundance, the *in vivo* enzyme activities, and the promoter activity analysis, ATSIP2 appears to fulfill a typical role for an enzyme involved in sink-source relationship, reminiscent of a putative function in phloem unloading (**Fig.12, 13**; Gaudreault and Webb, 1986; Bachmann et al., 1994; Carmi et al., 2003). Although Suc has been reported to be the primary phloem-mobile carbohydrate in Arabidopsis, there is also good evidence that some Raf is additionally transported in the phloem (Haritatos et al., 2000). In that indirect study, following exposure of Arabidopsis source leaves to <sup>14</sup>CO<sub>2</sub> and light, radio-label was clearly found in <sup>14</sup>C-Raf in sink leaves

(besides the predominant  $^{14}\text{C}$ -Suc). In this study, we have directly shown that the  $^{14}\text{C}$ -Raf produced in the photosynthetic leaves is present later in the phloem exudate (**Fig.10**). We have also shown ATSIP2 to be a Raf-specific alkaline  $\alpha\text{Gal}$  with a promoter active exclusively in sink tissues, suggesting that it may legitimately be involved in the unloading of phloem-mobile Raf in sink tissues. Although ATSIP1 promoter activity was somewhat similar to the ATSIP2 pattern, the transcript abundance and activities correlated positively but remained very low, suggesting a minor role for ATSIP1 in Raf phloem unloading.

In a final approach aiming at discriminating putative physiological functions of ATSIP1 and -2, we used T-DNA insertion mutants to perform preliminary seed germination and imbibition assays. It is established that RFO are degraded within the first few days of seed germination, to provide energy and carbon skeletons to sustain seed germination demands (Downie and Bewley, 2000; Blöchl et al., 2007; Blöchl et al., 2008). In Arabidopsis, however, very little information is available on RFO degradation during seed germination. We performed a germination assay, and the single mutant lines displayed the same germination rate as the WT. Only the double mutant line, *atsip1-atsip2*, showed a slight delay, suggesting that only the lack of both enzymes slightly impairs a proper germination. In parallel, we detected an alkaline  $\alpha\text{Gal}$  activity after 1d imbibition towards Raf at pH7.5 that could correspond to ATSIP2 activity and a low alkaline  $\alpha\text{Gal}$  activity towards Sta and Gol (pH8.5) that could correspond to ATSIP1 activity. Surprisingly, Raf and Sta concentration increased after 1d and 3d imbibition which controverted the fact that ATSIP1 or -2 could degrade RFO during this time frame. The data represent only one set of preliminary experiments and we need to repeat the experiment to generate reliable data. However, the actual result set shows that the RFO storage pool of Arabidopsis seeds is not degraded until at least 3d imbibition at 22°C in the dark.

## Chapter III:

### **AtDIN10 (At5g20250) is an alkaline $\alpha$ -galactosidase located in the chloroplast**

#### Statement of disclosure:

The work described in this chapter represents an academic collaboration between Dr. Shaun Peters (Institute for Plant Biotechnology, University of Stellenbosch, South Africa) and Prof. Dr. Stefan Hörtensteiner (Institute of Plant Biology, University of Zurich). Dr. Shaun Peters represents the lead principal investigator. Apart from myself, Ph.D. candidate Bastien Christ (Institute of Plant Biology, University of Zurich) and BSc. (Hons.) candidate Ross Rutherford-Jones (Department of Molecular & Cell Biology, University of Cape Town, South Africa) are currently active on the project.





### 3.1. Introduction

Upon exposure to darkness, chlorophyll, proteins and carbohydrate reserves in leaves are quickly depleted (Kerr et al., 1985; Stitt et al., 1985; Brouquisse et al., 1998). Leaf senescence in general involves complex and highly regulated molecular and cellular events that allow efficient recycling of nutrients to other sink tissues (Buchanan-Wollaston, 1997; Noodén et al., 1997). Chloroplasts are the first organelles subjected to degradation during leaf senescence, and breakdown of chlorophyll takes place when thylakoid membranes are disrupted. Thylakoid membranes are the most abundant membrane system in biology and may account for up to 90% of the membranes in a green leaf (Gray, 1996; Joyard et al., 2004). They are primarily composed of galactolipids which represent around 75% of the total membrane lipids in plant leaves. Two predominant galactolipids are found in higher plants. The first, MGDG, constitutes up to 50% of the chloroplast lipids and contains one Gal residue bound in a  $\beta$ 1,4-linkage. The second, DGDG, accounts for 20% of chloroplast lipids and contains a second Gal moiety bound in a  $\alpha$ 1,6-linkage (see section 1.2.1).

Dark-inducible (*DIN*) genes were first observed by their transcript up-regulation in radish cotyledons of seedlings transferred to the dark (Azumi and Watanabe, 1991; Nozawa et al., 1999). One of these genes, *DIN1*, was shown to encode a protein that was imported into the chloroplast (Shimada et al., 1998). In Arabidopsis, a series of *DIN* genes, upregulated in detached leaves during artificial dark-induced senescence, were cloned and analyzed (Fujiki et al. 2001). Additionally, this expression of *DIN* transcripts was shown to be suppressed by exogenous Suc application (Fujiki et al., 2000; Fujiki et al., 2001). Another study on *DIN* gene expression in Arabidopsis cell suspension cultures showed that sugar starvation triggered *DIN* expression (Fujiki et al., 2000). These experiments indicated that the expression of these genes, at least in part, depends on the cellular sugar level. Among the Arabidopsis *DIN* genes, *AtDIN10* (At5g20250), which encodes a protein with a predicted chloroplast transit peptide, is similar to seed imbibition proteins, sharing 48% identity to *Cicer arietum* SIP protein (X95875; Fujiki et al., 2001).

In rice, an alkaline  $\alpha$ Gal (Osak $\alpha$ Gal, Os08g38710) was reported to be associated with the chloroplasts. Indeed, immunoelectron microscopy analysis demonstrated that Osak $\alpha$ Gal was specifically localized in the chloroplasts of senescing leaves and the recombinant Osak $\alpha$ Gal protein expressed in *E. coli* displayed an  $\alpha$ Gal optimum activity at pH 8.0 with good hydrolytic activities towards  $\alpha$ 1,6-galactosyl oligosaccharides and DGDG (Lee et al., 2004). A recent study revealed that, besides localizing to the chloroplast, Osak $\alpha$ Gal appears to play an important role in thylakoid membrane degradation (*in vivo*) during rice leaf senescence (Lee et al., 2009).

Collectively, these data suggested *AtDIN10* to be a good candidate for a chloroplastic alkaline  $\alpha$ Gal with either  $\alpha$ 1,6-galactosyl oligosaccharides or galactolipid substrate specificities. However, *AtDIN10* was recently reported as a putative RafS transcriptionally up-regulated by abiotic stress (RS6; Nishizawa et al., 2008). In this work, I report on (i) a preliminary characterization of AtDIN10 by its expression in *Sf9* cells to determine whether this gene encodes a RafS or an  $\alpha$ Gal, and (ii) the subcellular localization of AtDIN10 in chloroplasts.

As aforementioned, this chapter constitutes the preliminary data of a new collaborative project between Dr. Shaun Peters (lead principal investigator) and Prof. Stefan Hörtensteiner. The data presented for the subcellular localization and confocal microscopy were generated by Bastien Christ. All other data described in this chapter was generated by myself.

## 3.2 Materials and methods

### 3.2.1 Plant material and growth conditions

Arabidopsis plants were grown as previously described (2.2.1).

### 3.2.2 Recombinant AtDIN10 expression and characterization in *Sf9* insect cells

The *AtDIN10* cDNA (At5g20250) was obtained as a full length RIKEN clone (pda08032, www.brc.riken.jp, Seki *et al.*, 1998; Seki *et al.*, 2002) and amplified using coding sequence specific (CDS) primers (*DIN10*<sub>fwd</sub>: 5-ATGACGATTAAACCGGCGGT-3'; *DIN10*<sub>rev</sub>: 5'TCATAACTCAACTTGGATC-3') with the Expand High Fidelity PCR system (Roche). After cloning in pGEM-Teasy, *AtDIN10* was sub-cloned into the pFastBac1 vector using *NotI*. The Bacmid construction and the expression of AtDIN10 in *Sf9* insect cells followed the protocol described in 2.2.3.

### 3.2.3 GFP fusion protein analysis

*AtDIN10* was amplified by PCR from the pGEM-TEasy construct (3.2.2) with *DIN10\_SpeI\_F* and *DIN10\_SpeI\_R* primers using Roche Expand High Fidelity polymerase (Roche).

<i>DIN10_speI_F</i>	5'-GACTAGTATGGCGTCACAGAGTTGCT-3'
<i>DIN10_speI_R</i>	5'- GACTAGTTAACTCAACTTGGATCAGATGA-3'

The PCR fragment was then cloned into the pGEM-Teasy vector and after *SpeI* restriction subcloned into pUC18-spGFP6 (Meyer *et al.*, 2006), thereby producing an N-terminal fusion of *AtDIN10* with GFP. Arabidopsis mesophyll protoplasts were isolated from 6-week-old soil-grown plants as previously described (Frelet-Barrand *et al.*, 2008) with modifications. Abraded leaves of six-week-old plants were incubated with 1.0% (w/v) Cellulase Y-C and 0.1% (w/v) Pectolyase Y-23 (Seishin Pharmaceutical, Tokyo, Japan) for cell wall digestion. The collected protoplasts were purified by centrifugation (2min at 500g, followed by 4min at 1250g) in a discontinuous Percoll gradient where resuspended protoplasts (bottom) were sequentially overlaid with one volume of Percoll solution [35% (v/v) Percoll, dissolved in MCP solution (0.5M sorbitol, 1mM CaCl<sub>2</sub>, 20mM MES-KOH, pH6)] and 0.5 volume of MCP solution. Protoplasts were recovered from the 0/35% Percoll interphase.

The protoplasts were transformed by 20% polyethylene glycol transformation (Meyer et al., 2006). Briefly, cell numbers were quantified with a Neubauer chamber and adjusted to a density of  $2 \times 10^6$  protoplasts  $\text{ml}^{-1}$ . Plasmid DNA (20 $\mu\text{g}$ ), denatured herring sperm DNA (20 $\mu\text{g}$ ) and protoplast solution (300 $\mu\text{l}$ ) were mixed and then 325 $\mu\text{l}$  of PEG solution [40% PEG 4000 (w/v), 400mM Mannitol, 100mM  $\text{Ca}(\text{NO}_3)_2 \cdot 4\text{H}_2\text{O}$ , 0.1% MES (w/v), pH 5.7] was added. The mixture was incubated for 30min at room temperature in the dark and then slowly diluted with 7.5ml W5 solution [154mM NaCl, 125mM  $\text{CaCl}_2$ , 5mM KCl, 5mM Glc, 0.03% MES (w/v), pH 5.8] to wash the protoplasts. The protoplasts were centrifuged (50g, 5min, 4°C, rotor brake off) and the washing step repeated once. Protoplasts were then incubated up to 48h in the dark at room temperature and subsequently analyzed using a laser scanning confocal microscope (LSCM DM IRE2; Leica Microsystems). GFP fluorescence was imaged at an excitation wavelength of 488nm, and the emission signal was recovered between 495 and 530nm. TIC110-GFP expressed from pCL60-TIC110-GFP (Schenk *et al.*, 2007) was used as a control for the inner chloroplast envelope localization. A free GFP construct was used (pUC18-GFP5T-sp; Meyer et al., 2006) as a control for cytosolic localization.

### 3.2.4 Biochemical characterization of recombinant AtDIN10

AtDIN10 enzyme assays were performed as described in section 2.2.4. The pH optimum of AtDIN10 was determined by incubating the *Sf9* crude extract with 3mM of the artificial substrates, pNP $\alpha$ Gal or pNP $\beta$ Gal, in 100mM MES-KOH (pH5.5-6.5), 100mM HEPES-HCl (pH7.0-8.0) or 100mM Bicine-KOH buffer (pH7.5-9.0) for 15min, following the procedure described in section 2.2.7. The specificity towards different substrates (Raf, Sta, Ver, Gol, and Mel) was tested at 50mM final concentrations at pH 8.0 and with an incubation of 1h. The desalting procedure and HPLC analysis were performed as described in sections 2.2.5 and 2.2.6.

Digalactosyl diacylglycerol (DGDG) and monogalactosyl diacylglycerol (MGDG) assays followed described methods (Dinur et al., 1984; Grossmann and Terra, 2001). Briefly, 1mg of DGDG or MGDG (Materya LLC, Pleasant Gap, USA) was solubilized in 1ml chloroform/methanol (2:1) solution containing 0.5% Triton X-100 and 0.12% taurocholate, followed by 10min of vacuum drying and re-suspension in 0.5ml assay buffer (100mM HEPES pH8.0) by 5min of sonication. For assays, 20 $\mu\text{l}$  of the protein crude extract (in 100mM HEPES pH8.0, 5mM  $\text{MgCl}_2$ , 1mM NaEDTA, 20mM DTT, 1mM PMSF, 0.05% Triton X-100) were incubated with 20 $\mu\text{l}$  of solubilized DGDG or MGDG (1mg  $\text{ml}^{-1}$  final concentration) at 30°C for 1h. The reaction was stopped by boiling the samples for 6min. After desalting (section 2.2.5), HPLC analysis was performed as described in section 2.2.6.

### 3.3 Results

#### 3.3.1 *AtDIN10* contains a putative chloroplast transit peptide (cTP)

*AtDIN10* shares amino acid identities of 54, 55 and 58%, respectively, with *ATSIP1*, *ATSIP2* and *Osakagall* (Os08g38710; Lee et al., 2004; Lee et al., 2009). When aligned with *AtSIP1* and *-2*, a 95 amino acid peptide sequence was clearly unique to *AtDIN10* (**Fig.1**). *In silico* analyzes using different prediction program tools (ChloroP, <http://www.cbs.dtu.dk/services/ChloroP/> ; WoLF PSORT, <http://wolfsort.org/>; AtSubP, <http://bioinfo3.noble.org/AtSubP/>; PredSL, <http://hannibal.biol.uoa.gr> /PredSL/) predicted the presence of a chloroplast transit peptide (cTP) at the amino terminus of the *AtDIN10* protein predicted to be cleaved after amino acid 76 (cleavage site [CS] score 4.091).

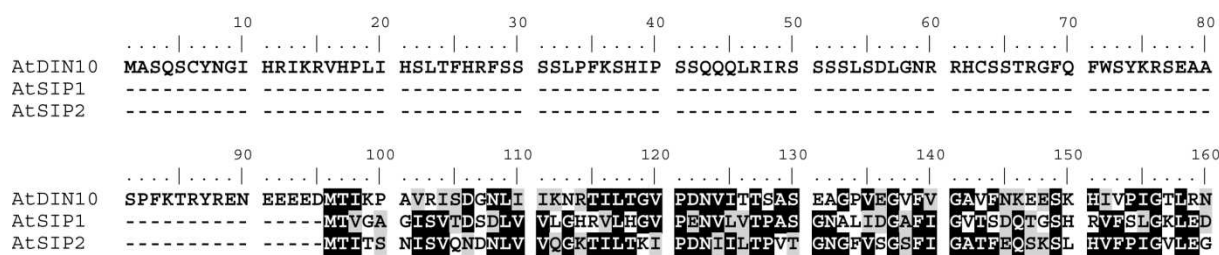


**Fig.1.** Alignment of the first 160 amino acids of *AtDIN10* (At5g20250) with the N-terminal parts of the *AtSIP1* (At1g55740) and *ATSIP2* (At3g57520) protein sequences. Alignment was performed using the BioEdit software (<http://www.mbio.ncsu.edu/bioedit/bioedit.html>).

#### 3.3.2 *AtDIN10* is located in the chloroplast

The putative cTP described for *AtDIN10* (above) suggested a chloroplastic location of the protein. When a C-terminal *AtDIN10-GFP* fusion construct was transiently transformed into *Arabidopsis* protoplasts, CLSM analyses revealed a strong fluorescence signal associated with GFP in the chloroplasts (**Fig.2** *AtDIN10-GFP* column C). Thereby, GFP fluorescence largely showed spots inside the chloroplast that largely co-localized with chlorophyll fluorescence, unlike free GFP (mainly found in the cytosol). By contrast, GFP fusions with translocon of the inner chloroplast envelope 110 (TIC110) showed distinct chlorophyll and GFP fluorescence signals as expected (Schenk et al., 2007; Schelbert et al., 2009), indicating envelope location (**Fig.2**, TIC110-GFP column C). From these results, we conclude that *AtDIN10* is located inside the chloroplast.

By investigating the topology of AtDIN10 using the plant membrane protein database ARAMEMNON (<http://aramemnon.botanik.uni-koeln.de/>), no transmembrane domain seems to be present in the corresponding protein (*i.e.* the protein is soluble), arguing for a stromal location of AtDIN10.

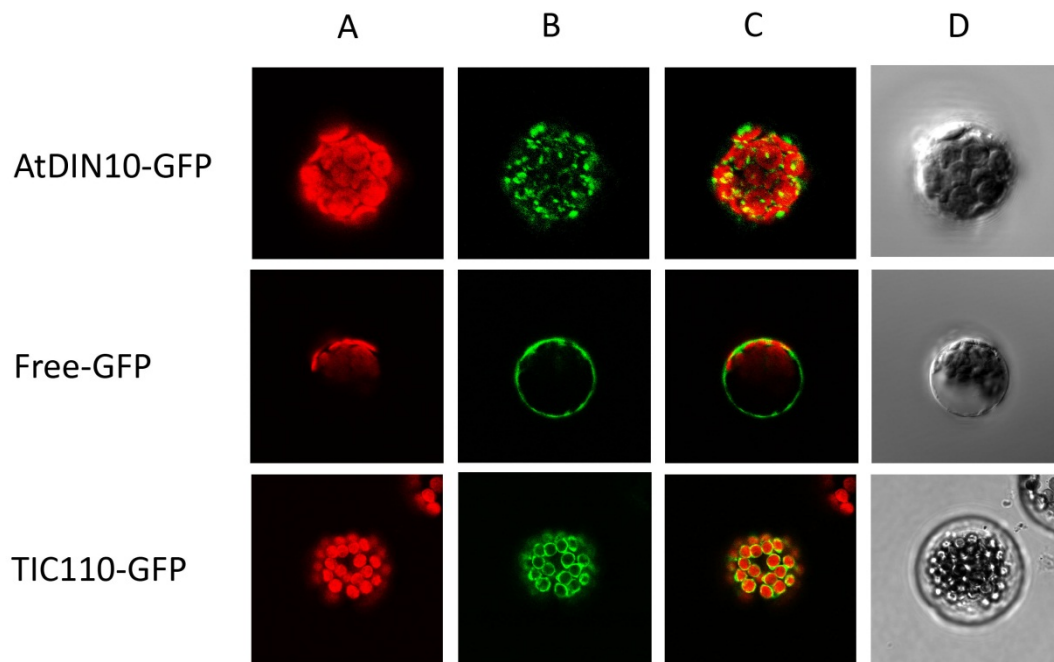


**Fig.2.** Transient expression in Arabidopsis mesophyll protoplasts of GFP fused in frame to the N-terminus of AtDIN10 (AtDIN10-GFP). Free GFP was used as a cytosolic control and TIC110-GFP for chloroplast envelope localization. Chlorophyll autofluorescence (column A) and GFP fluorescence (column B) were examined by confocal laser scanning microscopy. Column C: merge of GFP and autofluorescence; column D, bright field image. Protoplast diameter is approx. 20µm.

### 3.3.3 AtDIN10 is an alkaline $\alpha$ Gal

Crude extracts from *Sf9* cells infected with a baculovirus carrying *AtDIN10* cDNA were assayed for alkaline  $\alpha$ Gal activity with the artificial substrates pNP $\alpha$ Gal and pNP $\beta$ Gal. AtDIN10 showed an activity for the substrate pNP $\alpha$ Gal (1.26nkat mg<sup>-1</sup> total protein, HEPES-KOH pH8.0) but did not hydrolyze the  $\beta$ -linked pNPGal variant (pNP $\beta$ Gal), indicating that AtDIN10, like AtSIP1 and -2, shows hydrolytic activity specifically on  $\alpha$ -D-galactosidic linkages (**Fig.3A, B**). The recombinant protein was active between pH 6.5 and pH9.0 with maximum activity at pH 8.0 (**Fig.3B**). These define AtDIN10 as an alkaline  $\alpha$ Gal, as it is the case for AT SIP1 (pH optimum at 8.5) and AT SIP2 (pH optimum at 7.5). RafS activity was also investigated by incubating crude extracts with the appropriate substrates (100mM Suc and 10mM Gol) but no RafS was detected (data not shown), comparable to the results described for AT SIP1 and -2 see section 2.3.1).

Subsequently, the substrate specificity of AtDIN10 for various galacto-oligosaccharides and -lipids was determined (in HEPES buffer, pH8). AtDIN10 displayed good hydrolytic activities toward a broad spectrum of  $\alpha$ 1,6-galactosyl oligosaccharides with a preference for Raf (0.308nkat mg<sup>-1</sup> total protein) and Sta (0.299nkat mg<sup>-1</sup> total protein). However, all other tested oligosaccharides substrates, *i.e.* Mel (0.058nkat mg<sup>-1</sup> total protein), Ver (0.165nkat mg<sup>-1</sup> total protein) and Gol (0.126nkat mg<sup>-1</sup> total protein) were also hydrolyzed, albeit with lower activity (**Fig.3C**). When tested with 1mg ml<sup>-1</sup> MGDG or DGDG, the most highly abundant galactolipids present in the chloroplast membranes, no activity was detected. This was expected for MGDG because it contains an endo- $\beta$ -galactosidic linkage but unexpected for DGDG which does contain an endo- $\alpha$ -galactosidic linkage. One explanation for the absence of activity on DGDG could be problems with solubilization of this lipophilic substrate. Indeed, precipitates always appeared in the lipid preparation. It is also important to note that the oligosaccharide concentrations used for the assays were 50-fold higher than that of the galactolipids (50mM for the oligosaccharides, 1.05mM for DGDG and 1.27mM for MGDG). Because of the relatively low sensitivity of the HPLC system used, this could have led to a failure to detect the Gal product. We are planning to measure the Gal released from the reaction with an enzyme-linked assay using Gal dehydrogenase (section 4.2.10) like it was previously shown for the OsakaGal characterization (Lee et al., 2004).

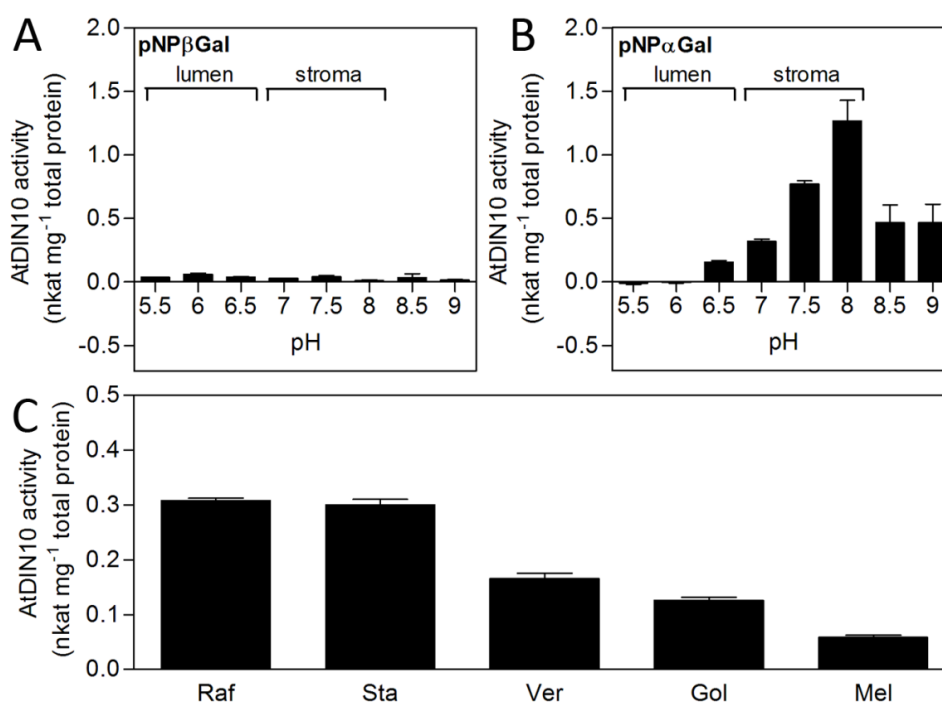


**Fig.3.** Preliminary biochemical characterization of recombinant AtDIN10. A. A crude extract of *Sf9* cells containing recombinant AtDIN10 is not active with 3mM pNPβGal in the pH range of 5.5-8.0. B. Crude extracts of *Sf9* containing recombinant AtDIN10 display a pH optimum at pH8.0 with 3mM of pNPαGal. The typical pH ranges of the lumenal and stromal compartments in chloroplasts are depicted above the diagrams. C. Recombinant AtDIN10 protein showed activity towards different oligosaccharides with a preference for Raf and Sta (measured at pH 8 with 50mM of each Raf, Sta, Ver, Gol, and Mel). Data are means  $\pm$  SE of six replicates.



### 3.4 Discussion

The structural and functional organization of thylakoid membranes is important for the dynamics and flexibility of the photosynthetic apparatus. Galactolipids play a crucial role in the structure and stability of photosynthetic complexes in the thylakoids. An appropriate ratio of MGDG to DGDG is required to maintain the intricate bilayer characteristics for insertion, folding, movement and conformational changes of membrane proteins (Webb and Green, 1991). However, very little work has been performed to understand the molecular and biochemical events that lead to the disassembly of thylakoid driving membrane senescence. Many studies have concentrated on chlorophyll and protein degradation during chloroplast breakdown (Martínez et al., 2008; Hörtensteiner, 2009). At the early stage of leaf senescence, a gradual breakdown of thylakoid membranes occurs, which is accompanied by chlorophyll breakdown (Woolhouse, 1984; Thompson et al., 1998; Lee and Chen, 2002). Plastoglobuli, which contain lipid-pigment-protein components originating from deteriorating thylakoids, are formed in the stroma of senescing chloroplasts and possibly secreted to the cytoplasm or vacuole for further degradation (Guamét et al., 1999; Lee and Chen, 2002). During senescence, their size and abundance increase, indicating an important function in lipid metabolism.

Nomenclature and annotation of *AtDIN10* is controversial in the literature as previously highlighted for *ATSIP1* and -2 (see chapter II). The first report dealing with this gene annotated *AtDIN10* as *AtSIP3* because of its homology to other members of the SIP family (Fujiki et al., 2001; Zhao et al., 2006), and the authors suggested a putative  $\alpha$ Gal function of the protein. However, *AtDIN10* was recently also described as a putative abiotic stress-inducible RafS (RS6; Nishizawa et al., 2008). By performing a protein sequence alignment with *ATSIP1* and -2, we identified a cTP consisting of 95 amino acids that suggested *AtDIN10* to be chloroplastic (**Fig.1**). Transient expression of an N-terminal *AtDIN10::GFP* fusion in *Arabidopsis* mesophyll protoplasts confirmed that *AtDIN10* is located in the chloroplast, possibly in the stroma, since (i) the *AtDIN10::GFP* fluorescence signal was comparable to a glucose-6-phosphate dehydrogenase-GFP signal that localizes in the stroma (Meyer et al., 2011) and (ii) comparison of the *AtDIN10::GFP* fluorescence signal with *TIC110::GFP*, which is located in the inner chloroplast membrane, could definitively place *AtDIN10::GFP* internal of the inner chloroplast envelope (**Fig.2**).

Interestingly, one alkaline  $\alpha$ Gal from rice (*Osak $\alpha$ Gal*), also localizing to the chloroplast and being up-regulated during dark-induced senescence in leaves, was shown to hydrolyze  $\alpha$ 1,6-galactosyl

oligosaccharides and DGDG (Lee et al., 2004). Furthermore, over-expression of the cDNA in rice led to transgenic plants with misformed chloroplasts. Collectively, these observations strongly suggest that OsakaGal is a chloroplastic alkaline  $\alpha$ -Gal responsible for thylakoid membrane turnover in rice chloroplasts undergoing senescence. *AtDIN10* transcripts were also up-regulated early during dark-induced senescence (3h dark-incubation; Fujiki et al., 2000; Fujiki et al., 2001) and besides AtDIN10 shares 58% amino acid identities with OsakaGal.

In this chapter, I showed that AtDIN10 is effectively a *bona fide* alkaline  $\alpha$ Gal and not a RafS. It has a pH optimum of 8.0 and hydrolyzes a broad range of galacto-oligosaccharide substrates such as Ver, Sta, Raf, Gol, and Mel (Fig.3). As demonstrated for OsakaGal, I tested the putative activity on MGDG and DGDG substrates. Unfortunately, I have thus far been unable to conclusively determine if recombinant AtDIN10 is active on the galactolipid substrates but I am currently optimizing the assay used to solubilize the lipid substrates prior to their use in activity assays and use more sensitive method to detect Gal units released from DGDG.

Interestingly, our initial biochemical characterization of recombinant AtDIN10 (using the artificial substrates pNP $\alpha$ Gal) yielded a strong  $\alpha$ -D-Gal hydrolytic activity in the alkaline pH range. Inside the chloroplast is the only alkaline pH compartment, the stroma (pH7.0-8.0; Raven, 1997). In addition to the observations that an AtDIN10::GFP fusion protein is targeted to the chloroplast (internal to the inner chloroplast envelope, Fig.2) and is a soluble protein, this strongly supports the assumption that AtDIN10 is a stromal protein.

Different roles for AtDIN10 have been hypothesized. For example, *AtDIN10* transcripts were up-regulated within hours after the addition of 50 $\mu$ M methylviologen, an enhancer of the production of O<sub>2</sub><sup>-</sup>, in four-week-old soil-grown plants, suggesting a putative role of AtDIN10 in response to oxidative stress (Nishizawa et al., 2008). Secondly, AtDIN10 would have a role in the mobilization of cold-stress induced Raf accumulation in chloroplasts of Arabidopsis. *AtDIN10* transcripts were shown to be up-regulated after 1d of cold treatment (Maruyama et al., 2009) and it was recently shown that Raf is indeed (partly) accumulated in the chloroplast (Schneider and Keller, 2009; Knaupp et al., 2011).

During senescence, RFOs seem to accumulate in leaves of *Populus nigra* (Fialho and B cker, 1996). A proposed role for AtDIN10 would be to hydrolyze DGDG in the chloroplast during leaf senescence, therefore releasing Gal which could potentially be mobilized to synthesize Raf in the cytosol. However, solving the technical problems concerning the galactolipid substrate preparation is

required to prove whether AtDIN10 is a galactolipid hydrolase *in vivo*. To follow this hypothesis suggesting that AtDIN10 could be the OsakaGal homolog in Arabidopsis and is able to degrade DGDG, we are currently investigating T-DNA mutant insertion lines for *AtDIN10* to test whether these lines are compromised in senescence-related lipid metabolism. This work will be followed within the framework of the collaboration project between Dr. Shaun Peters and Prof. Dr. Stefan Hörtensteiner.

## Chapter IV:

An *Arabidopsis* T-DNA insertion mutant for galactokinase (*AtGALK1*, At3g06580) hyper-accumulates free galactose and exhibits insensitivity to exogenous galactose



## 4.1. Introduction

Galactokinase (GALK) catalyzes the MgATP-dependent phosphorylation of  $\alpha$ -D-Gal to  $\alpha$ -D-Gal1P. GALK activity has been reported in purified extracts from *Phaseolus aureus* seedlings (mung bean; Chan and Hassid, 1975), fenugreek seeds (Foglietti and Percheron, 1976) and *Vicia faba* (broad bean; Dey, 1983). Arabidopsis GALK (*AtGALK*, At3g06580) was first identified via the ability of the cDNA to functionally rescue the Gal growth deficiency of a yeast GALK mutant ( $\Delta$ gal1, Kaplan et al., 1997). Further evidence for the identity of *AtGALK* was reported by expression of the cDNA in an *E. coli* GALK mutant deficient in GALK activity (Sherson et al., 1999). In that study, GALK activity was measured in mutants heterologously expressing *AtGALK*. More recently, *AtGALK* was comprehensively biochemically characterized after expression of the cDNA in *E. coli* (Yang et al., 2009). To date this remains the only GALK reported from Arabidopsis.

The toxicity of free Gal is well established across the taxonomic kingdom (see section 1.2.3). In humans it is quite clear that Gal1P accumulation is responsible of the toxicity (Lai et al., 2009). The mechanism of this toxicity in plants is largely unknown. One possibility is that it occurs as a consequence of the buildup of Gal1P which in turn inhibits phosphoglucomutase (catalyzing  $\text{Glc1P} \leftrightarrow \text{Glc6P}$ ), therefore preventing the incorporation of Glc into cellulose. Gal1P can also act as a competitive inhibitor of UTP: Glc1P uridylyltransferase thereby inhibiting the formation of UDP-Glc, a precursor of cellulose biosynthesis (Inouhe et al., 1986). Although these hypotheses argue for a direct role of GALK in Gal toxicity, other mechanisms of toxicity are also proposed to exist (Dey et al., 1980). For example, a study with a Gal-resistant sugar cane cell lines pointed to UDP-Gal being the toxic metabolite as this cell line had much higher levels of UDP-Glc/UDP-Gal 4-epimerase (catalyzing  $\text{UDP-Gal} \leftrightarrow \text{UDP-Glc}$ ), and as a result accumulated much less UDP-Gal than non-resistant cell lines (Maretzki and Thom, 1978). Another study also proposed that a possible UDP-Gal build-up could be toxic, due to a low endogenous UGE activity (Dörmann and Benning, 1998).

In this thesis, I report on the identification and characterization of an *AtGALK* T-DNA *loss-of-function* mutant (*atgalk*) that is (i) *AtGALK* transcript deficient, (ii) displays no GALK activity in vegetative tissues (leaves and roots), and (iii) and accumulates Gal up to 6.83mg g<sup>-1</sup> FW in vegetative tissues, contrary to WT plants. By constitutively overexpressing the *AtGALK* cDNA, *atgalk* was functionally rescued. Three independent transformed lines showed restored *AtGALK* transcripts and GALK activity and had low leaf Gal concentrations comparable to those observed in WT plants. Surprisingly, *in vitro*-grown *atgalk* plants were largely insensitive to the exogenous application of up to 100mM free Gal, whilst WT plants exhibited sensitivity to low Gal concentration (10mM), accumulating up to

57mg g<sup>-1</sup> FW in leaves. Leaves from soil-grown *atgalk* plants that exhibited no growth or morphological defects were used to demonstrate the accumulating Gal occurred exclusively in the vacuoles of mesophyll protoplasts. I provide evidence to suggest that a hitherto unknown detoxification pathway for Gal, which apparently targets Gal to the vacuoles is active in the of *atgalk* mutant background.

## 4.2. Materials and methods

### 4.2.1 Plant material and growth conditions

Arabidopsis plants were grown as previously described (2.2.1).

### 4.2.2 Screening for T-DNA insertion lines

Six independent T-DNA insertion lines for *AtGALK* were initially screened (SALK\_081223, SALK\_115263, SALK\_118504, SALK\_118505, SAIL\_315\_F01 and GABI-Kat 489D10). Genomic DNA was extracted from leaves as previously described (Edwards et al., 1991). Homozygosity determined by PCR using a combination of gene primers for *AtGALK* and a T-DNA specific primer as described in section 2.2.2 (**Table1**). Despite obtaining homozygous plants for the T-DNA insertion into *AtGALK* for all the lines tested, only the GABI-Kat 489D10 line displayed a high Gal “chemotype”.

**Table1.** Primer used for *AtGALK* T-DNA insertion lines screening. The wild-type allele was amplified with the primer pairs LP+RP and the mutant allele with the primer pairs LB+RP primer sets for SALK and SAIL lines. For GABI line the wild-type allele was amplified with *GABI<sub>fwd</sub>*+*GABI<sub>rev</sub>* and the mutant allele with *GABI<sub>fwd</sub>*+ *T-DNA<sub>GABI</sub>*.

Primer name	Sequence
<i>SALK_GALK<sub>LP</sub></i>	5'- TTAACATTTGCAATCCGAAGC-3'
<i>SALK_GALK<sub>RP</sub></i>	5'-AACAAACGGTTAACCGGAAAAC-3'
<i>LBb1.3</i>	5'-ATTTTGCCGATTTTCGGAAC-3'
<i>SAIL_315_f01<sub>LP</sub></i>	5'-TTGAACCCTAAACCCTATGGC-3'
<i>SAIL_315_f01<sub>RP</sub></i>	5'-TATCCTGACGAATAGCCATCG-3'
<i>PSCA110<sub>LB1</sub></i>	5'-GCCTTTTCAGAAATGGATAAATAGCCTTGCTTCC-3'
<i>GABI<sub>fwd</sub></i>	5'-GTTTGGAGCTTTGGTGTCTAT-3'
<i>GABI<sub>rev</sub></i>	5'-AATTGATGCGTACCTTAACAG-3'
<i>T-DNA<sub>GABI</sub></i>	5'- CCCATTTGGACGTGAATGTAGACAC-3'

### 4.2.3 Recombinant *AtGALK* expression in *Sf9* insect cells

The *AtGALK* cDNA (At3g06580) was obtained as a full length RIKEN clone (pda 09727, [www.brc.riken.jp](http://www.brc.riken.jp), Seki et al., 1998; Seki et al., 2002) and amplified using CDS specific primers (*GALK<sub>fwd</sub>*: 5' ATGGCGAAACCGGAAGAAGTAT-3', *GALK<sub>rev</sub>*: 5' TTAGAGGTTGAAGATGGC AGC-3') with the Expand High Fidelity PCR system (Roche). *AtGALK* was sub-cloned by standard restriction digest and ligation reactions, from pGEM-T Easy into the pFastBac1 vector, using the *NotI* restriction endonuclease. The construction and expression of *AtGALK* in *Sf9* insect cells followed the protocol described in 2.2.3.



#### 4.2.4. GALK activity assay and biochemical characterization of recombinant AtGALK

*Sf9* cells were collected as previously described (2.2.3). Total GALK activity was measured radiometrically with D-[ $^{14}$ C]-Gal as the substrate as previously described (Keller and Matile, 1985), with minor modifications. The incubation mixture (300 $\mu$ l) contained 25 $\mu$ l of clarified extract, 1mM ATP, 5mM MgCl<sub>2</sub>, 10mM NaF, 1mM DTT (1,4 dithiotreitol), 50mM HEPES-KOH pH7.5, 1mM D-Gal, 22.2kBq [ $^{14}$ C]-Gal (specific activity 2035MBq mmol<sup>-1</sup>, Hartmann Analytic, Braunschweig, Germany). The assay was conducted for 15min at 30°C. The pH optimum of AtGALK was determined with 50mM MES-KOH (pH5.0-6.5), 50mM HEPES-KOH (pH 6.5-8.5) and 50mM Tris-HCl (pH8.0-9.0).

#### 4.2.5 GALK analysis of plant crude extract

Freshly harvested leaf material (200mg) was ground in 400 $\mu$ l of chilled extraction buffer and desalted through Sephadex columns as previously described (see section 2.2.10). Total GALK activity was measured radiometrically with D-[ $^{14}$ C]-Gal as the substrate as described in 4.2.4 by incubating 50 $\mu$ l of plant desalted extract in a total volume of (300 $\mu$ l).

#### 4.2.6 Construction of *atgalk/35S::AtGALK* rescued lines

The *AtGALK* CDS (4.2.3) was cloned into the pCR8/GW/TOPO vector system (Invitrogen) and subcloned into the GATEWAY destination vector pMDC32 (Curtis and Grossniklaus, 2003) using a conventional LR clonase reaction (Invitrogen). This construct was transformed into *Agrobacterium tumefaciens* (GV3101) by electroporation, using a Genepulser (2.5kV; 100 $\Omega$ ; 25 $\mu$ F, Bio-Rad). Arabidopsis *atgalk* mutant plants were transformed and hygromycin-resistant (25 $\mu$ l ml<sup>-1</sup>) plants were selected as described in section 2.2.12. T2 and T3 transgenic plants were used for analysis.

#### 4.2.7 RNA isolation and semi-quantitative PCR (sqPCR)

Total RNA was extracted as previously described in 2.2.11. The sqPCR was carried out in 50 $\mu$ l containing 5 $\mu$ l cDNA, 0.5mM of each dNTP, and 0.5 $\mu$ mol of each primer, 1X PCR buffer and 1.25U GoTaq DNA polymerase (Promega), at a primer annealing temperature of 56°C for 24 cycles. (linear range of the constitutively expressed *RPS16A* (At2g09990); **Table2**) or 58°C for 23 cycles [linear range of the constitutively expressed *ACTIN2* (*ACT2*, At3g18780)]. *GALK* CDS specific primer pair (see 4.2.3) was used to amplify the corresponding cDNA. For the monosaccharide proton symporter *AtSTP1* sqPCR we designed a primer pair that amplified around 1kb CDS fragment (**Table2**).

**Table2.** Primer pairs used for sqPCR analyses.

Primer name	Sequence
<i>RPS16A</i> <sub>fwd</sub>	5' GGCGACTCAACCAGCTACTGA-3'
<i>RPS16A</i> <sub>rev</sub>	5' CGGTAACCTTCTGGTAACGA-3'
<i>ACT2</i> <sub>fwd</sub>	5' ATGGCTGAGGCTGATGATAT-3'
<i>ACT2</i> <sub>rev</sub>	5' TTAGAAACATTTTCTGTGAACGAT-3'
<i>AtSTP1</i> <sub>fwd</sub>	5' ATGCCTGCCGGTGGATTTC-3'
<i>AtSTP1</i> <sub>rev</sub>	5' CGGCCACGTTAACCGAGC-3'
<i>AtTMT1</i> <sub>fwd</sub>	5' ATGAAGGGAGCGACTCTCGTT-3'
<i>AtTMT1</i> <sub>rev</sub>	5' AATGAGCCGGTTTACCGTGA-3'
<i>AtTMT2</i> <sub>fwd</sub>	5' GACATGCCTCACACTGCTCA-3'
<i>AtTMT2</i> <sub>rev</sub>	5' TCACTCGTTTTTAGCAGCTTCA-3'
<i>AtTMT3</i> <sub>fwd</sub>	5' ATGAGGAGTGTAGTGCTTGTTGC-3'
<i>AtTMT3</i> <sub>rev</sub>	5' GGAGAAAGCAGAGGACTGTTTAA-3'

#### 4.2.8 Water soluble carbohydrate (WSC) extraction

WSCs were extracted and analyzed from 100mg six-week-old soil grown Arabidopsis leaf material as described in section 2.2.16.

#### 4.2.9 Isolation of mesophyll protoplasts and vacuoles from Arabidopsis

Arabidopsis protoplasts and vacuoles were prepared as previously described (see section 3.2.3). Recovered protoplasts were digested in 10 volumes of lysis solution described in Frelet-Barrand et al. (2008). Progression of vacuole release was continuously controlled by microscopy and vacuoles were purified and concentrated by centrifugation (1400g, 8min) using a step gradient as follows: lower phase, one volume of lysate; middle phase, one volume of a 1:1 mixture of lysis solution and betaine buffer (0.4M betaine, 30mM K-gluconate, 20mM HEPES-Imidazol pH 7.2, 1 mg ml<sup>-1</sup> BSA, 1 mM DTT) and upper phase, 1/3 volume of betain buffer. Vacuoles were collected from the interface between the middle and upper phase. For vacuolar yield determination, the activities of the soluble vacuolar enzymes,  $\alpha$ Gal,  $\alpha$ -mannosidase, and  $\beta$ -N-acetylglucosaminidase, were measured using the *p*-nitrophenyl substrates (see section 2.2.7; Keller and Matile, 1985). For extra-vacuolar contamination, NADH-malate dehydrogenase activity (mainly contamination by mitochondria, peroxisomes, and cytosol) and chlorophyll concentration (contamination by chloroplasts) were determined as previously described (Lichtenthaler and Wellburn, 1983; Schneider and Keller, 2009).

#### 4.2.10 Enzymatic quantification of Gal

To confirm the Gal quantification routinely obtained by the HPLC-PAD method, free Gal content was also quantified enzymatically. The enzymatic Gal determination was performed with  $\beta$ -D-Gal dehydrogenase from *Pseudomonas fluorescens* (Roche) which catalyzes the reaction:



The reaction was performed in a 96-well micro-titer plate (total volume 260µl) containing 35µl of desalted extract, 200µl of 100mM Tris-HCl, pH 8.6, 25µl of 16.5mM NAD and 3mU of  $\beta\text{-D-Gal}$  dehydrogenase. The assay was incubated for 1h at 37°C and the absorbance was read at 340nm and compared with a Gal standard curve.

#### 4.2.11 Gal toxicity assays

Surface-sterilized *Arabidopsis* seeds (WT, *atgalk* and *atgalk/35S:AtGALK*) were sown onto half-strength MS medium and grown for 7d in a controlled environment chamber (16h light, 100µmol photons m<sup>-2</sup> s<sup>-1</sup>, 22°C, 8h dark, 65% RH). Seedlings were then transferred onto half-strength MS supplemented with Gal (10 and 100mM). After a further 7d, leaf material was harvested and images of seedlings were captured using a digital camera. <sup>14</sup>C-Gal uptake was measured by transferring the plants after 7d initial growth onto half-strength MS medium supplemented with 0.1mM Gal and 3.7kBq <sup>14</sup>C-Gal for 7 additional days. Sugar phosphates were extracted as described (Sekiguchi et al., 2004). Briefly, leaf material was flash-frozen and ground in liquid nitrogen. Boiling water (500µl) was added to the sample and the extract was immediately mixed and irradiated with 600W in a microwave oven for 15s. After centrifugation (4°C, 10min), the supernatant was filtered through a 0.45µm filter and analyzed by HPLC, using a CarboPac PA1 column with a NaOH Na-acetate gradient (Table3). <sup>14</sup>C-carbohydrates and sugar phosphates were detected by separation on a BC100 column (see section 2.2.6) or CarboPac PA1 column with NaOH Na-acetate gradient coupled to a FLO-ONE radio chromatography detector (Model A-525X, Packard, Zürich, Switzerland).

**Table3.** HPLC system specifications used to analyze sugar phosphates.

Degassing	Helium				
Pump	Dionex GP 50				
Injector	Dionex ASI-100				
Stationary phase	CarboPac PA1 (4x250mm)				
Mobile phase	Eluent1: H <sub>2</sub> O, Eluent2: 1M NaOH, Eluent3: 1M Na-acetate, Eluent4: H <sub>2</sub> O				
Flow rate	1ml min <sup>-1</sup>				
Temperature	30°C				
Elution	NaOH, Na-acetate gradient				
	<b>Time (min)</b>	<b>1%</b>	<b>2%</b>	<b>3%</b>	<b>4%</b>
	<b>0</b>	40	10	10	40
	<b>20</b>	35	10	20	35
	<b>30</b>	20	10	50	20
	<b>40</b>	40	10	10	40
Post column addition	None				
Detection	Dionex ED 50				
Integration	Chromeleon v. 6.5 Dionex				

## 4.3 Results

### 4.3.1 AtGALK was functionally expressed and biochemically characterized

AtGALK was heterologously expressed in *Sf9* insect cells. The presence of AtGALK RNA in the infected cells was confirmed by sqRT-PCR. Crude extracts from *Sf9* cells infected with a baculovirus carrying the AtGALK cDNA was clearly able to convert Gal in the presence of MgATP to Gal1P, contrary to crude extracts from uninfected *Sf9* cells. The pH optimum of this reaction was determined to be about 7.5 (**Fig.1A**) with substrate concentrations of 1mM Gal and 1mM ATP. The AtGALK activity displayed an end-product inhibition of 50% inhibition at 20mM Gal1P (**Fig.1B**). AtGALK showed Michaelis-Menten type kinetics with apparent  $K_m$  and  $V_{max}$  values of  $89 \pm 13 \mu\text{M}$  and  $1.10 \pm 0.05 \text{ nkat mg}^{-1} \text{ protein}$  for ATP (**Fig.1C**) and apparent  $K_m$  and  $V_{max}$  of  $0.47 \pm 0.09 \text{ mM}$  and  $1.40 \pm 0.08 \text{ nkat mg}^{-1} \text{ protein}$  for Gal, respectively (**Fig.1D**).

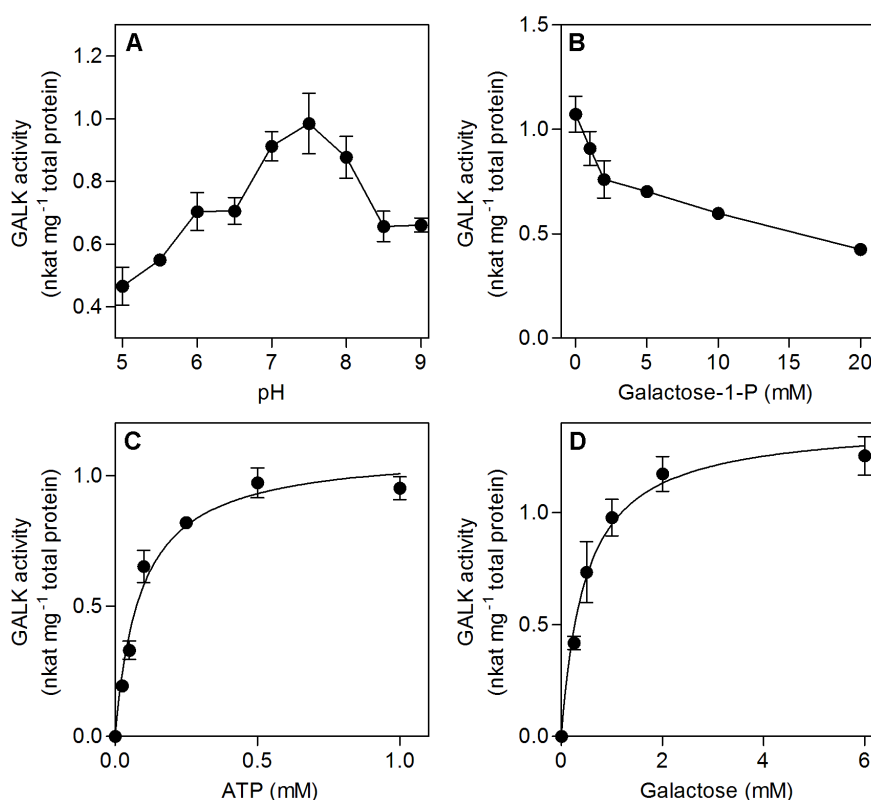


**Fig.1.** Biochemical characterization of recombinant AtGALK enzyme. A. The pH dependence shows a pH optimum around pH 7.5 with 1mMGal and 1mM ATP as substrates (MES, HEPES, TRIS buffers). B. The Gal1P inhibition curve of AtGALK at pH7.5 and with 1mM Gal and 1mM ATP shows 50% inhibition at 20mM Gal1P. C. The ATP concentration dependence shows Michaelis-Menten type kinetics with apparent  $K_m$  and  $V_{max}$  values of  $89 \pm 13 \mu\text{M}$  and  $1.10 \pm 0.05 \text{ nkat mg}^{-1} \text{ protein}$ , respectively. D. The Gal concentration dependence shows Michaelis-Menten type kinetics with apparent  $K_m$  and  $V_{max}$  values of  $0.47 \pm 0.09 \text{ mM}$  and  $1.40 \pm 0.08 \text{ nkat mg}^{-1} \text{ protein}$ , respectively. Data are means  $\pm$  SE of three replicates.

### 4.3.2 Characterization of an *atgalk* T-DNA insertion line

Of the six independent T-DNA insertion lines genotyped as homozygous for T-DNA insertions into *AtGALK* only one homozygous line (*atgalk*, GABI-Kat 489D10; **Fig.2**) showed distinct high free Gal in vegetative tissue (leaves and roots), when WSC extracts were analyzed by HPLC-PAD (**Fig.3B**). In independent experiments, WSC extracts from vegetative tissue of WT plants showed only trace amounts of free Gal (or none at all) (**Fig.3B, 4C, 6B, C**). Both WT-like plants (individuals genotyped as WT in zygosity screens) and WT plants (Col-0) had comparable WSC profiles; only WT-like plants were used in further experimentation (named WT in the rest of the chapter).

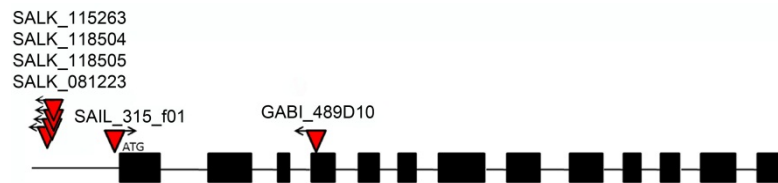


**Fig.2.** T-DNA insertion map in *AtGALK* gene. Lines identified and screened for T-DNA insertion in *AtGALK* (SALK\_081223, SALK\_115263, SALK\_118504, SALK\_118505, SAIL\_315\_F01 and GABI-Kat 489D10).

Interestingly, the first generation of the *atgalk* line showed growth retardation and a dwarf phenotype with smaller leaves and slower growth rate compared to WT plants (**Fig.3**). Subsequent generations of this parental *atgalk* plant lost this phenotype but the Gal “chemotype” was still present.

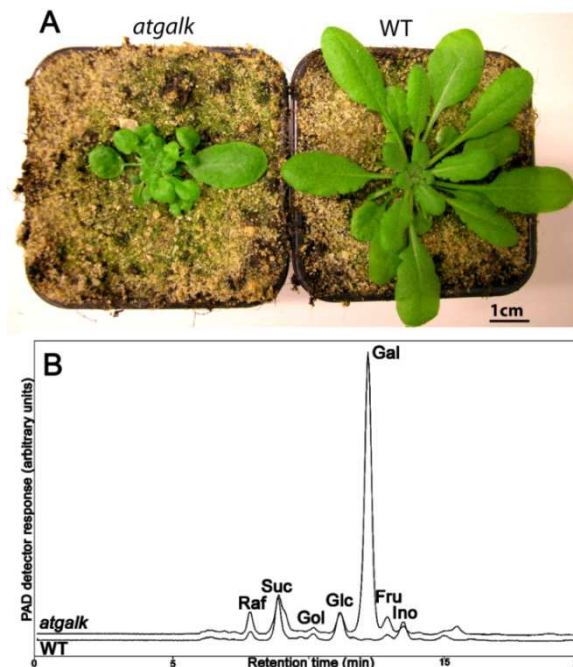


**Fig.3.** A. Phenotype of six-week-old first generation homozygous *atgalk* plants and WT plants (representative). B. HPLC traces showing the carbohydrate profile of *atgalk* compared to WT. Gal is present only in trace amount in WT leaves, whereas large quantities accumulate in the *atgalk* leaves. WT, wild-type-like; Raf, Raffinose; Suc, sucrose; Gol, galactinol; Gal, galactose; Fru, fructose; Ino, *myo*-inositol.

Using sqPCR, *AtGALK* transcripts were shown to be constitutively present in vegetative tissues (leaves and roots) of WT plants but to be absent in vegetative tissues of *atgalk* plants (Fig.4A, 6B). Similarly, total GALK activity was constitutive in the leaves (about 0.072nkat g<sup>-1</sup> FW) and roots (about 0.035nkat g<sup>-1</sup> F; Fig.4B, 6A) of WT plants and completely absent in leaves of *atgalk* plants (Fig. 4B, 6A). Quantitative HPLC-PAD analyses of WSCs from vegetative tissues of these plants demonstrated that free Gal accumulated up to 6.83mg g<sup>-1</sup> FW in the leaves and 5.76mg g<sup>-1</sup> FW in the roots of *atgalk* plants (Fig.3B, 4C, 6B).

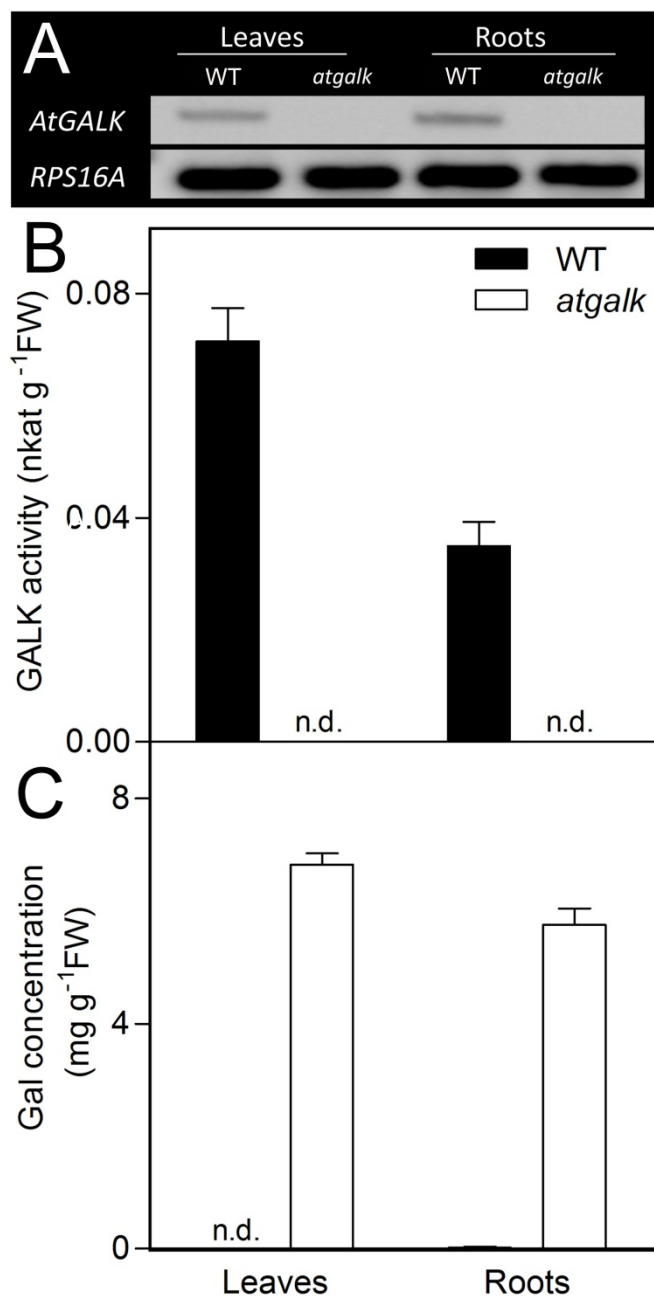


**Fig.4.** Analysis of the leaves and roots from soil-grown WT and *atgalk* plants. A. sqPCR with *AtGALK* CDS primers. The *RPS16A* gene was used as a constitutively expressed control. B. GALK activity in leaves and roots of soil-grown WT and *atgalk* plants. C. Gal concentration in the vegetative tissues of soil-grown WT and *atgalk* plants. Data are means  $\pm$  SE of five replicates.

### 4.3.3. Functional rescue of *atgalk*

The *atgalk* mutant was transformed with a construct carrying the *AtGALK* cDNA under the control of the *CaMV35S* promoter (*atgalk/35S::AtGALK*). Six independent, transformed lines were genotyped by PCR, screening amplifying mutant and WT alleles (Fig.5A). All the lines carrying the *AtGALK* overexpression construct were genotyped as homozygous for the T-DNA insertion into *AtGALK*. However, they contained *AtGALK* transcripts in leaves and displayed various GALK activities positively correlated to the transcript abundance (Fig.5B, C). Three transformed lines (L1, L4, L5) were chosen to analyze T2/T3 generations. GALK activity was detected in leaves and roots of the three *atgalk/35S::AtGALK* lines between 16 to 71% of the GALK activity in leaves of WT plants (values for T3: L1, 0.012nkat g<sup>-1</sup> FW; L4, 0.050nkat g<sup>-1</sup> FW; L5, 0.023nkat g<sup>-1</sup> FW, respectively, Fig.5C, 6A, C). Most importantly, HPLC-PAD analyses of WSC extracts from the leaves of all three lines showed a complete reversion of the high free Gal observed, in *atgalk*, to concentrations comparable to the leaves and roots of WT plants (Fig.6B, C).

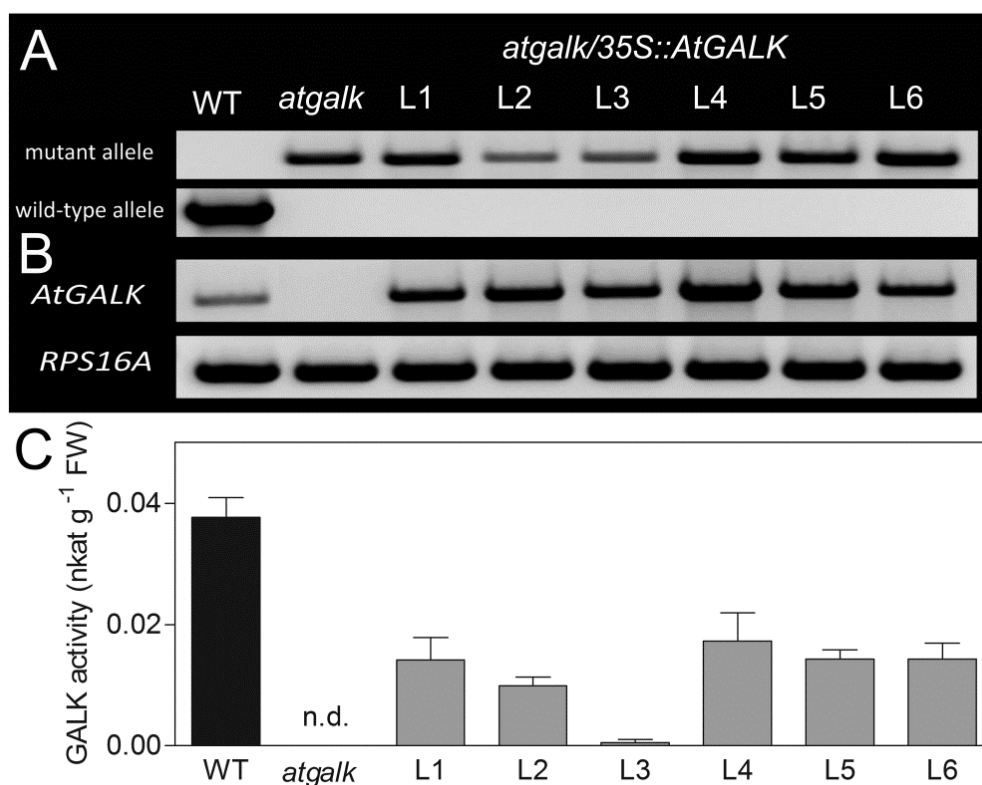


**Fig.5.** Characterization of hygromycin-resistant T2 *atgalk/35S::AtGALK* lines. A, zygosity screen on genomic DNA demonstrating that all *atgalk/35S::AtGALK* lines retain homozygosity for the T-DNA insertion in *AtGALK*. B, sqPCR of *atgalk/35S::AtGALK* lines confirming the restoration of *AtGALK* transcripts in the *atgalk* mutant background. The *RPS16A* gene (At2g09990) was used as a constitutively expressed control. C, The extractable GALK activities (in leaves) of the various lines were measured at pH 7.5 using 1 mM ATP, 1 mM Gal and 22.2 kBq [1-<sup>14</sup>C]Gal. Data are means ± SE of three replicates.



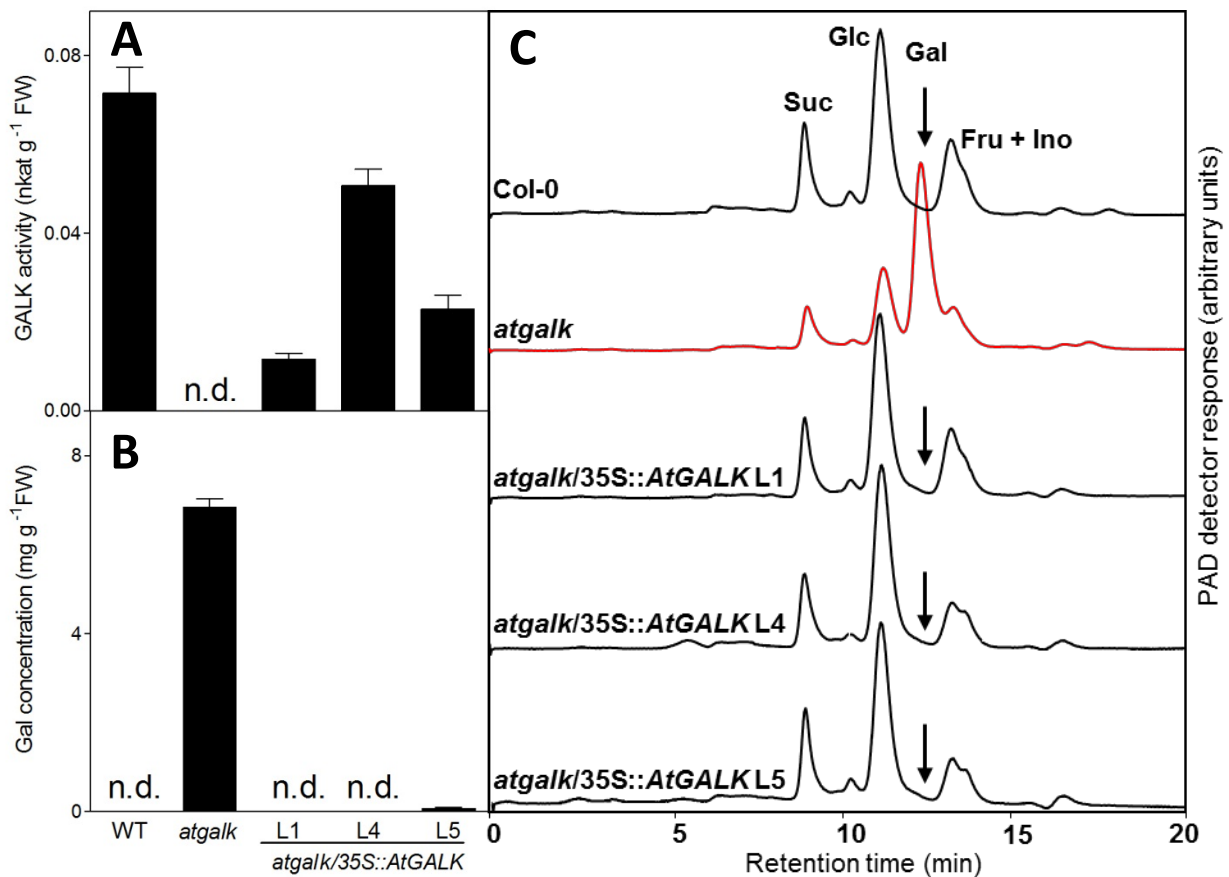


**Fig.6.** Characterization of WT, *atgalk* and *atgalk/35S::AtGALK* plants (T3 generation) A. *atgalk/35S::AtGALK* lines restored GALK activity partially. B. Gal concentration in WT, *atgalk* and *atgalk/35S::AtGALK* showed that *atgalk/35S::AtGALK* lines had a similar free Gal level than WT plants. Data are means  $\pm$  SE of six replicates. C. HPLC traces of carbohydrate content in WT, *atgalk* and the three chosen *atgalk/35S::AtGALK* rescued lines. WT, wild-type; Suc, sucrose; Glc, glucose; Gal, galactose; Fru, fructose; Ino, *myo*-inositol; n.d., not detected.

#### 4.3.4. *In vitro*-grown *atgalk* seedlings exhibit insensitivity to exogenous Gal

Seedlings grown on half-strength MS (7d-old) were transferred onto half-strength MS supplemented with Gal (10 or 100mM). After a further 7d, WT plantlets showed distinct growth defects on both 10mM Gal (some root elongation, but reduced lateral root formation) and 100mM Gal (complete growth arrest, **Fig.7**). Conversely, *atgalk* seedlings appeared little affected (some reduced lateral root formation and rosette size) by either of these Gal concentrations and growth was similar to WT and *atgalk* seedlings after 14d on Gal-free MS medium. Surprisingly, both T2 and T3 *atgalk/35S::AtGALK* lines retained this Gal insensitivity showing comparable growth characteristics to *atgalk* seedlings grown under 10 and 100mM free Gal (**Fig.7**), despite complete functional rescue (described above).



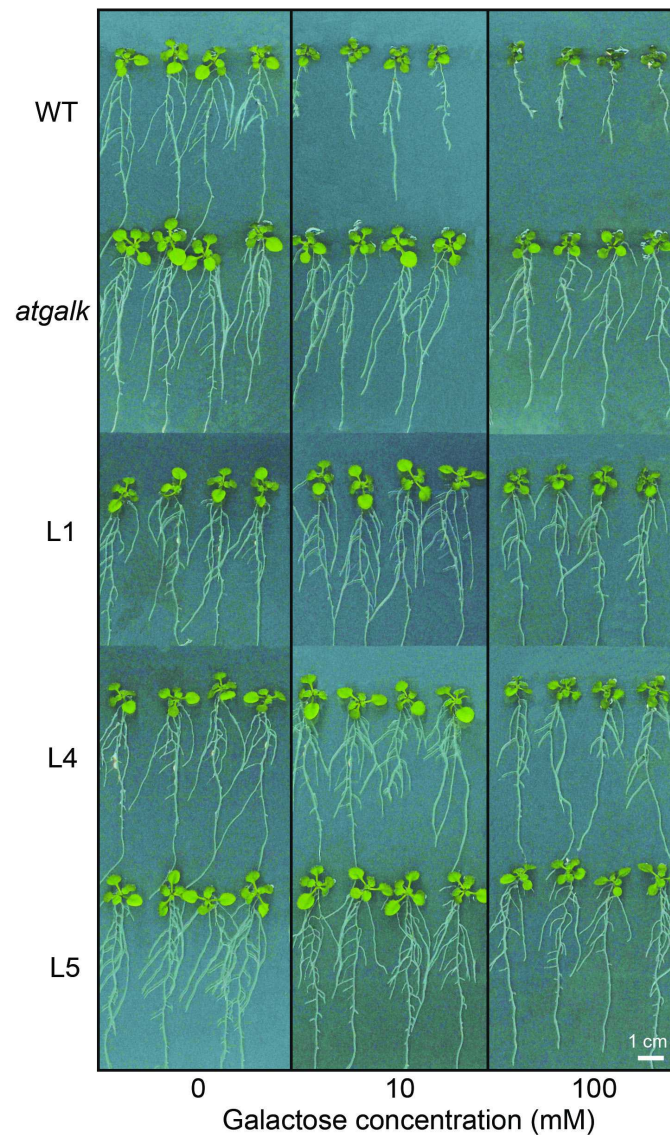


**Fig.7.** Representative images of seedlings from wild-type, *atgalk* and *atgalk/35S::AtGALK* lines L1, L4 and L5 grown on half-strength MS medium for 7 d and subsequently transferred to half-strength MS medium supplemented with Gal (10 or 100 mM) for a further 7 d.

#### 4.3.5 Free Gal accumulates in leaf mesophyll vacuoles of *atgalk* plants

To determine the subcellular localization of the Gal accumulation observed in leaves of *atgalk* plants, vacuoles were isolated from *atgalk* leaf mesophyll protoplasts (**Fig.8**). In three independent experiments, the vacuolar fractions were shown to be very pure; no activity of the combined mitochondrial, peroxisomal and cytosolic marker, NADH-malate dehydrogenase (NADH-MDH) and only traces (1.99%) of chlorophyll present in the protoplasts were detected in isolated vacuoles (**Table4**). The distribution of Gal closely paralleled that of the vacuolar marker enzyme,  $\beta$ -N-acetylglucosaminidase, allowing the conclusion that the free Gal present in the leaves of the *atgalk* mutant occurs exclusively in the vacuole (**Table4**). This was strikingly different to protoplast and

vacuole preparations from WT plants where no Gal was detected in the protoplasts. By performing Gal enzymatic determination we observed exactly the same Gal concentration values than those measured with HPLC-PAD (data not shown).

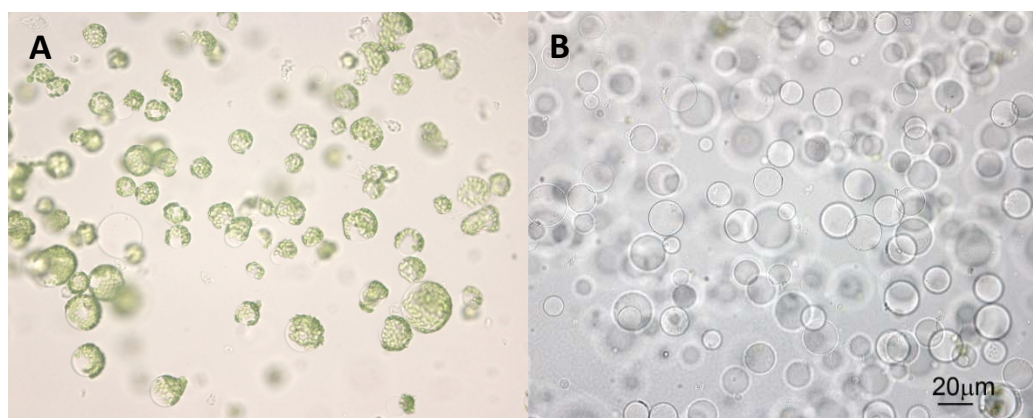


**Fig.8.** Bright field microscopy of protoplasts and vacuoles isolated from 6-week-old soil grown *Arabidopsis atgalk*. A. Protoplast fraction. B. Vacuolar fraction.

**Table4.** Vacuolar localization of Gal in mesophyll protoplasts isolated from leaves of *atgalk* plants. Mesophyll protoplasts and vacuoles were isolated from leaves of six-week-old *atgalk* plants. NADH-malate dehydrogenase activity (mainly indicating contamination by mitochondria, peroxisomes, and cytosol) and chlorophyll concentration (indicating contamination by chloroplasts) served as extra-vacuolar markers.  $\beta$ -*N*-acetylglucosaminidase activity was assumed to be exclusively located in the vacuole. This was confirmed in a control experiment using an additional, well-established vacuolar marker enzyme,  $\alpha$ -mannosidase (Keller and Matile, 1985; data not shown). Gal was analyzed by HPLC-PAD on a BC-100 column and the data confirmed by enzymatic Gal determination using the  $\beta$ -*D*-Gal dehydrogenase method. Data are means  $\pm$  SE of three independent experiments. Chl, Chlorophyll; n.d., not detected.

Substance/enzyme	Protoplasts	Percentage in vacuoles
	$\mu\text{g or nkat ml}^{-1}$	
NADH-malate dehydrogenase	$12.8 \pm 0.8$	n.d.
Chl	$256 \pm 90$	$1.99 \pm 1.78$
$\beta$ - <i>N</i> -acetylglucosaminidase	$0.44 \pm 0.26$	100
Gal	$225 \pm 31$	$123 \pm 13$

#### 4.3.6 Uptake mechanisms for free Gal are unaffected in *atgalk* plants

To determine if the Gal insensitivity displayed in the *atgalk* mutant background was not due to cessation of Gal uptake mechanisms, I firstly tested if *atgalk* plants were able to take up exogenously supplied Gal through the roots, seedlings were propagated on half-strength MS supplemented with either 10mM (WT) or 100mM Gal (*atgalk*, L1, L4, L5). After 7d, WSCs were extracted from the seedlings and analyzed by HPLC-PAD. Gal concentrations were slightly higher in WT seedlings ( $0.35\text{mg g}^{-1}$  FW, **Fig.9A**). Since 100mM Gal resulted in complete growth arrest in WT plants, I then analyzed the WSC profiles of WT seedlings grown on 10mM exogenous Gal and *atgalk* seedlings on

100mM exogenous Gal. In *atgalk* seedlings, Gal concentrations were found to be 10-fold higher ( $57.38\text{mg g}^{-1}\text{FW}$ ) when they were grown on 100mM Gal. The *atgalk/35S::AtGALK* lines (L1, 4 and 5) all showed varying degrees of Gal accumulation when grown on 100mM Gal ( $1.27\text{mg g}^{-1}\text{FW}$  to  $11.44\text{mg g}^{-1}\text{FW}$  Fig.9A) but never to the extent of Gal accumulation observed in *atgalk* seedlings. The *atgalk/35S::AtGALK* L4, closest to the WT (Fig.6) showed the lowest Gal concentration, probably because these plants metabolized Gal more rapidly than the others. Additionally, *atgalk* seedlings grown for 7d on 0.1mM Gal supplemented with  $3.7\text{kBq }^{14}\text{C}$ -Gal per plate showed a massive  $^{14}\text{C}$ -Gal accumulation in their leaves (Fig.9B). The leaves of WT plants exposed to the same treatment did not show any  $^{14}\text{C}$ -Gal (Fig.9B) nor the potentially toxic  $^{14}\text{C}$ -Gal1P as determined by radio-HPLC analysis of leaf  $^{14}\text{C}$ -sugar phosphates (data not shown). WT plants grown on toxic concentration of Gal (10mM) supplemented with  $3.7\text{kBq }^{14}\text{C}$ -Gal per plate did not show any  $^{14}\text{C}$ -Gal nor  $^{14}\text{C}$ -Gal1P accumulation in their leaves either (data not shown).

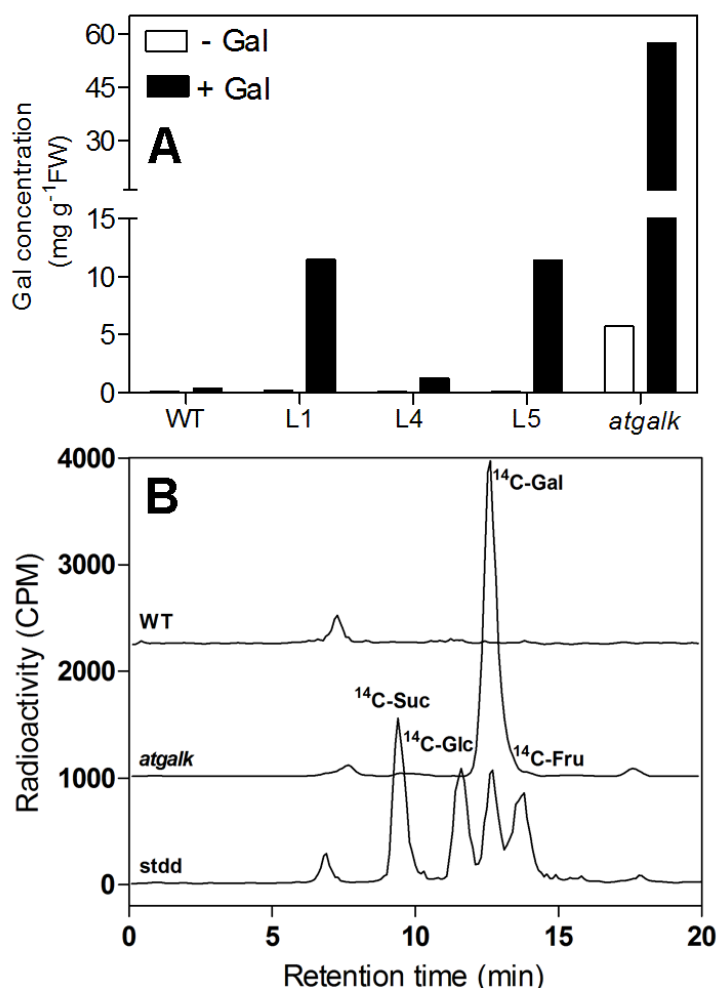


**Fig.9.** Seedlings grown for 7d on Gal medium are transporting Gal in their leaves. A. Carbohydrate concentration of two weeks old seedlings exposed to high Gal concentration for 7d (10mM Gal for WT, 100mM for *atgalk/35S::AtGALK* L1, L4, L5 and *atgalk*). B. HPLC traces representing radio-labeled carbohydrate peaks of WT and *atgalk* seedlings supplemented with  $3.7\text{kBq }^{14}\text{C}$ -Gal per plate and 0.1mM Gal for 7d analyzed with the BC-100 column coupled with a FLO-ONE radio chromatography detector. CPM, counts per minute.

In parallel, using sqPCR I analyzed the *atgalk* roots for the presence of transcripts of the *AtSTP1* (At1g11260) gene. This monosaccharide proton symporter was previously suggested to be the primary Gal root transporter in Arabidopsis (Sherson et al., 2000). *AtSTP1* transcript levels of were comparable in both WT and *atgalk* roots grown on half-strength MS without Gal (**Fig.10A**). However, we observed a down-regulation of *AtSTP1* transcripts in the WT plants grown on toxic levels of Gal and no difference in transcript abundance in the *atgalk* grown on 100mM Gal. SqPCR of three well-described tonoplast monosaccharide transporters (*AtTMT1*, *AtTMT2* and *AtTMT3*) revealed that the TMTs transcripts were expressed similarly and at a low level in WT and *atgalk* leaves of plants grown on half-strength MS without Gal (**Fig.10B**).

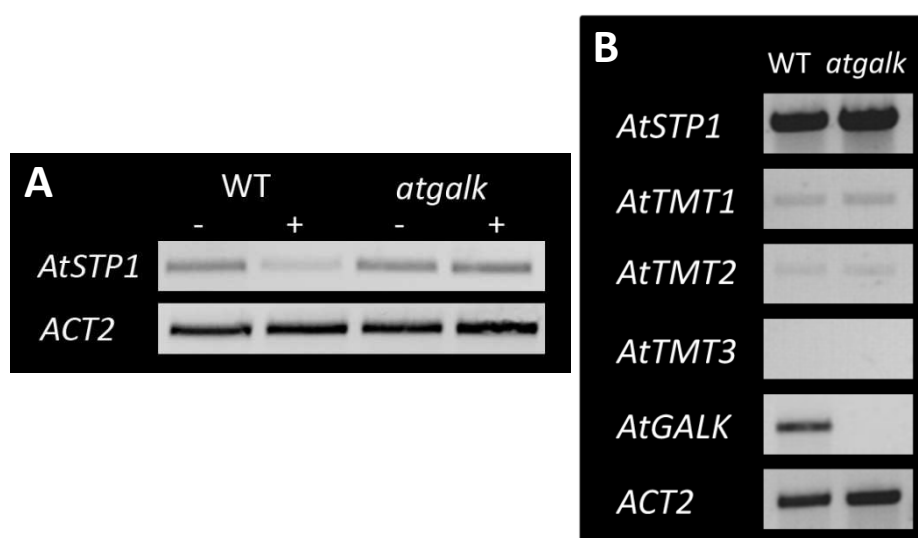


**Fig.10.** SqPCR of cDNA from WT and *atgalk*. A. Analyzes of roots of two weeks-old plants grown 7d on half-strength MS (-) or half-strength MS medium supplemented with Gal (+; 10mM for WT and 100mM for *atgalk* seedlings). B. Analyzes of leaves of plants grown 14d on half-strength MS. The *ACTIN2* gene was used as a constitutively expressed control. *AtSTP1* (At1g11260), *AtTMT1* (At1g20840), *AtTMT2* (At4g35300), *AtTMT3* (At3g51490).

## 4.4 Discussion

GALK is a cytosolic enzyme which catalyzes the MgATP-dependent phosphorylation of  $\alpha$ -D-Gal at the C1 position to  $\alpha$ -D-Gal1P. To date only one GALK has been reported in Arabidopsis. Our first goal was to biochemically characterize AtGALK using the Sf9 insect cell system. Crude extracts from Sf9 cells infected with a baculovirus carrying *AtGALK* showed a GALK activity *in vitro*, contrary to crude extracts from uninfected Sf9 cells. This activity was showed by typical Michaelis-Menten type kinetics with apparent  $K_m$  and  $V_{max}$  values of  $89 \pm 13 \mu\text{M}$  and  $1.09 \pm 0.04 \text{ nkat mg}^{-1} \text{ protein}$  for ATP and  $470 \pm 90 \mu\text{M}$  and  $1.4 \pm 0.08 \text{ nkat mg}^{-1} \text{ protein}$  for Gal, respectively. The pH optimum was about 7.5 (**Fig.1**). These findings are quite different from those recently reported when *AtGALK* was heterologously expressed in *E. coli* [ $K_m$  of  $701 \mu\text{M}$  for ATP,  $K_m$  of  $701 \mu\text{M}$  for Gal; Yang et al., 2009], i.e. the  $K_m$  values for *E. coli*-expressed AtGALK protein (7.86-fold higher for ATP and 1.42-fold higher for Gal) was compared to our Sf9 cell expressed AtGALK protein. The exact reason for this discrepancy using these two vastly different expression systems is currently not known.

Having confirmed that AtGALK encodes a genuine GALK, we investigated GALK deficient mutant lines. Analyses of six independent T-DNA insertion lines identified only a single unique T-DNA *loss-of-function* mutant (*atgalk*) for *AtGALK* (At3g06580) where both *AtGALK* expression and GALK activity in vegetative tissues (leaves and roots) were completely abolished. In WT plants, *AtGALK* transcripts were present in vegetative tissues and a constitutive GALK activity could be measured. Consequent to *AtGALK loss-of-function (atgalk)* mutants hyper-accumulated Gal in vegetative tissues up to 7 and  $6 \text{ mg g}^{-1} \text{ FW}$  in leaves and roots, respectively, whereas only traces could be detected in the vegetative tissues of WT plants (**Fig.3, 4, 6**). Collectively, these observations point to *AtGALK* occurring as a single copy gene in Arabidopsis, as previously suggested (Sherson et al., 1999). Despite free Gal being reported to be cytotoxic to plants (Maretzki and Thom, 1978; Yamamoto et al., 1988) even at very low concentrations ( $\text{LD}_{50} = 0.7 \mu\text{M}$  for maize; Roberts et al., 1971), *atgalk* plants showed no obvious morphological or growth defects when grown in soil or *in vitro*. We could, however, detect a dwarf phenotype, but only in the first generation of *atgalk* plants. Further generation lost this growth retardation.

Since our initial analyses yielded only one single T-DNA *loss-of-function* mutant characterized by the absence of GALK activity and hyper-accumulation of Gal in vegetative tissues, *AtGALK* was constitutively over-expressed in the *atgalk* background. Three independent *atgalk/35S::AtGALK* lines were selected where leaf GALK activity was restored to between 15-70% of the activity of WT leaves.



Even the lowest activity recovered (15%, line 1) was wholly sufficient to reduce the high free Gal concentrations in the leaves of this line to concentrations comparable to those in WT leaves (**Fig.6**). All three *atgalk/35S::AtGALK* lines were confirmed to still genotype as homozygous for the T-DNA insertion into *AtGALK* demonstrating explicitly, that the absence of *AtGALK* in the *atgalk* background was alone responsible for the high Gal concentrations observed in vegetative tissues.

An astonishing finding was that *in vitro*-grown *atgalk* seedlings were completely insensitive to exogenous application of Gal up to 100mM, whilst WT seedlings showed growth defects such as epinastic leaves, reduction in root length, and lateral root abundance on concentrations as low as 5mM and severe growth retardation as low as 10mM (cessation of leaf and root growth). An identical Gal insensitivity has been previously reported for a T-DNA *loss-of-function* mutant for the monosaccharide proton symporter *AtSTP1* (At1g11260) which exhibits substrate specificity for mannose and Gal (Sherson et al., 1999). In that study, *atstp1* mutants were also insensitive to exogenous Gal application up to 100mM. The authors concluded that since diffusional uptake of hexoses across the plasma membrane is negligible, hexose uptake in Arabidopsis seedlings (under normal physiological conditions) was entirely *AtSTP1*-dependent. This would effectively explain the Gal insensitivity of the *atstp1 loss-of-function* mutant (no Gal uptake when grown on 100mM Gal). However, such explanations were insufficient when considering the Gal insensitivity observed in the *atgalk* mutant since vegetative tissues already contain up to 7 mg g<sup>-1</sup> FW Gal prior to the addition of exogenous Gal and would be predicted to still contain a functional *STP1*. To confirm that the exogenous Gal-insensitive phenotype of *atgalk* seedlings was not due to a cessation of Gal uptake, the roots of 7d-old *in vitro* grown seedlings were exposed to exogenous <sup>14</sup>C-Gal and 1mM Gal for additional 7d. Leaf WSCs were then analyzed by HPLC-PAD. We could conclusively demonstrate that <sup>14</sup>C-Gal appeared in the leaves of *atgalk* seedlings, confirming that the proposed *AtSTP*-mediated hexose uptake pathway was still active in the *atgalk* background. In parallel, we performed sqPCR on roots of seedlings grown 7d in the presence or absence of toxic Gal concentrations and *AtSTP1* transcripts could be detected in both WT and *atgalk* in Gal and no Gal conditions supporting that *AtSTP1* would still be active in *atgalk* plants.

Under our normal growing conditions (for soil-grown plants) and during routine HPLC-PAD analyses we have never observed leaf Gal concentrations exceeding 0.3mg g<sup>-1</sup> FW in Arabidopsis WT leaves. Since *atgalk loss-of-function* (i) completely abolished *GALK* activity, (ii) led to Gal hyper-accumulation (with no growth defects), and (iii) to an exogenous Gal-insensitive phenotype, we believed that a hitherto unknown detoxification pathway for free Gal could explain the Gal insensitivity of *atgalk*. Furthermore, we speculated that the existence of such a pathway may have only become apparent

because of the artificial physiological state (high free Gal) in the *atgalk* mutant background. In further experiments, we looked to the most obvious detoxification compartment in the cell, the vacuole, and asked if the vacuoles of WT and *atgalk* plants showed differences in their WSC profiles. Protoplasts and subsequently vacuoles were isolated from the leaves of soil-grown WT and *atgalk* plants. Compartmentation analyses of WSCs revealed that *atgalk* vacuoles contained all the free Gal occurring in *atgalk* protoplasts, while no Gal was present in the vacuoles of WT plants (Table 4). This observation would appear to support our argument for a novel free Gal detoxification pathway being activated in the *atgalk* mutant background, allowing the mutant to sequester the excess Gal already present in vegetative tissues to the vacuoles. This would also explain the lack of any morphological defects and, possibly, the Gal insensitivity apparent in *atgalk*.

Our hypothesis that a novel Gal detoxification pathway becomes active in the *atgalk* mutant relies on the presence of a tonoplastic monosaccharide transporter able to transport Gal into the vacuole. As a first step to understand how the putative Gal detoxification mechanism might work, *in vivo*, we looked to three well-described tonoplast monosaccharide transporters in Arabidopsis (*AtTMT1* to -3, *At1g20840*, *At4g35300* and *At3g51490*, respectively; Wormit et al., 2006). In that study, analyses of TMT *loss-of-function* mutants strongly suggested their function in Glc transport into the vacuole. However, none have been tested for their ability to transport Gal. Using sqPCR, we analyzed the transcript abundance of the three TMTs in the leaves of *atgalk* and WT plants. All three TMTs transcripts were expressed at a low level and there was no significant up-regulation of one of these genes in the *atgalk* leaves compared to WT.

Surprisingly, the Gal insensitivity observed in *atgalk* seedlings was retained in the three *atgalk/35S::AtGALK* lines (T2, Fig. 7). We additionally tested T3 generation seedlings and still found them to be completely insensitive to 100mM exogenous Gal as *atgalk* seedlings are. We assumed that the retention of the Gal insensitivity, despite an apparently complete functional rescue of the *atgalk* mutant background, may imply that the putative Gal detoxification pathway was still active in the *atgalk/35S::AtGALK* lines. We compared leaf Gal concentrations of these lines after they had been exposed to exogenous Gal application (half-strength MS + 100mM Gal) for 7d. We could indeed measure high Gal concentrations (up to 11.44mg g<sup>-1</sup> FW) in the leaves of plants exposed to Gal and no Gal in control plants (half-strength MS alone), suggesting that *atgalk/35S::AtGALK* plants take up Gal actively (presumably STP-mediated).

When two-week-old WT plants were analyzed for sugar phosphates, no Gal1P or <sup>14</sup>C-Gal1P was detected under all the conditions tested (half-strength MS alone, half-strength MS supplemented

with 10mM Gal, half-strength MS supplemented with 3.7kBq  $^{14}\text{C}$ -Gal and 1mM Gal per plate or half-strength MS supplemented with 3.6kBq  $^{14}\text{C}$ -Gal per plate and 10mM Gal), suggesting that, in the WT plants, there is no accumulation of the direct GALK product, Gal1P, even under stressed conditions (10mM Gal) which denies the hypothesis of Gal1P being the toxic compound (Yamamoto et al., 1988). As proposed by Dörmann and Benning (1998), a possible UDP-Gal build-up due to a low endogenous UGE activity could be responsible for the Gal toxicity.

In summary, I have functionally expressed and characterized AtGALK in *Sf9* cells isolated and characterized a T-DNA *loss-of-function* mutant for AtGALK that (i) shows no GALK activity, (ii) hyper-accumulates free Gal up to  $6.83\text{mg g}^{-1}$  FW Gal, (iii) appears to sequester the free Gal to the vacuoles, and (iv) presents a distinct exogenous Gal-insensitive phenotype. Collectively, these observations led us to speculate that a novel free Gal detoxification was active in the *atgalk* background, but we were unable to show any difference in the transcript abundance of three characterized tonoplast monosaccharide transporters, suggesting that another tonoplastic transporter may exist.





## **Chapter V:**

### **General discussion, conclusions and outlook**



## 5.1 General discussion and conclusions

Research interest in RFOs has historically focused on (i) their role in carbon translocation in plants which use RFOs as their primary phloem mobile-carbohydrates (*e.g.* Turgeon, 1996; Gao et al., 1999), (ii) genes involved in biosynthesis and their role/s in the acquisition of abiotic stress-resistance (*e.g.* Taji et al., 2002; Pennycooke et al., 2003; Pukacka et al., 2009; dos Santos et al., 2011; Li et al., 2011) and (iii) the process leading to the accumulation on storage RFOs. It is now well established that Raf plays a crucial role in the abiotic stress tolerance response of *Arabidopsis* (Cook et al., 2004; Rhodes et al., 2004; Kaplan et al., 2007; Knaupp et al., 2011). However, attempts to dissect RFO functional roles *in vivo* have resulted in controversy, particularly in the cold acclimation response of *Arabidopsis*, where Raf was shown to accumulate but suggested to have no functional role (Zuther et al., 2004). In spite of ample evidence demonstrating a significant shift in RFO status of plants during stress events, most of the studies have focused on the RFO biosynthesis and only few studies were devoted to the equally important process of RFO catabolism, such as stress relief (*e.g.* Pennycooke et al., 2004), phloem unloading (*e.g.* Gao and Schaffer, 1999; Carmi et al., 2003) and seed germination (for a review see Keller and Pharr, 1996). During seed germination, one study revealed that the inhibition of Raf breakdown delayed germination in pea (Blöchl et al., 2007), but another study claimed that RFO breakdown is not essential for proper germination in soybean (Dierking and Bilyeu, 2009). These seemingly controversial results illustrate that the exact function(s) of RFOs during abiotic stress and seed germination are far from being clearly understood.

The only known mechanism by which Gal units of RFOs or other  $\alpha$ -D-galactosides is liberated for further metabolism in vascular plants is through hydrolysis of the galactosidic bonds in these compounds by  $\alpha$ Gals (**Fig.1**).  $\alpha$ Gals have been well studied, probably because of their industrial applications. For example,  $\alpha$ Gals can be used to hydrolyze the galactoside residues typically found in RFOs of legume seeds and that are not digestible in our intestine and thus causing flatulence (Wang et al., 2003a). In plants,  $\alpha$ Gals have mainly received attention in fundamental research the main foci being seed germination and phloem unloading. In *Arabidopsis*, no alkaline  $\alpha$ Gal has been characterized thus far and only one acid  $\alpha$ Gal (AtGAL2; At5g08370) has been investigated with the analysis of heterozygous T-DNA insertion lines. This acid  $\alpha$ Gal was suggested to play an important role in leaf development, *i.e.* cell wall loosening during cell growth (Chrost et al., 2007).

Contrary to Gal hydrolysis Gal phosphorylation (the second step of RFO catabolism) has received more research attention in Arabidopsis, where the only GALK, AtGALK, was recently identified and biochemically characterized (Kaplan et al., 1997; Yang et al., 2009). Further steps downstream of  $\alpha$ Gal and GALK include the production of UDP-Gal by the action of UDPGal/Glc pyrophosphorylases (Gronwald et al., 2008) and of UDP-Glc by the action of UDP-Glc 4-epimerases (Barber et al., 2006) and are quite well studied.

The goals of my thesis were to dissect the first two steps of RFO catabolism in Arabidopsis and functionally characterize the putative and ambiguously annotated corresponding genes. **Fig.1** summarizes the first steps of RFO catabolism, schematically. The focal points of my thesis are indicated in red and include the alkaline  $\alpha$ Gals, ATSIP1, ATSIP2 and AtDN10, as well as the GALK, AtGALK.

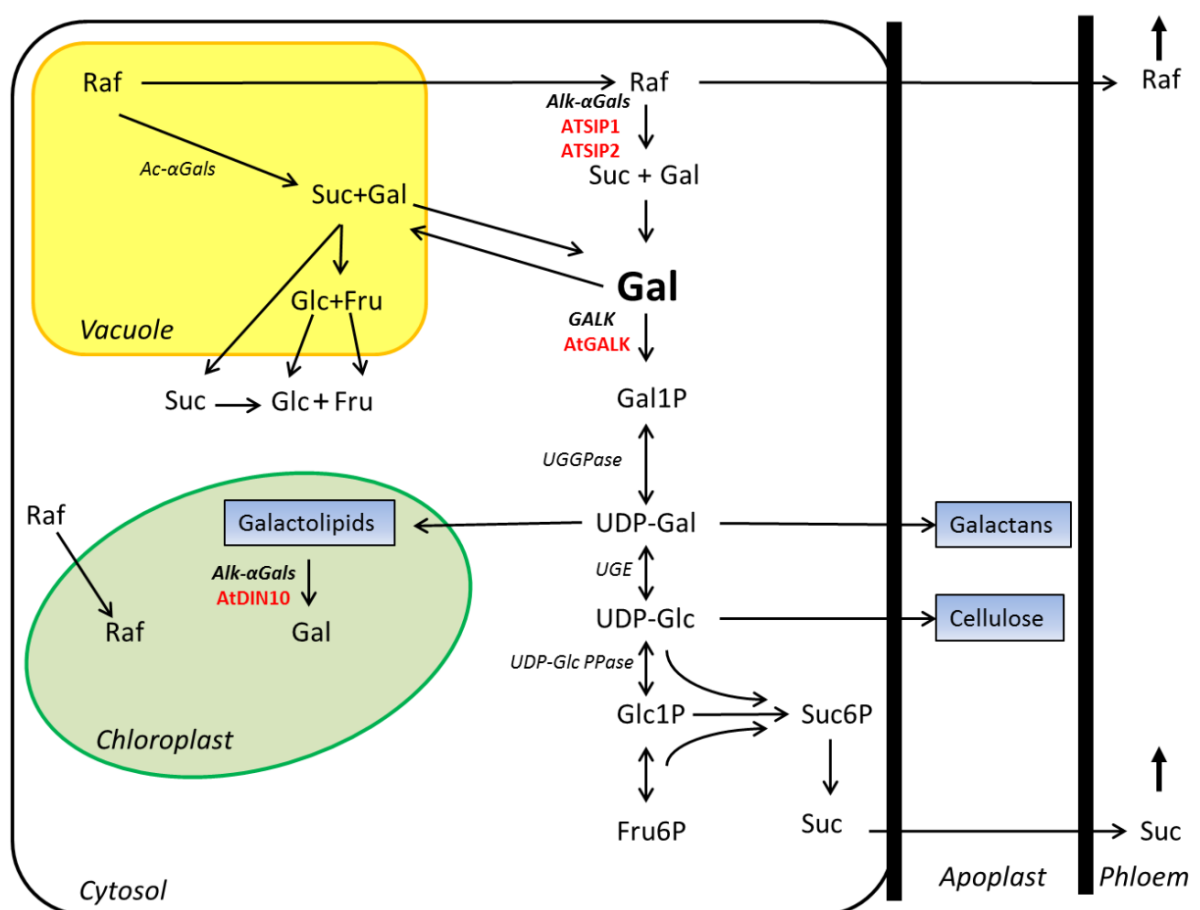


**Fig.1.** RFO catabolism in plants. Enzymes/genes studied during my thesis are indicated in red. Cell wall-bound Gal is designated as “galactans”. Ac- $\alpha$ Gals, acid  $\alpha$ -galactosidase (EC 3.2.1.2.2); Alk- $\alpha$ Gals, alkaline  $\alpha$ -galactosidase (EC 3.2.1.2.2); GALK, galactokinase (EC 2.7.1.6); UGGPase, UDP-galactose/glucose pyrophosphorylase (EC 2.7.7.10); UGE, UDP-glucose 4-epimerase (EC 5.1.3.2), UDP-Glc PPase, UDP-glucose pyrophosphorylase (EC 2.7.7.9). Adapted from Dörmann and Benning, 1998.

### 5.1.1 *ATSIP2* is a *bona fide* Raf-specific alkaline $\alpha$ Gal proposed to be involved in phloem unloading

The project of my thesis represents a continuation of work initiated by Dr. Shaun Peters who focused on the first step of RFO catabolism of Arabidopsis catalyzed by  $\alpha$ Gals. The original inspiration came from two publications (Gao and Schaffer, 1999; Carmi et al., 2003) where the authors identified two alkaline  $\alpha$ Gals from melon fruit, CmAGA1 and CmAGA2, that displayed distinct substrate specificities for Raf and Sta, respectively. Interestingly, these two genes shared high amino acid sequence identities with Arabidopsis SIP proteins, which remained ambiguously annotated. Dr. Shaun Peters expressed the *ATSIP2* gene functionally and obtained preliminary results showing that it encodes an alkaline  $\alpha$ Gal and not a RafS as suggested by recent reports (Nishizawa et al., 2008; Maruyama et al., 2009). I completed the biochemical characterization of *ATSIP2* recombinant protein expressed in *Sf9* insect cells and demonstrated that *ATSIP2* was able to hydrolyze the  $\alpha$ -linkage variant of the artificial substrate pNPGal but not the  $\beta$ -linkage variant. Furthermore, *ATSIP2* activity was abolished by the specific  $\alpha$ Gal inhibitor, DJG, and no RafS was detected, confirming that *ATSIP2* is definitively a *bona fide*  $\alpha$ Gal. The pH optimum of recombinant *ATSIP2* was between 7.5 and 8.0, the enzyme was highly specific towards Raf (2.42nkat mg<sup>-1</sup> total protein) and was partially inhibited by the end-product Gal (sections 2.2.2 and 2.2.3).

I further analyzed the possible physiological roles for such a specific alkaline  $\alpha$ Gal in Arabidopsis and precluded a possible role for *ATSIP2* in the hydrolysis of low temperature (4°C) stress-induced Raf. A T-DNA *loss-of-function* mutant (*atsip2*) behaved as a wild-type (WT) plant following a 3d deacclimation from 4°C, showing comparable rates of stress-induced Raf decline during deacclimation at 22°C, suggesting that *ATSIP2* does not seem to play a major role in Raf hydrolysis during the deacclimation process (section 2.3.3). The studies were extended to include water-deficit stress when dehydrated Arabidopsis plants were rehydrated (section 2.3.4). Taken together, these two stress/de-stress situations indicate Raf was quickly depleted in both the *atsip2* lines and the WT plants. *ATSIP2* does not seem to be important for stress relief-associated Raf hydrolysis. To study the other possible roles of *ATSIP2*, I created *ATSIP2* promoter/ $\beta$ -glucuronidase fusion constructs and transformed them into Arabidopsis. Stained plants showed strong GUS activity in sink leaves and roots. This GUS activity correlated positively with *ATSIP2* transcript levels and alkaline  $\alpha$ Gal activities in these organs, with the highest activities evident in crude extracts from sink leaves and roots (section 2.3.5.1). This observation suggests that *ATSIP2* may be involved in phloem unloading, similar to other alkaline  $\alpha$ Gals previously described (Keller and Pharr, 1996; Gao and Schaffer, 1999). This finding is particularly interesting because although Arabidopsis has been reported to mainly

transport Suc in its phloem it still transports some Raf which needs to be catabolized in the sink (Haritatos et al., 2000). In Arabidopsis, the mode of phloem unloading mechanism is not known (symplastic or apoplastic). Symplastic phloem unloading is the “normal”, most common mode (see section 1.4.1). Interestingly, it was recently shown that cucumber, a predominantly Raf and Sta translocator (besides some Suc), follows an apoplastic pathway, which suggests the involvement of acid  $\alpha$ Gals, present in the cell wall that could degrade RFOs in the apoplast (Hu et al., 2011). My ATSIP2 results argue rather for a symplastic unloading pathway in Arabidopsis, since a cytosolic alkaline  $\alpha$ Gal is up-regulated in sink tissues, potentially degrading RFOs at their arrival in the sink. A detailed study aimed at dissecting the mode of phloem unloading of both Suc and Raf (which might differ) is clearly needed.

#### **5.1.2. ATSIP1 is a *bona fide* Sta- and Gol-specific alkaline $\alpha$ Gal with a yet unknown physiological function**

Further, I biochemically characterized the second member of the SIP family, *ATSIP1*, through functional expression in *Sf9* insect cells. I showed that *ATSIP1*, like *ATSIP2*, was only able to hydrolyze the  $\alpha$ -linkage variant of the artificial substrate, pNPGal, and not the  $\beta$ -variant. *ATSIP1* activity was also abolished by the DGJ inhibitor, and no RafS or VerS was detected, confirming that *ATSIP1* is definitively a *bona fide*  $\alpha$ Gal and not a RafS (Nishizawa et al., 2008) or a VerS (Anderson and Kohorn, 2001) as previously hypothesized. The pH optimum of 8.5 was higher than that of *ASIP2* (7.5 to 8.0). The natural substrate specificity also differed, *ATSIP1* being more specific for Sta and Gol (0.45nkat  $\text{mg}^{-1}$  total protein and 0.81nkat  $\text{mg}^{-1}$  total protein, respectively) than for Raf as with *ATSIP2*. Finally, *ATSIP1*, like *ATSIP2*, was partially inhibited by the end product Gal (section 2.3.1 and 2.3.2).

Considering the *ATSIP1* Sta specificity, the most logical putative function of *ATSIP1* would be that of RFO degradation in seeds, the only known organ where Sta accumulates in Arabidopsis (Ooms et al., 1993; Bentsink et al., 2000; Baud et al., 2002). According to their original nomenclature, both *ATSIP1* and -2 belong to the seed imbibition protein family, suggesting that they might play a role during seed germination when RFOs are known to be degraded rapidly. I investigated the putative physiological function of *ATSIP1* in parallel with that of *ATSIP2* by creating the double mutant, *atsip1-atsip2*, besides *atsip1*, *atsip2* and WT plants to compare their germination performance. The single mutant lines germinated like the WT lines. A slight delay was observed in the double mutant seeds and could reveal that the lack of both enzymes would have an influence on the germination (section 2.3.6). By measuring  $\alpha$ Gal activities after 1d of imbibition on extracts of seeds kept in the dark at 22°C, with the corresponding substrates and pH optima of both *ATSIP1* and -2, we detected a good

activity towards Raf but the activity towards Gol and Sta remained low (section 2.3.6). This suggests, somewhat surprisingly, a putative role of ATSIP2 (rather than ATSIP1) in RFO degradation during seed germination. Considering the ATSIP1 Gol specificity, no physiological role has become obvious and awaits further experimentation. Finally, it is worth noting that WSC contents in seeds did not decrease during the 3d of imbibition experimented, suggesting that the RFOs are probably degraded at of Arabidopsis germination. In dry seeds, the relative amounts of Suc, Sta and Raf corresponded to published data (Bentsink et al., 2000; Baud et al., 2002). Almost all the studies concerning Arabidopsis seeds have so far focused on the acquisition of seed desiccation tolerance and maturation. To my knowledge, only one study presented data on the fate of RFOs during Arabidopsis seed vernalization and germination (Fait et al., 2006). In that paper, the authors did not see any changes in Raf concentration before and after seed vernalization at 4°C for 3d followed by germination at 21°C for 3d. This indicates that Raf does not decrease, at least in the first day of germination, which is in accordance with my own results. However, this available information is very limited because (i) the germination conditions were different from mine and (ii) the authors did not measure Sta, which is the main RFO accumulating in Arabidopsis mature seeds. We are currently investigating when exactly the seed Raf and Sta are catabolized during seed imbibition and germination.

### **5.1.3 AtDIN10 is an alkaline $\alpha$ Gal located in the chloroplast, proposed to degrade DGDG during dark-induced senescence**

AtDIN10, also named ATSIP3, was identified and cloned following a screen intending to find genes upregulated during detached dark-induced leaf senescence of Arabidopsis (Fujiki et al., 2001). AtDIN10 shares high amino acid identity with other SIP proteins and also with the newly characterized rice alkaline  $\alpha$ Gal, Osak $\alpha$ Gal, located in the chloroplast (Lee et al., 2004; Lee et al., 2009). This particular rice alkaline  $\alpha$ Gal was able to hydrolyze  $\alpha$ 1,6-galactosyl oligosaccharides and the galactolipid, DGDG. It was suggested that Osak $\alpha$ Gal plays an important role in thylakoid membrane degradation during rice leaf senescence. Our initial idea was that AtDIN10 could be the homolog of the rice Osak $\alpha$ Gal. We therefore cloned, functionally expressed and partially characterized AtDIN10 in *Sf9* cell system and confirmed that AtDIN10 is indeed a *bona fide* alkaline  $\alpha$ Gal with a pH optimum of 8.0 and broad substrate specificity towards  $\alpha$ -galactosyl oligosaccharides (section 3.3.3). Further, we identified that *AtDIN0* possesses a chloroplast transit peptide and showed its location in the chloroplast by transient protoplast transformation. The location pattern of AtDIN10 compared to that of GFP patterns of control genes indicated that AtDIN10 is possibly located in the stroma (sections 3.3.1 and 3.3.2). We still need to perform and optimize the enzyme



assays with DGDG as a substrate to confirm if AtDIN10 is really able to hydrolyze galactolipids present in the chloroplasts. The project is currently followed up by Dr. Shaun Peters who will manage research on three confirmed T-DNA *loss-of-function* mutant lines to see if these mutants display a delay in leaf senescence or retention of chlorophyll due to the lack of galactolipid degradation.

It is important to notice that DGDG only contributes to 20% to the chloroplast lipids whereas MGDG contributes up to 50%. Galactolipid degradation occurring during leaf senescence involves the hydrolysis of the external Gal residue of DGDG by an  $\alpha$ Gal to yield MGDG, which is in turn degraded by a  $\beta$ -galactosidase ( $\beta$ Gal; EC 3.2.1.23; Bhalla and Dalling, 1984). The internal Gal of DGDG and that of MGDG are hydrolyzed by  $\beta$ Gals. It is still unclear whether galactolipids are first cleaved by galactolipases (*i.e.* removing the acyl groups), and the remaining digalactosylglycerol or galactosylglycerol moieties are then hydrolyzed by  $\alpha$ - and  $\beta$ Gals, respectively, or whether  $\alpha$ Gals or  $\beta$ Gals directly act on the two galactolipids, DGDG and MGDG (Andersson and Dörmann, 2009). In *Triticum aestivum* (wheat), it was shown that chloroplast contain more than 50% of the cellular  $\beta$ Gal activity and more than 80% of this chloroplastic activity is located in the stroma while the remainder is thought to be bound to the thylakoids (Bhalla and Dalling, 1984). An alternative view is that the  $\beta$ Gal is able to release digalactose (galactobiose) from digalactosylglycerol. The digalactose could then be exported and hydrolyzed by the extra-chloroplastic  $\alpha$ Gal (Bhalla and Dalling, 1984). This suggests that the Gal pool resulting from galactolipid mobilization is mostly attributed to  $\beta$ Gal activity and only a limited proportion is hydrolyzed by  $\alpha$ Gals. It is therefore obvious that our  $\alpha$ Gal studies need to be extended to include  $\beta$ Gals because their contribution to the Gal salvage pathway will be most substantial.

#### 5.1.4 Are the other annotated RafSs genuine RafSs?

RafS annotations are very controversial. In Arabidopsis, six genes have been reported to date to encode RafSs (Nishizawa et al., 2008; Maruyama et al., 2009). In this thesis, I showed that from these six genes, three are alkaline  $\alpha$ Gals without any biosynthetic (RafS) activity (Table1). At the structural level,  $\alpha$ Gals, RafSs and StaSs have similarities and common motifs and the three classes of enzymes belong the GH36 family (<http://www.cazy.org/GH36.html>; Peterbauer et al., 1999; Peterbauer et al., 2002a; Tapernoux-Lüthi et al., 2004). It is, therefore, difficult to predict distinct functions of each without a proper biochemical characterization. Interestingly, the situation might even be more complex as indicated by the fact that certain RafSs were also suggested to be active in both the biosynthetic and degradation directions, respectively (Peterbauer et al., 2002b).

**Table1.** Inventory of the annotated RafSs referenced in databases.

Name	Gene code	Location	Determination
<b>RS1 (ATSIP1)</b>	At1g55740	cytosolic	This thesis
<b>RS2 (ATSIP2)</b>	At3g57520	cytosolic	This thesis and Peters et al., 2010
<b>RS3</b>	At4g01265	?	-
<b>RS4 (RS14)</b>	At4g01970	?	Zuther et al., 2004
<b>RS5</b>	At5g40390	?	annotation in TAIR
<b>RS6 (AtDIN10/ATSIP3)</b>	At5g20250	chloroplastic	This thesis

It would be interesting to characterize the three remaining members of the gene family (RS3, RS4, RS5; **Table1**) to know if they really encode RafSs or StaSs and, therefore, increase the knowledge in this poorly documented area of research. We are currently investigating the biochemical and functional characterization of RS4 by a reverse genetic approach using T-DNA *loss-of-function* mutant lines and testing whether the plants lacking the enzyme could abolish Raf accumulation under abiotic stress conditions. This project has been initiated by Dr. Shaun Peters and I am involved to perform some of the experiments.

#### **5.1.5 AtGALK is a *bona fide* GALK and the study of *atgalk* reveals a putative new Gal detoxification pathway involving a tonoplast transporter**

When I started my investigations on the AtGALK biochemical characterization, no published data was available other than rudimentary information (Kaplan et al., 1997; Sherson et al., 1999). In 2009, a publication became available with detailed biochemical characterization of AtGALK expressed in the prokaryotic system, *E. coli* (Yang et al., 2009). From my side I expressed AtGALK in eukaryotic *Sf9* insect cell system and I could confirm some of the data of Yang et al. (2009) such as the pH optimum (7.5), but the *K<sub>m</sub>* values for the two substrates, ATP and Gal, were different (section 4.3.1). The exact reason of this divergence is currently not known, but it could be explained by the distinct heterologous systems used and also by a possible self-inhibition of the enzyme that would result in activities variation. Despite these biochemical characterization variations, *AtGALK* was clearly demonstrated to be a *bona fide* GALK.

Totally new were my studies using T-DNA *loss-of-function* mutants (*atgalk*). Having confirmed that the vegetative tissues (leaves and roots) of mutant plants lacked *atgalk*, I found that the leaves and roots of mutant plants contain up to 6.8mg g<sup>-1</sup> FW Gal, contrary to WT plants which only had trace amounts of Gal (section 4.3.2). The *atgalk* mutant was also transformed with the *ATGALK* cDNA under the control of a double CaMV35S promoter and shown to partially restore GALK activity which

was sufficient to reduce the Gal level to a similar level than the WT (section 4.3.3). Free Gal itself has long been suggested to be cytotoxic and hence we have developed an intriguing hypothesis that a free Gal detoxifying mechanism may be active in *atgalk* plants. We suggest that such a mechanism would (i) use the large central vacuole as the Gal detoxification store and (ii) involve a tonoplasmic Gal transporter. Recent metabolomics approaches have identified some Gal in the vacuoles of soybean (Benkeblia et al., 2007) and barley (Tohge et al., 2011). It would thus appear that vacuolar uptake mechanisms for free Gal in plants are inherent, but due to the low abundance of free Gal in the cytosol under normal physiological conditions the absolute concentrations of free Gal in the vacuole is negligible. Under our normal growing conditions (for soil-grown plants) and during routine HPLC-PAD analyses we never observed Gal concentrations exceeding 0.063 mg g<sup>-1</sup> FW in Arabidopsis WT leaves.

Monosaccharide transporters (MSTs) are well characterized in Arabidopsis. A subset of these MSTs consisting of 14 genes are defined as sugar transport proteins (STPs) and eight of them have been characterized extensively (Büttner, 2007). A few AtSTPs have been shown to transport Gal. The most obvious candidates for a Gal tonoplast transporter would be the tonoplast monosaccharide transporters (TMTs; Wormit et al., 2006; Schulze et al., 2011; Wingenter et al., 2011) or the vacuolar glucose transporters (VGTs; Aluri and Büttner, 2007) most of which have been demonstrated to localize to the tonoplast. Apart from VGT1 which showed minimal vacuolar Gal uptake (Aluri and Büttner, 2007), neither of the TMTs or VGTs have been tested for their capacity to transport Gal. We tested by sqPCR if one of the major TMTs (AtTMT1, AtTMT2 and AtTMT3) was highly expressed in *atgalk* compared to the WT plants. But it seems that none of them are up-regulated in the mutant plant (section 4.3.6). All the observations taken together provide promising hints that our hypothesis may be correct and warrant further investigations, including the determination if a tonoplasmic transporter is indeed able to transport Gal. Recently, the first Gal-specific transporter (AtSTP14; At1g77210) was identified (Poschet et al., 2010), however it was described as a plasma membrane transporter and, therefore, is it unlikely that this transporter fulfill a possible role for the transport of Gal in *atgalk* plant vacuoles.

If such a detoxifying pathway was constitutively active in *atgalk* plants, then exogenous application of free Gal should result in *atgalk* plants being insensitive. Indeed, *atgalk* and *atgalk/35S::AtGALK* plants showed Gal insensitivity up to 100mM external Gal compared to WT plants, which displayed reduced root length, reduced lateral roots and epinastic leaf phenotype (section 4.3.4). The reason why *atgalk/35S::AtGALK* did not restore the Gal sensitivity is still unclear. This could be explained by the constitutive detoxification pathway being still active in those plants. A similar Gal insensitivity has

been previously reported for a T-DNA *loss-of-function* mutant for the monosaccharide proton symporter *AtSTP1* (At1g11260) which exhibits a broad spectrum substrate specificity (mainly Glc, mannose and Gal; Sherson et al., 2000). We tested whether the *atgalk* insensitivity could be due to the cessation of Gal uptake and we conclusively demonstrated that  $^{14}\text{C}$ -Gal appeared in the leaves of *atgalk* seedlings after 7d exposure of the roots to  $^{14}\text{C}$ -Gal, confirming that the proposed AtSTP-mediated hexose uptake pathway was still active in the *atgalk* background (section 4.3.6). The WT, however, did not show any  $^{14}\text{C}$ -Gal accumulation with the same treatment and also no  $^{14}\text{C}$ -Gal1P was formed. Vacuole isolation from *atgalk* plants confirmed that all of the Gal accumulated was sequestered into the vacuole (section 4.3.5). Collectively, these observations led us to speculate that a novel mechanism of detoxification for free Gal became constitutively active in the *atgalk* background (artificially high free Gal accumulation). In the future, we plan to investigate the Gal transport capacity of mesophyll vacuoles isolated from *atgalk* plants to determine if they show an enhanced rate of Gal uptake. Additionally, we will also test candidate genes of tonoplast transporters that may prove to be responsible for Gal uptake into vacuoles.

#### 5.1.6 Does the conversion of $\beta$ -form of Gal to $\alpha$ -form via a mutarotase exist in Arabidopsis?

GALK from bacteria, yeast, Arabidopsis and human are selective for the  $\alpha$ -configuration of Gal as substrate. At equilibrium in solution and at a temperature of 37°C, around 36% of Gal exists in the  $\alpha$ -configuration and 64% in the  $\beta$ -form (Yang et al., 2009). In aqueous solution, the two forms are spontaneously interconverted until equilibrium in the mixture is formed (Beebe et al., 2003). However, in humans, a Gal mutarotase converts the thermodynamically more stable  $\beta$ -Gal to the bioactive  $\alpha$ -form (Timson and Reece, 2003). It is thought that Gal mutarotase may be required to rapidly generate and maintain a sufficient pool of  $\alpha$ -form of Gal needed by the GALK that catalyze the conversion of Gal to Gal1P. Indeed, the Gal mutarotase enzyme was defined as an integral part of the Leloir pathway (Holden et al., 2003). In plants, a Gal mutarotase (also named aldose 1-epimerase), was purified 1400-fold in *Capsicum frutescens* (green pepper; Bailey et al., 1967) over 40 years ago and shown to be present in many dicotyledonous plant families such as *Solanaceae*, *Cucurbitaceae* and *Fabaceae* and also in monocotyledons such as *Liliaceae* or *Gramineae* (Bailey et al., 1966). Since these two early reports on Gal mutarotase no recent publication has reported on this enzyme in plants and particularly in Arabidopsis.

By performing an *in silico* co-expression analysis of *AtGALK* with the tools, GeneCAT (<http://genecat.mpg.de>) and GeneMANIA (<http://genemania.org>), we identified a putative Arabidopsis aldose-1-epimerase (At3g17940) strongly connected to *AtGALK* (Fig.2). The gene

expression network of At3g17940 suggested that, besides being co-expressed, the two genes are co-localized. Two other enzymes from the Leloir pathway, UDP-Glc/UDP-Gal 4'-epimerases (UGE3 and UGE5) were also closely linked to At3g17940 suggesting that this aldose-1-epimerase could be a good Gal mutarotase candidate involved in the Gal catabolism pathway.

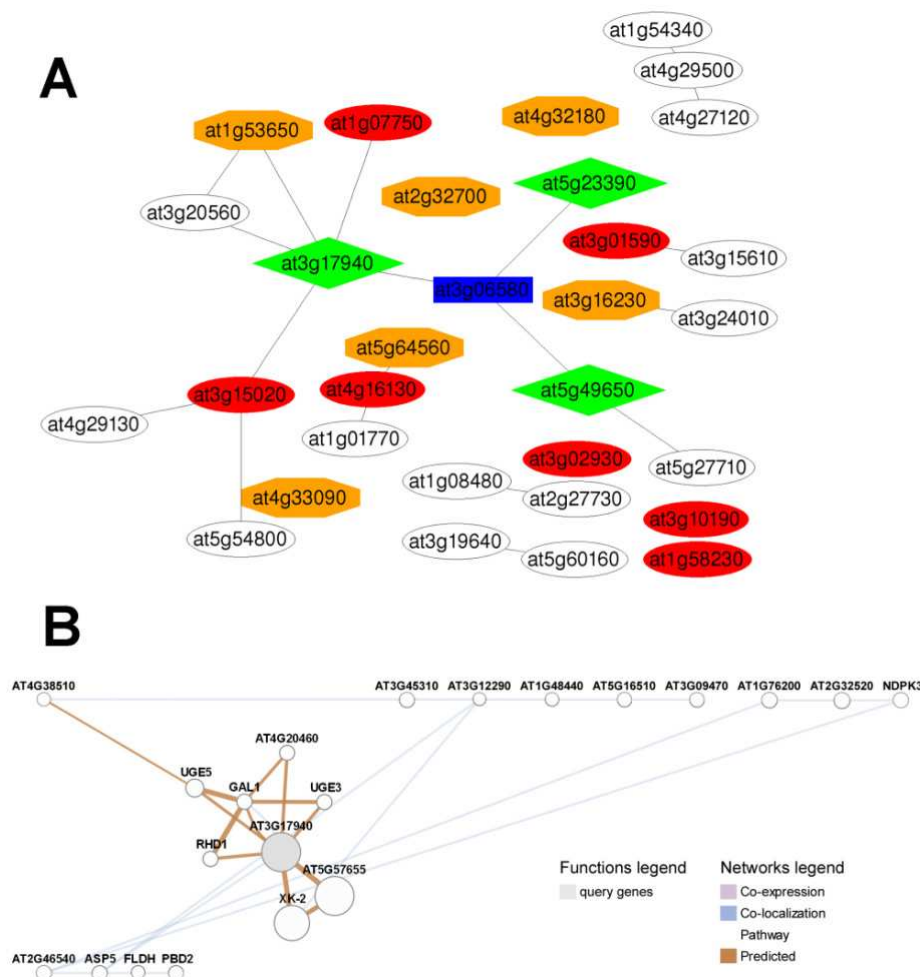


**Fig.2.** *In silico* co-expression and co-localization gene network of AtGALK (At3g06580) and At3g17940. A. GeneCAT co-expression analysis of AtGALK. Blue, gene query; Green, strong connection; orange, intermediate connection; Red, weak connection. White, insignificantly connection. At3g17940, aldose1-epimerase family protein; At5g23390, unknown protein; At5g49650, putative xylulose synthase (<http://genecat.mpg.de>). B. GeneMANIA co-expression and co-localization network of At3g17940. GAL1, galactokinase (At3g06580); UGE3, UDP-Glc/UDP-Gal 4-epimerase 5 (At4g10960); UGE3, UDP-Glc/UDP-Gal 4-epimerase 3 (At1g63180); RHD1, NAD(P)-binding Rossmann-fold superfamily protein (At1g64440); XK-2, xylulose kinase 2 (At5g49650) (<http://genemania.org>).

In 2004, the human mutarotase was crystallized (HsGALM; Thoden et al., 2004). From that study, the authors discovered that the sugar ligand is surrounded by specific residues (Asn-81, Arg-82, His-107, His-176, Asp-243, Gln-279 and Glu-307, **Fig.3A**). These residues are absolutely conserved in all Gal mutarotases. An alignment of the putative Arabidopsis mutarotase (AtGALM, At3g17940) amino acid

sequence against HsGALM showed 45% identity between the two sequences and the conserved amino acids were present in AtGALM (**Fig.3B**).

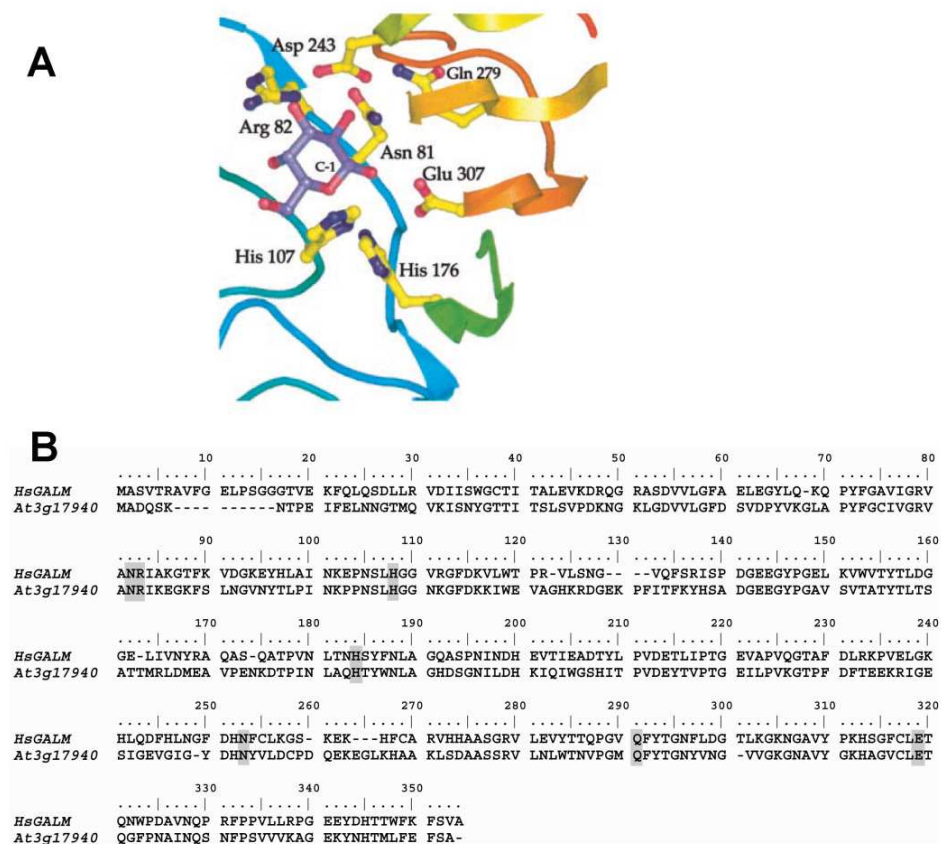


**Fig.3.** The active site for human Gal mutarotase compared with At3g17940. A. Close-up stereo view of HsGALM amino acid residues involved in sugar binding (Thoden et al., 2004). B. Amino acid alignment between HsGALM and At3g17940. In grey are highlighted the conserved residues involved in sugar binding. In order of appearance, Asn-81, Arg-82, His-107, His-176, Asp-243, Gln-279 and Glu-307.

In summary, we identified a new candidate for an Arabidopsis Gal mutarotase homolog, At3g17940, by *in silico* analyses of gene co-expression and co-localization. A further sequence alignment confirmed that the essential and conserved amino acid residues of the catalytic site are present in this gene. It would be interesting to analyze T-DNA insertion mutants of this gene and test whether they accumulate Gal in their leaves.

## 5.2 Outlook

To increase our understanding of RFO catabolism in Arabidopsis, I suggest the following additional experiments:

- (i) To examine Arabidopsis seed germination in more details to define when exactly the RFO pool is mobilized and test whether ATSIP1 or -2 play a role for Sta and Raf hydrolysis in seed germination. Because of the numerous controversies occurring in databases concerning the annotation of RafS genes, it would be interesting to further analyze and dissect the roles of the different genes annotated as RafS.
- (ii) To resolve the reported technical problems of DGDG solubilization and of Gal detection following AtDIN10 alkaline  $\alpha$ Gal assay on lipids. We are currently characterizing three *atdin10 loss-of-function* T-DNA insertion lines and planning to perform dark-induced senescence tests to determine if AtDIN10 loss causes a delay in chlorophyll catabolism. This work will be followed in the framework of the newly established collaboration between Dr. Shaun Peters and Prof. Dr. Stefan Hörtensteiner and will further our understanding of the temporal events appearing during leaf senescence in the chloroplast.
- (iii) To investigate the analysis of putative tonoplastic transporters involved in Gal sequestration. To date, no tonoplastic transporters distinctly specific for Gal have been characterized.
- (iv) To biochemically characterize the putative Gal mutarotase identified by *in silico* analyses (At3g17940) by the expression of the corresponding protein in the *Sf9* insect cell system. It is interesting to study this enzyme, because if it truly exists in Arabidopsis, it could be one explanation for the extreme rapid metabolization of free Gal to Gal1P via the subsequent action of AtGALK. Currently, two T-DNA insertions are being investigated in our laboratory to see if a lack of a Gal mutarotase involves the generation of free Gal in those lines growing on a medium supplemented with exogenous Gal.



## REFERENCE LIST

- Ai Y, Jenkins NA, Copeland NG, Gilbert DH, Bergsma DJ, Stambolian D** (1995) Mouse galactokinase: isolation, characterization, and location on chromosome 11. *Genome Research* **5**: 53-59
- Ainsworth EA, Bush DR** (2011) Carbohydrate export from the leaf: a highly regulated process and target to enhance photosynthesis and productivity. *Plant Physiology and Biochemistry* **155**: 64-69
- Aluri S, Büttner M** (2007) Identification and functional expression of the *Arabidopsis thaliana* vacuolar glucose transporter 1 and its role in seed germination and flowering. *Proceedings of the National Academy of Sciences of the United States of America* **104**: 2537-2542
- Anderson CM, Kohorn BD** (2001) Inactivation of Arabidopsis SIP1 leads to reduced levels of sugars and drought tolerance. *Journal of Plant Physiology* **158**: 1215-1219
- Andersson M, Dörmann P** (2009) Chloroplast membrane lipid biosynthesis and transport. In A Sandelius, H Aronsson (eds), *The Chloroplast*, Vol 13. Springer Berlin / Heidelberg, pp 125-158
- Anker L** (1974) Auxin synthesis inhibition by sugars, notably by galactose. *Acta botanica neerlandica* **23**: 705-714
- Ashworth EN, Stirn VE, Volenec JJ** (1993) Seasonal variations in soluble sugars and starch within woody stems of *Cornus sericea* L. . *Tree Physiology* **13**: 379-388
- Avigad G, Dey PM** (1997) Carbohydrate metabolism: storage carbohydrates. In PM Dey, J Harborne (eds), *Plant Biochemistry*. Academic Press, San Diego, pp 143-204
- Ayre BG, Keller F, Turgeon R** (2003) Symplastic continuity between companion cells and the translocation stream: long-distance transport is controlled by retention and retrieval mechanisms in the phloem. *Plant Physiology* **131**: 1518-1528
- Azumi Y, Watanabe A** (1991) Evidence for a senescence-associated gene induced by darkness. *Plant Physiology* **95**: 577-583
- Bachmann M, Inan C, Keller F** (1995) Raffinose oligosaccharide storage. In M Madore, W Lucas (eds), *Carbon partitioning and source-sink interactions in plants*. American Society of Plant Physiologists, Rockville, MD, pp 215-225
- Bachmann M, Keller F** (1995) Metabolism of the raffinose family oligosaccharides in leaves of *Ajuga reptans* L. Inter- and intracellular compartmentation. *Plant Physiology* **109**: 991-998
- Bachmann M, Matile P, Keller F** (1994) Metabolism of the raffinose family oligosaccharides in leaves of *Ajuga reptans* L. Cold acclimation, translocation, and sink to source transition: discovery of chain elongation enzyme. *Plant Physiology* **105**: 1335-1345
- Bailey JM, Fishman PH, Pentchev PG** (1966) Mutarotase in higher plants: distribution and properties. *Science* **152**: 1270-1271
- Bailey JM, Fishman PH, Pentchev PG** (1967) Studies on mutarotases. *Journal of Biological Chemistry* **242**: 4263-4269
- Barber C, Rösti J, Rawat A, Findlay K, Roberts K, Seifert GJ** (2006) Distinct properties of the five UDP-D-glucose/UDP-D-galactose 4-epimerase isoforms of *Arabidopsis thaliana*. *Journal of Biological Chemistry* **281**: 17276-17285
- Barham D, Dey PM, Griffith D, Pridham JB** (1971) Studies on distribution of alpha-galactosidases in seeds. *Phytochemistry* **10**: 1759-1763
- Baud S, Boutin J-P, Miquel M, Lepiniec L, Rochat C** (2002) An integrated overview of seed development in *Arabidopsis thaliana* ecotype WS. *Plant Physiology and Biochemistry* **40**: 151-160
- Beck EH, Heim R, Hansen J** (2004) Plant resistance to cold stress: mechanisms and environmental signals triggering frost hardening and dehardening. *Journal of biosciences* **29**: 449-459
- Beebe JA, Arabshahi A, Clifton JG, Ringe D, Petsko GA, Frey PA** (2003) Galactose mutarotase: pH dependence of enzymatic mutarotation. *Biochemistry* **42**: 4414-4420
- Benkeblia N, Shinano T, Osaki M** (2007) Metabolite profiling and assessment of metabolome compartmentation of soybean leaves using non-aqueous fractionation and GC-MS analysis. *Metabolomics* **3**: 297-305
- Bentsink L, Alonso-Blanco C, Vreugdenhil D, Tesnier K, Groot SPC, Koornneef M** (2000) Genetic analysis of seed-soluble oligosaccharides in relation to seed storability of Arabidopsis. *Plant Physiology* **124**: 1595-1604
- Bewley J, Black M** (1994) *Seeds: physiology of development and germination*. Plenum Press, New York



- Bhalla PL, Dalling MJ** (1984) Characteristics of a  $\beta$ -galactosidase associated with the stroma of chloroplasts prepared from mesophyll protoplasts of the primary leaf of wheat. *Plant Physiology* **76**: 92-95
- Bhatnagar-Mathur P, Vadez V, Sharma K** (2008) Transgenic approaches for abiotic stress tolerance in plants: retrospect and prospects. *Plant Cell Reports* **27**: 411-424
- Blackman SA, Obendorf RL, Leopold AC** (1992) Maturation proteins and sugars in desiccation tolerance of developing soybean seeds. *Plant Physiology* **100**: 225-230
- Blöchl A, March GG, Sourdoux M, Peterbauer T, Richter A** (2005) Induction of raffinose oligosaccharide biosynthesis by abscisic acid in somatic embryos of alfalfa (*Medicago sativa* L.). *Plant Science* **168**: 1075-1082
- Blöchl A, Peterbauer T, Hofmann J, Richter A** (2008) Enzymatic breakdown of raffinose oligosaccharides in pea seeds. *Planta* **228**: 99-110
- Blöchl A, Peterbauer T, Richter A** (2007) Inhibition of raffinose oligosaccharide breakdown delays germination of pea seeds. *Journal of Plant Physiology* **164**: 1093-1096
- Blom D, Speijer D, Linthorst GE, Donker-Koopman WG, Strijland A, Aerts JMFG** (2003) Recombinant enzyme therapy for fabry disease: absence of editing of human  $\alpha$ -galactosidase A mRNA. *American Journal of Human Genetics* **72**: 23-31
- Bohnert HJ, Nelson DE, Jensen RG** (1995) Adaptations to environmental stresses. *The Plant Cell* **7**: 1099-1111
- Bourquelot E, Bridel M** (1910) Oligosaccharide isolated from roots of mullein *Verbascum thapsus* L., *Scrophulariaceae*. *Comptes rendus* **151**: 760
- Braun R, Keller F** (2000) Vacuolar chain elongation of raffinose oligosaccharides in *Ajuga reptans*. *Australian Journal of Plant Physiology* **27**: 743-746
- Bray EA** (1997) Plant responses to water deficit. *Trends in Plant Science* **2**: 48-54
- Brenac P, Smith ME, Obendorf RL** (1997) Raffinose accumulation in maize embryos in the absence of a fully functional *Vp1* gene product. *Planta* **203**: 222-228
- Brouquisse R, Gaudillere JP, Raymond P** (1998) Induction of a carbon-starvation-related proteolysis in whole maize plants submitted to Light/Dark cycles and to extended darkness. *Plant Physiology* **117**: 1281-1291
- Brown RJ, Serro RF** (1953) Isolation and identification of O- $\alpha$ -galactopyranosyl-myo-inositol and of myo-inositol from juice of the sugar beet (*Beta vulgaris*). *Journal of the American Chemical Society* **75**: 1040-1042
- Buchanan-Wollaston V** (1997) The molecular biology of leaf senescence. *Journal of Experimental Botany* **48**: 181-199
- Bulpin PV, Gidley MJ, Jeffcoat R, Underwood DR** (1990) Development of a biotechnological process for the modification of galactomannan polymers with plant  $\alpha$ -galactosidase. *Carbohydrate Polymers* **12**: 155-168
- Butters TD, Dwek RA, Platt FM** (2005) Imino sugar inhibitors for treating the lysosomal glycosphingolipidoses. *Glycobiology* **15**: 43R-52R
- Büttner M** (2007) The monosaccharide transporter(-like) gene family in Arabidopsis. *FEBS Letters* **581**: 2318-2324
- Calhoun DH, Bishop DF, Bernstein HS, Quinn M, Hantzopoulos P, Desnick RJ** (1985) Fabry disease: isolation of a cDNA clone encoding human alpha-galactosidase A. *Proceedings of the National Academy of Sciences of the United States of America* **82**: 7364-7368
- Cantarel BL, Coutinho PM, Rancurel C, Bernard T, Lombard L, Henrissat B** (2009) The carbohydrate-active enzyme database (CAZy): an expert resource for glycogenomics. *Nucleic Acids Research* **37**: D233-D238
- Caputto R, Leloir L, Trucco RE, Cardini C, Paladini A** (1948) A coenzyme for phosphoglucomutase. *Archives of Biochemistry and Biophysics* **18**: 201-203
- Carmi N, Zhang GF, Petreikov M, Gao ZF, Eyal Y, Granot D, Schaffer AA** (2003) Cloning and functional expression of alkaline alpha-galactosidase from melon fruit: similarity to plant SIP proteins uncovers a novel family of plant glycosyl hydrolases. *The Plant Journal* **33**: 97-106
- Castillo EM, De Lumen BO, Reyes PS, De Lumen HZ** (1990) Raffinose synthase and galactinol synthase in developing seeds and leaves of legumes. *Journal of Agricultural and Food Chemistry* **38**: 351-355
- Chan PH, Hassid WZ** (1975) One step purification of D-galactose and D-arabinose kinases from *Phaseolus aureus* seedlings by ATP-Sepharose affinity chromatography. *Analytical Biochemistry* **64**: 372-379
- Chaves MM** (1991) Effects of water deficits on carbon assimilation. *Journal of Experimental Botany* **42**: 1-16
- Chaves MM, Flexas J, Pinheiro C** (2009) Photosynthesis under drought and salt stress: regulation mechanisms from whole plant to cell. *Annals of Botany* **103**: 551-560

- Chaves MM, Maroco JP, Pereira JS** (2003) Understanding plant responses to drought - from genes to the whole plant. *Functional Plant Biology* **30**: 239-264
- Chen TH, Murata N** (2008) Glycinebetaine: an effective protectant against abiotic stress in plants. *Trends in Plant Science* **13**: 499-505
- Chrost B, Kolukisaoglu U, Schulz B, Krupinska K** (2007) An alpha-galactosidase with an essential function during leaf development. *Planta* **225**: 311-320
- Chrost B, Schmitz K** (1997) Changes in soluble sugar and activity of  $\alpha$ -galactosidases and acid invertase during muskmelon (*Cucumis melo* L.) fruit development. *Journal of Plant Physiology* **151**: 41-45
- Clough SJ, Bent AF** (1998) Floral dip: a simplified method for *Agrobacterium*-mediated transformation of *Arabidopsis thaliana*. *The Plant Journal* **16**: 735-743
- Cook DJ, Fowler S, Fiehn O, Thomashow MF** (2004) A prominent role for the CBF cold response pathway in configuring the low-temperature metabolome of *Arabidopsis*. *Proceedings of the National Academy of Sciences of the United States of America* **101**: 15243-15248
- Crowe JH, Hoekstra FA, Crowe LM** (1992) Anhydrobiosis. *Annual Review of Physiology* **54**: 579-599
- Curtis MD, Grossniklaus U** (2003) A Gateway cloning vector set for high-throughput functional analysis of genes in planta. *Plant Physiology* **133**: 462-469
- Dai N, Cohen S, Portnoy V, Tzuri G, Harel-Beja R, Pompan-Lotan M, Carmi N, Zhang G, Diber A, Pollock S, Karchi H, Yeselson Y, Petreikov M, Shen S, Sahar U, Hovav R, Lewinsohn E, Tadmor Y, Granot D, Ophir R, Sherman A, Fei Z, Giovannoni J, Burger Y, Katzir N, Schaffer AA** (2011) Metabolism of soluble sugars in developing melon fruit: a global transcriptional view of the metabolic transition to sucrose accumulation. *Plant Molecular Biology* **76**: 1-18
- Dai N, Petreikov M, Portnoy V, Katzir N, Pharr DM, Schaffer AA** (2006) Cloning and expression analysis of a UDP-galactose/glucose pyrophosphorylase from melon fruit provides evidence for the major metabolic pathway of galactose metabolism in raffinose oligosaccharide metabolizing plants. *Plant Physiology* **142**: 294-304
- Dey P** (1990) Oligosaccharides. In H JB (ed), *Methods in plant biochemistry*, Vol 2. CA: Academic Press, San Diego, pp 189-218
- Dey PM** (1983) Galactokinase of *Vicia faba* seeds. *European Journal of Biochemistry* **136**: 155-159
- Dey PM** (1984) UDP-galactose 4'-epimerase from *Vicia faba* seeds. *Phytochemistry* **23**: 729-732
- Dey PM** (1985) D-Galactose-containing oligosaccharides. In PM Dey, R Dixon (eds), *Biochemistry of storage carbohydrates in green plants*. Academic Press, London, pp 53-129
- Dey PM, del Campillo E** (1984) Biochemistry of the multiple forms of glycosidases in plants. *Advances in Enzymology & Related Areas of Molecular Biology* **56**: 141-249
- Dey PM, Pridham J** (1972) Biochemistry of alpha-galactosidases. *Advances in enzymology*. pp 91-130
- Dey PM, Tipson R, Horton D** (1980) Biochemistry of  $\alpha$ -D-Galactosidic linkages in the plant kingdom. In *Advances in Carbohydrate Chemistry and Biochemistry*, Vol Volume 37. Academic Press, pp 283-372
- Dierking EC, Bilyeu KD** (2009) Raffinose and stachyose metabolism are not required for efficient soybean seed germination. *Journal of Plant Physiology* **166**: 1329-1335
- Dinur T, Grabowski GA, Desnick RJ, Gatt S** (1984) Synthesis of a fluorescent derivative of glucosyl ceramide for the sensitive determination of glucocerebrosidase activity. *Analytical Biochemistry* **136**: 223-234
- Dörmann P, Benning C** (1998) The role of UDP-glucose epimerase in carbohydrate metabolism of *Arabidopsis*. *The Plant Journal* **13**: 641-652
- Dörmann P, Benning C** (2002) Galactolipids rule in seed plants. *Trends in Plant Science* **7**: 112-118
- Dörmann P, Hoffmann-Benning S, Balbo I, Benning C** (1995) Isolation and characterization of an *Arabidopsis* mutant deficient in the thylakoid lipid digalactosyl diacylglycerol. *The Plant Cell* **7**: 1801-1810
- dos Santos TB, Budzinski IGF, Marur CJ, Petkowicz CLO, Pereira LFP, Vieira LGE** (2011) Expression of three galactinol synthase isoforms in *Coffea arabica* L. and accumulation of raffinose and stachyose in response to abiotic stresses. *Plant Physiology and Biochemistry* **49**:
- Downie B, Bewley JD** (2000) Soluble sugar content of white spruce (*Picea glauca*) seeds during and after germination. *Physiologia Plantarum* **110**: 1-12
- Downie B, Gurusinghe S, Dahal P, Thacker RR, Snyder JC, Nonogaki H, Yim K, Fukanaga K, Alvarado V, Bradford KJ** (2003) Expression of a galactinol synthase gene in tomato seeds is up-regulated before maturation desiccation and again after imbibition whenever radicle protrusion is prevented. *Plant Physiology* **131**: 1347-1359
- Drew A** (1984) Physiology and metabolism of cyclitols. In DH Lewis (ed), *Storage Carbohydrates in Vascular Plants*. Cambridge University Press, pp 133-155

- Edwards K, Johnstone C, Thompson C** (1991) A simple and rapid method for the preparation of plant genomic DNA for PCR analysis. *Nucleic Acids Research* **19**: 1349
- Fait A, Angelovici R, Less H, Ohad I, Urbanczyk-Wochniak E, Fernie AR, Galili G** (2006) Arabidopsis seed development and germination is associated with temporally distinct metabolic switches. *Plant Physiology* **142**: 839-854
- Farrant JM** (2000) A comparison of mechanisms of desiccation tolerance among three angiosperm resurrection plant species. *Plant Ecology* **151**: 29-39
- Feingold DS, Avigad G** (1980) Sugar nucleotide transformations in plants. *The Biochemistry of Plants* **3**: 101-170
- Ferguson J, Street HE, David SB** (1958) The carbohydrate nutrition of tomato roots: V. The promotion and inhibition of excised root growth by various sugars and sugar alcohols. *Annals of Botany* **22**: 513-523
- Fernandez-Leiro R, Pereira-Rodriguez Á, Cerdan ME, Becerra M, Sanz-Aparicio J** (2010) Structural analysis of *Saccharomyces cerevisiae*  $\alpha$ -galactosidase and its complexes with natural substrates reveals new insights into substrate specificity of GH27 glycosidases. *Journal of Biological Chemistry* **285**: 28020-28033
- Feurtado JA, Banik M, Bewley JD** (2001) The cloning and characterization of alpha-galactosidase present during and following germination of tomato (*Lycopersicon esculentum* Mill.) seed. *Journal of Experimental Botany* **52**: 1239-1249
- Fialho RC, Bucker J** (1996) Changes in levels of foliar carbohydrates and myo-inositol before premature leaf senescence of *Populus nigra* induced by a mixture of O<sub>3</sub> and SO<sub>2</sub>. *Canadian Journal of Botany* **74**: 965-970
- Foglietti MJ, Percheron F** (1974) Présence d'une galactokinase dans les graines germées de Fenugrec. *Biochimie* **56**: 473-475
- Foglietti MJ, Percheron F** (1976) Purification et mécanisme d'action d'une galactokinase. *Biochimie* **58**: 499-504
- Frelet-Barrand A, Kolukisaoglu HU, Plaza S, Ruffer M, Azevedo L, Hörtensteiner S, Marinova K, Weder B, Schulz B, Klein M** (2008) Comparative mutant analysis of Arabidopsis ABC-Type ABC transporters: AtMRP2 contributes to detoxification, vacuolar organic anion transport and chlorophyll degradation. *Plant and Cell Physiology* **49**: 557-569
- Frey PA** (1996) The Leloir pathway: a mechanistic imperative for three enzymes to change the stereochemical configuration of a single carbon in galactose. *The FASEB Journal* **10**: 461-470
- Fridovich-Keil JL** (2006) Galactosemia: the good, the bad, and the unknown. *Journal of Cellular Physiology* **209**: 701-705
- Frydman RB, Neufeld EF** (1963) Synthesis of galactosylinositol by extracts from peas. *Biochemical and Biophysical Research Communications* **12**: 121-125
- Fujiki Y, Ito M, Nishida I, Watanabe A** (2000) Multiple signaling pathways in gene expression during sugar starvation. Pharmacological analysis of *din* gene expression in suspension-cultured cells of Arabidopsis. *Plant Physiology* **124**: 1139-1148
- Fujiki Y, Yoshikawa Y, Sato T, Inada N, Ito M, Nishida I, Watanabe A** (2001) Dark-inducible genes from *Arabidopsis thaliana* are associated with leaf senescence and repressed by sugars. *Physiologia Plantarum* **111**: 345-352
- Gaff D** (1989) Responses of desiccation tolerant 'resurrection' plants to water stress. In K Kreeb, H Richter, T Hinckley (eds), Structural and functional responses to environmental stress: water shortage. SPB Academic Publishers, The Hague, The Netherlands, pp 255-268
- Gao Z, Petreikov M, Zamski E, Schaffer AA** (1999) Carbohydrate metabolism during early fruit development of sweet melon (*Cucumis melo*). *Physiologia Plantarum* **106**: 1-8
- Gao ZF, Schaffer AA** (1999) A novel alkaline alpha-galactosidase from melon fruit with a substrate preference for raffinose. *Plant Physiology* **119**: 979-987
- Gaudreault P, Webb J** (1986) Alkaline  $\alpha$ -galactosidase activity and galactose metabolism in the family Cucurbitaceae. *Plant Science* **45**: 71-75
- Gaudreault PR, Webb JA** (1981) Stachyose synthesis in leaves of *Cucurbita pepo*. *Phytochemistry* **20**: 2629-2633
- Gaudreault PR, Webb JA** (1982) Alkaline  $\alpha$ -galactosidase in leaves of *Cucurbita pepo*. *Plant Science Letters* **24**: 281-288
- Gaudreault PR, Webb JA** (1983) Partial purification and properties of an alkaline  $\alpha$ -galactosidase from mature leaves of *Cucurbita pepo*. *Plant Physiology* **71**: 662-668
- Gilbert GA, Wilson C, Madore MA** (1997) Root-zone salinity alters raffinose oligosaccharide metabolism and transport in *Coleus*. *Plant Physiology* **115**: 1267-1276

- Göring H, Reckin E (1968) Einfluss von D-Galaktose auf den Kohlenhydratstoffwechsel pflanzlicher Gewebe. *Flora* **159**: 82-103
- Graf A, Schlereth A, Stitt M, Smith AM (2010) Circadian control of carbohydrate availability for growth in Arabidopsis plants at night. *Proceedings of the National Academy of Sciences of the United States of America* **107**: 9458-9463
- Granot D (2008) Putting plant hexokinases in their proper place. *Phytochemistry* **69**: 2649-2654
- Gray J (1996) Biogenesis of chloroplasts in higher plants. In M Smallwood, J Knox, D Bowles (eds), *Membranes: specialized functions in plants*. Bios Scientific Publishers, Oxford, pp 441-458
- Grennan AK (2006) High impact. *Plant Physiology* **139**: 563-565
- Greutert H, Keller F (1993) Further evidence for stachyose and sucrose/H<sup>+</sup> antiporters on the tonoplast of Japanese artichoke (*Stachys sieboldii*) tubers. *Plant Physiology* **101**: 1317-1322
- Gronwald JW, Miller SS, Vance CP (2008) Arabidopsis UDP-sugar pyrophosphorylase: Evidence for two isoforms. *Plant Physiology and Biochemistry* **46**: 1101-1105
- Gross KC, Pharr DM (1982) A potential pathway for galactose metabolism in *Cucumis-Sativus* L, a stachyose transporting species. *Plant Physiology* **69**: 117-121
- Grossmann GA, Terra WR (2001)  $\alpha$ -Galactosidases from the larval midgut of *Tenebrio molitor* (Coleoptera) and *Spodoptera frugiperda* (Lepidoptera). *Comparative Biochemistry and Physiology Part B: Biochemistry and Molecular Biology* **128**: 109-122
- Guce AI, Clark NE, Salgado EN, Ivanen DR, Kulminkaya AA, Brumer H, Garman SC (2010) Catalytic mechanism of human alpha-galactosidase. *Journal of Biological Chemistry* **285**: 3625-3632
- Guamét JJ, Pichersky E, Noodén LD (1999) Mass exodus from senescing soybean chloroplasts. *Plant and Cell Physiology* **40**: 986-992
- Guimaraes VM, de Rezende ST, Moreira MA, de Barros EG, Felix CR (2001) Characterization of alpha-galactosidases from germinating soybean seed and their use for hydrolysis of oligosaccharides. *Phytochemistry* **58**: 67-73
- Häfliger B, Kindhauser E, Keller F (1999) Metabolism of d-glycero-d-manno-heptitol, volemitol, in *Polyanthus*. Discovery of a novel ketose reductase1. *Plant Physiology* **119**: 191-198
- Handley L, Pharr DM (1982) Ion stimulation, UDP inhibition and effects of sulphydryl reagents on the activity of galactinol synthase from leaves of cucumber, *Cucumis sativus* L. *Zeitschrift für Pflanzenphysiologie* **108**: 47-55
- Handley L, Pharr DM, Mc Feeters R (1983) Relationship between galactinol synthase activity and sugar composition of leaves and seeds of several crop species. *Journal of the American Society for Horticultural Sciences* **108**: 600-605
- Hannah MA, Zuther E, Buchel K, Heyer AG (2006) Transport and metabolism of raffinose family oligosaccharides in transgenic potato. *Journal of Experimental Botany* **57**: 3801-3811
- Hara M, Tokunaga K, Kuboi T (2008) Isolation of a drought-responsive alkaline  $\alpha$ -galactosidase gene from New Zealand spinach. *Plant Biotechnology* **25**: 497-501
- Hare PD, Cress WA, Van Staden J (1998) Dissecting the roles of osmolyte accumulation during stress. *Plant, Cell & Environment* **21**: 535-553
- Haritatos E, Medville R, Turgeon R (2000) Minor vein structure and sugar transport in *Arabidopsis thaliana*. *Planta* **211**: 105-111
- Harrison SJ, Mott EK, Parsley K, Aspinall S, Gray JC, Cottage A (2006) A rapid and robust method of identifying transformed *Arabidopsis thaliana* seedlings following floral dip transformation. *Plant Methods* **2**: 19
- Hashimoto H, Katayama C, Goto M, Okinaga T, Kitahata S (1995) Transgalactosylation catalyzed by  $\alpha$ -galactosidase from *Candida guilliermondii* H-404. *Bioscience Biotechnology and Biochemistry* **59**: 619-623
- Heck G, Dorsett C, Ho T-H (1991) Cloning and characterization of a gene Sip1 associated with seed imbibition in barley. *Direct submission to gene bank*, M77475.
- Henrissat B, Davis GJ (2000) Glycoside hydrolases and glycosyltransferases. Families, modules, and implications for genomics. *Plant Physiology* **124**: 1515-1519
- Heredia A, Guillén R, Jiménez A, Fernández-Bolaños J (1993) Activity of glycosidases during development and ripening of olive fruit. *Zeitschrift für Lebensmitteluntersuchung und Forschung A* **196**: 147-151
- Hoch G, Peterbauer T, Richter A (1999) Purification and characterization of stachyose synthase from lentil (*Lens culinaris*) seeds: galactopinitol and stachyose synthesis. *Archives of Biochemistry and Biophysics* **366**: 75-81
- Hoekstra FA, Golovina EA, Buitink J (2001) Mechanisms of plant desiccation tolerance. *Trends in Plant Science* **6**: 431-438

- Holden HM, Rayment I, Thoden J** (2003) Structure and function of enzymes of the Leloir pathway for galactose metabolism. *Journal of Biological Chemistry* **278**: 43885-43888
- Holthaus U, Schmitz K** (1991) Stachyose synthesis in mature leaves of *Cucumis melo*: purification and characterization of stachyose synthase (EC 2.4.1.67). *Planta* **184**: 525-531
- Horbowicz M, Obendorf R** (1994) Seed desiccation tolerance and storability: dependence on flatulence-producing oligosaccharides and cyclitols: review and survey. *Seed Science Research* **4**: 385-405
- Hörtensteiner S** (2009) Stay-green regulates chlorophyll and chlorophyll-binding protein degradation during senescence. *Trends in Plant Science* **14**: 155-162
- Hu L, Sun H, Li R, Zhang L, Wang S, Sui X, Zhang Z** (2011) Phloem unloading follows an extensive apoplasmic pathway in cucumber (*Cucumis sativus* L.) fruit from anthesis to marketable maturing stage. *Plant, Cell & Environment* in Press
- Huang J, Hirji R, Adam L, Rozwadowski KL, Hammerlindl JK, Keller WA, Selvaraj G** (2000) Genetic engineering of glycinebetaine production toward enhancing stress tolerance in plants: metabolic limitations. *Plant Physiology* **122**: 747-756
- Huber J, Pharr DM, Huber SC** (1990) Partial purification of stachyose synthase in leaves of *Cucumis sativus* and *Cucumis melo*: utilization of a rapid assay for myo-inositol. *Plant Science* **69**: 179-188
- Inan Haab C, Keller F** (2002) Purification and characterization of the raffinose oligosaccharide chain elongation enzyme, galactan:galactan galactosyltransferase (GGT), from *Ajuga reptans* leaves. *Physiologia Plantarum* **114**: 361-371
- Ingram J, Bartels D** (1996) The molecular basis of dehydration tolerance in plants *Annual Review of Physiology and Plant Molecular Biology* **47**: 377-403
- Inouhe M, Yamamoto R, Masuda Y** (1986) Inhibition of IAA-induced cell elongation in *Avena* coleoptile segments by galactose: Its effect on UDP-glucose formation. *Physiologia Plantarum* **66**: 370-376
- Irving D, Hurst P, Ragg J** (1997) Changes in carbohydrates and carbohydrate metabolism enzymes during the development, maturation, and ripening of buttercup squash (*Cucurbita maxima* D. Delica). *Journal of the American Society for Horticultural Sciences* **122**: 310-314
- Jewell MC, Campbell BC, Godwin ID** (2010) Transgenic plants for abiotic stress resistance. In C Kole, CH Michler, AG Abbott, TC Hall (eds), *Transgenic Crop Plants*, Brisbane
- Johnston M** (1987) A model fungal gene regulatory mechanism: the GAL genes of *Saccharomyces cerevisiae*. *Microbiological reviews* **51**: 458-476
- Jones H, Jones M, Flowers T** (1989) Introduction: some terminology and common mechanisms. Plants under stress. In: Cambridge University Press, pp 1-10
- Joyard J, Marechal E, Block MA, Douce R** (1996) Plant galactolipids and sulfolipid: structure, distribution and biosynthesis. In M Smallwood, J Knox, D Bowles (eds), *Specialized Functions in Plants*. BIOS Scientific Publishers Limited, pp 179-194
- Joyard J, Maréchal E, Miège C, Block MH, Dorne A-J, Douce R** (2004) Structure, distribution and biosynthesis of glycerolipids from higher plant chloroplasts. In P-A Siegenthaler, N Murata (eds), *Lipids in Photosynthesis: Structure, Function and Genetics*, Vol 6. Springer Netherlands, pp 21-52
- Kabat E, Mac Donald D, Ballou C, Fischer H** (1953) On the structure of galactinol. *Journal of the American Chemical Society* **75**: 4507-4509
- Kandler O, Hopf H** (1982) Oligosaccharides based on sucrose (sucrosyl oligosaccharides). In FA Loewus, W Tanner (eds), *Encyclopedia of plant physiology: Plant Carbohydrates I, Intracellular Carbohydrates* New Series, Vol 13a. Springer-Verlag, Berlin, pp 348-383
- Kaplan CP, Tugal HB, Baker A** (1997) Isolation of a cDNA encoding an Arabidopsis galactokinase by functional expression in yeast. *Plant Molecular Biology* **34**: 497-506
- Kaplan F, Kopka J, Sung DY, Zhao W, Popp M, Porat R, Guy CL** (2007) Transcript and metabolite profiling during cold acclimation of Arabidopsis reveals an intricate relationship of cold-regulated gene expression with modifications in metabolite content. *The Plant Journal* **50**: 967-981
- Keller F** (1992) Galactinol synthase is an extravacuolar enzyme in tubers of Japanese artichoke (*Stachys sieboldii*). *Plant Physiology* **99**: 1251-1253
- Keller F** (1992) Transport of stachyose and sucrose by vacuoles of Japanese artichoke (*Stachys sieboldii*) tubers. *Plant Physiology* **98**: 442-445
- Keller F, Matile P** (1985) The role of the vacuole in storage and mobilization of stachyose in tubers of *Stachys sieboldii*. *Journal of Plant Physiology* **119**: 369-380
- Keller F, Pharr DM** (1996) Metabolism of carbohydrates in sinks and sources: galactosyl-sucrose oligosaccharides. In E Zamski, AA Schaffer (eds), *Photoassimilate distribution in plants and crops: source-sink relationships*. Dekker, M., New York, pp 157-183

- Kerr PS, Rufty TW, Huber SC (1985) Changes in nonstructural carbohydrates in different parts of soybean (*Glycine max* [L.] Merr.) Plants during a light/dark cycle and in extended darkness. *Plant Physiology* **78**: 576-581
- Kim J, Gross K, Solomos T (1991) Galactose metabolism and ethylene production during development and ripening of tomato fruit. *Postharvest Biology and Technology* **1**: 67-80
- Kim MS, Cho SM, Kang EY, Im YJ, Hwangbo H, Kim YC, Ryu C-M, Yang KY, Chung GC, Cho BH (2008) Galactinol is a signaling component of the induced systemic resistance caused by *Pseudomonas chlororaphis* O6 root colonization. *Molecular Plant-Microbe Interactions* **21**: 1643-1653
- King RW, Zeevaert JA (1974) Enhancement of phloem exudation from cut petioles by chelating-agents. *Plant Physiology* **53**: 96-103
- Kleczkowski LA (1994) Glucose activation and metabolism through UDP-glucose pyrophosphorylase in plants. *Phytochemistry* **37**: 1507-1515
- Kleczkowski LA, Decker D, Wilczynska M (2011) UDP-sugar pyrophosphorylase: a new old mechanism for sugar activation. *Plant Physiology* **156**: 3-10
- Knaupp M, Mishra KB, Nedbal L, Heyer AG (2011) Evidence for a role of raffinose in stabilizing photosystem II during freeze-thaw cycles. *Planta* **234**: 477-486
- Korn M, G  rtner T, Erban A, Kopka J, Selbig J, Hinch DK (2010) Predicting Arabidopsis freezing tolerance and heterosis in freezing tolerance from metabolite composition. *Molecular Plant* **3**: 224-235
- Kosterlitz HW (1943) The structure of the galactosephosphate present in the liver during galactose assimilation. *Biochemical Journal* **37**: 318-310
- Kotake T, Hojo S, Yamaguchi D, Aohara T, Konishi T, Tsumuraya Y (2007) Properties and physiological functions of UDP-sugar pyrophosphorylase in Arabidopsis. *Bioscience Biotechnology and Biochemistry* **71**: 761-771
- Kotiguda G, Peterbauer T, Mulimani VH (2006) Isolation and structural analysis of ajugose from *Vigna mungo* L. *Carbohydrate Research* **341**: 2156-2160
- Krul WR, Colclasure GC (1977) Effect of galactose and other monosaccharides on IAA movement in bean hypocotyl segments. *Physiologia Plantarum* **41**: 249-253
- Kulik N, Weignerova L, Filipi T, Pompach P, Novak P, Mrazek H, Slamova K, Bezouska K, Kren V, Ettlich R (2010) The  $\alpha$ -galactosidase type A gene aglA from *Aspergillus niger* encodes a fully functional  $\alpha$ -N-acetylgalactosaminidase. *Glycobiology* **20**: 1410-1419
- Lahuta LB, Goszczynska J (2009) Inhibition of raffinose family oligosaccharides and galactosyl pinitols breakdown delays germination of winter vetch (*Vicia villosa* Roth.) seeds. *Acta Societatis Botanicorum Poloniae* **78**: 203-208
- Lahuta LG, R. (2010) Raffinose in seedlings of winter vetch (*Vicia villosa* Roth.) under osmotic stress and followed by recovery. *Acta Physiologiae Plantarum* **33**: 725-733
- Lai K, Elsas LJ, Wierenga KJ (2009) Galactose toxicity in animals. *IUBMB Life* **61**: 1063-1074
- Lalonde S, Tegeder M, Throne-Holst M, Frommer WB, Patrick JW (2003) Phloem loading and unloading of sugars and amino acids. *Plant, Cell & Environment* **26**: 37-56
- Lee R-H, Chen S-CG (2002) Programmed cell death during rice leaf senescence is nonapoptotic. *New Phytologist* **155**: 25-32
- Lee RH, Hsu JH, Huang HJ, Lo SF, Chen SC (2009) Alkaline  $\alpha$ -galactosidase degrades thylakoid membranes in the chloroplast during leaf senescence in rice. *New Phytologist* **184**: 596-606
- Lee RH, Lin MC, Chen SC (2004) A novel alkaline  $\alpha$ -galactosidase gene is involved in rice leaf senescence. *Plant Molecular Biology* **55**: 281-295
- Lehle L, Tanner W (1973) The function of myo-inositol in the biosynthesis of raffinose. Purification and characterization of galactinol:sucrose 6-galactosyltransferase from *Vicia faba* seeds. *European Journal of Biochemistry* **38**: 103-110
- Leloir LF (1951) The enzymatic transformation of uridine diphosphate glucose into a galactose derivative. *Archives of Biochemistry and Biophysics* **33**: 186-190
- Li SB, Li T, Kim W-D, Kitaoka M, Yoshida S, Nakajima M, Kobayashi H (2007) Characterization of raffinose synthase from rice (*Oryza sativa* L. var. *Nipponbare*). *Biotechnology Letters* **29**: 635-640
- Li X, Zhuo J, Jing Y, Liu X, Wang X (2011) Expression of a galactinol synthase gene is positively associated with desiccation tolerance of *Brassica napus* seeds during development. *Journal of Plant Physiology* **168**: 1761-1770
- Lichtenthaler H, Wellburn A (1983) Determinations of total carotenoids and chlorophylls a and b of leaf extracts in different solvents. *Biochemical Society Transactions* **11**: 591 - 592

- Lichtenthaler HK** (1998) The stress concept in plants: an introduction. *Annals of the New York Academy of Sciences* **851**: 187-198
- Lim P, Kim H, Nam H** (2007) Leaf senescence. *Annual Review of Plant Biology* **58**: 115-136
- Liu JJJ, Krenz DC, Galvez AF, de Lumen BO** (1998) Galactinol synthase (GS): increased enzyme activity and levels of mRNA due to cold and desiccation. *Plant Science* **134**: 11-20
- Loescher W, Everard J** (2000) Regulation of sugar alcohol biosynthesis. In R Leegood, T Sharkey, S Caemmerer (eds), *Photosynthesis: Physiology and Metabolism*. Kluwer Academic, Dordrecht, The Netherlands, pp 275-299
- Loiseau D** (1876) Correspondenzen von A. Henninger aus Paris, 9. Mai 1876 (Akademie, Sitzung vom 1. Mai). *Berichte der Deutschen Chemischen Gesellschaft* **9**: 732
- Mahajan S, Tuteja N** (2005) Cold, salinity and drought stresses: an overview. *Archives of Biochemistry and Biophysics* **444**: 139-158
- Main EL, Pharr DM, Huber SC, Moreland DE** (1983) Control of galactosyl-sugar metabolism in relation to rate of germination. *Physiologia Plantarum* **59**: 387-392
- Majumder AL, Sengupta S, Goswami L** (2010) Osmolyte regulation in abiotic stress. In A Pareek, SK Sopory, HJ Bohnert (eds), *Abiotic Stress Adaptation in Plants*. Springer, Netherlands, pp 349-370
- Maretzki A, Thom M** (1978) Characteristics of a galactose-adapted sugarcane cell line grown in suspension culture. *Plant Physiology* **61**: 544-548
- Marraccini P, Rogers WJ, Caillet V, Deshayes A, Granato D, Lausanne F, Lechat S, Pridmore D, Petiard V** (2005) Biochemical and molecular characterization of  $\alpha$ -D-galactosidase from coffee beans. *Plant Physiology and Biochemistry* **43**: 909-920
- Martínez DE, Costa ML, Guamet JJ** (2008) Senescence-associated degradation of chloroplast proteins inside and outside the organelle. *Plant Biology* **10**: 15-22
- Maruyama K, Takeda M, Kidokoro S, Yamada K, Sakuma Y, Urano K, Fujita M, Yoshiwara K, Matsukura S, Morishita Y, Sasaki R, Suzuki H, Saito K, Shibata D, Shinozaki K, Yamaguchi-Shinozaki K** (2009) Metabolic pathways involved in cold acclimation identified by integrated analysis of metabolites and transcripts regulated by DREB1A and DREB2A. *Plant Physiology* **150**: 1972-1980
- Matile P** (1992) Chloroplast senescence. In N Baker, H Thomas (eds), *Crop photosynthesis: spatial and temporal determinants*. Elsevier Science Publishers, New York, NY, USA, pp 413-440
- McCaskill A, Turgeon R** (2007) Phloem loading in *Verbascum phoeniceum* L. depends on the synthesis of raffinose-family oligosaccharides. *Proceedings of the National Academy of Sciences of the United States of America* **104**: 19619-19624
- McNeil SD, Nuccio ML, Hanson AD** (1999) Betaines and related osmoprotectants. Targets for metabolic engineering of stress resistance. *Plant Physiology* **120**: 945-949
- Meyer A, Eskandari S, Grallath S, Rentsch D** (2006) AtGAT1, a high affinity transporter for gamma-aminobutyric acid in *Arabidopsis thaliana*. *Journal of Biological Chemistry* **281**: 7197-7204
- Meyer T, Hölscher C, Schwöppe C, von Schaewen A** (2011) Alternative targeting of Arabidopsis plastidic glucose-6-phosphate dehydrogenase G6PD1 involves cysteine-dependent interaction with G6PD4 in the cytosol. *The Plant Journal* **66**: 745-758
- Mitchell DE, Gadus MV, Madore MA** (1992) Patterns of Assimilate Production and Translocation in Muskmelon (*Cucumis melo* L.) : I. Diurnal Patterns. *Plant Physiology* **99**: 959-965
- Morre DJ** (1968) Cell wall dissolution and enzyme secretion during leaf abscission. *Plant Physiology* **43**: 1545-1559
- Mullen JA, Koller HR** (1988) Trends in carbohydrate depletion, respiratory carbon loss, and assimilate export from soybean leaves at night. *Plant Physiology* **86**: 517-521
- Munns R** (2002) Comparative physiology of salt and water stress. *Plant, Cell & Environment* **25**: 239-250
- Murashige T, Skoog F** (1962) A revised medium for rapid growth and bio assays with tobacco tissue cultures. *Physiologia Plantarum* **15**: 473-497
- Nakai H, Baumann MJ, Petersen BO, Westphal Y, Hachem MA, Dilokpimol A, Duus J, Schols HA, Svensson B** (2010) *Aspergillus nidulans*  $\alpha$ -galactosidase of glycoside hydrolase family 36 catalyses the formation of  $\alpha$ -galacto-oligosaccharides by transglycosylation. *FEBS Journal* **277**: 3538-3551
- Nanjo T, Kobayashi M, Yoshida Y, Kakubari Y, Yamaguchi-Shinozaki K, Shinozaki K** (1999) Antisense suppression of proline degradation improves tolerance to freezing and salinity in *Arabidopsis thaliana*. *FEBS Letters* **461**: 205-210
- Neufeld EF, Feingold DS, Hassid WZ** (1960) Phosphorylation of D-galactose and L-arabinose by extracts from *Phaseolus aureus* seedlings. *Journal of Biological Chemistry* **235**: 906-909

- Nishizawa-Yokoi A, Yabuta Y, Shigeoka S** (2008) The contribution of carbohydrates including raffinose family oligosaccharides and sugar alcohols to protection of plant cells from oxidative damage. *Plant Signaling and Behaviour* **3**: 1016-1018
- Nishizawa A, Yabuta Y, Shigeoka S** (2008) Galactinol and raffinose constitute a novel function to protect plants from oxidative damage. *Plant Physiology* **147**: 1251-1263
- Nishizawa A, Yabuta Y, Yoshida E, Maruta T, Yoshimura K, Shigeoka S** (2006) Arabidopsis heat shock transcription factor A2 as a key regulator in response to several types of environmental stress. *The Plant Journal* **48**: 535-547
- Noodén LD, Guamét JJ, John I** (1997) Senescence mechanisms. *Physiologia Plantarum* **101**: 746-753
- Nozawa A, Ito M, Hayashi H, Watanabe A** (1999) Dark-induced expression of genes for asparagine synthetase and cytosolic glutamine synthetase in radish cotyledons is dependent on the growth stage. *Plant and Cell Physiology* **40**: 942-948
- Nunan KJ, Davies C, Robinson SP, Fincher GB** (2001) Expression patterns of cell wall-modifying enzymes during grape berry development. *Planta* **214**: 257-264
- Obendorf RL** (1997) Oligosaccharides and galactosyl cyclitols in seed desiccation tolerance. *Seed Science Research* **7**: 63-74
- Olien CR, Smith MN** (1977) Ice adhesions in relation to freeze stress. *Plant Physiology* **60**: 499-503
- Ooms J, Leon-Kloosterziel KM, Bartels D, Koornneef M, Karssen CM** (1993) Acquisition of desiccation tolerance and longevity in seeds of *Arabidopsis thaliana* (A Comparative Study Using Absciscic Acid-Insensitive *abi3* Mutants). *Plant Physiology* **102**: 1185-1191
- Oparka KJ, Duckett CM, Prior DAM, Fisher DB** (1994) Real-time imaging of phloem unloading in the root tip of *Arabidopsis*. *The Plant Journal* **6**: 759-766
- Ordin L, Bonner J** (1957) Effect of galactose on growth and metabolism of *Avena* coleoptile sections. *Plant Physiology* **32**: 212-215
- Panikulangara TJ, Eggers-Schumacher G, Wunderlich M, Stransky H, Schöffl F** (2004) Galactinol synthase1. A novel heat shock factor target gene responsible for heat-induced synthesis of raffinose family oligosaccharides in *Arabidopsis*. *Plant Physiology* **136**: 3148-3158
- Parcy F, Nilsson O, Busch MA, Lee I, Weigel D** (1998) A genetic framework for floral patterning. *Nature* **395**: 561-566
- Patrick JW** (1997) Phloem unloading: sieve element unloading and post-sieve element transport. *Annual review of plant physiology and plant molecular biology* **48**: 191-222
- Penna S** (2003) Building stress tolerance through over-producing trehalose in transgenic plants. *Trends in Plant Science* **8**: 355-357
- Pennycooke JC, Jones ML, Stushnoff C** (2003) Down-regulating alpha-galactosidase enhances freezing tolerance in transgenic petunia. *Plant Physiology* **133**: 901-909
- Pennycooke JC, Vepachedu R, Stushnoff C** (2004) Expression of an  $\alpha$ -galactosidase gene in petunia is upregulated during low-temperature deacclimation. *Journal of the American Society for Horticultural Science* **129**: 491-496
- Peterbauer T, Lahuta LB, Blochl A, Mucha J, Jones DA, Hedley CL, Gorecki RJ, Richter A** (2001) Analysis of the raffinose family oligosaccharide pathway in pea seeds with contrasting carbohydrate composition. *Plant Physiology* **127**: 1764-1772
- Peterbauer T, Mach L, Mucha J, Richter A** (2002b) Functional expression of a cDNA encoding pea (*Pisum sativum* L.) raffinose synthase, partial purification of the enzyme from maturing seeds, and steady-state kinetic analysis of raffinose synthesis. *Planta* **215**: 839-846
- Peterbauer T, Mucha J, Mach L, Richter A** (2002a) Chain elongation of raffinose in pea seeds. Isolation, characterization, and molecular cloning of multifunctional enzyme catalyzing the synthesis of stachyose and verbascose. *Journal of Biological Chemistry* **277**: 194-200
- Peterbauer T, Mucha J, Mayer U, Popp M, Glössl J, Richter A** (1999) Stachyose synthesis in seeds of adzuki bean (*Vigna angularis*): molecular cloning and functional expression of stachyose synthase. *The Plant Journal* **20**: 509-518
- Peterbauer T, Richter A** (1998) Galactosylononitol and stachyose synthesis in seeds of adzuki bean . Purification and characterization of stachyose synthase. *Plant Physiology* **117**: 165-172
- Peterbauer T, Richter A** (2001) Biochemistry and physiology of raffinose family oligosaccharides and galactosyl cyclitols in seeds. *Seed Science Research* **11**: 185-197
- Peters S, Egert A, Stieger B, Keller F** (2010) Functional identification of *Arabidopsis* ATSIP2 (At3g57520) as an alkaline  $\alpha$ -galactosidase with a substrate specificity for raffinose and an apparent sink-specific expression pattern. *Plant and Cell Physiology* **51**: 1815-1819



- Peters S, Keller F** (2009) Frost tolerance in excised leaves of the common bugle (*Ajuga reptans* L.) correlates positively with the concentrations of raffinose family oligosaccharides (RFOs). *Plant, Cell & Environment* **32**: 1099–1107
- Peters S, Mundree SG, Thomson JA, Farrant JM, Keller F** (2007) Protection mechanisms in the resurrection plant *Xerophyta viscosa* (Baker): both sucrose and raffinose family oligosaccharides (RFOs) accumulate in leaves in response to water deficit. *Journal of Experimental Botany* **58**: 1947–1956
- Pharr DM, Hubbard N** (1994) Melons: biochemical and physiological control of sugar accumulation. In C Arntzen (ed), *Encyclopedia of Agricultural Science*. Academic Press, New York, pp 1912–1934
- Pharr DM, Sox HN** (1984) Changes in carbohydrate and enzyme levels during sink to source transition of leaves of *Cucumis sativus* L., a stachyose transporter. *Plant Science Letters* **35**: 187–193
- Pharr DM, Sox HN, Locy RD, Huber SC** (1981) Partial characterization of the galactinol forming enzyme from leaves of *Cucumis-Sativus* L. *Plant Science Letters* **23**: 25–33
- Pinheiro C, Chaves MM, Ricardo CP** (2001) Alterations in carbon and nitrogen metabolism induced by water deficit in the stems and leaves of *Lupinus albus* L. *Journal of Experimental Botany* **52**: 1063–1070
- Planta A, Schultze E** (1890) *Berichte der Deutschen Chemischen Gesellschaft* **23**: 1692
- Porter JE, Herrmann KM, Ladisch MR** (1990) Integral kinetics of alpha-galactosidase purified from *Glycine max* for simultaneous hydrolysis of stachyose and raffinose. *Biotechnology and bioengineering* **35**: 15–22
- Poschet G, Hannich B, Büttner M** (2010) Identification and characterization of AtSTP14, a novel galactose transporter from Arabidopsis. *Plant and Cell Physiology* **51**: 1571–1580
- Pridham JB, Walter MW, Worth HGJ** (1969) The metabolism of raffinose and sucrose in germinating broad-bean (*Vicia faba*) seeds. *Journal of Experimental Botany* **20**: 317–324
- Pukacka S, Ratajczak E, Kalembe E** (2009) Non-reducing sugar levels in beech (*Fagus sylvatica*) seeds as related to withstanding desiccation and storage. *Journal of Plant Physiology* **166**: 1381–1390
- Rathinasabapathi B** (2000) Metabolic engineering for stress tolerance: installing osmoprotectant synthesis pathways. *Annals of Botany* **86**: 709–716
- Raven JA** (1997) CO<sub>2</sub>-concentrating mechanisms: a direct role for thylakoid lumen acidification? *Plant, Cell & Environment* **20**: 147–154
- Reid J, Meier H** (1973) Enzymatic activities and galactomannan mobilization in germinating seeds of fenugreek (*Trigonella foenum-graecum* L. *Leguminosae*). Secretion of  $\alpha$ -galactosidase and  $\beta$ -mannosidase by the aleurone layer. *Planta* **112**: 301–308
- Reid JSG** (1971) Reserve carbohydrate metabolism in germinating seeds of *Trigonella foenum-graecum* L. (*Leguminosae*). *Planta* **100**: 131–142
- Reidel EJ, Rennie EA, Amiard V, Cheng L, Turgeon R** (2009) Phloem loading strategies in three plant species that transport sugar alcohols. *Plant Physiology* **149**: 1601–1608
- Rennie EA, Turgeon R** (2009) A comprehensive picture of phloem loading strategies. *Proceedings of the National Academy of Sciences of the United States of America* **106**: 14162–14167
- Rhodes D, Nadolska-Orczyk A, Rich PJ** (2004) Salinity, osmolytes and compatible solutes. In *Salinity: Environment - Plants - Molecules*. Springer Netherlands, pp 181–204
- Roberts RM, Heishman A, Wicklin C** (1971) Growth inhibition and metabolite pool levels in plant tissues fed D-glucosamine and D-galactose. *Plant Physiology* **48**: 36–42
- Romo S, Labrador E, Dopico B** (2001) Water stress-regulated gene expression in *Cicer arietinum* seedlings and plants. *Plant Physiology and Biochemistry* **39**: 1017–1026
- Rontein D, Basset G, Hanson AD** (2002) Metabolic engineering of osmoprotectant accumulation in plants. *Metabolic Engineering* **4**: 49–56
- Rösti J, Barton CJ, Albrecht S, Dupree P, Pauly M, Findlay K, Roberts K, Seifert GJ** (2007) UDP-glucose 4-epimerase isoforms UGE2 and UGE4 cooperate in providing UDP-galactose for cell wall biosynthesis and growth of *Arabidopsis thaliana*. *The Plant Cell* **19**: 1565–1579
- Sakai A, Larcher W** (1987) Frost survival of plants. Responses and adaptation to freezing stress. Springer-Verlag, Berlin
- Saravitz D, Pharr DM, Carter T** (1987) Galactinol synthase activity and soluble sugars in developing seeds of four soybean genotypes. *Plant Physiology* **83**: 185–189
- Sastry PS, Kates M** (1964) Hydrolysis of monogalactosyl and digalactosyl diglycerides by specific enzymes in runner-bean leaves. *Biochemistry* **3**: 1280–1287
- Sauer N** (2007) Molecular physiology of higher plant sucrose transporters. *FEBS Letters* **581**: 2309–2317
- Schelbert S, Aubry S, Burla B, Agne B, Kessler F, Krupinska K, Hortensteiner S** (2009) Pheophytin pheophorbide hydrolase (pheophytinase) is involved in chlorophyll breakdown during leaf senescence in Arabidopsis. *The Plant Cell* **21**: 767–785

- Schenk N, Schelbert S, Kanwischer M, Goldschmidt EE, Dörmann P, Hörtensteiner S (2007) The chlorophyllases AtCLH1 and AtCLH2 are not essential for senescence-related chlorophyll breakdown in *Arabidopsis thaliana*. *FEBS Letters* **581**: 5517-5525
- Schneider T, Keller F (2009) Raffinose in chloroplasts is synthesized in the cytosol and transported across the chloroplast envelope. *Plant and Cell Physiology* **50**: 2174-2182
- Schulze ED (1986) Carbon dioxide and water vapor exchange in response to drought in the atmosphere and in the soil. *Annual Review of Plant Physiology* **37**: 247-274
- Schulze W, Schneider T, Starck S, Martinoia E, Trentmann O (2011) Cold acclimation induces changes in Arabidopsis tonoplast protein abundance and activity and alters phosphorylation of tonoplast monosaccharide transporters. *The Plant Journal* no-no
- Schümperli D, Howard BH, Rosenberg M (1982) Efficient expression of *Escherichia coli* galactokinase gene in mammalian cells. *Proceedings of the National Academy of Sciences of the United States of America* **79**: 257-261
- Scott P (2000) Resurrection plants and the secrets of eternal leaf. *Annals of Botany* **85**: 159-166
- Seifert GJ, Barber C, Wells B, Roberts K (2004) Growth regulators and the control of nucleotide sugar flux. *The Plant Cell* **16**: 723-730
- Seki M, Carninci P, Nishiyama Y, Hayashizaki Y, Shinozaki K (1998) High-efficiency cloning of Arabidopsis full-length cDNA by biotinylated CAP trapper. *The Plant Journal* **15**: 707-720
- Seki M, Narusaka M, Kamiya A, Ishida J, Satou M, Sakurai T, Nakajima M, Enju A, Akiyama K, Oono Y, Muramatsu M, Hayashizaki Y, Kawai J, Carninci P, Itoh M, Ishii Y, Arakawa T, Shibata K, Shinagawa A, Shinozaki K (2002) Functional annotation of a full-length Arabidopsis cDNA collection. *Science* **296**: 141-145
- Sekiguchi Y, Mitsuhashi N, Inoue Y, Yagisawa H, Mimura T (2004) Analysis of sugar phosphates in plants by ion chromatography on a titanium dioxide column with pulsed amperometric detection. *Journal of Chromatography A* **1039**: 71-76
- Senser M, Kandler O (1967a) Galactinol, ein Galactosyldonor für die Biosynthese der Zucker der Raffinosefamilien in Blättern. *Zeitschrift für Pflanzenphysiologie* **57**: 376-388
- Senser M, Kandler O (1967b) Vorkommen und Verbreitung von Galactinol in Blättern höherer Pflanzen. *Phytochemistry* **6**: 1533-1540
- Serraj R, Sinclair TR (2002) Osmolyte accumulation: can it really help increase crop yield under drought conditions? *Plant, Cell & Environment* **25**: 333-341
- Shen B, Jensen RG, Bohnert HJ (1997) Mannitol protects against oxidation by hydroxyl radicals. *Plant Physiology* **115**: 527-532
- Sherson S, Gy I, Medd J, Schmidt R, Dean C, Kreis M, Lecharny A, Cobbett C (1999) The arabinose kinase, ARA1, gene of Arabidopsis is a novel member of the galactose kinase gene family. *Plant Molecular Biology* **39**: 1003-1012
- Sherson SM, Hemmann G, Wallace G, Forbes S, Germain V, Stadler R, Bechtold N, Sauer N, Smith SM (2000) Monosaccharide/proton symporter AtSTP1 plays a major role in uptake and response of Arabidopsis seeds and seedlings to sugars. *Plant Journal* **24**: 849-857
- Sheveleva E, Chmara W, Bohnert HJ, Jensen RG (1997) Increased salt and drought tolerance by D-ononitol production in transgenic *Nicotiana tabacum* L. *Plant Physiology* **115**: 1211-1219
- Shimada Y, Wu GJ, Watanabe A (1998) A protein encoded by *din1*, a dark-inducible and senescence-associated gene of radish, can be imported by isolated chloroplasts and has sequence similarity to sulfide dehydrogenase and other small stress proteins. *Plant and Cell Physiology* **39**: 139-143
- Shinozaki K, Yamaguchi-Shinozaki K (1997) Gene expression and signal transduction in water-stress response. *Plant Physiology* **115**: 327-334
- Shinozaki K, Yamaguchi-Shinozaki K (1999) Molecular responses to drought stress. In K Shinozaki, K Yamaguchi-Shinozaki (eds), *Molecular Responses to Cold, Drought, Heat and Salt Stress in Higher Plants*. RG Landes, Austin, TX, pp 11-28
- Slewinski TL, Braun DM (2010) Current perspectives on the regulation of whole-plant carbohydrate partitioning. *Plant Science* **178**: 341-349
- Smart EL, Pharr DM (1980) Characterization of alpha-galactosidase from cucumber leaves. *Plant Physiology* **66**: 731-734
- Smart EL, Pharr DM (1981) Separation and characteristics of galactose-1-phosphate and glucose-1-phosphate uridylyltransferase from fruit peduncles of cucumber. *Planta* **153**: 370-375
- Smith AM, Zeeman SC, Smith SM (2005) Starch degradation. *Annual Review of Plant Biology* **56**: 73-98

- Smith PT, Kuo TM, Crawford C** (1991) Purification and characterization of galactinol synthase from mature zucchini squash leaves. *Plant Physiology* **96**: 693-698
- Soh CP, Ali ZM, Lazan H** (2006) Characterisation of an alpha-galactosidase with potential relevance to ripening related texture changes. *Phytochemistry* **67**: 242-254
- Sprenger N, Keller F** (2000) Allocation of raffinose family oligosaccharides to transport and storage pools in *Ajuga reptans*: the roles of two distinct galactinol synthases. *The Plant Journal* **21**: 249-258
- Stagoj MN, Komel R** (2008) The GAL induction response in yeasts with impaired galactokinase Gal1p activity. *World Journal of Microbiology & Biotechnology* **24**: 2159-2166
- Stitt M, Cséke C, Buchanan BB** (1985) Regulation of fructose 2,6-bisphosphate concentration in spinach leaves. *European Journal of Biochemistry* **143**: 89-93
- Stitt M, Gibon Y, Lunn JE, Piques M** (2007) Multilevel genomics analysis of carbon signalling during low carbon availability: coordinating the supply and utilisation of carbon in a fluctuating environment. *Functional Plant Biology* **34**: 526-549
- Suzuki H, Ozawa Y, Oota H, Yoshida H** (1969) Studies on decomposition of raffinose by alpha-galactosidase of mold. I. Alpha-galactosidase formation and hydrolysis of raffinose by enzyme preparation. *Agricultural and Biological Chemistry* **33**: 506
- Taji T, Ohsumi C, Iuchi S, Seki M, Kasuga M, Kobayashi M, Yamaguchi-Shinozaki K, Shinozaki K** (2002) Important roles of drought- and cold-inducible genes for galactinol synthase in stress tolerance in *Arabidopsis thaliana*. *The Plant Journal* **29**: 417-426
- Tanner W** (1969) The function of myo-inositol glycosides in yeasts and higher plants. In M Krauss (ed), Cyclitols and phosphoinositides: chemistry, metabolism, and function, Vol 164. Annals of the New York Academy of Sciences pp 726-742
- Tanner W, Kandler O** (1966) Biosynthesis of stachyose in *Phaseolus vulgaris*. *Plant Physiology* **41**: 1540-1542
- Tanner W, Kandler O** (1968) Myo-inositol a cofactor in biosynthesis of stachyose. *European Journal of Biochemistry* **4**: 233-239
- Tanner W, Lehle L, Kandler O** (1967) Myo-Inositol, a cofactor in the biosynthesis of verbascose. *Biochemical and Biophysical Research Communications* **29**: 166-171
- Tapernoux-Lüthi EM, Böhm A, Keller F** (2004) Cloning, functional expression, and characterization of the raffinose oligosaccharide chain elongation enzyme, galactan:galactan galactosyltransferase, from common bugle leaves. *Plant Physiology* **134**: 1377-1387
- Tapernoux-Lüthi EM, Schneider T, Keller F** (2007) The C-terminal sequence from common bugle leaf galactan : galactan galactosyltransferase is a non-sequence-specific vacuolar sorting determinant. *FEBS Letters* **581**: 1811-1818
- Tarczynski MC, Jensen RG, Bohnert HJ** (1993) Stress protection of transgenic tobacco by production of the osmolyte mannitol. *Science* **259**: 508-510
- Thanankul D, Tanaka M, Chichester C, Li T** (1976) Degradation of raffinose and stachyose in soybean milk by alpha-galactosidase from *Mortierella vinacea*. *Journal of Food Science* **41**: 173-175
- Thoden JB, Timson DJ, Reece RJ, Holden HM** (2004) Molecular structure of human galactose mutarotase. *Journal of Biological Chemistry* **279**: 23431-23437
- Thomashow MF** (1999) Plant cold acclimation: freezing tolerance genes and regulatory mechanisms. *Annual review of plant physiology and plant molecular biology* **50**: 571-599
- Thomashow MF** (2001) So what's new in the field of plant cold acclimation? Lots! *Plant Physiology* **125**: 89-93
- Thompson J, Froese C, Madey E, Smith M, Hong Y** (1998) Lipid metabolism during plant senescence. *Progress in Lipid Research* **37**: 119-141
- Timasheff S** (1992) Water as ligand: preferential binding and exclusion of denaturants in protein unfolding. *Biochemistry* **31**: 9857-9864
- Timson DJ, Reece RJ** (2002) Kinetic analysis of yeast galactokinase: implications for transcriptional activation of the GAL genes. *Biochimie* **84**: 265-272
- Timson DJ, Reece RJ** (2003) Sugar recognition by human galactokinase. *BMC Biochem* **4**: 16
- Tohge T, Ramos MS, Nunes-Nesi A, Mutwil M, Giavalisco P, Steinhäuser D, Schellenberg M, Willmitzer L, Persson S, Martinola E, Fernie AR** (2011) Toward the storage metabolome: profiling the barley vacuole. *Plant Physiology* **157**: 1469-1482
- Turgeon R** (1996) Phloem loading and plasmodesmata. *Trends in Plant Science* **1**: 418-423
- Turgeon R** (2010) The role of phloem loading reconsidered. *Plant Physiology* **152**: 1817-1823
- Turgeon R, Ayre BG** (2005) Pathways and mechanisms of phloem loading. In N Holbrook, M Zwieniecki (eds), Vascular Transport in Plants. Elsevier/Academic Press, Oxford, pp 45-67

- Turgeon R, Beebe D, Gowan E** (1993) The intermediary cell: Minor-vein anatomy and raffinose oligosaccharide synthesis in the Scrophulariaceae. *Planta* **191**: 446-456
- Turgeon R, Medville R** (2004) Phloem Loading. A reevaluation of the relationship between plasmodesmatal frequencies and loading strategies. *Plant Physiology* **136**: 3795-3803
- Turgeon R, Wolf S** (2009) Phloem transport: cellular pathways and molecular trafficking. *Annual Review of Plant Biology* **60**: 207-221
- Uddin MI, Qi Y, Yamada S, Shibuya I, Deng X-P, Kwak S-S, Kaminaka H, Tanaka K** (2008) Overexpression of a new rice vacuolar antiporter regulating protein OsARP improves salt tolerance in tobacco. *Plant and Cell Physiology* **49**: 880-890
- Uemura M, Steponkus PL** (2003) Modification of the intracellular sugar content alters the incidence of freeze-induced membrane lesions of protoplasts isolated from *Arabidopsis thaliana* leaves. *Plant, Cell & Environment* **26**: 1083-1096
- Ueno Y, Ikami T, Yamauchi R, Kato K** (1980) Purification and some properties of alpha galactosidase from tubers of *Stachys affinis*. . *Agricultural and Biological Chemistry* **44**: 2623-2630
- Valluru R, Van den Ende W** (2008) Plant fructans in stress environments: emerging concepts and future prospects. *Journal of Experimental Botany* **59**: 2905-2916
- Verbruggen N, Hermans C** (2008) Proline accumulation in plants: a review. *Amino Acids* **35**: 753-759
- Vicré M, Farrant JM, Driouich A** (2004) Insights into the cellular mechanisms of desiccation tolerance among angiosperm resurrection plant species. *Plant, Cell & Environment* **27**: 1329-1340
- Viola R, Roberts AG, Haupt S, Gazzani S, Hancock RD, Marmioli N, Machray GC, Oparka KJ** (2001) Tuberization in potato involves a switch from apoplastic to symplastic phloem unloading. *The Plant Cell* **13**: 385-398
- Voitsekhovskaja OV, Rudashevskaya EL, Demchenko KN, Pakhomova MV, Batashev DR, Gamalei YV, Lohaus G, Pawlowski K** (2009) Evidence for functional heterogeneity of sieve element-companion cell complexes in minor vein phloem of *Alonsoa meridionalis*. *Journal of Experimental Botany* **60**: 1873-1883
- Wang TL, Domoney C, Hedley CL, Casey R, Grusak MA** (2003a) Can we improve the nutritional quality of legume seeds? *Plant Physiology* **131**: 886-891
- Wang W, Vinocur B, Altman A** (2003b) Plant responses to drought, salinity and extreme temperatures: towards genetic engineering for stress tolerance. *Planta* **218**: 1-14
- Wang Z-Y, Li F-M, Xiong Y-C, Xu B-C** (2008) Soil-water threshold range of chemical signals and drought tolerance was mediated by ROS homeostasis in winter wheat during progressive soil drying. *Journal of Plant Growth Regulation* **27**: 309-319
- Wanner LA, Junttila O** (1999) Cold-induced freezing tolerance in Arabidopsis. *Plant Physiology* **120**: 391-400
- Webb MS, Green BR** (1991) Biochemical and biophysical properties of thylakoid acyl lipids. *Biochimica et Biophysica Acta* **1060**: 133-158
- Werner D, Gerlitz N, Stadler R** (2011) A dual switch in phloem unloading during ovule development in Arabidopsis. *Protoplasma* **248**: 225-235
- Wilkinson JF** (1949) The pathway of the adaptive fermentation of galactose by yeast. *Biochemical Journal* **44**: 460-460
- Williams J, Villarroya H, Petek F** (1978) Alpha-Galactosidases II, III and IV from seeds of *Trifolium repens*. Purification, physicochemical properties and mode of galactomannan hydrolysis *in vitro*. *Biochemical Journal* **175**: 1069-1077
- Wingenter K, Trentmann O, Winschuh I, Hörmiller II, Heyer AG, Reinders J, Schulz A, Geiger D, Hedrich R, Neuhaus HE** (2011) A member of the mitogen-activated protein 3-kinase family is involved in the regulation of plant vacuolar glucose uptake. *The Plant Journal* **68**: 890-900
- Wong L, Sheu K, Lee S, Frey P** (1977) Galactose-1-phosphate uridylyltransferase: isolation and properties of a uridylyl-enzyme intermediate. *Biochemistry* **16**: 1010-1016
- Woolhouse H** (1984) The biochemistry and regulation of senescence in chloroplasts. *Canadian Journal of Botany* **62**: 2934-2942
- Wormit A, Trentmann O, Feifer I, Lohr C, Tjaden J, Meyer S, Schmidt U, Martinoia E, Neuhaus HE** (2006) Molecular identification and physiological characterization of a novel monosaccharide transporter from Arabidopsis involved in vacuolar sugar transport. *The Plant Cell* **18**: 3476-3490
- Wu X, Kishitani S, Ito Y, Toriyama K** (2009) Accumulation of raffinose in rice seedlings overexpressing OsWRKY11 in relation to desiccation tolerance. *Plant Biotechnology* **26**: 431-434
- Yamaguchi-Shinozaki K, Shinozaki K** (2006) Transcriptional regulatory networks in cellular responses and tolerance to dehydration and cold stresses. *Annual Review of Plant Biology* **57**: 781-803

- Yamamoto R, Inouhe M, Masuda Y** (1988) Galactose inhibition of auxin-induced growth of mono- and dicotyledonous plants. *Plant Physiology* **86**: 1223-1227
- Yancey P** (1994) Compatible and counteracting solutes. In K Strange (ed), *Cellular and Molecular Physiology of Cell Volume Regulation*. CRC Press, Boca Raton
- Yancey PH, Clark ME, Hand SC, Bowlus RD, Somero GN** (1982) Living with water stress: evolution of osmolyte systems. *Science* **217**: 1214-1222
- Yang T, Bar-Peled L, Gebhart L, Lee SG, Bar-Peled M** (2009) Identification of galacturonic acid-1-phosphate kinase, a new member of the GHMP kinase superfamily in plants, and comparison with galactose-1-phosphate kinase. *Journal of Biological Chemistry* **284**: 21526-21535
- Zeng L, Das SC, Burne RA** (2010) Utilization of Lactose and Galactose by *Streptococcus mutans*: Transport, Toxicity, and Carbon Catabolite Repression. *Journal of Bacteriology* **192**: 2434-2444
- Zhang C, Turgeon R** (2009) Downregulating the sucrose transporter VpSUT1 in *Verbascum phoeniceum* does not inhibit phloem loading. *Proceedings of the National Academy of Sciences of the United States of America* **106**: 18849-18854
- Zhang Q, Hrmova M, Shirley NJ, Lahnstein J, Fincher GB** (2006a) Gene expression patterns and catalytic properties of UDP-D-glucose 4-epimerases from barley (*Hordeum vulgare* L.). *Biochemical Journal* **394**: 115-124
- Zhang X-Y, Wang X-L, Wang X-F, Xia G-H, Pan Q-H, Fan R-C, Wu F-Q, Yu X-C, Zhang D-P** (2006b) A shift of phloem unloading from symplasmic to apoplasmic pathway is involved in developmental onset of ripening in grape berry. *Plant Physiology* **142**: 220-232
- Zhang YP, Gong F, Bao GQ, Gao HW, Ji SP, Tan YX, Li SB, Li LL, Wang YL, Xu H, Xu LJ, Tian SG, Zhang ZX, Lu QS, Qiu Y, Bai JS, Chen JT** (2007) B to O erythrocyte conversion by the recombinant alpha-galactosidase. *Chinese medical journal* **120**: 1145-1150
- Zhao H, Lu L, Xiao M, Wang Q, Lu Y, Liu C, Wang P, Kumagai H, Yamamoto K** (2008) Cloning and characterization of a novel  $\alpha$ -galactosidase from *Bifidobacterium breve* 203 capable of synthesizing Gal- $\alpha$ -1,4 linkage. *FEMS Microbiology Letters* **285**: 278-283
- Zhao TY, Corum JW, Mullen J, Meeley RB, Helentjaris T, Martin D, Downie B** (2006) An alkaline alpha-galactosidase transcript is present in maize seeds and cultured embryo cells, and accumulates during stress. *Seed Science Research* **16**: 107-121
- Zhu JK** (2001) Plant salt tolerance. *Trends in Plant Science* **6**: 66-71
- Zhu JK** (2002) Salt and drought stress signal transduction in plants. *Annual Review of Plant Biology* **53**: 247-273
- Zuther E, Büchel K, Hundertmark M, Stitt M, Hinch DK, Heyer AG** (2004) The role of raffinose in the cold acclimation response of *Arabidopsis thaliana*. *FEBS Letters* **576**: 169-173

## List of abbreviations

ABA	abscisic acid
ABF	ABA-responsive element binding factor
ABRE	abscisic acid responsive element
$\alpha$ Gal	$\alpha$ -D-galactosidase
AREB	abscisic acid responsive element binding
AsA	ascorbate
ATP	adenosine triphosphate
Aju	ajugose
$\beta$ Gal	$\beta$ -galactosidase
bp	base pair
bZIP	basic leucine zipper
CBF	C-repeat binding factor
CC	companion cells
cDNA	copy-DNA
CDS	coding sequence
CLSM	confocal laser scanning microscopy
Col-0	columbia-0 ecotype
COR	cold responsive genes/proteins
CPM	counts per minute
CRT	C-repeat
DGDG	digalactosyl diacylglycerol
DMSP	3-dimethylsulfoniopropionate
DNA	deoxyribose nucleic acid
dNTP	deoxynucleotide triphosphate
DP	degree of polymerization
DRE	dehydration responsive element
DREB	dehydration-responsive element binding protein
DW	dry weight
ERD	early responsive to dehydration
Fru	fructose
FW	fresh weight
Gol	galactinol
GolS	galactinol synthase
Gal	galactose
Gal1P	galactose-1-phosphate
GALK	galactokinase
GALE	UDP-Gal 4'epimerase
GALT	Gal1P uridylyltransferase
GGT	galactan:galactan galactosyltransferase
GH	glycosylhydrolase
Glc1P	glucose-1-phosphate
Glc6P	glucose-6-phosphate
GSH	glutathione
GUS	$\beta$ -glucuronidase
HPLC	high-performance liquid chromatography
HPLC-PAD	HPLC with pulsed amperometric detector
HSF	heat shock factor
IC	intermediary cells
Ino	<i>myo</i> -inositol
LTI	low-temperature induced
KDa	kilodalton
KIN	cold induced
Kb	kilobase

K <sub>m</sub>	Michaelis-Menten constant
Mel	melibiose
MGDG	monogalactosyl diacylglycerol
MOI	multiplicity of infection
MST	monosaccharide transporter
n.d.	not detected
PCR	polymerase chain reaction
PPase	pyrophosphorylase
Raf	raffinose
RafS	raffinose synthase
RD	responsive to dehydration
RFO	raffinose family of oligosaccharides
RH	relative humidity
RNA	ribonucleic acid
ROS	reactive oxygen species
RT	room temperature
RWC	relative water content
SE	sieve element
Sf9	<i>Spodoptera frugiperda</i> cell line 9
Sf21	<i>Spodoptera frugiperda</i> cell line 21
SIP	seed imbibition protein
sqPCR	semi-quantitative PCR
Sta	stachyose
SAP	shrimp alkaline phosphatase
StaS	stachyose synthase
Suc	sucrose
T-DNA	transfer DNA
UDP-Gal	uridindiphosphate-galactose
UDP-Glc	uridindiphosphate-glucose
UGE	UDP-Glc 4'-epimerase
UGGPase	UDP-Gal/Glc pyrophosphorylase
UT	uridylyltransferase
v/v	volume/volume
Ver	verbascose
VerS	verbascose synthase
WSC	water soluble carbohydrate
WT	wild-type

#### List of chemicals:

DGJ	1-deoxygalactonojirimycin
DTT	dithiothreitol
EDTA	ethylenediaminetetraacetic acid
EtOH	ethanol
FAA	formalin-acetic-alcohol
HEPES	4-(2-hydroxyethyl)-1-piperazineethanesulfonic acid
LB	Luria-Bertani medium
MES	2-(N-morpholino)ethanesulfonic acid
MS medium	Murashige and Skoog medium
PEG	polyethylene glycol
PMSF	phenylmethanesulfonylfluoride
pNP $\alpha$ Gal	para-nitrophenyl- $\alpha$ -D-galactopyranoside
pNP $\beta$ Gal	para-nitrophenyl- $\beta$ -D-galactopyranoside
PVPP	polyvinylpyrrolidone
SOC	super optimal broth with catabolic repression medium
TE buffer	Tris-EDTA buffer
X-Gluc	5-bromo-4-chloro-3-indolyl-beta-D-glucuronic acid



# Functional Identification of Arabidopsis *ATSIP2* (At3g57520) as an Alkaline $\alpha$ -Galactosidase with a Substrate Specificity for Raffinose and an Apparent Sink-Specific Expression Pattern

Shaun Peters<sup>1,3</sup>, Aurélie Egert<sup>1,3</sup>, Bruno Stieger<sup>2</sup> and Felix Keller<sup>1,\*</sup>

<sup>1</sup>Institute of Plant Biology, University of Zürich, Zollikerstrasse 107, 8008 Zürich, Switzerland

<sup>2</sup>Division of Clinical Pharmacology and Toxicology, University Hospital Zürich, Rämistrasse 100, 8091 Zürich, Switzerland

<sup>3</sup>These authors contributed equally to this work

\*Corresponding author: E-mail, fkel@botinst.uzh.ch; Fax, +41-44-634-82-04

(Received June 30, 2010; Accepted August 16, 2010)

*Arabidopsis ATSIP2* has recently been suggested to be a raffinose synthase gene. However, it has high amino acid identity to functionally characterized alkaline  $\alpha$ -galactosidases from *Cucumis melo* and *Zea mays*. Using the *Sf9* insect cell expression system, we demonstrate that recombinant *ATSIP2* is a genuine alkaline  $\alpha$ -galactosidase with a distinct substrate specificity for raffinose, and not a raffinose synthase. A  $\beta$ -glucuronidase reporter construct using the *ATSIP2* promoter shows that *ATSIP2* is strongly expressed in sink tissues of *Arabidopsis*, i.e. sink leaves and non-xylem parts of the root stele, suggesting a physiological function in raffinose phloem unloading.

**Keywords:** Alkaline  $\alpha$ -galactosidase • Phloem unloading • Raffinose • *Sf9* insect cells • Sink metabolism.

**Abbreviations:** DGJ, 1-deoxygalactonojirimycin;  $\alpha$ -Gal,  $\alpha$ -galactosidase; Gal, galactose; Gol, galactinol; GUS,  $\beta$ -glucuronidase; Mel, melibiose; pNP $\alpha$ Gal, *p*-nitrophenyl  $\alpha$ -D-galactopyranoside; pNP $\beta$ Gal, *p*-nitrophenyl  $\beta$ -D-galactopyranoside; PAD, pulsed amperometric detection; Raf, raffinose; RafS, raffinose synthase; SIP, seed imbibition protein; sqPCR, semi-quantitative PCR; Sta, stachyose; Suc, sucrose; Ver, verbascose.

The *Arabidopsis* gene, *ATSIP2* (At3g57520), presently has controversial annotations and functions. It has been annotated as a putative raffinose synthase (RafS) or a seed imbibition protein (SIP) with *O*-glycosyl hydrolase (e.g.  $\alpha$ -D-galactoside hydrolase,  $\alpha$ -Gal) activity and suggested to function accordingly in both the biosynthetic and hydrolytic pathways of raffinose (Raf) metabolism, especially under certain abiotic stress conditions (drought, high salinity or high temperature; Nishizawa et al. 2008, Maruyama et al. 2009). The aim of this study was (i) to functionally express and characterize *ATSIP2* to determine if it encodes a RafS or an  $\alpha$ -Gal; and (ii) to identify a possible physiological function in sink tissues.

Interestingly, *ATSIP2* shares 76% amino acid similarity with CmAGA1 and 67% with CmAGA2, both functionally identified as alkaline  $\alpha$ -Gals from melon fruit with distinct substrate preferences for stachyose (Sta) and Raf, respectively (Gao and Schaffer 1999, Carmi et al. 2003). Numerous higher plant  $\alpha$ -Gals have been identified and described from a variety of species (for reviews, see Keller and Pharr 1996, Peterbauer and Richter 2001). Most studies have dealt with acidic isoforms, which appear to play important roles in seed development and germination and in sprouting of Sta-containing tubers (see Keller and Pharr 1996, Peterbauer and Richter 2001). Alkaline  $\alpha$ -Gals, however, have been mostly associated with sink activities, hydrolyzing phloem-translocated Raf and Sta in sink leaves and developing fruits (Gaudreault and Webb 1986, Bachmann et al. 1994, Carmi et al. 2003) as well as with thylakoid galactolipid breakdown during leaf senescence (Lee et al. 2009).

The cloning and functional expression of two cDNAs from melon fruit (*CmAGA1* and *CmAGA2*) showed that they displayed distinct  $\alpha$ -Gal activity at alkaline pH. Most importantly, these genes showed the highest homology to SIP genes, suggesting that SIPs are likely to represent alkaline  $\alpha$ -Gals in plants and revealing a hitherto unknown subfamily of glycosyl hydrolases (Carmi et al. 2003). On the basis of sequence homology, SIP genes have been identified in at least four other plant families including Poacea (barley, SIP: M77475), Leguminosae (Cicer, SIP: X95875), Solanaceae (tomato, SIP: TC94379) and Brassicaceae (*Arabidopsis*, SIPs: AAC83062, CAB66109). We here provide clear evidence that *ATSIP2* encodes a Raf-specific alkaline  $\alpha$ -Gal (and not a RafS) and suggest that it is involved in sink metabolism, most probably in phloem unloading of Raf.

*ATSIP2* was heterologously expressed in *Sf9* insect cells. Crude extracts from *Sf9* cells infected with a baculovirus carrying the *ATSIP2* cDNA were clearly able to hydrolyze Raf to sucrose (Suc) and galactose (Gal) at pH 7.5, in contrast to crude extracts from uninfected *Sf9* cells (Fig. 1A). Furthermore, this hydrolase activity was completely abolished when the



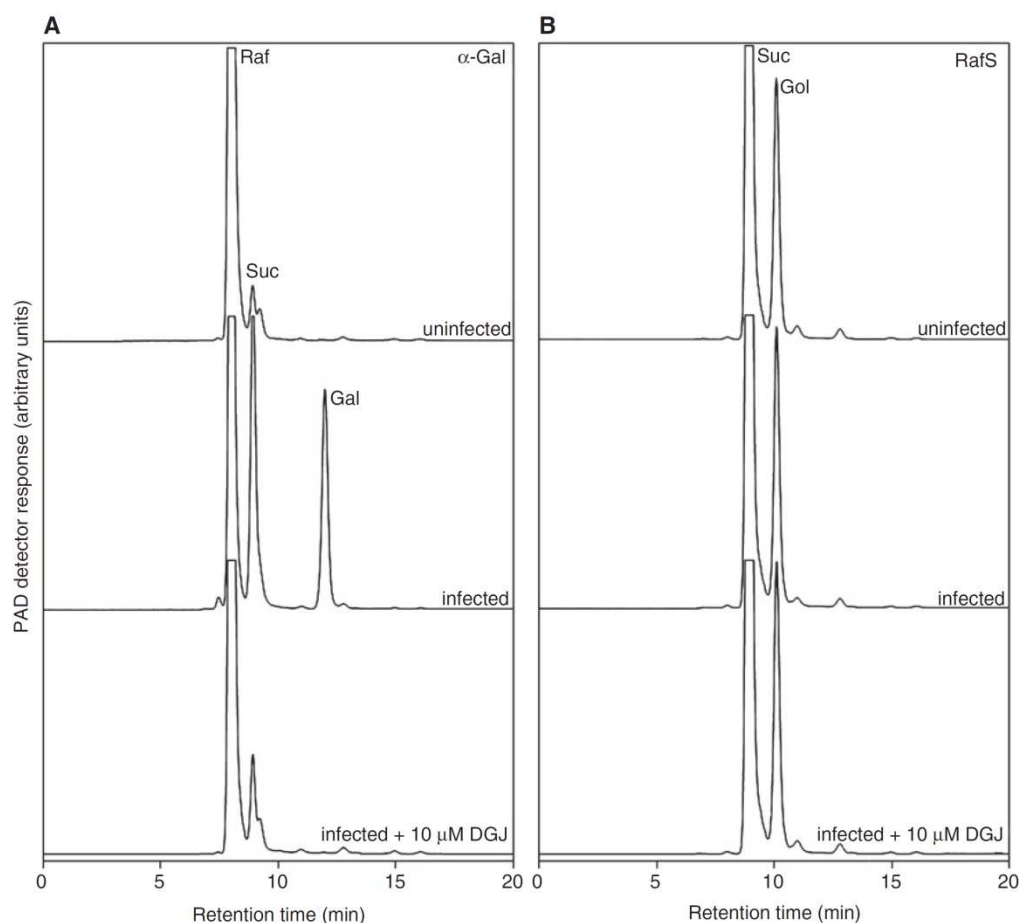


**Fig. 1** Enzyme activities of Sf9 cells infected or uninfected (controls) with an *ATSIP2*-carrying baculovirus. Crude cell lysates were incubated at pH 7.5 either with 50 mM Raf to assay for alkaline  $\alpha$ -Gal activity (A) or with 10 mM Gol and 100 mM Suc to assay for RafS activity (B). DGJ, 1-deoxygalactonojirimycin, is a potent inhibitor of  $\alpha$ -Gals (Butters et al. 2005, Blöchl et al. 2007).

enzyme assay was performed in the presence of 10  $\mu$ M 1-deoxygalactonojirimycin (DGJ), a potent  $\alpha$ -Gal inhibitor (Butters et al. 2005, Blöchl et al. 2007; **Fig. 1A**). The recombinant *ATSIP2* activity showed Michaelis–Menten-type kinetics with apparent  $K_m$  and  $V_{max}$  values of  $105 \pm 18$  mM and  $1.80 \pm 0.16$  nkat  $\text{mg}^{-1}$  protein, respectively (**Fig. 2A**), with a pH optimum around pH 7.5–8.0 (**Fig. 2B**) for Raf as substrate. The  $\alpha$ -Gal activity was end product-inhibited by Gal, displaying a 50% inhibition at 7.4 mM Gal (with 50 mM Raf as substrate). It was also very specific. When tested with the natural  $\alpha$ -galactosyl substrates, Raf, Sta, verbascose (Ver), galactinol (Gol) and melibiose (Mel), only Raf was recognized as an efficient substrate (**Fig. 2C**). When tested with the artificial substrate, *p*-nitrophenyl  $\alpha$ -D-galactopyranoside (pNP $\alpha$ Gal), a very high activity was observed ( $432 \mu\text{kat mg}^{-1}$  protein), in contrast to the  $\beta$ -linked variant of pNPGal, *p*-nitrophenyl  $\beta$ -D-galactopyranoside (pNP $\beta$ Gal; activity not detectable), confirming that it is indeed an  $\alpha$ -Gal (and not a  $\beta$ -Gal).

Using Suc and Gol as substrates, recombinant *ATSIP2* exhibited no ability to produce Raf, clearly excluding it from being a functional RafS (**Fig. 1B**).

Collectively, these observations unambiguously identify *ATSIP2* as an alkaline  $\alpha$ -Gal in *Arabidopsis* with a substrate preference for Raf, and not a RafS as recently reported (Nishizawa et al. 2008, Maruyama et al. 2009, Wu et al. 2009).

To investigate *ATSIP2*'s putative physiological function in sink metabolism, an *ATSIP2* promoter: $\beta$ -glucuronidase (GUS) fusion was created, using the Gateway-compatible vector, pMDC163 (Curtis and Grossniklaus 2003), and a 0.5 kb fragment of genomic DNA, upstream of the start codon of *ATSIP2* (–500 bp). A second fusion included this 0.5 kb plus an additional 1 kb of upstream DNA. *Arabidopsis* (Col-0) transformed with these constructs showed strong GUS activity in sink leaves of 5-week-old soil-grown plants (**Fig. 3A, B**), suggesting that *ATSIP2* is expressed in these tissues. *ATSIP2* promoter expression was also found in steles of lateral roots (**Fig. 3C, D**).

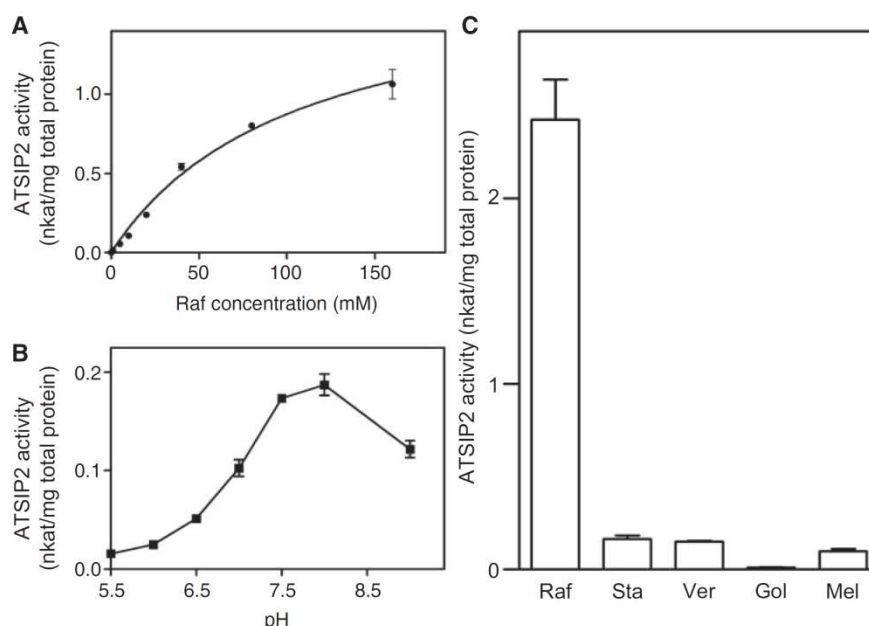


**Fig. 2** Biochemical characterization of the recombinant ATSIP2 enzyme. (A) The Raf concentration dependence shows Michaelis–Menten-type kinetics with apparent  $K_m$  and  $V_{max}$  values of  $105 \pm 18$  mM and  $1.80 \pm 0.16$  nkat  $\text{mg}^{-1}$  protein, respectively. (B) The pH dependence shows a pH optimum at around pH 7.5–8.0 with 50 mM Raf as substrate. (C) The ATSIP2 activity shows clear Raf specificity when different natural substrates are compared (measured at pH 7.5 with 50 mM each of Raf, Sta, Ver, Gol and Mel). Data are means  $\pm$  SE of 3–6 replicates.

Cross-sections of young roots further revealed that this expression is located in the non-xylem parts of the stele, including the phloem (Fig. 3E, F). Finally, we were able to correlate this GUS expression pattern to *in vivo* alkaline  $\alpha$ -Gal activity. Using Raf as substrate at pH 7.5, the  $\alpha$ -Gal activity was significantly higher in sink tissues (roots and young leaves) than in source tissues (old leaves) (Fig. 3G). Using semi-quantitative reverse-transcription PCR (sqPCR), these  $\alpha$ -Gal activities were positively correlated to the presence of *ATSIP2* transcripts in all tissue types described (Fig. 3H). Such an expression pattern for alkaline  $\alpha$ -Gal is reminiscent of a putative function in phloem unloading (Gaudreault and Webb 1986, Bachmann et al. 1994, Carmi et al. 2003). Although Suc has been reported to be the primary phloem-mobile carbohydrate in *Arabidopsis*, there is also good evidence that some Raf is additionally transported in the phloem (Haritatos et al. 2000). In that study, following exposure of *Arabidopsis* source leaves to  $^{14}\text{CO}_2$  and light, radio-label was clearly found in [ $^{14}\text{C}$ ]Raf in sink leaves (in addition to the predominant [ $^{14}\text{C}$ ]Suc). In this study, we have shown *ATSIP2* to be a Raf-specific alkaline  $\alpha$ -Gal with a promoter active exclusively in sink tissues, suggesting that it may legitimately be involved in the unloading of phloem-mobile Raf in sink tissues. This finding does not rule out the possibility of additional putative physiological functions for *ATSIP2* in *Arabidopsis*, for instance in abiotic stress tolerance or seed germination, and these are currently being investigated using a reverse genetic approach.

## Materials and Methods

Following stratification (48 h, 4°C), *Arabidopsis* Col-0 ecotype seeds were propagated on soil (Einheitserde, type ED73, Gebr. Patzer GmbH & Co. KG, Schopfheim, Germany) in a controlled-environment chamber (8 h light, 120  $\mu\text{mol photons m}^{-2}\text{s}^{-1}$ , 22°C, 16 h dark, 60% relative humidity).

*ATSIP2* (At3g57520) was obtained as a full-length cDNA from the Riken *Arabidopsis* full-length clone database (pda02775, [www.brc.riken.jp](http://www.brc.riken.jp)). This cDNA was amplified using a high fidelity PCR (Expand High Fidelity PCR System, Roche) according to the manufacturer's instructions, using open reading frame-specific primers (*ATSIP2*<sub>fwd</sub> 5'-ATGACGATTA CATCAATATCTCTG and *ATSIP2*<sub>rev</sub> 5'-CTAGACCAGAATC TCAACATG). *ATSIP2* was subcloned by standard restriction digest and ligation reactions, from pGEM-T Easy into the pFastBac HTc vector (Invitrogen AG), using the *NotI* restriction endonuclease. Bacmid preparation, insect cell transfection and recombinant protein expression were conducted as outlined in the bac-to-bac manual (Invitrogen), using Sf9 cells grown in monolayer cultures.

Sf9 cells were collected by centrifugation (500  $\times$ g, room temperature, 5 min) 72 h after baculovirus infection. Cell pellets were re-suspended in 2 ml of extraction buffer [100 mM HEPES-KOH, pH 7.5, 5 mM  $\text{MgCl}_2$ , 1 mM EDTA, 10 mM dithiothreitol (DTT), 1 mM benzamidine, 1 mM phenylmethylsulfonyl fluoride (PMSF), 0.05% (v/v) Triton X-100] and homogenized on



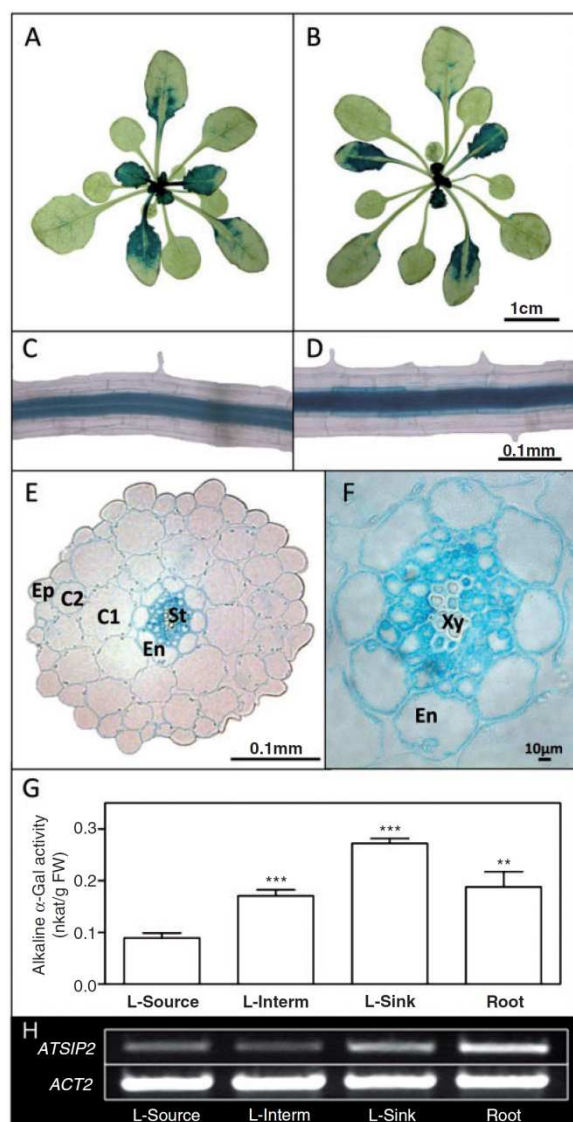


**Fig. 3** The *ATSIP2* promoter is active in sink leaves and the non-xylem parts of the root stele (blue GUS staining). (A) Sink leaf-specific expression pattern in the 1.14 stage rosettes of *pATSIP2*<sub>500</sub>::*pMDC163* and (B) of *pATSIP2*<sub>1500</sub>::*pMDC163*. (C) Root stele-specific expression of *pATSIP2*<sub>500</sub>::*pMDC163* and (D) of *pATSIP2*<sub>1500</sub>::*pMDC163*. (E and F) Cross-sections of roots of young *pATSIP2*<sub>500</sub>::*pMDC163* plants showing promoter activity in the non-xylem parts of the root stele. (G) The extractable alkaline α-Gal activity of wild-type plants is highest in the sink tissues. α-Gal activity was measured at pH 7.5 with 50 mM Raf. All plants were of the same age (5 weeks; soil-grown), except for E and F (10-day-old, MS agar-grown). (H) SqPCR of cDNA from the four tissues described shows that the *ATSIP2* transcripts are most abundant in sink tissues. The *ACTIN2* gene was used as a constitutively expressed control. Ep, epidermis; C1-C2, cortex; En, endodermis; St, stele; Xy, xylem vessels; L-Source, source leaves; L-Interm, intermediate leaves; L-Sink, sink leaves. The statistical probabilities represented by asterisks reflect an unpaired *t*-test (\*\**P* < 0.0001; \*\**P* < 0.006).

ice using a Potter homogenizer connected to an electric drill. After centrifugation (12,000×*g*, 4°C, 10 min), 30 μl aliquots of clarified crude extracts were incubated with 30 μl of Raf assay buffer (100 mM HEPES-KOH, pH 7.5, 100 mM Raf) at 30°C for 1 h. Samples were desalted and analyzed by HPLC with pulsed amperometric detection (HPLC-PAD), using a Ca<sup>2+</sup>/Na<sup>+</sup>-moderated ion partitioning carbohydrate column (Peters et al. 2007, Peters and Keller 2009). The pH optimum of recombinant *ATSIP2* was determined using 50 mM Raf in the following buffers: full-strength Mcllvaine buffer (pH 5.0, 5.5 and 6.0), 100 mM MES-KOH buffer (pH 6.0, 6.5 and 7.0) and 100 mM HEPES-KOH buffer (pH 7.0, 7.5, 8.0 and 9.0).

The specificity of recombinant *ATSIP2* for α- or β-galactosides was tested using the artificial substrate, *p*-nitrophenyl-*D*-galactopyranoside (pNPGal) as previously described (Gao and Schaffer 1999). Briefly, 10 μl of clarified crude extract was incubated with 90 μl of assay buffer (100 mM HEPES-KOH pH 7.5) containing 3 mM pNPGal or pNPβGal. The assay mixture was incubated in a 96-well microtiter plate at 30°C and the reaction stopped by the addition of 160 μl of 1 M Na<sub>2</sub>CO<sub>3</sub>. Absorbance was read at 405 nm. The specificity for the natural substrates, Raf, Sta, Ver, Gol and Mel, was tested at 50 mM final concentrations using the HPLC-PAD method as described above.

For the determination of α-Gal activities in crude leaf extracts, 5-week-old soil-grown *Arabidopsis* plants were separated into source, intermediary and sink leaves, as well as roots. Tissue (100 mg) was homogenized in 200 μl of an alkaline extraction buffer as previously described (Peters et al. 2007, Peters and Keller 2009). Aliquots (10 μl) of clarified crude extracts were incubated with 10 μl of Raf assay buffer at 30°C for 1 h and the activity was determined as described above.

Total RNA was extracted from source, intermediary and sink leaves as well as roots using the Plant RNeasy kit (Qiagen AG). The cDNA template for sqPCR was obtained by reverse transcribing 1 μg of total RNA with an oligo(dT)<sub>15</sub> primer and M-MLV (H<sup>-</sup>) reverse transcriptase (Promega AG) according to the manufacturer's protocol. The sqPCR was carried out in 50 μl containing 5 μl of cDNA, 1.25 U of GoTaq DNA polymerase (Promega), 1× PCR buffer, 0.5 mM of each dNTP and 0.5 μmol of each primer, at a primer annealing temperature of 58°C for 23 cycles. The number of cycles chosen for the sqPCR was determined to occur in the linear range of the constitutively expressed *ACTIN2* gene (*ACT2*, At3g18780). The *ACT2* primer pair (*ACT2*<sub>fwd</sub> 5'-ATGGCTGAGGCTGATGATAT and *ACT2*<sub>rev</sub> 5'-TTAGAAACATTTTCTGTGAACGAT) amplified a 1.1 kb fragment of the cDNA. The *ATSIP2* primer pair (*ATSIP2*<sub>fwd</sub> 5'-ATGACGATTACATCAATATCTCTG and *ATSIP2*<sub>rev</sub> 5'-TGAAGTGGGTATGCTAATGC) amplified a 1.0 kb fragment of the cDNA.

A 0.5 kb fragment of *Arabidopsis* genomic DNA, upstream from the *ATSIP2* start codon, was amplified using a high fidelity PCR (Expand High Fidelity PCR System, Roche), following the manufacturer's instructions. This fragment was cloned into the pCR8/GW/TOPO vector system (Invitrogen) and subcloned into the Gateway destination vector *pMDC163* (Curtis and



Grossniklaus 2003) using a conventional LR clonase reaction (Invitrogen). This ATSIP2–promoter–GUS reporter construct was transformed into *Agrobacterium tumefaciens* (GV3101) by electroporation, using a Genepulser (2.5 kV; 100  $\Omega$ ; 25  $\mu$ F; Bio-Rad). A second reporter construct included the 0.5 kb described above and an additional 1 kb of upstream sequence, containing a putative TATA consensus sequence. Col-0 *Arabidopsis* plants were transformed using a floral dip method (Clough and Bent 1998). Hygromycin B-resistant plants were selected as previously described (Harrison et al. 2006). Transgenic plants ( $T_3$ ) were used to assay for GUS activity.

$T_3$  *Arabidopsis* seeds transformed with the reporter construct described above were sown onto MS agar supplemented with Suc (5%, w/v) and hygromycin B (25  $\mu$ g ml<sup>-1</sup>). One week after germination, plants were transferred onto soil and used to stain for GUS activity (Parcy et al. 1998) 4 weeks later.

For the preparation of root cross-sections, roots of 10-day-old plants grown on MS agar were used. They were stained for GUS activity, fixed for 3 min under vacuum in 4% (v/v) glutaraldehyde and incubated for 4 h at room temperature. The tissue was washed three times with ddH<sub>2</sub>O and dehydrated using an ethanol series (70%, 30 min; 90%, 30 min; 100%, 1 h). The final dehydration step using 100% ethanol was repeated once. Embedding of the tissue was conducted using Technovit 7100 (Heraeus Kulzer), following the manufacturer's instructions, and root cross-sections (2–3  $\mu$ m) were cut using a hand-operated microtome.

### Funding

This work was supported by the Swiss National Foundation [grant number 31-116599].

### References

- Bachmann, M., Matile, P. and Keller, F. (1994) Metabolism of the raffinose family oligosaccharides in leaves of *Ajuga reptans* L. Cold acclimation, translocation, and sink to source transition: discovery of chain elongation enzyme. *Plant Physiol.* 105: 1335–1345.
- Blöchl, A., Peterbauer, T. and Richter, A. (2007) Inhibition of raffinose oligosaccharide breakdown delays germination of pea seeds. *J. Plant Physiol.* 164: 1093–1096.
- Butters, T.D., Dwek, R.A. and Platt, F.M. (2005) Imino sugar inhibitors for treating the lysosomal glycosphingolipidoses. *Glycobiology* 15: 43–52.
- Carmi, N., Zhang, G., Petreikov, M., Gao, Z., Eyal, Y., Granot, D., et al. (2003) Cloning and functional expression of alkaline  $\alpha$ -galactosidase from melon fruit: similarity to plant SIP proteins uncovers a novel family of plant glycosyl hydrolases. *Plant J.* 33: 97–106.
- Clough, S.J. and Bent, A.F. (1998) Floral dip: a simplified method for *Agrobacterium*-mediated transformation of *Arabidopsis thaliana*. *Plant J.* 16: 735–743.
- Curtis, M.D. and Grossniklaus, U. (2003) A gateway cloning vector set for high-throughput functional analysis of genes in planta. *Plant Physiol.* 133: 462–469.
- Gao, Z. and Schaffer, A.A. (1999) A novel alkaline  $\alpha$ -galactosidase from melon fruit with a substrate preference for raffinose. *Plant Physiol.* 119: 979–988.
- Gaudreault, P. and Webb, J. (1986) Alkaline  $\alpha$ -galactosidase activity and galactose metabolism in the family Cucurbitaceae. *Plant Sci.* 45: 71–75.
- Haritatos, E., Medville, R. and Turgeon, R. (2000) Minor vein structure and sugar transport in *Arabidopsis thaliana*. *Planta* 211: 105–111.
- Harrison, S., Mott, E., Parsley, K., Aspinall, S., Gray, J. and Cottage, A. (2006) A rapid and robust method of identifying transformed *Arabidopsis thaliana* seedlings following floral dip transformation. *Plant Methods* 2: 19.
- Keller, F. and Pharr, M. (1996) Metabolism of carbohydrates in sinks and sources: galactosyl-sucrose oligosaccharides. In *Photoassimilate Distribution in Plants and Crops: Source–Sink Relationships*. Edited by Zamski, E. and Schaffer, A.A. pp. 157–183. Marcel Dekker, New York.
- Lee, R.-H., Hsu, J.-H., Huang, H.-J., Lo, S.-F. and Chen, S.-C.G. (2009) Alkaline  $\alpha$ -galactosidase degrades thylakoid membranes in the chloroplast during leaf senescence in rice. *New Phytol.* 184: 596–606.
- Maruyama, K., Takeda, M., Kidokoro, S., Yamada, K., Sakuma, Y., Urano, K., et al. (2009) Metabolic pathways involved in cold acclimation identified by integrated analysis of metabolites and transcripts regulated by DREB1A and DREB2A. *Plant Physiol.* 150: 1972–1980.
- Nishizawa, A., Yabuta, Y. and Shigeoka, S. (2008) Galactinol and raffinose constitute a novel function to protect plants from oxidative damage. *Plant Physiol.* 147: 1251–1263.
- Parcy, F., Nilsson, O., Busch, M.A., Lee, I. and Weigel, D. (1998) A genetic framework for floral patterning. *Nature* 395: 561–566.
- Peterbauer, T. and Richter, A. (2001) Biochemistry and physiology of raffinose family oligosaccharides and galactosyl cyclitols in seeds. *Seed Sci. Res.* 11: 185–187.
- Peters, S. and Keller, F. (2009) Frost tolerance in excised leaves of the common bugle (*Ajuga reptans* L.) correlates positively with the concentrations of raffinose family oligosaccharides (RFOs). *Plant Cell Environ.* 32: 1099–1107.
- Peters, S., Mundree, S.G., Thomson, J.A., Farrant, J.M. and Keller, F. (2007) Protection mechanisms in the resurrection plant *Xerophyta viscosa* (Baker): both sucrose and raffinose family oligosaccharides (RFOs) accumulate in leaves in response to water deficit. *J. Exp. Bot.* 58: 1947–1956.
- Wu, X.L., Kishitani, S., Ito, Y. and Toriyama, K. (2009) Accumulation of raffinose in rice seedlings overexpressing OsWRKY11 in relation to desiccation tolerance. *Plant Biotechnol.* 26: 431–434.



## Curriculum Vitae

### Personalien

Name: EGERT

Vorname: Aurélie

Geboren am: 15.01.1984

Heimatort: Saint-Louis, France

### Ausbildung

- 2007-2011     **Doctor of Philosophy** (Ph.D.), Institute of Plant Biology, University of Zürich, Switzerland
- 2005-2007     **Master** (Master sciences, Mention Vie et Santé, spécialité Sciences du Végétal), Strasbourg, France
- 2002-2005     **Bachelor** (Licence de biochimie), Strasbourg, France.
- 2002           **Maturität** (Baccalaureat serie S), Saint-Louis, France

### Erfahrung

- 2007-2011     Assistentin am Institut für Pflanzenbiologie der Universität Zürich
- 2007-2011     Teilnahme am Graduiertenprogramm des Zürich-Basel Plant-Science Centers
- 2007           Teilnahme am Tempus Project SWRC in Russland (Securing Water Resources Through Educational Change)
- 2007           Masterarbeit am Albert-Ludwigs-Universität Freiburg, Deutschland (unter der Leitung von Prof. Dr. Wagner)
- 2006-2007     Laborantin am Botanischen Institut der Universität Basel (unter der Leitung von Prof. Dr. Heinlein)

### Publikation

**Peters S, Egert A, Stieger B, Keller F** (2010) Functional identification of Arabidopsis AT5G10330 (At3g57520) as an alkaline  $\alpha$ -galactosidase with a substrate specificity for raffinose and an apparent sink-specific expression pattern. *Plant and Cell Physiology* 51(10): 1815-1819



## Acknowledgments

First of all I am grateful to Prof. Dr. Felix Keller who gave me the opportunity to work in his laboratory. Many thanks for your support, trust, corrections, ideas, discussions and for helping me to develop my own thinking. I will never forget this wonderful time in your lab as your last PhD student.

Thanks to my PhD committee, Prof. Dr. Enrico Martinoia and Dr. Norbert Sprenger for devoting time being members of my PhD committee and for their guidance and words of encouragement during my thesis.

Many thanks to Prof. Dr. Stefan Hörtensteiner for being part of my examiners, for the corrections and help concerning the AtDIN10 project.

Thanks to Prof. Dr. Bruno Stieger who gave me the opportunity to use and learn the *Sf9* insect cell system and thanks to Dr. Christelle Guyot, Lia Hofstetter, Stéphanie Häusler and Dr. Krasimira Marinova for the technical assistance with *Sf9* cells and cell stocks maintenance.

Thanks to Prof. Dr. Francoise Corbineau for her advice and collaboration concerning the seed germination experiments.

Special thanks to Shaun Peters for the interesting discussions we often had, the common projects we shared, also for his help in correcting my English, this thesis and our publication. We had a good time together and I really appreciated your humor and all your spicy stories.

Thanks to Bastien, Silvia and Kathrin for the good atmosphere we had in the lab and free beds always available for me to stay in Zurich!

Thanks to all the people from the P1 floor for the good time spent together and the discussions during coffee breaks.

Un grand merci à ma famille et mes amis, en particulier ma mère que je ne remercierai jamais assez de m'avoir toujours poussé et soutenu dans tous mes choix.

Enfin je remercie mon fiancé Cédric pour son soutien quotidien moral autant qu'informatique et son amour. Notre couple a grandi en même temps que mon projet scientifique, le premier servant de socle solide à l'épanouissement du second.



